UNIVERSITY OF NEWCASTLE UPON TYNE

DYNAMICS AND CONTROL

of

LINKAGE MECHANISMS

having

TWO DEGREES OF FREEDOM

BY

A.H. YOUSSEF M.Sc.

A Thesis submitted for the

Degree of Doctor of Philosophy in the

Faculty of Applied Science,

University of Newcastle upon Tyne

March 1974

BEST COPY
AVAILABLE
Variable print
quality

S Y N O P S I S

The work described in this thesis concerns the dynamics and control of linkage mechanisms having two degrees of freedom. The work, basically, deals with three topics. The first concerns the derivation of equations of motion, their numerical solution and linearised analysis involving the studies of resonance and stability. The second concerns optimisation of a general planar linkage to generate a given output and also controlling some of the linkage inputs to generate an output more closely. The third concerns experimental investigations to check the validity of the numerical solutions and the linearised analysis.

ACKNOWLEDGEMENTS

I am greatly indebted to Professor L. Maunder for his constant encouragement and guidance throughout this work and also for making available the facilities of the Mechanical Engineering Department.

My thanks to Mr. J. Burdess, Dr. J.R. Hewit, Mr. C. Grant and Mr. K. Oldham and other colleagues for their helpful comments.

My thanks to the workshop and design office staff of the Department of Mechanical Engineering for their help in manufacturing the experimental rigs and preparing some of the figures in this thesis.

My thanks to Mrs. M. Macpherson for typing this thesis.

Lastly, my special thanks and appreciation to my wife Kathy for her encouragement and understanding.

C O N T E N T S

PART I

INTRODUCTION

Chapter 1

GENERAL INTRODUCTION

1. 0. Introduction

Mechanisms of various types are present in great numbers in present day engineering industry. It is not surprising, therefore, to find a substantial interest in investigating the various aspects of motion, function and design of mechanisms, ref. (1 - 3).

The main function of a mechanism is, in most cases, to generate a specified output motion. In doing so, the mechanism must work in harmony with its surroundings, be efficient and have acceptable dynamic characteristics. The first step towards designing a mechanism is therefore kinematic synthesis, that is finding the dimensions and the inputs that will generate the desired output motion. The second step is a kinematical motion analysis investigating the motion of the constitutive parts and ensuring they work in harmony and do not interfere with the motion or components of neighbouring mechanisms. The third step is the study of the dynamic effects resulting from the distribution of masses and inertias and the flexibility of the various components. These dynamic studies include items such as balancing, resonance and stability, and power transmission characteristics.

Linkages constitute an important class of mechanisms. A number of researchers have therefore focused their attention on studying the various phenomena concerning this type of mechanism. The greatest part of these studies fall into two categories (a) kinematic, which constitute the major part and (b) dynamic.

The kinematic studies concern two aspects : synthesis and kinematic analysis. Examples of the work in synthesis may be found in refs. (4 - 16) which, briefly, concern ways of finding the type of linkage and dimensions to achieve a desired output motion. The most widely used method of specifying the desired motion is by means of a number of points or positions often called in the literature "precision points". A limit on the number of precision points is determined by the type and form of the linkage being studied. For example, in a four-bar linkage the number of parameters sufficient to define the linkage is four (five, if the initial configuration is considered) and hence only four precision points in the output may be considered in finding the values of these parameters. Briefly the methods adopted in obtaining the results include such methods as solving a simultaneous set of N equations, when N is the number of parameters sufficient to define the mechanism, describing the different

configurations corresponding to the prescribed output motion or methods such as constructing an error function in output generation and finding the stationary values with respect to the mechanism parameters. Various techniques are used in achieving the solution. Among them are included least square fit, iterative techniques such as Newton-Raphson, displacement matrix and others. Other methods are based on graphical solutions in which, again, different techniques are used. These include techniques such as inversion of the mechanism, taking the tracing point through the output and choosing a linkage, fixing the values of some of its parameters and pin joint locations and determining the dimensions and form of the remaining links.

Recently there has been an interest in applying optimal control methods, ref. (17 - 22), in synthesis problems. Such work may be found in refs. (23 - 31). The methods employed are gradient methods, non linear programming and random methods and direct search methods. In the opinion of the author gradient methods are difficult to apply in linkages,except in simple ones,because of the difficulty in obtaining the gradient and the existence of numerous stationary values in the error criterion. All the methods rely on initial guesses to start them. The gradient methods descend along the gradient until a minimum is located. The direct

search methods search along n-orthogonal vectors in linkage parameter space and choose values of the linkage parameters that produce a reduction in the value of the error criterion. The random methods investigate the values of the error criterion for random values of linkage parameters and choose the best set of parameters that yield minimum error. All these methods obviously need an error and convergence criteria, the choice of which depends upon the type of problem being studied. This choice, however, greatly influences the progress and efficiency of the type of method used.

Examples of the work in kinematic analysis may be found in refs. (32 - 40). Briefly the work consists of setting up the kinematic equations of motion describing the loop closure of the mechanism and solving them to find the displacements of the individual links of the mechanism. The velocities and accelerations are obtained by taking the first and second time derivatives of the displacements respectively. The kinematic equations are set up in vector or scalar forms and various techniques ranging from use of complex harmonic analysis to iterative techniques and straight forward elimination are used in the solution.

Studies concerning the dynamics of mechanisms have received less attention than those concerning the kinematics. A number of workers have, however. contributed to this field and examples of their work

may be found in ref. (41 - 69). The work on balancing (41, 44) concerns adding counterweights and springs and finding the distribution of masses and inertias to yield minimum values of pin forces, shaking moments and input torques. The dynamics of mechanisms with flexible elements have also been studied, refs. (45 - 54), in which in most cases the equations of motion are linearised to yield Hill's type equations on which standard solutions are performed. Other work in dynamics, refs. (55 - 64), constitute dynamical analysis involving the solution of the non linear equations of motion; finding the torques, pin forces, response, velocities and accelerations. Recently there has been some work done on the dynamic effects of clearance in linkages. Such work may be found in refs. (65 - 69) and briefly concerns the effects of the clearance on the pin forces transmitted to the bearings and currently ref. (68) deals with eliminating the undesirable effects of clearances and altering the shapes of the loci plots of pin forces to minimise wear in the bearings.

The complexity of modern devices demand a sophisticated class of mechanisms. ROSE (70) considered the use of a five bar linkage with two inputs to generate a complex motion. His method consisted of determining graphically a five bar loop to bound any desired plane motion by an area, establishing functional relationships between the two

inputs and coupling them together with a simple mechanism to match the output motion requirements. The work that follows springs from a comparable idea by finding the optimum four bar to approximate an output and releasing the rocker-to-ground joint, which effectively results in a five bar loop, and controlling this joint in such a manner that the output is achieved closely. The dynamics of this type of mechanism when the slider is constrained by a linear spring and opposed by viscous friction is also studied and experimental investigations are performed to support some of the computer solutions obtained in the theoretical analysis.

1. 1. Scope of Investigation

The following investigation proceeds to study the dynamics and kinematics of a two degree of freedom mechanism. The mechanism chosen is a four bar linkage with the rocker-to-ground joint replaced by a slider. The slider movement is opposed by viscous friction and constrained by a linear spring along its direction of travel. The mechanism is a representative two degree of freedom linkage and the methods of solution may be applied to any other two degree of freedom linkage. The mechanism can also generate a variety of outputs by using different spring rates or controlling the slider movement. It can also be looked upon as a four bar linkage with a flexible mounting and hence may be treated as a vibration problem.

The investigation falls into three phases. The first studies the dynamics, the second finds the optimum four bar to generate a given output and controls its slider in an optimum fashion and the third performs an experimental investigation.

1. 1. 1 The dynamics.

The equations of motion are derived using the Lagrangian multiplier method. The multipliers are associated with the corresponding pin forces and torques. A method of solution is established giving minimum errors in the numerical integration of the equations of motion. The equations of motion are solved for three cases of (a) constant speed input, (b) torsion bar input and (c) free motion condition. In each case the motion of the slider is investigated for different spring rates and viscous coefficient values and in case (a) the input torque required to maintain constant speed input is found. In the free motion case, (c), a phase plane plot of the slider motion and the variation of the crank speed with time are obtained.

The equations of motion are linearised and solutions are obtained. The resonance frequency and resonance curves are obtained for various values of viscous coefficient values and rocker inertias. The stability of the slider motion is studied using a perturbation method and a numerical computer orientated method. The numerical method is used

when the damping terms are included in the analysis and relies on an optimisation method to locate the unstable regions. These unstable regions are found for a constant spring stiffness and a viscous coefficient varying the crank length, the coupler length and rocker inertia. The value of the viscous coefficient to eliminate instability for all ranges of crank speeds within a range of values of the rocker inertia is also found. The method is established to deal with any Mathieu type equation and produces results which when compared with the perturbation results give good agreement.

1. 1. 2. Optimisation and Control

A general and conversational optimisation procedure is written to deal with finding the optimum of any general planar linkage to produce minimum errors, in generating a given output. The procedure is applied to a four bar linkage to produce outputs in the form of a path dependent or independent of time. The procedure can cope with equality and non equality constraints explicit or implicit and is able to generate portions of an output more accurately by introducing weighting factors.

The optimum four bar produced by the above optimisation is considered with a sliding rocker-to-ground pivot to which an input is introduced. This input is controlled in an optimum manner leading to

acceptable errors in the output. Alternatively as a result of releasing the pivot an output area becomes accessible and a desired output defined within this area may be achieved by proper control of the pivot.

1. 1. 3. Experimental investigations

Two experimental rigs are used, the first is built by the author and the second built under his supervision,ref. (53). The investigation carried out on the first rig concerns finding the steady state motion of the slider for different spring rates and crank constant input speeds and also compares them with the theoretical results. The second rig is used to investigate the resonance of the slider with the linkage having a small crank length relative to the other links and a small viscous coefficient value for different spring rates. The results are also compared with those obtained from the theoretical analysis.

1. 2. Layout of thesis

The thesis is divided into five parts, the layout of which is as follows. Part I includes the general introduction; Part II consists of four chapters, the first contains the derivation of equations of motion, the second the solutions of the equations of motion, the third resonance analysis and the fourth stability analysis. Part III consists of two chapters, the first deals with parameter optimisation and the second with control. Part IV consists of two

chapters,the first contains the experimental investigations and the second the conclusions. Part V contains the references and appendices.

P A R T I I

DYNAMICS

CHAPTER II

EQUATIONS OF MOTION

Consider the linkage shown in fig. (2.1). It is a two degree of freedom mechanism, the degrees being the crank angle "θ_2" and the displacement of the slider "u". The imposed external forces are the driving torque $T_1(\theta_2)$, the loading force F_1 acting on point p and the controller or constraint force F_2 acting on the slider. The viscous damping force is represented by F_3 and the coefficient of damping by μ. The link dimensions, masses and inertias are as shown in the figure and the reference coordinates are X and Y with origin at A.

2. 1. The Kinematics

The kinematics may be defined by writing the two constraint equations along and perpendicular to the ground link ℓ_1, i.e.

$$\ell_2 \mathrm{Cos}\theta_2 + \ell_3 \mathrm{Cos}\theta_3 - \ell_4 \mathrm{Cos}(\theta_4 + \alpha) - u\,\mathrm{Cos}\alpha = 0$$

$$\ell_2 \mathrm{Sin}\theta_2 + \ell_3 \mathrm{Sin}\theta_3 - \ell_4 \mathrm{Sin}(\theta_4 + \alpha) - u\,\mathrm{Sin}\alpha = 0 \qquad (2.1)$$

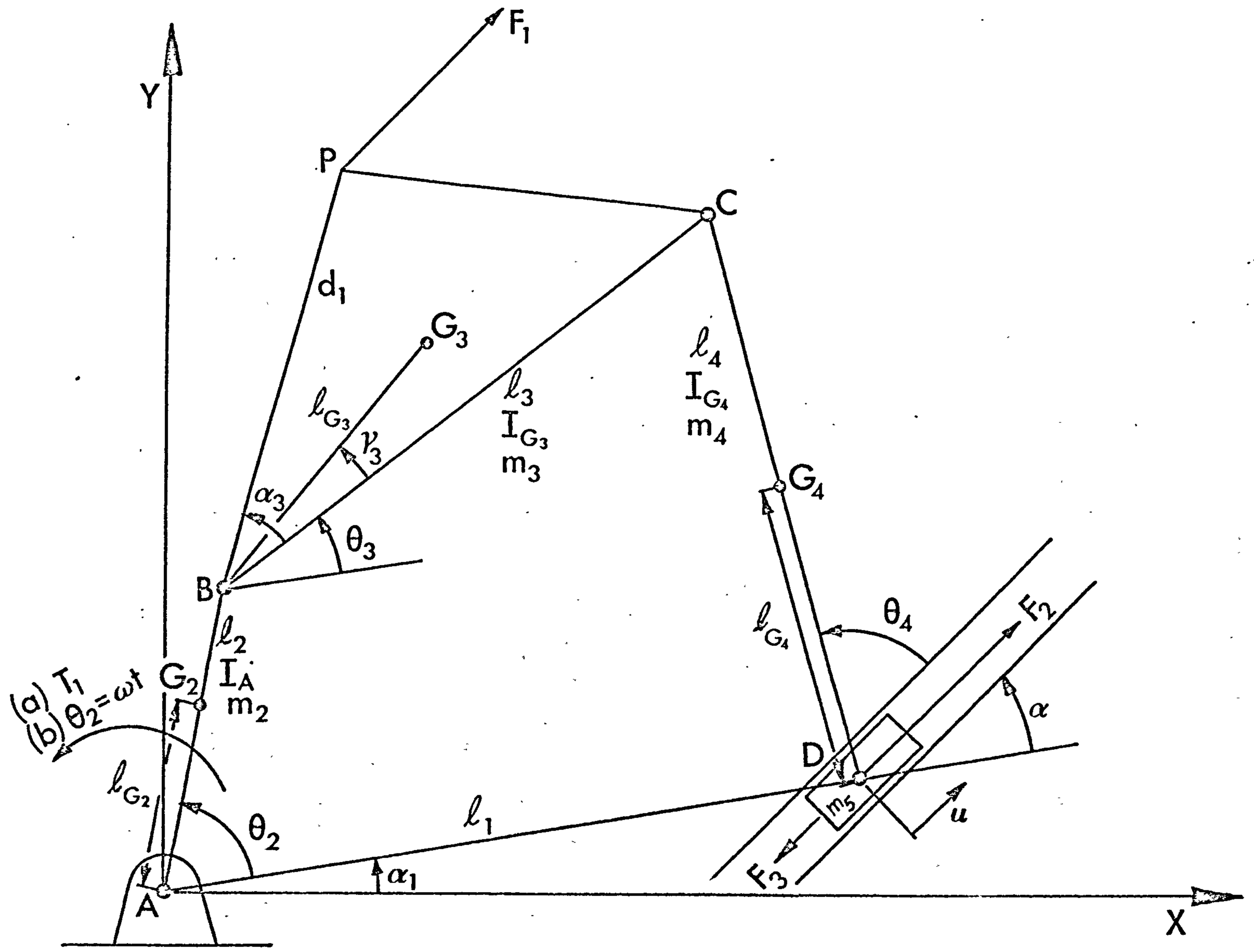

Fig(2·1) ; PLANAR LINKAGE A,B,C,D

In addition, in the case of a constant speed input ω of the crank, a further equation of the form

$$\theta_2 - \omega t = 0 \qquad (2.2)$$

is required. The above equations may be represented in suffix notation as

$$f_j\ (\theta_2, \theta_3, \theta_4, u) = 0, \qquad (2.3)$$

where $j = 1, 2, 3$.

The constraint equations expressed in terms of velocities may be derived from (2.3) and written in suffix notation as,

$$v_j(\theta_2, \theta_3, \theta_4, u, \dot{\theta}_2, \dot{\theta}_3, \dot{\theta}_4, \dot{u}) = 0 \qquad (2.4)$$

Equation (2.3) can be solved explicitly to give the angles θ_3 and θ_4 as functions of angle θ_2 and displacement u. Similarly the angular velocities $\dot{\theta}_3$ and $\dot{\theta}_4$ may be obtained from (2.4) as functions of positions and speeds of crank and slider. The accelerations may also be obtained by taking the first derivative of equation (2.4). It is, therefore, clear that equation (2.3) is sufficient for the complete kinematic solution of the linkage.

2. 2. The Derivation of Equations of Motion

The equations of motion are derived using the Lagrangian multipliers method. This may be stated as follows :-

$$\frac{\partial}{\partial t}\frac{\partial T}{\partial \dot{q}_i} - \frac{\partial T}{\partial q_i} = Q_i + \sum_{j=1}^{n} \lambda_j \cdot \frac{\partial f_j}{\partial q_i} \qquad (2.5)$$

where T is the total kinetic energy of the system q_i and $\dot{q}_i$ are the generalised coordinates and velocities, Q_i the generalised forces including conservative and non conservative effects, n the number of constraint equations, λ_j the Lagrangian multipliers and f_j the Constraint equations.

The generalised forces Q_i may be written in the form

$$Q_i = m_j \cdot (\tilde{g} \cdot \frac{\partial \tilde{r}_j}{\partial q_i}) + \tilde{F}_j \cdot \frac{\partial \tilde{r}_i}{\partial q_i} + \tilde{T}_j \frac{\partial \tilde{\Theta}_j}{\partial q_i} \qquad (2.6)$$

where m_j represents the masses, $\tilde{g}$ the gravitational vector, $\tilde{r}_j$ the coordinate vector of the point of application of the external forces $\tilde{F}_j$ and $\tilde{T}_j$ the vector of torques.

Let the generalised coordinates q_i be $\Theta_2, \Theta_3, \Theta_4$ and u. Now in order to obtain the kinetic energy in terms of these coordinates the velocities of the centres of masses must be found. These can be obtained by writing the x and Y coordinates of the centres of masses and taking the first derivative. This yields, for centres G_3 and G_4, the following velocities.

$$V_{G3} = \left[\ell_2^2 \dot{\theta}_2^2 + \ell_{G3}^2 \dot{\theta}_3^2 + 2\ell_{G3} \cdot \ell_2 \cos(\theta_2 - \theta_3 - \nu_3) \dot{\theta}_3 \dot{\theta}_3 \right]^{\frac{1}{2}} .$$

$$V_{G4} = \left[\dot{u}^2 + \ell_{G4}^2 \dot{\theta}_4^2 - 2\ell_{G4} \cdot \sin\theta_4 \cdot \dot{\theta}_4 \cdot \dot{u} \right]^{\frac{1}{2}} . \qquad (2.8)$$

Hence the total kinetic energy of the mechanism may be expressed as

$$T = \frac{1}{2} I_A \cdot \dot{\theta}_2^2 + \frac{1}{2} I_{G3} \cdot \dot{\theta}_3^2 + \frac{1}{2} I_{G4} \cdot \dot{\theta}_4^2 + \frac{1}{2} m_5 \dot{u}^2 + \frac{1}{2} m_3 V_{G3}^2 + \frac{1}{2} m_4 V_{G4}^2 . \qquad (2.9)$$

Finally, in order that equation (2.5) may be expanded and written for this linkage the coordinates of the points of application of the external forces must be known. These are

$$x_p = \ell_2 \cos(\theta_2 + \alpha_1) + d_1 \cos(\theta_3 + \alpha_3 + \alpha_1)$$

$$y_p = \ell_2 \sin(\theta_2 + \alpha_1) + d_1 \sin(\theta_3 + \alpha_3 + \alpha_1) \qquad (2.10)$$

and

$$X_D = \ell_1 \cos\alpha_1 + u \cos(\alpha + \alpha_1)$$

$$Y_D = \ell_1 \sin\alpha_1 + u \sin(\alpha + \alpha_1)$$

Assuming ideal pin joints, gravitational forces and no frictional forces apart from a viscous force acting on the slider with a damping coefficient of μ the equations of motion may be written for the following two cases.

2. 2. 1 Constant Speed Input.

Assume a constant crank angular speed, ω, i.e.,

$$\theta_2 = \omega t$$

This is considered as a further constraint equation in addition to equations (2.1) and replaces the need for specifying an expression for the torque T_1. In fact it leads to a Lagrangian multiplier λ_3 which, as will be shown later, is itself the external torque.

Assuming that F_1^x and F_1^y are the values of the force F_1 in the x and y directions the equations of motion may be written as follows :

$$m_3\ell_2\ell_{G3}\cos(\theta_2-\theta_3-\nu_3)\ddot{\theta}_3+m_3\ell_2\ell_{G3}\sin(\theta_2-\theta_3-\nu_3)\cdot\dot{\theta}_3^2$$
$$+\lambda_1\ell_2\sin\theta_2-\lambda_2\ell_2\cos\theta_2-\lambda_3+m_2\, g\,\ell_{G2}\cos(\theta_2+\alpha_1) \qquad (1.11)$$
$$+m_3g\ell_2\cos(\theta_2+\alpha_1)+F_1^x\ell_2\sin(\theta_2+\alpha_1)-F_1^y\ell_2\cos(\theta_2+\alpha_1)=0$$

$$(I_{G3}+m_3\ell_{G3}^2)\ddot{\theta}_3-m_3\ell_2\ell_{G3}\sin(\theta_2-\theta_3-\nu_3)\dot{\theta}_2^2+\lambda_1\ell_3\sin\theta_3$$
$$-\lambda_2\ell_3\cos\theta_3+m_3g\ell_{G3}\cos(\theta_3+\nu_3+\alpha_1)+F_1^x d_1\sin(\theta_3+\alpha_3+\alpha_1)$$
$$-F_1^y\cdot d_1\cdot\cos(\theta_3+\alpha_3+\alpha_1)=0 \qquad (2.12)$$

$$(I_{G4}+m_4\ell_{G4}^2)\ddot{\theta}_4-m_4\ell_{G4}\sin\theta_4\cdot\ddot{u}-\lambda_1\ell_4.\sin(\theta_4+\alpha)$$
$$+\lambda_2\ell_4\cos(\theta_4+\alpha)+m_4g\ell_{G4}\cos(\theta_4+\alpha+\alpha_1)=0 \qquad (2.13)$$

$$(m_4+m_5)\ddot{u}-m_4\ell_{G4}\sin\theta_4.\ddot{\theta}_4-m_4\ell_{G4}\cos\theta_4.\dot{\theta}_4^2+\lambda_1\cos\alpha$$
$$+\lambda_2\sin\alpha+m_5g\cdot\sin(\alpha+\alpha_1)-F_2+\mu_1\dot{u}=0 \qquad (2.14)$$

Equations (2.11) through to (2.14) are second order non-linear differential equations. Together with the following two equations which are obtained by taking the second derivatives of equations (2.1) they may be solved for $\ddot{\theta}_3, \ddot{\theta}_4, \ddot{u}$, λ_1, λ_2, and λ_3.

$$\ell_3 \sin\theta_3 \cdot \ddot{\theta}_3 - \ell_4 \sin(\theta_4+\alpha) \cdot \ddot{\theta}_4 + \ddot{u}\cos\alpha + \ell_2 \cos\theta_2 \cdot \dot{\theta}_2^2 + \ell_3 \cos\theta_3 \cdot \dot{\theta}_3^2 - \ell_4 \cos(\theta_4+\alpha) \cdot \dot{\theta}_4^2 = 0 \cdot \tag{2.15}$$

$$\ell_3 \cos\theta_3 \cdot \ddot{\theta}_3 - \ell_4 \cos(\theta_4+\alpha) \ddot{\theta}_4 - \ddot{u}\sin\alpha - \ell_2 \sin\theta_2 \cdot \dot{\theta}_2^2 - \ell_3 \sin\theta_3 \dot{\theta}_3^2 + \ell_4 \sin(\theta_4+\alpha) \cdot \dot{\theta}_4^2 = 0 \tag{2.16}$$

2. 2. 2 Torque Input

Assume an input torque T_1 acting on the crank. This may be a function of the crank angular position, as in the case of a torsion bar input or a function of the crank angular speed, as in the case of an induction motor. These may be expressed in the forms of

$$T_1 = T_{1_b}(\theta_2) \quad \text{(a)} \qquad \text{and} \quad T_1 = T_{1_m}(\dot{\theta}_2) \quad \text{(b)} \tag{2.17}$$

respectively. It is clear that, in both cases, the

constraints are only the two equations specified in (2.1). By application of equations (2.5) and as before assuming gravitational forces, ideal pin joints and no frictional forces apart from the viscous force acting on the slider, a set of four differential equations may be obtained. Two of these equations are :

$$(I_A+m_3\ell_2^2)\ddot{\theta}_2 + m_3\ell_2\ell_{G3}\cos(\theta_2-\theta_3-\nu_3)\ddot{\theta}_3 + m_3\ell_2\ell_{G3}\sin(\theta_2-\theta_3-\nu_3)\dot{\theta}_3^2$$
$$+ \lambda_1\ell_2\sin\theta_2 - \lambda_2\ell_2\cos\theta_2 - T_1 + m_2g\ell_{G2}\cos(\theta_2+\alpha_1)$$
$$+ m_3g\ell_2\cos(\theta_2+\alpha_1) + F_1^{\dot{x}}\ell_2.\sin(\theta_2+\alpha_1) - F_1^{y}\ell_2\cos(\theta_2+\alpha_1) = 0. \quad (2.18)$$

$$(I_{G3}+m_3\ell_{G3}^2)\ddot{\theta}_3 + m_3\ell_3\ell_{G3}\cos(\theta_2-\theta_3-\nu_3)\ddot{\theta}_2 - m_3\ell_2\ell_{G3}\sin(\theta_2-\theta_3-\nu_3)\dot{\theta}_2^2$$
$$+ \lambda_1.\ell_3\sin\theta_3 - \lambda_2\ell_3\cos\theta_3 + m_3g\ell_{G3}\cos(\theta_3+\nu_3+\alpha_1)$$
$$+ F_1^{x}.d_1.\sin(\theta_3+\alpha_3+\alpha_1) - F_1^{y}.d_1.\cos(\theta_3+\alpha_3+\alpha_1) = 0 \quad (2.19)$$

The remaining two equations are similar to equations (2.13) and (2.14) exactly. As mentioned before the set of four equations may be solved simultaneously with equations obtained from the second derivatives of equations (2.1). In this case these are :

$$\ell_2\sin\theta_2.\ddot{\theta}_2 + \ell_3\sin\theta_3\ddot{\theta}_3 - \ell_4\cos(\theta_4+\alpha)\ddot{\theta}_4 + \ddot{u}\cos\alpha$$
$$+\ell_2\cos\theta_2.\dot{\theta}_2^2 + \ell_3\cos\theta_3\dot{\theta}_3^2 - \ell_4\cos(\theta_4+\alpha)\dot{\theta}_4^2 \doteq 0. \quad (2.20)$$

$$\ell_2 \cos\theta_2 . \ddot{\theta}_2 + \ell_3 \cos\theta_3 . \ddot{\theta}_3 - \ell_4 \cos(\theta_4+\alpha)\ddot{\theta}_4 - \ddot{u} \sin\alpha$$

$$-\ell_2 \sin\theta_2 . \dot{\theta}_2^{\,2} - \ell_3 \sin\theta_3 \dot{\theta}_3^{\,2} + \ell_4 \sin(\theta_4+\alpha)\dot{\theta}_4^{\,2} = 0. \qquad (2.21)$$

2. 3. Associating the Lagrangian Multipliers with Pin Forces and Torques.

In many mechanisms the Newtonian approach to formulating the equations of motion is usually cumbersome and time consuming. However, the Lagrangian formulation is easier and more compact. The Lagrangian multiplier method facilitates the formulation even more but at the expense of dealing with larger numbers of differential equations. The present day numerical methods and computer hard and soft wear make the solution of large number of equations a straightforward matter. The Lagrangian multiplier, unfortunately, does not include the internal forces explicitly but as will be seen later an association between the two is possible. Once this association is accomplished all the remaining internal forces are easily obtainable since the accelerations are available from the solution of the equations of motion.

2. 3. 1 Analysis

The number of lower pairs in a linkage may be expressed in the form :-

$$h = \frac{3(N-1)-n}{2} \qquad (2.22)$$

where N is the number of links and n is the degree of freedom of the linkage. All linkages constitute one or more loops each containing a number of lower pairs. Each loop yields two constraint equations, one along each coordinate of the reference system (planar linkages only).

Now let m be number of loops in a linkage and $f_j(q_1, q_2 \cdots, q_k)$ are the constraint equations where q_k are the generalised coordinates then j = 2m and the equations of motion will contain 2m multipliers. If the linkage inputs are in the forms of constant speeds then the number of constraint equations becomes (2m + ℓ), where ℓ is the number of inputs, and hence (2m + ℓ) multipliers are obtained. Each pair of the 2m multipliers constitute a pin force and the ℓ multipliers constitute the input torques. Therefore, it only remains to associate the λ's with the corresponding lower pairs and input links to get the forces at the joints and the input torques.

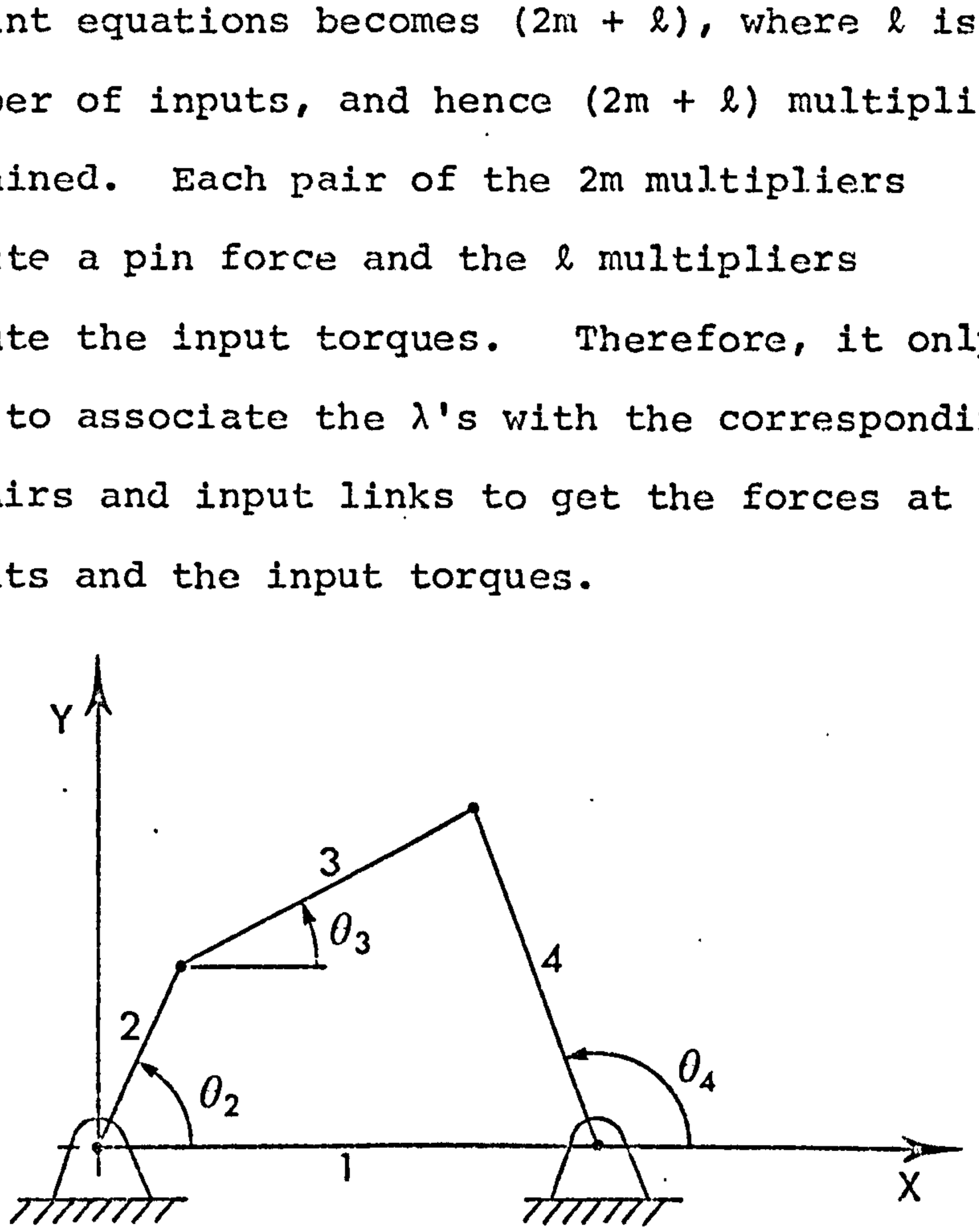

Fig(2·2)

The values of λ_j depend upon the choice of coordinates and direction of looping around the linkage when specifying the coordinates of the constitutive links. As an example the kinetic energy of link 3 in fig. (2.2) may be calculated as a function of $\dot{\theta}_2$ and $\dot{\theta}_3$ or as a function of $\dot{\theta}_4$ and $\dot{\theta}_3$. Both are essentially equivalent but lead to different forms of equations of motion. Therefore it is possible to obtain four different forms of equations of motion by considering the linkage of fig. (2.2) in any of the forms shown in fig. (2.3).

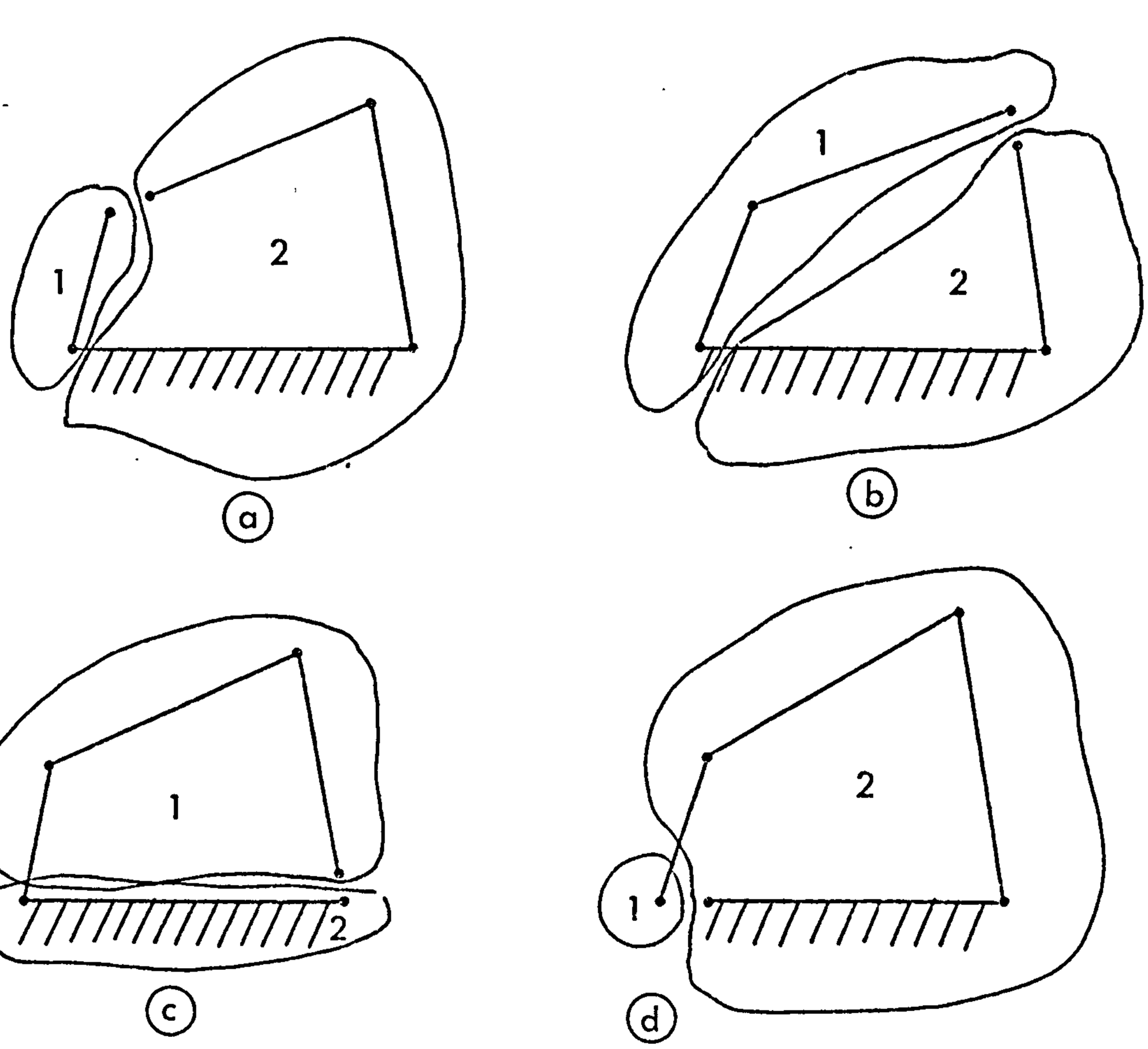

Fig. (2.3) Alternative treatments of system for purposes of analysis.

This means that four sets of values of λ_j are obtainable. Each set corresponds to the pin force at the joint where the linkage is broken. Therefore as an example, system of fig. (2.3.b) leads to values of multipliers λ_1 and λ_2 corresponding to the two components of the pin force at the coupler-rocker joint.

A simple proof of the above argument may be stated as follows. Consider the linkage of fig. (2.2) in two but exactly equivalent configurations as shown in fig. (2.4) where the coupler-rocker joint is replaced by four constraint forces in fig. (2.4.b). These forces formulate the pin force.

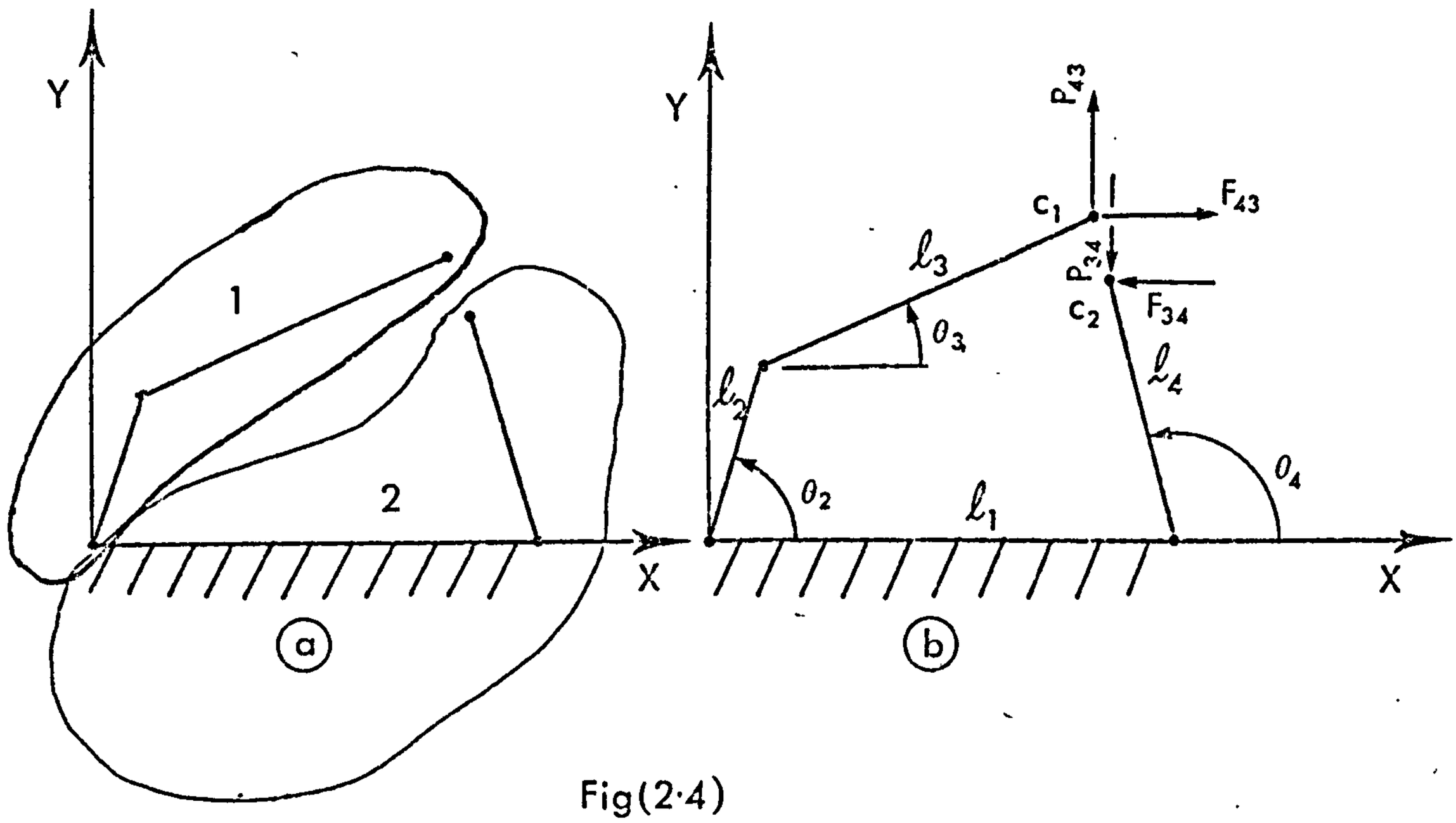

Fig(2·4)

Now let us write the equations of motion using the Lagrangian multiplier method for fig. (2.4.a.) and the basic Euler-Lagrange method for fig. (2.4.b) and assume a constant crank speed input ω which is treated in fig. (2.4.b) as a torque T_2 maintaining this constant speed and in fig. (2.4.a) as an extra constraint equation $\Theta_2 = \omega t$. We obtain

$$\frac{\partial}{\partial t}\frac{\partial T}{\partial \dot{q}_i} - \frac{\partial T}{\partial q_i} = Q_i + \lambda_j \frac{\partial f_j}{\partial q_i} \qquad \lambda\text{- method} \qquad (2.23)$$

$$\frac{\partial}{\partial t}\frac{\partial T}{\partial \dot{q}_i} - \frac{\partial T}{\partial q_i} = Q_i + F_k \frac{\partial r_k}{\partial q_i} + \frac{T_2 \partial \Theta_2}{\partial q_i} \qquad \text{Euler method} \qquad (2.24)$$

where F_k are the four constraint forces in (2.4.b) along r_k their respective coordinates in the positive x, y directions and f_j are the two loop-constraint equations plus the equation $\Theta_2 = \omega t$. Equations (2.23) and (2.24) are similar apart from the last terms. Therefore if

$$\frac{\partial f_j}{\partial q_i} \equiv \frac{\partial r_j}{\partial q_i} \quad \text{for } j = 1, 2 \qquad (2.25)$$

$$\text{and } \frac{\partial f_j}{\partial q_i} \equiv \frac{\partial \Theta_2}{\partial q_i} \quad \text{for } j = 3$$

Then,

$$\lambda_j = F_j \quad \text{for } j = 1, 2$$

$$\text{and} \quad \lambda_j = T_2 \quad \text{for } j = 3 \qquad (2.26)$$

i.e., the multipliers are equal to the internal forces components and the input torque.

The coordinates of forces acting on C_1 are :

$$X_{c_1} = \ell_2 \text{Cos}\Theta_2 + \ell_3 \text{Cos}\Theta_3$$

$$Y_{c_1} = \ell_2 \text{Sin}\Theta_2 + \ell_3 \text{Sin}\Theta_3$$

and of forces on C_2 are :

$$X_{c_2} = - (\ell_1 + \ell_4 \text{Cos}\Theta)_4$$

$$Y_{c_1} = - \ell_4 \text{Sin}\Theta_4$$

Now fig. (2.4.b) has three degrees of freedom because; by releasing the lower pair C two degrees are added. Hence (2.23) yields three equations and similarly (2.24). Thus by expanding $\frac{\partial f_j}{\partial q_i}$ and $\frac{\partial r_j}{\partial q_i}$ we have

$\frac{\partial f_1}{\partial \Theta_2} = -\ell_2 \text{Sin}\Theta_2$ and $\frac{\partial x_{c1}}{\partial \Theta_2} = - \ell_2 \text{Sin}\Theta_2$.
$\frac{\partial f_2}{\partial \Theta_2} = \ell_2 \text{Cos}\Theta_2$ and $\frac{\partial y_{c1}}{\partial \Theta_2} = \ell_2 \text{Cos}\Theta_2$
$\frac{\partial f_3}{\partial \Theta_2} = 1$ $\frac{\partial \Theta_2}{\partial \Theta_2} = 1$

} Last terms in 1st equation of motion.

$\frac{\partial f_1}{\partial \Theta_3} = -\ell_3 \text{Sin}\Theta_3$ and $\frac{\partial x_{c1}}{\partial \Theta_3} = -\ell_3 \text{Sin}\Theta_3$
$\frac{\partial f_2}{\partial \Theta_3} = \ell_3 \text{Cos}\Theta_3$ and $\frac{\partial x_{c1}}{\partial \Theta_3} = \ell_3 \text{Cos}\Theta_3$
$\frac{\partial f_3}{\partial \Theta_3} = 0$ $\frac{\partial f_3}{\partial \Theta_3} = 0$

} Last terms in 2nd equation of motion.

$\frac{\partial f_1}{\partial \theta_4} = \ell_4 \, \mathrm{Sin}\theta_4$ and $\frac{\partial x_{c2}}{\partial \theta_4} = \ell_4 \, \mathrm{Sin}\theta_4$)

$\frac{\partial f_2}{\partial \theta_4} = -\ell_4 \, \mathrm{Cos}\theta_4$ and $\frac{\partial y_{c2}}{\partial \theta_4} = -\ell_4 \, \mathrm{Cos}\theta_4$) Last terms in 3rd equation of motion.

$\frac{\partial f_3}{\partial \theta_4} = 0$ $\qquad$ $\frac{\partial f_3}{\partial \theta_4} = 0.$

i.e., equation (2.25) is true and therefore

$\lambda_1 = F_{43}$, $\lambda_2 = P_{43}$ and $\lambda_3 = T_2$.

Since the accelerations, velocities and positions are given from the solution, the remaining pin forces at A, B and D may be easily obtained.

2. 4 METHODS OF SOLUTION

The equations of motion stated earlier are highly non-linear second order differential equations. A straightforward generalised analytic solution is an impossible task with present day mathematical methods. An attempt to linearise the equations in the variable u is possible bearing in mind that the coefficients of the then obtained equation will be the results of the solution of the four-bar linkage with no movable pivot; this can only be obtained using a computer. Therefore, even if the equations have been linearised a solution can only be obtained for a particular case. However, in some cases, as will be seen later in chapters IV and V, if further simplifying assumptions are made a

linearised equation with periodic coefficients, which can be evaluated by straightforward analytic algebraic methods, may be obtained.

Consequently, a near exact solution can only be obtained using either an analogue or digital computer. The analogue, once set up, is quick and efficient; however, the setting up stage can be complex and time consuming. On the other hand, the digital computer is more flexible, easily set up and possesses time sharing characteristics; this is compared with the analogue which can be used by one researcher only at one time. Owing to the above and the availability of a time sharing digital computer installation, the IBM 360/67, it was decided upon a digital solution.

The accuracy and efficiency of a numerical solution depend on the method of integration adopted. The most widely used methods of integration are the Runge-kutta methods, the series methods and the predicted-corrector methods. Each has its own advantages and disadvantages and the choice depends on the nature and complexity of the equations.

The equations of motion derived earlier can be expressed in a form equivalent to (see 3.1)

$$\dot{Z} = \Phi(t, Z) \qquad (2.27)$$

where Z represents the unknowns of the equations θ_2, θ_3, θ_4 and u and $\dot{Z}$ the derivatives. The Runge-kutta methods are one step methods, i.e. to

evaluate Z at time t+δt we only require the information available at point Z at time t. Secondly, they do not require the evaluation of the derivative of the function to be integrated. This makes them suitable for digital computer applications, especially in cases where the derivative is not easily obtained. Their serious drawbacks are, firstly, the lack of simple means of estimating the errors; this makes them highly susceptible to numerical instabilities and, secondly, the large number of evaluation of the function Φ; four times for each step in a fourth order method. The second of these drawbacks makes them unfavourable for use with our Lagrangian multiplier formulation of the equations of the motion because of the large number of equations and hence the lengthy time involved in computation of the function Φ.

Series methods such as Taylor Series and Picard's method are the most straightforward methods. However, they involve tedious work in finding the derivatives of the function Φ. For example, to obtain a solution equivalent to a fourth order Runge-kutta method we need to evaluate the fourth derivative of the function Φ. A simple look at the equations of motion stated earlier shows immediately the impracticability of these methods in this case.

Lastly, there are the predictor-corrector methods. They provide an easy estimate of the errors, inherent, roundoff or truncation, from the information already calculated. These errors are in all cases convergent and thus the methods are highly stable. One of their most attractive qualities is that they require only two evaluations of the function Φ per step of integration. Their only relative drawback is that since they use information about prior points they are not self-starting. This drawback is easily solved by employing a Runge-kutta method to start them. Owing to these above qualities they are the most suitable for use with this type of formulation of equations of motion.

The Hamming fourth order modified predictor-corrector is the method chosen here but in some cases where simulation is performed using the IBM Continuous system modelling program (CSMP) the Milne method is employed. The only reason for choosing the Milne, which is incidentally a predictor-corrector, is its availability for use in the IBM subroutine package. The various steps involved in application of the Hamming's methods are as follows:-

1. A predicted value for Z in (2.27) is obtained using the formula

$$z^{p}_{j+1} = z_{j-3} + 4\frac{h}{3}\left\{2\dot{z}_{j} - \dot{z}_{j-1} + 2\dot{z}_{j-2}\right\} \qquad (2.28)$$

where h represents the time step, j the number of integration step and $\dot{Z}_j$, $\dot{Z}_{j-1}$ and $\dot{Z}_{j-2}$ are the function Φ at the current point and the previous two points respectively.

2. A modified value of this predicted point is obtained using the predicted and corrected values of the current point, i.e.,

$$Z^{m}_{j+1} = Z^{p}_{j+1} - \frac{112}{121}\left\{Z^{p}_{j} - Z^{c}_{j}\right\} \qquad (2.29)$$

where letters m, p and c above Z indicate modified, predicted and corrected values respectively.

3. The corrected point is obtained using the derivatives and values of the modified point, the current and previous points as follows :

$$\dot{Z}^{c}_{j+1} = \frac{1}{8}\left[9\,Z_{j} - Z_{j-2} + 3h\left\{\dot{Z}^{m}_{j+1} + 2\,\dot{Z}_{j} - \dot{Z}_{j-1}\right\}\right] \qquad (2.30)$$

4. The final values Z_{j+1} is obtained using the above predicted and corrected points, thus

$$Z_{j+1} = Z^{c}_{j+1} + \frac{9}{121}\left\{Z^{p}_{j+1} - Z^{c}_{j+1}\right\} \qquad (2.31)$$

This above method is used on the equations of motion formulated in the form of equation (2.27). The method of transformation to this form is discussed in the next chapter.

CHAPTER III

DIGITAL COMPUTER SOLUTION OF EQUATIONS OF MOTION

It was stated earlier that an analytic solution cannot be found owing to the gross non-linearities of the equations. It was also decided that a digital solution would be performed. Hamming's integration method was also chosen to find the solution. It only remains therefore, to put the equations into a form to which the integration can be applied directly.

Solutions for both the cases of forced and free motion will be considered. It will also be assumed that the slider will either be free or constrained by viscous friction and/or linear spring.

3. 1 The Formulation of Equations of Motion for Digital Solution.

It is desired that the equations of motion be transformed into a form similar to that of equation (2.27). In order to make this possible we must isolate each of the second order quantities $\ddot{\theta}_2$, $\ddot{\theta}_3$, $\ddot{\theta}_4$ and $\ddot{u}$ and express them in terms of velocities, positions and other already known or calculated quantities.

The equations of motion may be written in the form

$$A_{ij}\, W_j = B_i \qquad (3.1)$$

Where W_j ; j = 1,2, ... 6 is the column vector $(\lambda_3, \ddot{\theta}_3, \ddot{\theta}_4, \ddot{u}, \lambda_1\ \lambda_2)$ for the constant speed input case or $(\ddot{\theta}_2, \ddot{\theta}_3, \ddot{\theta}_4, \ddot{u}, \lambda_1, \lambda_2)$ for the known torque input case, matrix A_{ij}; i = 1, 2, ... 6, j = 1, 2, ... 6 is the square matrix of coefficients and B_i is the remaining terms independent of W_j.

If A_{ij} is non singular, equation (3.1) may be written in the form

$$W_j = C_{ji} \cdot B_i \tag{3.2}$$

where

$$C_{ji} = A_{ij}^{-1}$$

Two relations may now be obtained from this equation, these are

$$\ddot{z}_k = C_{ki} \cdot B_i \tag{3.3}$$

and

$$\lambda_m = C_{mi} \cdot B_i \tag{3.4}$$

Where k=1,2, ...3, m=1,2,....3 for a constant speed input or k=1,2,....4, m=1,2 for a torque input and i=1,2,.....6. $\ddot{z}_k$ represents the second order derivatives and λ_m the Langrangian multipliers.

Equation (3.3) may be written in the form

$$\ddot{z}_k = \phi_1(t, \dot{z}_k) \tag{3.5}$$

and integrated giving

$$\dot{z}_k = \phi_2(t, z_k) \tag{3.6}$$

Where $\ddot{z}_k$ is calculated using the values of z_k and $\dot{z}_k$ obtained from the previous integration step. Equations (3.5) and (3.6) are in the form of equation (2.27) and hence numerical integration can be applied directly.

Equation (3.1) is solved by using the Gaussian direct elimination method with provisions for row and column interchanges and error bounds corrections. The error corrections are made as follows :
The values of W_j obtained from (3.2) are substituted in (3.1) and $B_i^{(o)} = A_{ij}$. W_j is calculated. If round off errors are small; i.e.

$$\text{if } \left| B_i - B_i^{(o)} \right| \leq \varepsilon \,, \tag{3.7}$$

where ε is small positive error constant, then we proceed with the integration. If this condition is not satisfied then

$$A_{ij} \cdot \delta_j^{(o)} = (B_i - B_i^{(o)})$$

is solved. The values of $\delta_j^{(o)}$ are added to the already found values for W_j. These are in turn substituted in equation (3.1) and the process is repeated until equation (3.7) is satisfied.

The preceding analysis allows for integration of all the second order derivatives $\ddot{\theta}_2, \ddot{\theta}_3, \ddot{\theta}_4$ and $\ddot{u}$. This means that the kinematic equations described in equation (2.1) and (2.4) need only be solved once in order to find the initial conditions. Contrasting with this approach is that in which the second order derivatives of θ_2 and u are calculated once and are integrated to give $\dot{\theta}_2$ and $\dot{u}$. The remaining first order derivatives may be obtained from the solution of equation (2.4). $\dot{\theta}_2$ and $\dot{u}$ are then integrated giving θ_2 and u which when used in equation (2.1) give the remaining angular positions. It is clearly seen that this latter approach requires the solution of the

kinematics at every time step in contrast with the first which requires it only at the initial point. The first approach may be useful especially when dealing with mechanisms having complex kinematic equations. It also has the further advantage that it gives a complete solution carried out wholly by the computer and at no stage is there any tedious work involved on the part of the designer. In contrast with this the kinematic solution must either be performed by elimination or iteration. The first of these is manual and can be lengthy and time consuming in complex mechanisms;the second can be computationally difficult.

It is strongly recommended, albeit, unmentioned in all literature, that the first approach be used at first hand no matter how simple or complex the mechanism may be. The accuracy or even the debugging of the integration procedure may then be examined by simple checks on loop closure. It is important to recognise that a loop closure check is meaningful other than for trivial arithmetical checks, only if used in conjunction with the first approach. This is so, because the second approach integrates only the derivatives of the generalised coordinates determining the degree of freedom of the system. The remaining ones are obtained from the kinematics thus large errors may be involved in the numerical integrations yet they are not realised by the designer because the kinematics are used to force the closure of the mechanism and hence no simple check is available to indicate whether

the solution is accurate. On the other hand the first approach is wholly dependent on the results of the integration thus if the designer obtains large erros in loop closure checks he can immediately recognise that the integration needs further refinement.

Based on the above arguments our policy in the coming solutions will be to integrate all the second order derivatives and make sure that the errors in loop closure are within acceptable bounds, then due to the relatively simple kinematic solution of our mechanism, the second approach of integration will be adopted. This will ensure that the integration method is reliable and leads to accurate results.

3.2 Forced Motion

3.2.1 Constant Speed Input

Consider the mechanism shown in Fig. (3.1) and assume that the crank rotates at a constant angular speed ω and its centre of gravity lies on pin joint A. Also assume that the force opposing the motion of the slider consists of a viscous force of coefficient μ and a spring force of coefficient K. By assuming the linkage to be in the vertical plane the equations of motion may be written in the form of equation (3.1) where A_{ij} is the square matrix.

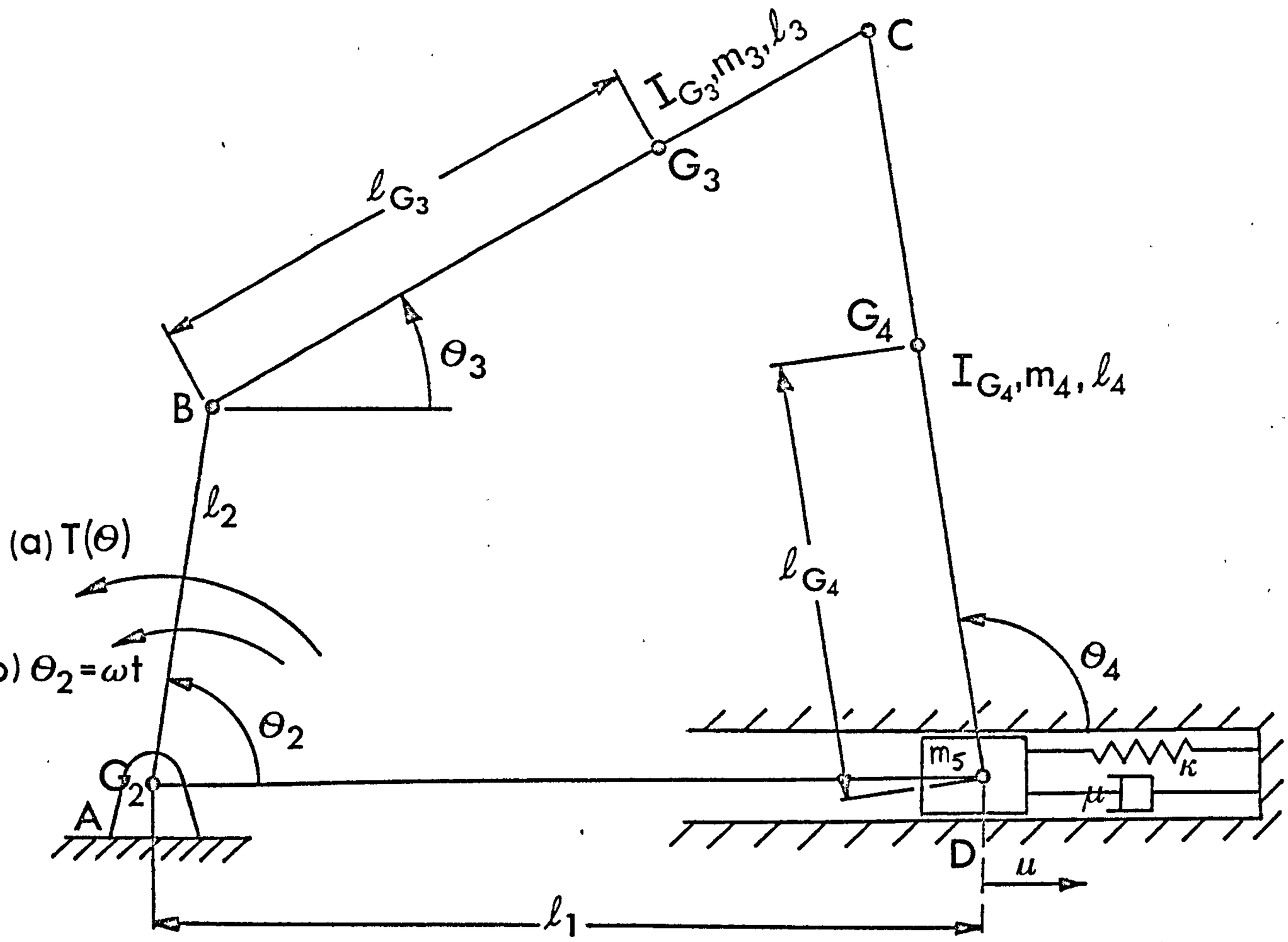

Fig (3·1) PLANAR LINKAGE A,B,C,D

$$\begin{bmatrix}
-1 & -\ell_2 \cos\theta_2 & \ell_2 \sin\theta_2 & 0 & 0 & m_3\ell_2\ell_{G3}\cos(\theta_2-\theta_3) \\
0 & -\ell_3 \cos\theta_3 & \ell_3 \sin\theta_3 & 0 & 0 & I_{G3}+m_3\ell_{G3}^2 \\
0 & \ell_4 \cos\theta_4 & -\ell_4 \sin\theta_4 & -m_4\ell_{G4}\sin\theta_4 & I_{G4}+m\ell_{G4} & 0 \\
0 & 0 & 1 & m_4 + m_5 & -m_4\ell_{G4}\sin\theta_4 & \\
0 & 0 & 0 & 1 & -\ell_4 \sin\theta_4 & \ell_3 \sin\theta_3 \\
0 & 0 & 0 & 0 & -\ell_4 \cos\theta_4 & \ell_3 \cos\theta_3
\end{bmatrix} \tag{3.8}$$

W_j is the column vector

$$W_j = (\lambda_3, \lambda_2, \lambda_1, \ddot{u}, \ddot{\theta}_4, \ddot{\theta}_3) \tag{3.9}$$

where λ_1 and λ_2 are the pin forces along the x and y directions at joint c in Fig. (3.1) and λ_3 is the input torque required to maintain constant speed input.

The matrix B_i is the column vector

$$\begin{bmatrix}
-m_3 g\ell_2 \cos\theta_2 - m_3\ell_2\ell_{G3}\sin(\theta_2-\theta_3)\dot{\theta}_3^2 \\
-m_3 g\ell_{G3}\cos\theta_3 + m_3\ell_2\ell_{G3}\sin(\theta_2-\theta_3)\dot{\theta}_2^2 \\
-m_4 g\ell_{G4}\cos\theta_4 \\
-\mu.\dot{u} - k_2 u + m_4\ell_{G4}\cos\theta_4\dot{\theta}_4^2 \\
-\ell_2 \cos\theta_2.\dot{\theta}_2^2 - \ell_3\cos\theta_3\dot{\theta}_3^2 + \ell_4\cos\theta_4.\dot{\theta}_4^2 \\
\ell_2\sin\theta_2\dot{\theta}_2^2 + \ell_3\sin\theta_3\dot{\theta}_3^2 - \ell_4\sin\theta_4\dot{\theta}_4^2
\end{bmatrix} \tag{3.10}$$

a) Assume the spring stiffness K = 0

Fig. (3.2) shows the motion of the slider versus the crank angle θ_2 for values of the viscous

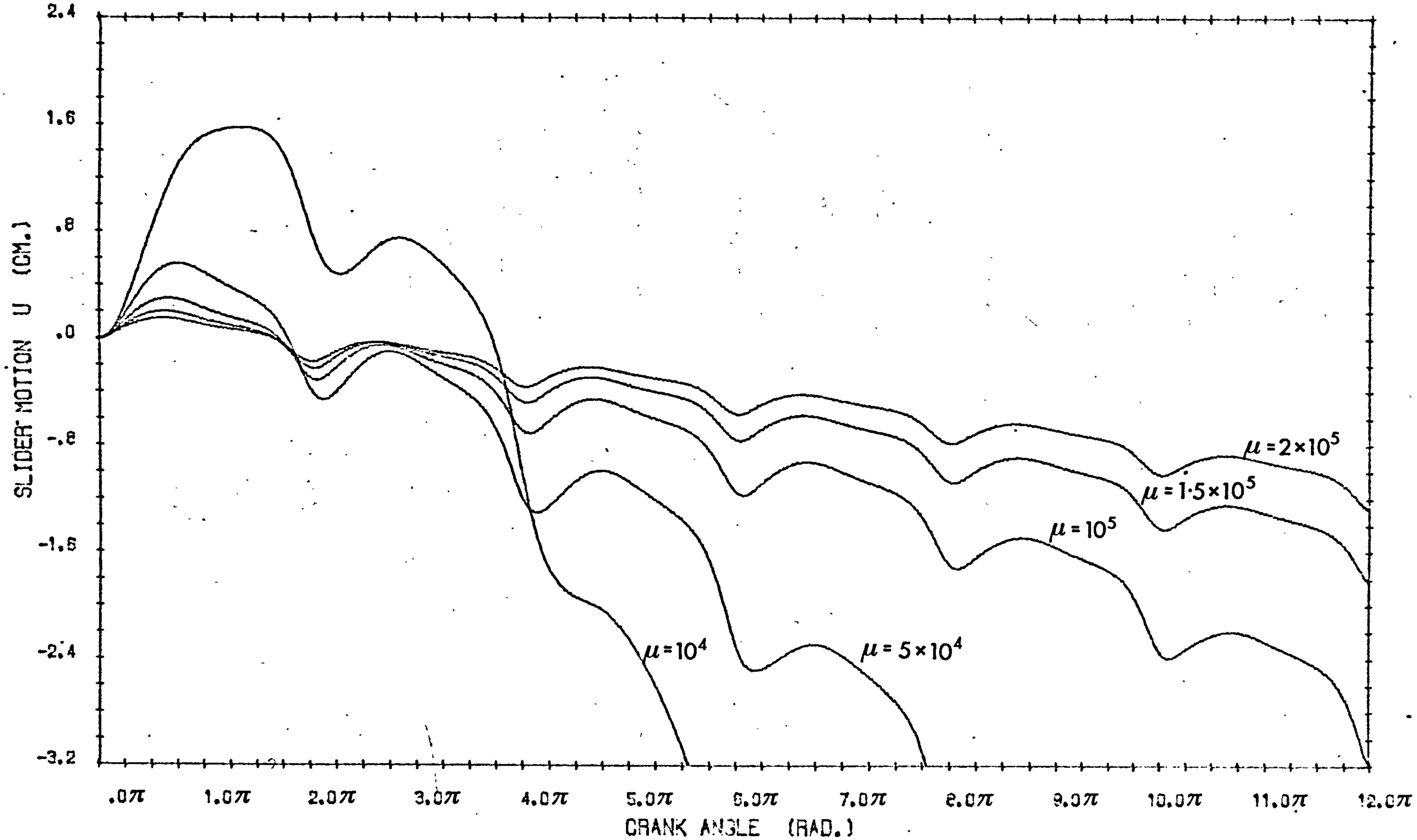

FIG. (3·2). THE MOTION OF THE SLIDER VERSUS THE CRANK ANGLE θ_2 . (SPRING STIFF. κ=0.0)

coefficient $\mu = 10^4$, 5×10^4, 10^5, 5×10^5 and 10^6 dyne. sec/cm. The constant input speed ω = 420 RPM and the input data of the linkage is as shown in the following table:

length (cm)	ℓ_1	ℓ_2	ℓ_3	ℓ_4	ℓ_{G3}	ℓ_{G4}
	15.35	5	15	15	9.82	7.5
mass (gms)	m_3	m_4	m_5			
	209	206	590			
inertia ($gm.cm^2$.)	I_{G3}	I_{G4}	I_{G2}			
	5250	3863	12500			
Initial conditions	θ_2=0., $\dot{u}$=0,	u=0				

Gravitational Constant g = 981. $cm/sec.^2$

Table (3.1)

The figure shows that the response consists of two distinct regions. The first of these is a transient region of duration approximately two cycles. The second consists of a steady periodic motion superimposed upon a drift. The drift is linear with crank angle and may be described by the equation

$$U = M.\theta_2 + U_o \qquad (3.9)$$

where M and U_o are constants depending on μ. This indicates that for a small viscous force the linkage tends to collapse quickly into a collinear configuration. However, as the viscous force is increased this tendency is counteracted. The effects of the gravitational constant equated to zero on the response curves is shown

in fig. (3.3). It is clear from this figure that because the gravitational forces are eliminated the value of M in equation (3.9) is slightly reduced.

b) Assume a constant viscous coefficient $\mu = 3 \times 10^4$.

Fig. (3.4) shows the motion of the slider versus the crank angle θ_2 for values of the spring stiffness coefficient $k = 5 \times 10^5$, 10^6 and 2×10^6 dyne/cm. The input data is as shown in table (3.1) and the input speed is 420 rpm. The figure shows that due to the initial condition assumptions that u and $\dot{u} = 0$ a transient effect is shown over the first cycle. The steady state motion is periodic and oscillates about a mean position between the initial position of the slider and the crank shaft. This mean position shifts towards the slider initial position as the spring stiffness is increased. The minimum value of the oscillation for the case of $k = 5 \times 10^5$ dyne/cm occurs at crank angle $\theta_2 = 22^o$. However, as k is increased this minimum oscillation occurs at smaller crank angle and eventually occurs at zero degrees for $k = 2 \times 10^6$ dyne/cm. The rate of change of the slider position is approximately the same for all the response curves between the minimum and maximum values. However, as the spring stiffness is increased the spring force becomes dominant and the width of the response curve is decreased. Eventually, although not shown on this figure, as k increases further the slope of the response curve takes a constant value between the maximum and minimum values of the oscillation on the portions of the curve below the zero degree crank angle positions.

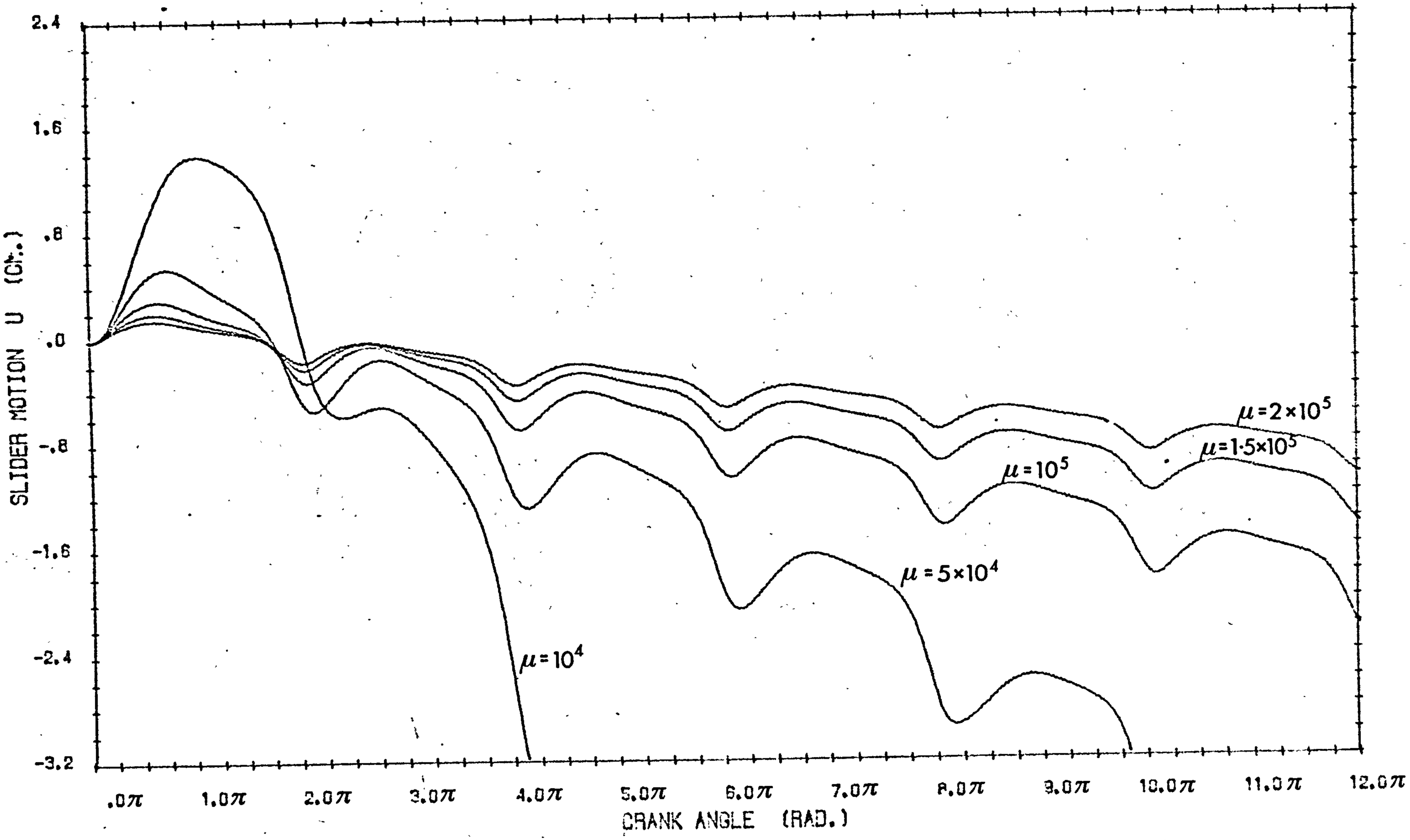

FIG. (3-3). THE MOTION OF THE SLIDER VERSUS THE CRANK ANGLE θ_2 . (SPRING STIFF. κ=0.0)
GRAVITATIONAL CONSTANT G=0.)

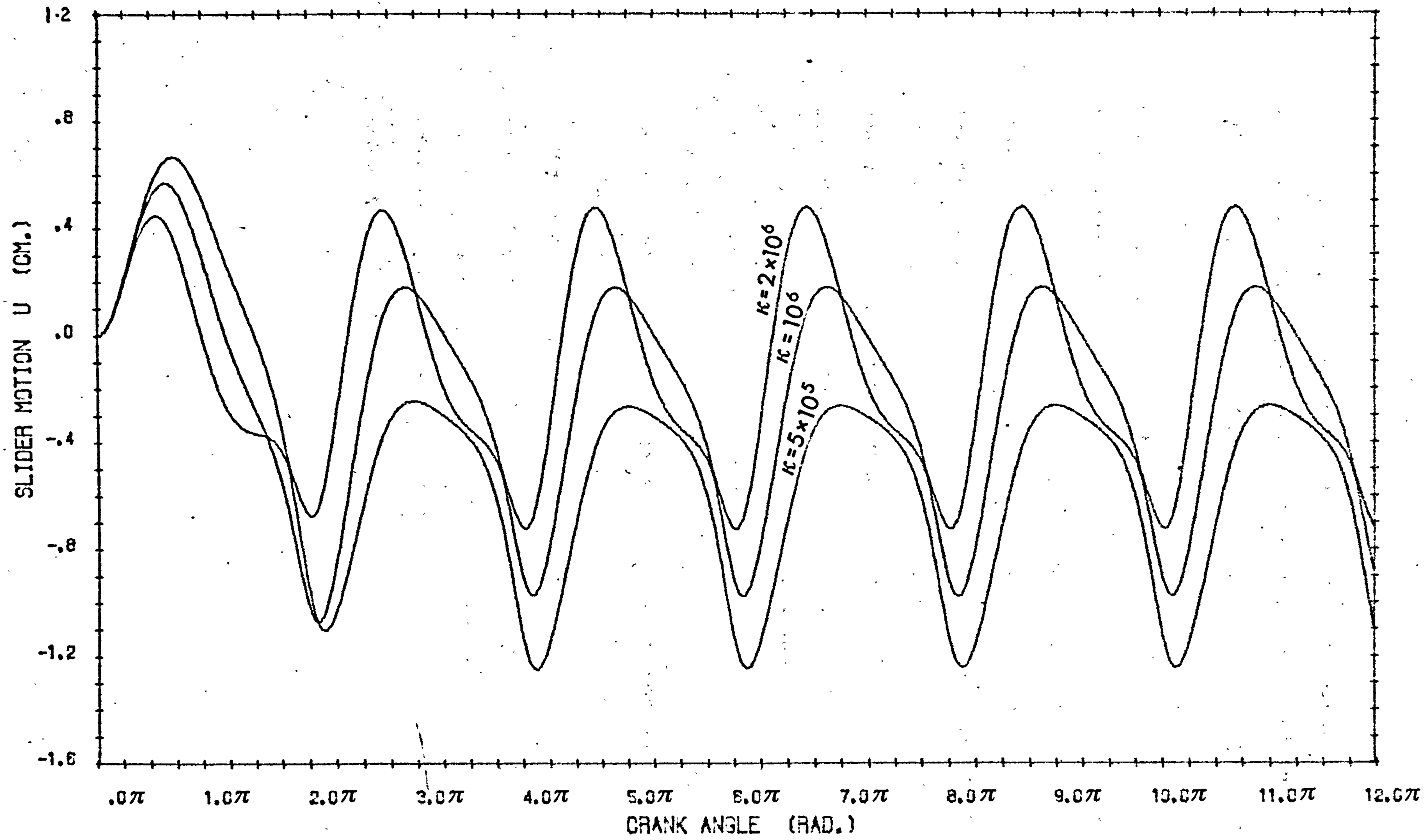

FIG. (3·4). THE MOTION OF THE SLIDER VERSUS THE CRANK ANGLE θ_2. (VISCOS COEF. μ=3.E 04)

Fig. (3.5) shows the input torque required to be applied to the crank to maintain constant speed input of 420 rpm. The striking feature of the figure is the sudden reversal in torque in the region of $\theta_2 = 0^o$. The other feature is that on the scale of the graph this torque is independent of the spring stiffness k. The exception is at the maximum and minimum values where a slight variation is recorded. These variations are due to the differences in the slider accelerations at these instances. The independence of the torque of the stiffness k may be explained by the fact that the spring presents no external load on the mechanism. The only effect results from the slight change in the geometry which leads to changes in inertial loads. The energy dissipation in the slider guide due to viscous friction also accounts for variations in torque. However, the overall conclusion is that the only appreciable difference in the torque requirements for different springs for this particular mechanism occurs only at the instances when appreciable differences in the slider accelerations leading to different inertial loads are present.

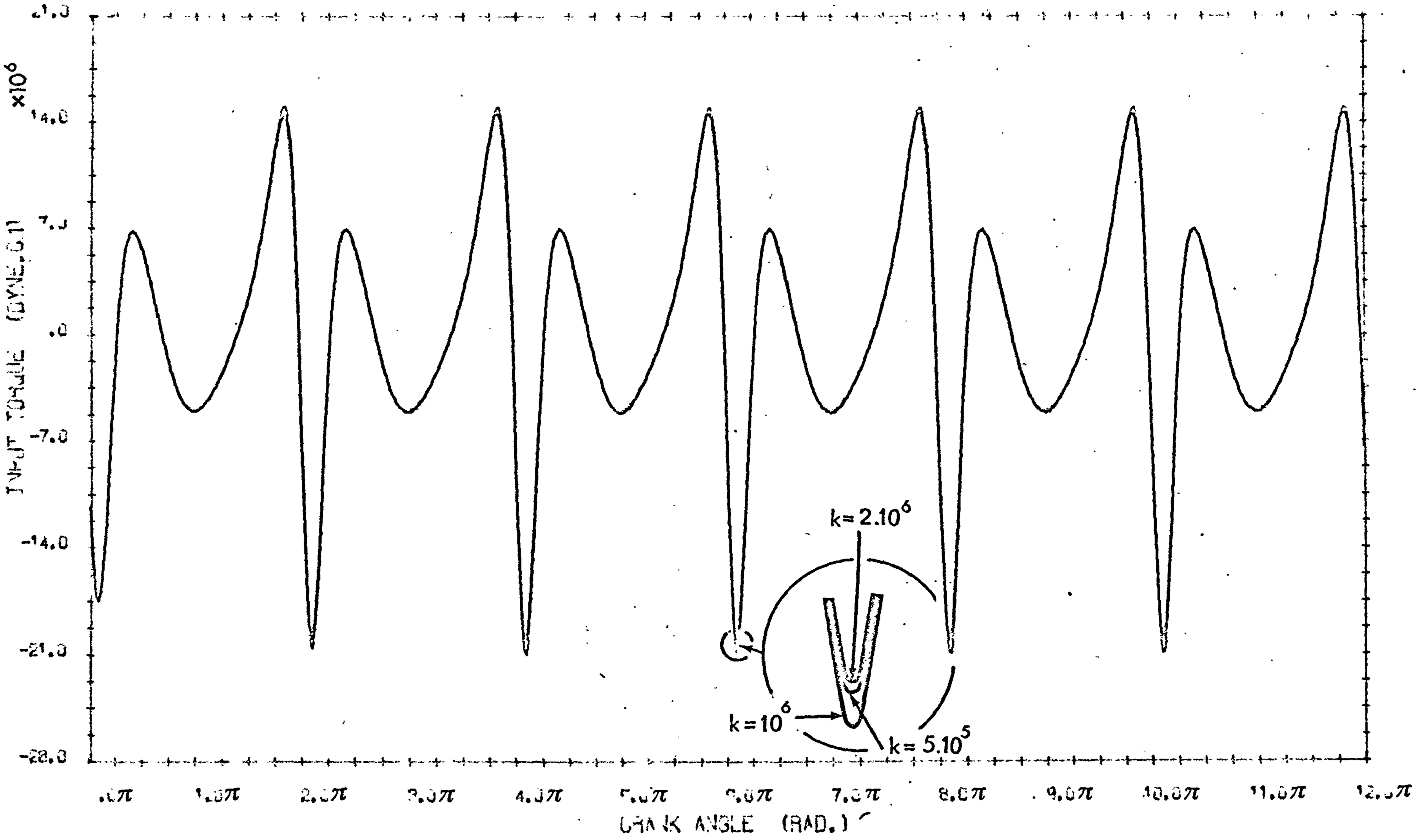

FIG. (3·5) . THE INPUT TORQUE REQUIRED TO MAINTAIN CONSTANT INPUT SPEED VERSUS THE CRANK ANGLE θ2 (μ = , k=5.10⁵,10⁶,2.10⁶)

3.2.2 Torque Input

There are only two constraint equations for the input torque case. These equations define the loop closure of the linkage along the x and y direction. Therefore only two Lagrangian multipliers exist for this case as opposed to three in the previous case. These multipliers are λ_1 and λ_2 representing the pin forces along the x and y directions in pin joint C of fig. (3.1).

The torque input

$$T = T_o(1-\theta_2) \quad \text{if} \quad \theta_2 \leq \theta_2$$

and $T = 0$ thereafter

is applied to the crank, where T_o is the initial value of the torque and θ_2 is a pre-given constant value of crank angle θ_2. Assuming the centre of gravity of the crank lies on the crank shaft A the equation of motion (3.1) can be expressed in the following terms. The matrix A_{ij} is as given in equation (3.8) except for the following elements.

$$A_{11} = I_{2A} + m_3 \ell_2^2 .$$

$$A_{21} = m_3 \ell_2 \ell_{G3} \cos(\theta_2 - \theta_3).$$

$$A_{51} = \ell_2 \sin\theta_2.$$

$$A_{61} = \ell_2 \cos\theta_2.$$

Where I_{2A} is the crank inertia about the crank shaft A.

The column vecror W_j is given by

$$W_j = (\ddot{\theta}_2, \lambda_2, \lambda_1, \ddot{u}, \ddot{\theta}_4, \ddot{\theta}_3).$$

And the matrix B_i is as given in equation (3.10) except for the following element.

$$B_1 = -m_3.g.\ell_2 \cos\theta_2 - m_3\ell_2\ell_{G3} \sin(\theta_2-\theta_3)\dot{\theta}_3^2 + T_o(1-\theta_2).$$

The crank speed and the slider response are both investigated varying

(1) the input torque T_o and keeping the spring stiffness k and viscous coefficient μ constants, and

(2) varying the stiffness k and keeping the input torque T_o and viscous coefficient μ constants.

In both cases the torque is assumed to act during the first 57.3 degrees (1 rad.) rotation of the crank. The kinematic and dynamic input data and the initial conditions are as shown in table (3.1).

Fig. (3.6) shows the crank speed plotted against time for values of initial torque $T_o = 10^7$, 10^8 and 2×10^8 dyne·cm. The torque T becomes zero, when the points $\theta_2 = 1$ rad. marked on the curves are reached. It is clear from the figure that during the time in which the torque T is acting the crank speed behaves in a linear manner up to the stage when the input torque becomes less than the torque sufficient to accelerate the mechanism. This stage occurs when the points p_1 and p_2 are reached. A plot of the initial torque T_o against the time taken to reach $\theta_2 = 1$ rad. is shown in Fig. (3.7). It shows a hyperbolic relationship between T_o and τ asymptotic to $T_o = o$ and $\tau = o$. The behaviour of the crank speed beyond $\theta_2 = 1$ rad. in Fig. (3.6) is governed by the free motion equations of motion. However, it is

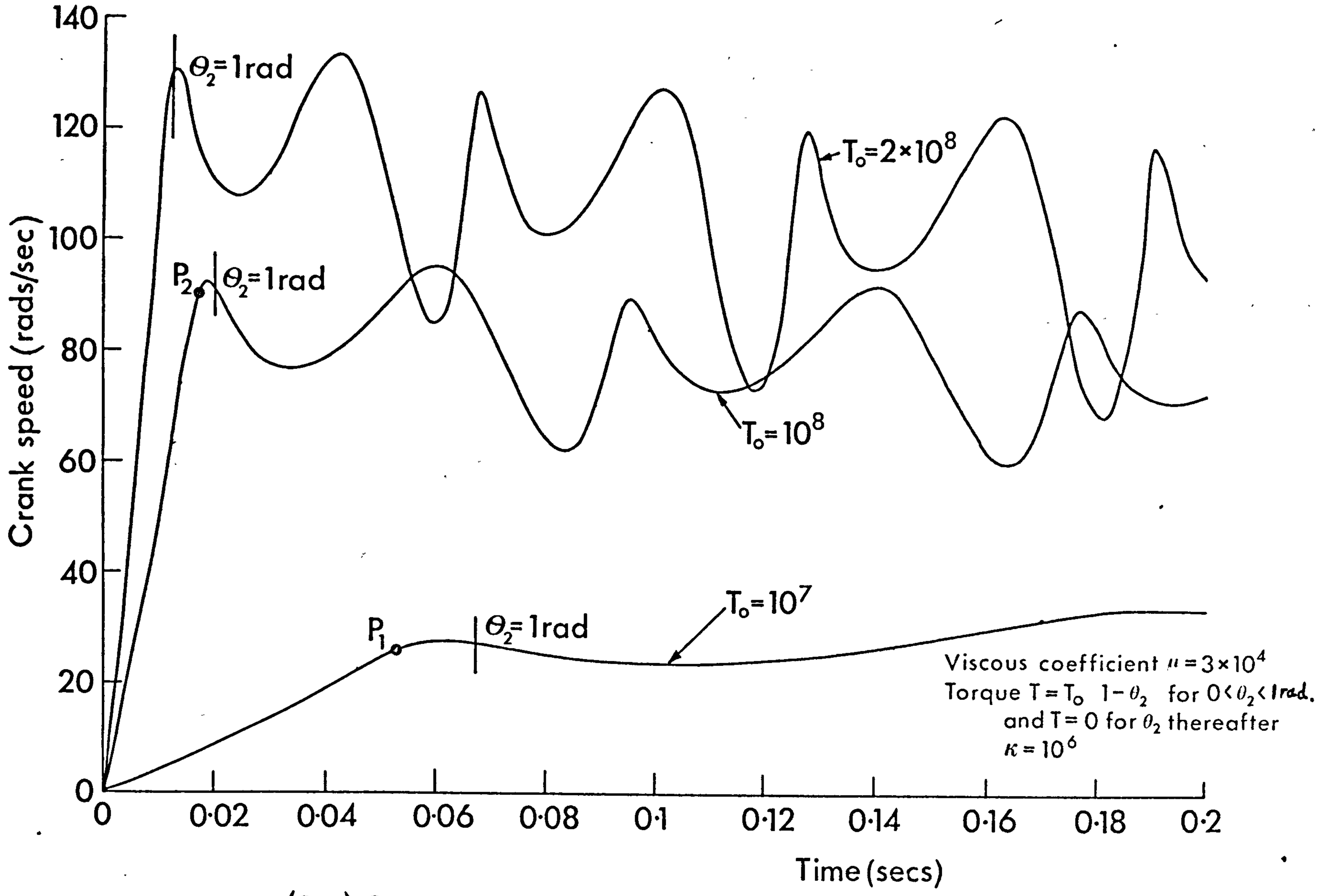

Fig(3·6) CRANK SPEED RESPONSE

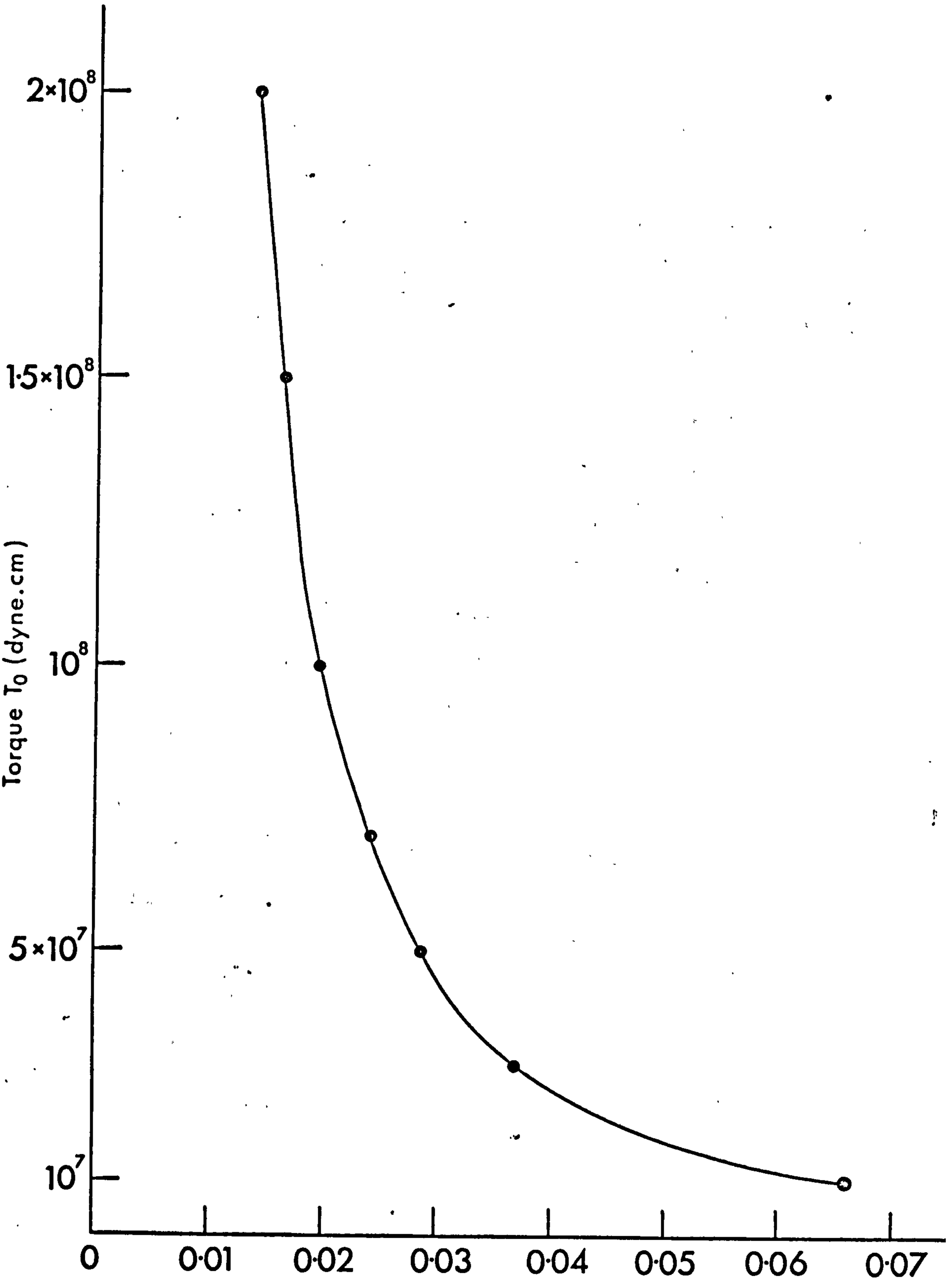

Fig(3·7) INITIAL TORQUE T_0 VERSUS TIME TAKEN TO REACH CRANK ANGLE $\theta_2 = 1$rad

oscillatory and decaying. The decaying aspect is due to the energy dissipation in the slider guide and will be studied in the next section.

Fig. (3.8) shows the slider response corresponding to the inputs of Fig. (3.6). As would be expected the response for $T_o = 2 \times 10^8$ takes longer before it settles and then starts a steady state decay. The three responses show the slider oscillates between its initial position and the crank shaft and as would be expected the shift from its initial position is greatest in the highest input torque case.

Fig. (3.9) shows the crank speed versus time curves for spring stiffness values of 5×10^5, 10^6 and 2×10^6 dyne/cm. The value of the initial torque T_o is 10^8 dyne. cm. The figure shows the crank speed increasing linearly up to the point when the torque input becomes smaller than the torque required to accelerate the mechanism. The speed fluctuates when the torque is removed and then decays due to the viscous dissipation of energy in the slider guide. Because the speed response is the same throughout the time region in which the torque acts, it suggests similar loads and movement of slider. The latter is verified in Fig. (3.10) in which the slider response is shown. Fig. (3.10) also shows that as the torque is removed a transient free motion response prevails after which occurs a free motion steady state decay which is studied in the next section. The duration of the transient free motion stage depends on the stiffness k and the initial input torque values.

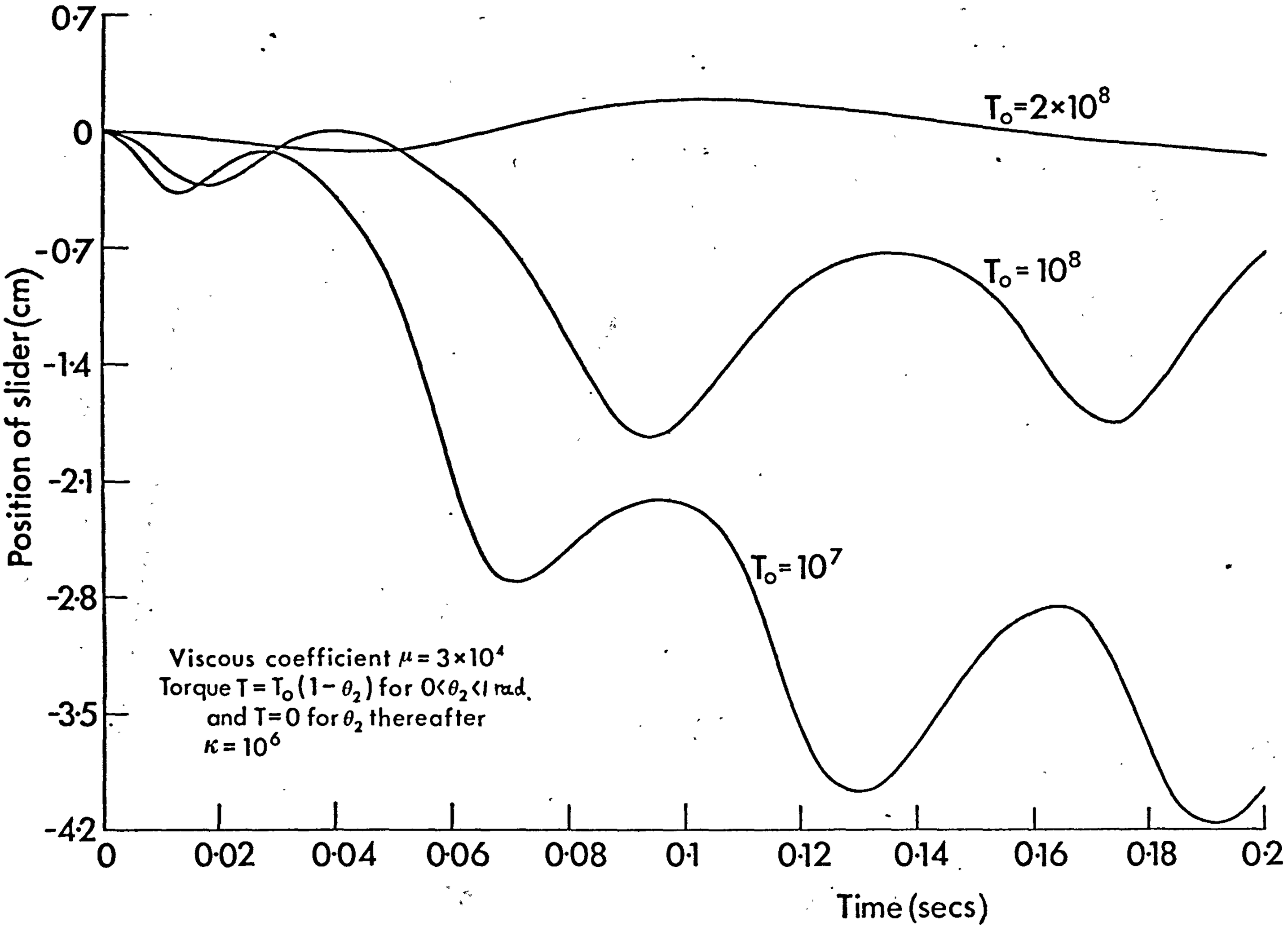

Fig(3·8) THE SLIDER RESPONSE

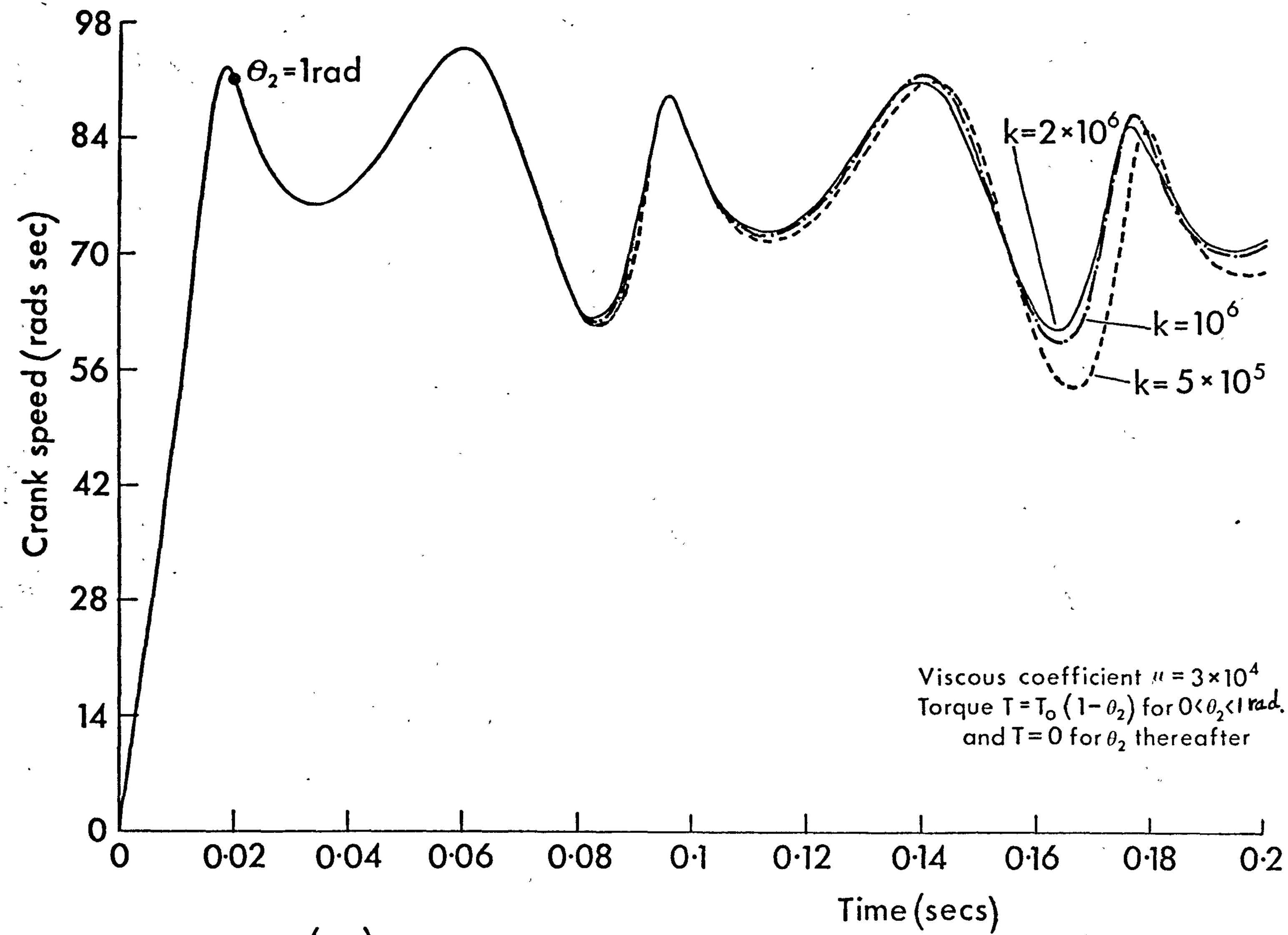

Fig(3·9) CRANK SPEED RESPONSE

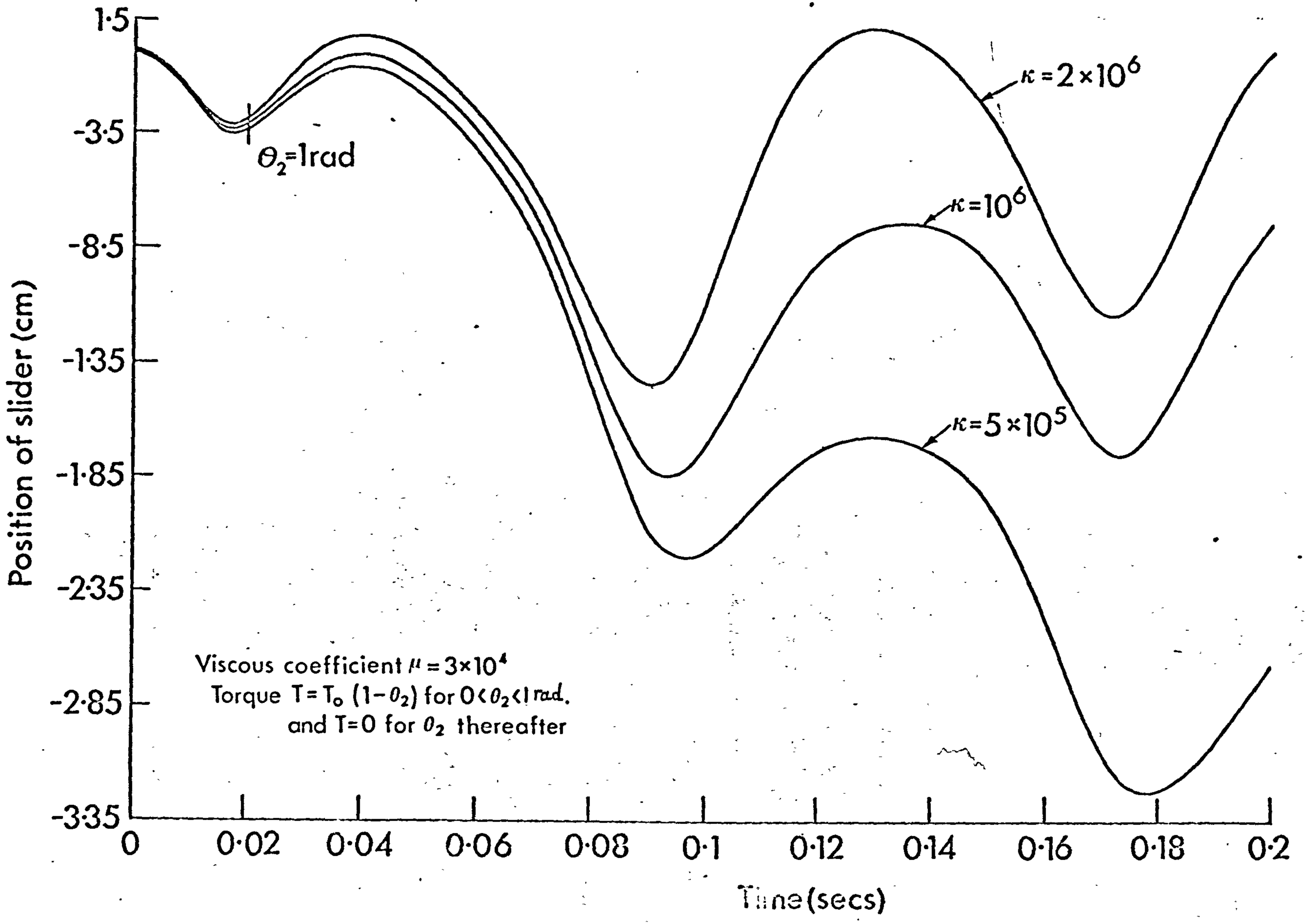

Fig (3·10) THE SLIDER RESPONSE

3. 3 Free Motion

The equations of motion for the free motion are the same as for the forced motion input torque case except that the element B_1 in matrix B_j has no torque component, i.e.

$$B_1 = -m_3 g \ell_2 \, \mathrm{Cos}\Theta_2 - m_3 \ell_2 \ell_{G3} \, \mathrm{Sin}(\Theta_2 - \Theta_3) \dot{\Theta}_3^{\,2}$$

In order to investigate the response of the mechanism in its free motion let us assume that initially we have a forced motion with constant speed input. The input torque to maintain the constant speed input is then removed and the responses of the slider and crank are studied. Figs. (3.11) and (3.12) show the crank speed versus crank angle for $k = 5 \times 10^5$ and 2×10^6 dyne/cm respectively. The initial speed of the crank is 420 rpm and the viscous coefficient $\mu = 3 \times 10^4$ dyne.sec/cm. The input data is as shown in table (3.1).

Both figures show that

(1) The crank speed behaviour is oscillatory

(2) The amplitude of oscillations decreases with crank angle and

(3) The mean position of oscillation reduces with crank angle.

The oscillatory behaviour of the speed is due to the non-linearities of the system and the reduction in speed is due to viscous dissipation of energy in the slider.

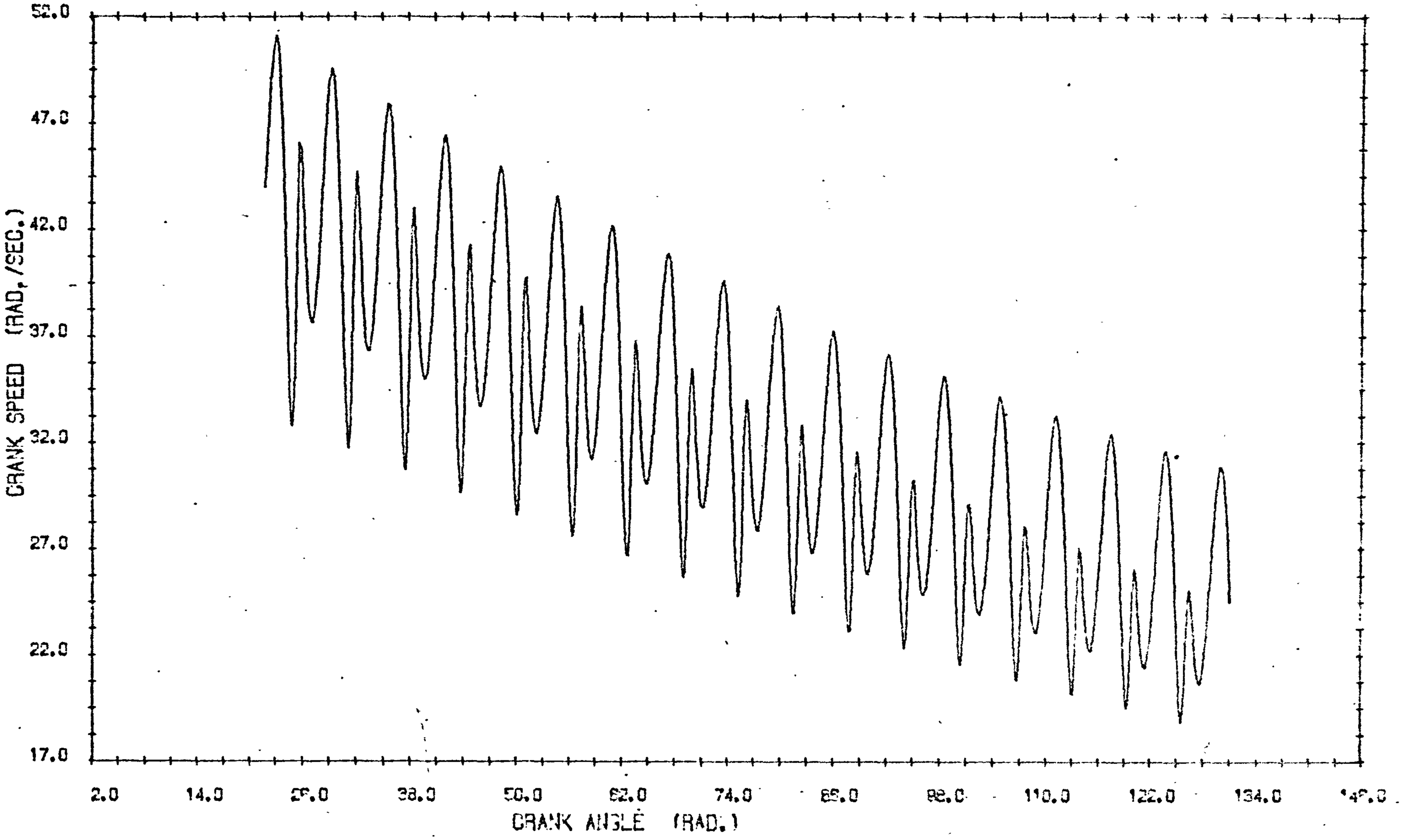

FIG(3-11). THE CRANK SPEED VERSUS THE CRANK ANGLE. (K=5.E 05, μ =3.E 04)

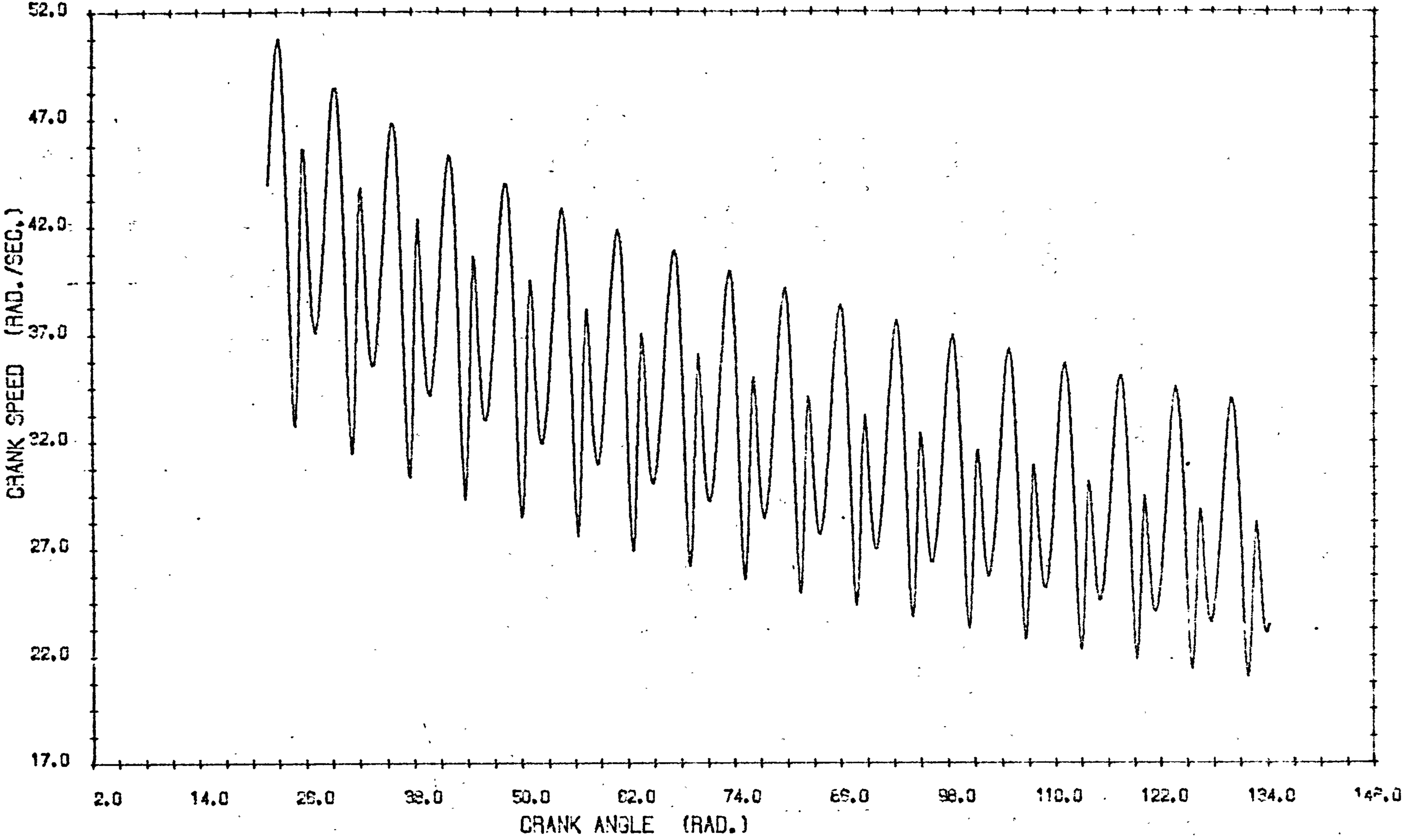

FIG(3-12). THE CARANK SPEED VERSUS THE CRANK ANGLE. (K=2.E 06, μ =3.E 04)

Figs. (3.13) and (3.14) show the phase plane plots of the slider for $k = 5 \times 10^5$ and 2×10^6 dyne/cm respectively. The points S and F indicate the start and finish of the plots. Due to sampling of output data straight-line segments appear on the curves. These segments should in fact be smooth curves following the line pattern of the curves and appear as straight lines only because no points were sampled between the end points of each segment. Both figures show the tendency of the phase plane plot towards the region $u = o$, $\dot{u} = o$. In so doing the amplitude of the oscillation decreases and a superimposed shift on the slider position, in the form of a drift towards $u = o$, is noticeable. The drift is greater in Fig. (3.13) due to the value of k being smaller which puts the mean position of oscillation further away from $u = o$. Non-linear effects leading to higher harmonics in the slider motion are clearly shown in both figures. However, these non-linearities are more manifested in Fig.(3.14) around the crank angular speed of 27 rad/sec. This speed is in fact an approximation to half the natural frequency of the system. This suggests that the non-linearity is a second subharmonic resonance. It is however appreciated that a natural frequency of the mechanism in study is not a sharply defined value but extends over a range. This is due to the variable mass and inertia of the mechanism experienced by the slider.

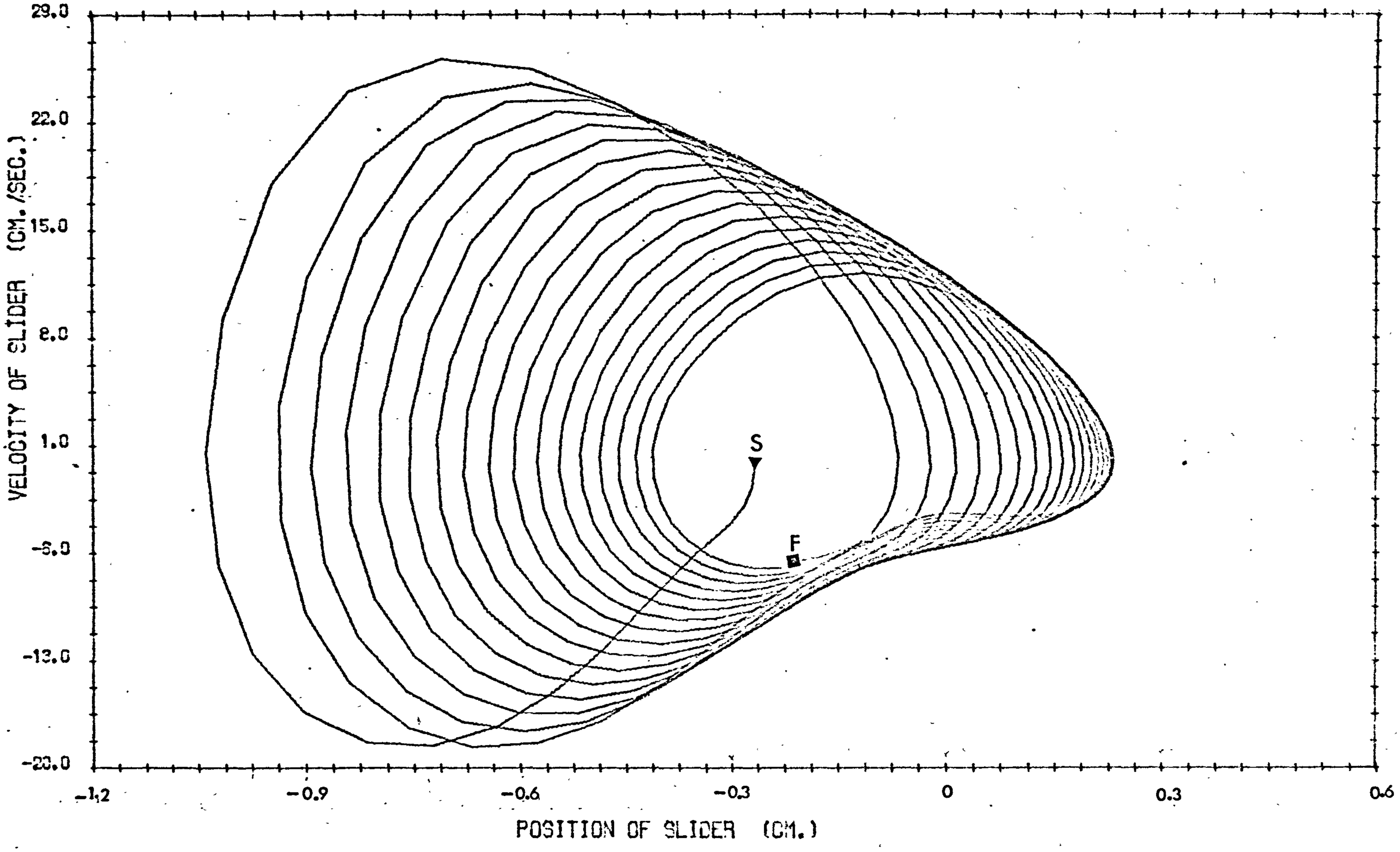

FIG. (3-13). THE VELOCITY OF THE SLIDER VERSUS ITS POSITION. (K=5.E 05, μ =3.E 04)

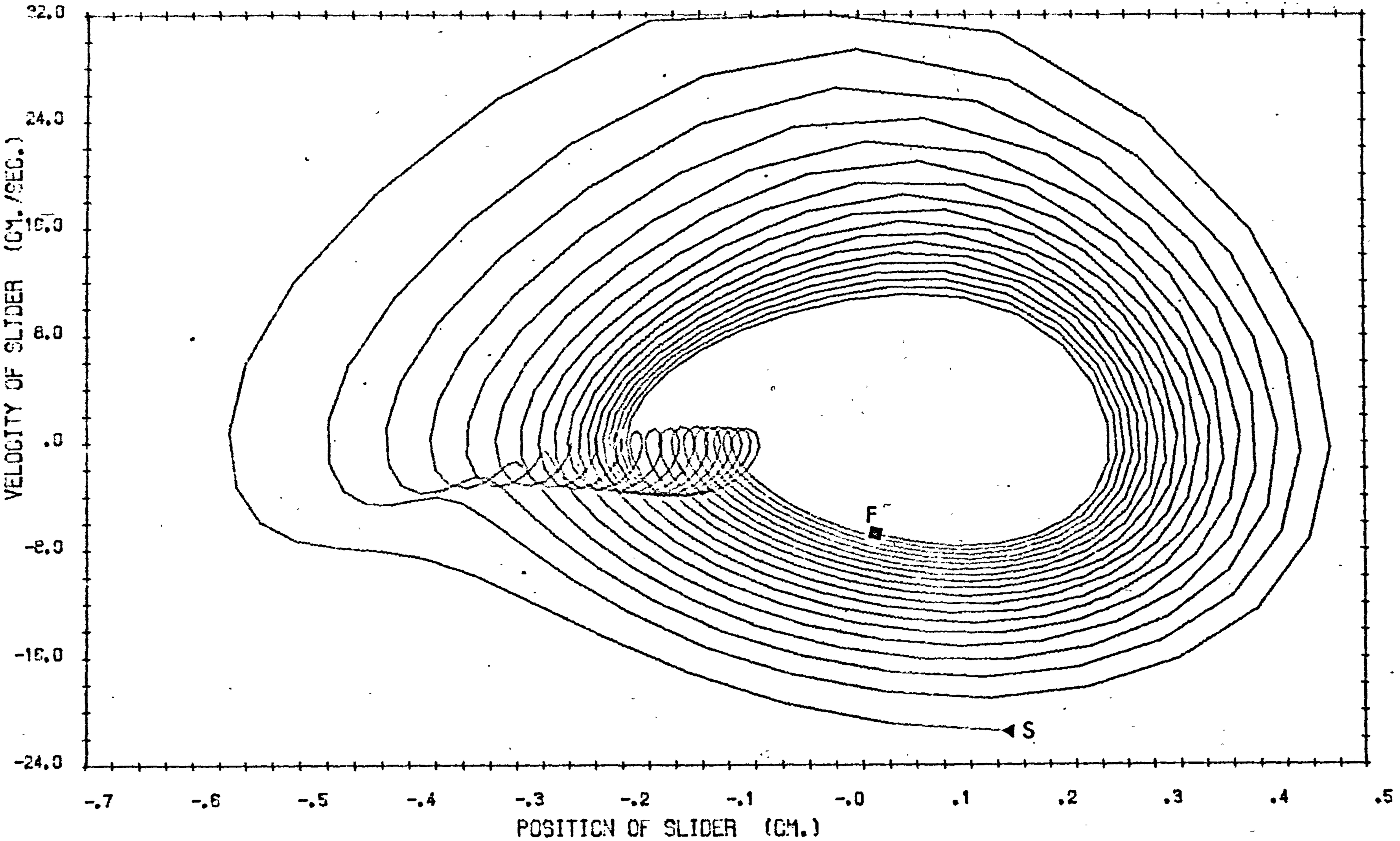

FIG. (3-14). THE VELOCITY OF THE SLIDER VERSUS ITS POSITION. (K=2.E 06, μ=3.E 04)

3.4 Computer Program

A computer program, the details of which are shown in Appendix , 1, was written to solve the equations of motion. It consists of a main program which calls for several subroutines. The Hamming's method which performs the numerical integration is shown in subroutine "DHAM" and the Gaussian elimination method which performs the solution for the second order derivatives is shown in subroutine "Gauss". The solution of the kinematics is shown in subroutine "Kine" and subroutines "Block data" and "Outp" are used for input and output requirements respectively.

The language in which the program is written is FORTRAN IV and double precision arithmetics are used throughout.

Chapter IV

THE LINEARISED EQUATIONS

AND

RESONANCE ANALYSIS

The dynamic analysis performed in Chapter II led to a set of highly non-linear differential equations. These equations can be linearised in parameters describing the deviation of motion from that of the four-bar with no movable pivot. This can be performed by expressing each of the generalised coordinates as the sum of two quantities. The first of these quantities accounts for the motion of the fixed four bar, the second only for the deviation from this motion due to the movable pivot. It must, however, be appreciated that in order that the results are true and meaningful the motion of the movable pivot must be small.

Two important aspects of the mechanism may be directly studied from the linearised motion; these are resonance and stability. The first will be studied in this chapter, the second in the next.

4. 1 The Linearised Kinematics

In order to facilitate the linearised treatment it will be assumed in the subsequent analysis that the crank length is small relative to the other links.

Consider the linkage shown in fig. (4.1). The configurations $A_oB_oC_oD_o$ and ABCD represent the datum and perturbed linkages of the fixed four bar with no movable pivot and the five bar respectively.

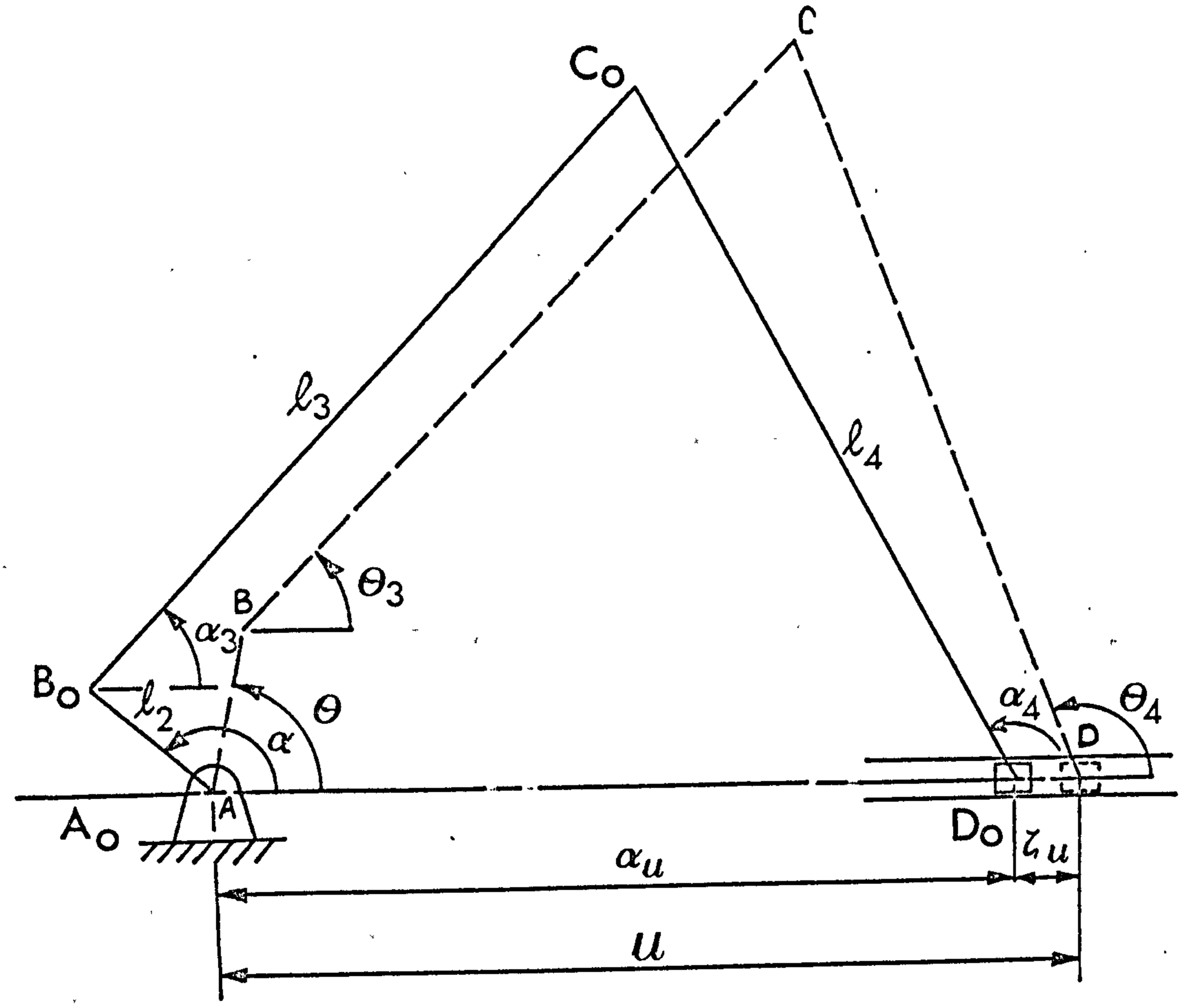

Fig(4·1) PLANAR LINKAGE ; $\frac{\ell_2}{\ell_4} \ll 1, \frac{\ell_2}{\ell_4} \ll \frac{\ell_3}{\ell_4}, \frac{\ell_2}{\ell_4} \ll \frac{\alpha_u}{\ell_4}$

$A_oB_oC_oD_o$ is arrived at by defining :-

$$\alpha_4 = \frac{\alpha_{4\ max.} + \alpha_{4\ min.}}{2} \qquad (4.1)$$

where α_4 max and α_4 min are the maximum and minimum angles of the rocker C_oD_o when the crank A_oB_o is rotated through 360 degrees in the fixed four bar case. The angles α and α_3 are then calculated accordingly.

The constraint equations may be written :-

$$\begin{aligned} \ell_2\ \mathrm{Cos}\Theta + \ell_3\mathrm{Cos}\Theta_3 - \ell_4\ \mathrm{Cos}\Theta_4 - u = 0 \\ \ell_2\ \mathrm{Sin}\Theta + \ell_3\mathrm{Sin}\Theta_3 - \ell_4\ \mathrm{Sin}\Theta_4 = 0 \end{aligned} \qquad (4.2)$$

Now, dividing equation (4.2) by ℓ_4 and defining

$$\Theta_3 = \alpha_3 + \zeta_3\ ,\ \Theta_4 = \alpha_4 + \zeta_4,\ u = \alpha_u + \zeta_u \qquad (a)$$

and

$$\sigma_2 = \frac{\ell_2}{\ell_4} << 1,\ \sigma_3 = \frac{\ell_3}{\ell_4}\ ,\ \sigma = \frac{\alpha_u}{\ell_4}\ ,\ \zeta = \frac{\zeta_u}{\ell_4} \qquad (b) \qquad (4.3)$$

where ζ_3, ζ_4 and ζ_u are the deviations from the four bar motion, and assuming

$$\mathrm{Cos}\zeta_3 = \mathrm{Cos}\zeta_4 = 1,\ \ \mathrm{Sin}\zeta_3 = \zeta_3\ ,\ \mathrm{Sin}\zeta_4 = \zeta_4\ , \qquad (4.4)$$

the following two equations may be obtained :-

$$\begin{aligned} -\mathrm{Cos}\alpha_4 + \mathrm{Sin}\alpha_4.\ \zeta_4 + \sigma_2\ \mathrm{Cos}\Theta\ + \sigma_3\ \mathrm{Cos}\alpha_3 \\ - \sigma_3\ \mathrm{Sin}\alpha_3\ \zeta_3 - \sigma - \zeta\ = 0 \end{aligned} \qquad (4.5)$$

$$\begin{aligned} -\mathrm{Sin}\alpha_4 - \mathrm{Cos}\alpha_4.\ \zeta_4 + \sigma_2\ \mathrm{Sin}\Theta\ + \sigma_3\ \mathrm{Sin}\alpha_3 \\ + \sigma_3\ \mathrm{Cos}\alpha_3.\ \zeta_3\ = 0. \end{aligned}$$

Now using the datum configuration $A_oB_oC_oD_o$ we obtain :-

$$\begin{aligned} \sigma_2\ \mathrm{Cos}\alpha\ &= \sigma + \mathrm{Cos}\alpha_4 - \sigma_3\ \mathrm{Cos}\alpha_3 \\ \sigma_2\ \mathrm{Sin}\alpha\ &= \mathrm{Sin}\alpha_4 - \sigma_3\ \mathrm{Sin}\alpha_3. \end{aligned} \qquad (4.6)$$

Substituting equations (4.6) into equations (4.5) we obtain:-

$$\begin{aligned} -\sigma_3 \sin\alpha_3 \zeta_3 + \sin\alpha_4 \zeta_4 - \zeta &= -\sigma_2 \cos\theta + \sigma_2 \cos\alpha \\ \sigma_3 \cos\alpha_3 \zeta_3 - \cos\alpha_4 \zeta_4 &= -\sigma_2 \sin\theta + \sigma_2 \sin\alpha \end{aligned} \qquad (4.7)$$

and hence

$$\zeta_3 = \frac{\cos\alpha_4 \zeta - \sigma_2 \cos(\theta-\alpha_4) + \sigma_2 \cos(\alpha - \alpha_4)}{\sigma_3 \sin(\alpha_4-\alpha_3)}$$

$$\zeta_4 = \frac{\cos\alpha_3 \zeta - \sigma_2 \cos(\theta - \alpha_3) + \sigma_2 \cos(\alpha - \alpha_3)}{\sin(\alpha_4 - \alpha_3)} \qquad (4.8)$$

4. 2 The Linearised Equations of Motion

Consider the linkage shown in fig. (4.2) with a spring of stiffness k and a damping friction of coefficient μ. The symbols indicated on the figure are as follows :

ℓ, m and I denote length, mass and inertia respectively. Subscript G denotes centre of gravity. Subscripts 2, 3, 4 denote crank, coupler and rocker respectively.

4.2.1 Derivation

Assuming a constant crank angular speed ω, i.e.

$$\theta = \omega t \qquad (4.9)$$

and no gravitational forces, then by application of the Lagrangian multiplier method stated in equation (2.5) the following equations are obtained.

$$m_3\ell_2\ell_{G3} \cos(\theta - \theta_3)\ddot{\theta}_3 + m_3\ell_3 \ell_{G3} \sin(\theta - \theta_3)\dot{\theta}_3^2 + \lambda_1\ell_2 \sin\theta - \lambda_2\ell_2 \cos\theta - \lambda_3 = 0 \qquad (4.10)$$

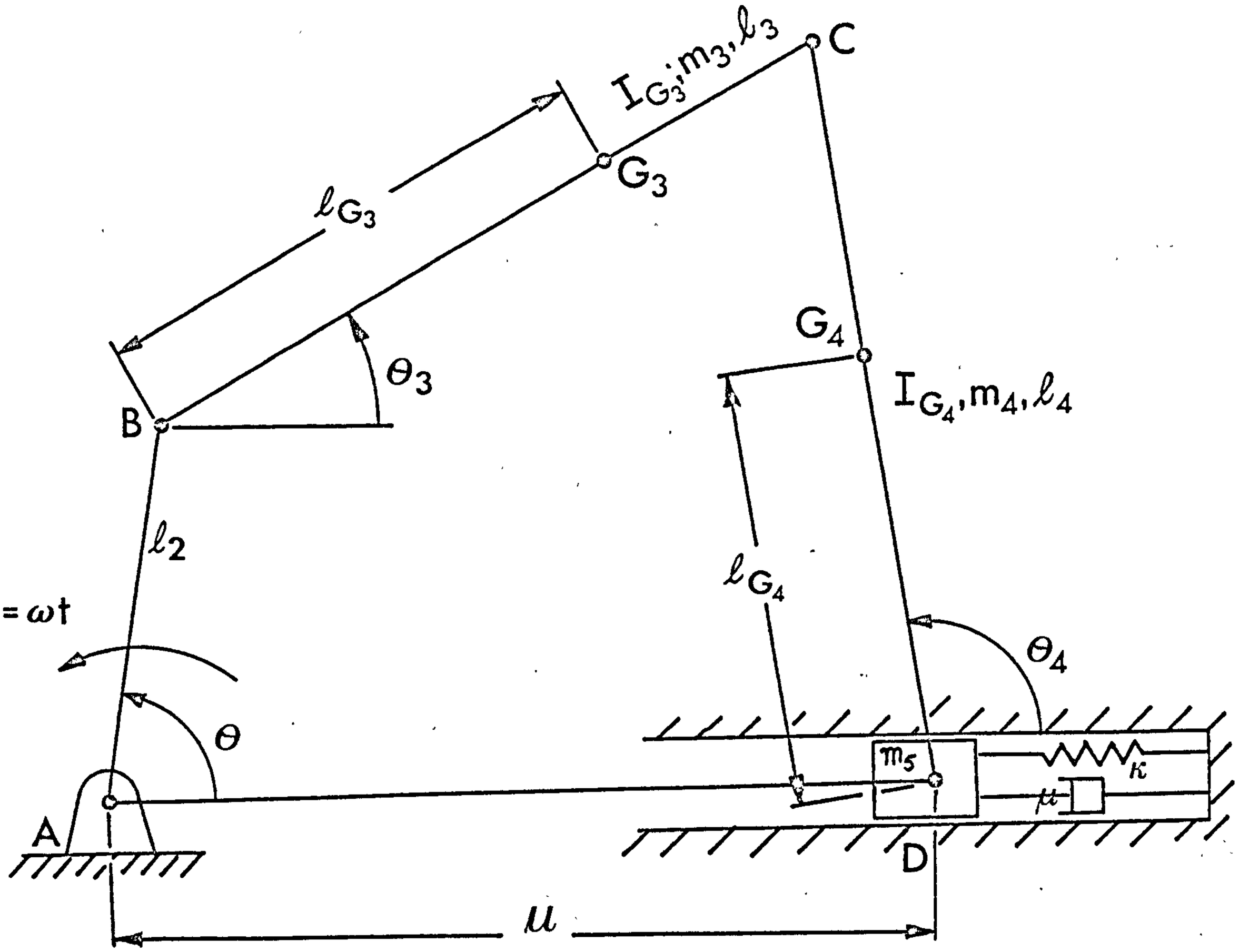

Fig (4·2) PLANAR LINKAGE A,B,C,D

$$(I_{G3} + m_3\ell_{G3}^2)\ddot{\theta}_3 - m_3\ell_2\ell_{G3}\,\mathrm{Sin}(\theta-\theta_3)\dot{\theta}^2 + \lambda_1\ell_3\,\mathrm{Sin}\theta_3 - \lambda_2\ell_3\,\mathrm{Cos}\theta_3 = 0. \quad (4.11)$$

$$(I_{G4} + m_4\ell_{G4}^2)\ddot{\theta}_4 - m_4\ell_{G4}\,\mathrm{Sin}\theta_4\,\ddot{\zeta}_u - \lambda_1\ell_4\,\mathrm{Sin}\theta_4 + \lambda_2\ell_4\,\mathrm{Cos}\theta_4 = 0. \quad (4.12)$$

$$(m_4 + m_5)\ddot{\zeta}_u - m_4\ell_{G4}\,\mathrm{Sin}\theta_4\ddot{\theta}_4 - m_4\ell_{G4}\,\mathrm{Cos}\theta_4\cdot\dot{\theta}_4^2 + \lambda_1 + \mu\cdot\dot{\zeta}_u + k\cdot\zeta_u = 0. \quad (4.13)$$

Divide equations (4.10), (4.11) and (4.12) by $(m_4\omega^2\ell_4^2)$ and equation (4.13) by $(m_4\omega^2\cdot\ell_4)$ and let

$$m_{r3} = \frac{m_3\cdot\ell_2\cdot\ell_{G3}}{m_4\cdot\ell_4^2}\ ,\quad I_3 = \frac{I_{G3} + m_3\ell_{G3}^2}{m_4\,\ell_4^2}$$

$$I_4 = \frac{I_{G4} + m_4\ell_{G4}^2}{m_4\,\ell_4^2}\ ,\quad r_4 = \ell_{G4}/\ell_4$$

$$\omega_c = \mu/(m_4+m_5)\ ,\quad \omega_k = \sqrt{\frac{k}{(m_4 + m_5)}} \quad (4.14)$$

$$\rho_{45} = \frac{m_4}{(m_4 + m_5)}\ ,\quad \lambda_c = \frac{\omega_c}{\omega}\ ,\quad \lambda_k = \frac{\omega_k}{\omega}$$

$$\xi_1 = \frac{\lambda_1}{m_4\,\omega^2\ell_4}\ ,\quad \xi_2 = \frac{\lambda_2}{m_4\omega^2\ell_4}\ ,\quad \xi_3 = \frac{\lambda_3}{m_4\omega^2\ell_4^2}\ ,$$

Now, transform the differentiation with respect to time to that with respect to crank angle θ and denote the first derivative of this by ' ' ' above the variable symbol, and

the second by '''. The equations of motion may then be written :-

$$m_{r3}.\cos(\theta-\theta_3)\ddot{\theta}_3 + \sigma_2 \sin\theta \,.\xi_1 - \sigma_2 \cos\theta \,.\xi_2' - \xi_3 = -m_{r3}\sin(\theta-\theta_3)\dot{\theta}_3^{\,2} \qquad (4.15)$$

$$I_3\ddot{\theta}_3 + \sigma_3\sin\theta_3\xi_1 - \sigma_3\cos\theta_3\xi_2 = m_{r3}\sin(\theta-\theta_3) \qquad (4.16)$$

$$I_4\ddot{\theta}_4 - r_4\sin\theta_4\ddot{\zeta} - \sin\theta_4\xi_1 + \cos\theta_4\xi_2 = 0. \qquad (4.17)$$

$$\ddot{\zeta} - \rho_{45}.r_4\sin\theta_4\ddot{\theta}_4 + \lambda_c\dot{\zeta} + \lambda_k^{\,2}\zeta + \rho_{45}\xi_1 = \rho_{45}r_4\cos\theta_4\dot{\theta}_4^{\,2} \qquad (4.18)$$

Divide Equations (4.2) by ℓ_4 and differentiate twice with respect to θ, we obtain

$$\sigma_3\sin\theta_3\ddot{\theta}_3 - \sin\theta_4\ddot{\theta}_4 + \ddot{\zeta} = -\sigma_2.\cos\theta - \sigma_3\cos\dot{\theta}_3\theta_3^{\,2} + \cos\theta_4\dot{\theta}_4^{\,2} \qquad (4.19)$$

$$\sigma_3\cos\theta_3\ddot{\theta}_3 - \cos\theta_4\ddot{\theta}_4 = \sigma_2\sin\theta + \sigma_3\sin\theta_3\dot{\theta}_3^{\,2} - \sin\theta_4\,\dot{\theta}_4^{\,2}\,. \qquad (4.20)$$

By eliminating $\ddot{\theta}_3$, $\ddot{\theta}_4$, ξ_1, ξ_2 and ξ_3 from the above equations a second order differential equation describing the motion of the slider may be obtained. If equations (4.3a) and (4.8) are substituted into this slider equation, and second and higher order multiples of ζ and its derivatives are ignored the following linearised equation of motion of the slider may be obtained.

$$\ddot{\zeta} + \frac{\lambda_c\,(A_1 + B_1.\cos\theta + C_1.\sin\theta)}{D_1 + E_1.\cos\theta + F_1.\sin\theta}\,\dot{\zeta} + \frac{\lambda_k^{\,2}\,(A_1+B_1\cos\theta+C_1\sin\theta) + (G_1+H_1\cos\theta+P_1\sin\theta)}{D_1+E_1.\cos\theta + F_1.\sin\theta}\,\zeta = \frac{Q_1+R_1\cos\theta+S_1.\sin\theta}{D_1+E_1\cos\theta + F_1\sin\theta} \qquad (4.21)$$

This may also be written as :

$$\zeta'' + \psi_1(\Theta)\zeta' + \psi_2(\Theta)\zeta = \psi_3(\Theta)$$

i.e. a second order linear differential equation with periodic coefficients of $\psi_1(\Theta)$ and $\psi_2(\Theta)$ and a forcing term of $\psi_3(\Theta)$.

The various coefficients of equation (4.21) are as follows :-

$$A_1 = \sigma_3^2\{\mathrm{Sin}^2(\alpha_4-\alpha_3) - 2\sigma_2\mathrm{Cos}(\alpha_4-\alpha_3)\left[\frac{\mathrm{Cos}(\alpha-\alpha_4)}{\sigma_3} - \mathrm{Cos}(\alpha-\alpha_3)\right]\} .$$

$$B_1 = -\sigma_3^2\{2\sigma_2\mathrm{Cos}(\alpha_4-\alpha_3)\left[-\frac{\mathrm{Cos}\alpha_4}{\sigma_3} + \mathrm{Cos}\alpha_3\right]\} .$$

$$C_1 = -\sigma_3^2\{2\sigma_2\mathrm{Cos}(\alpha_4-\alpha_3)\left[-\frac{\mathrm{Sin}\alpha_4}{\sigma_3} + \mathrm{Sin}\alpha_3\right]\} .$$

$$\begin{aligned} D_1 = A_1 &- 2\rho_{45}r_4\sigma_3^2\{\mathrm{Sin}\alpha_4\mathrm{Cos}\alpha_3\mathrm{Sin}(\alpha_4-\alpha_3) \\ &- \frac{\sigma_2}{\mathrm{Sin}(\alpha_4-\alpha_3)}\left[\frac{\mathrm{Sin}\alpha_4\mathrm{Cos}(\alpha_4-2\alpha_3)\mathrm{Cos}(\alpha-\alpha_4)}{\sigma_3}\right. \\ &\left. - \mathrm{Cos}\alpha_3\mathrm{Sin}(2\alpha_4-\alpha_3)\mathrm{Cos}(\alpha-\alpha_3)\right]\} \\ &+ \rho_{45}\{I_4\sigma_3^2\left[\mathrm{Cos}^2\alpha_3 - \frac{\sigma_2\mathrm{Sin}2\alpha_3\mathrm{Cos}(\alpha-\alpha_4)}{\sigma_3\mathrm{Sin}(\alpha_4-\alpha_3)}\right] \\ &+ I_3\left[\mathrm{Cos}^2\alpha_4 - \frac{\sigma_2\mathrm{Sin}2\alpha_4\mathrm{Cos}(\alpha-\alpha_3)}{\mathrm{Sin}(\alpha_4-\alpha_3)}\right]\} . \end{aligned}$$

$$\begin{aligned} E_1 = B_1 &- \rho_{45}r_4\sigma_3\sigma_2\{\frac{\mathrm{Sin}2\alpha_4\mathrm{Cos}(\alpha_4-2\alpha_3) - 2\sigma_3\mathrm{Cos}^2\alpha_3\mathrm{Sin}(2\alpha_4-\alpha_3)}{\mathrm{Sin}(\alpha_4-\alpha_3)} \\ &+ \rho_{45}\{I_4\sigma_3\sigma_2\left[\frac{\mathrm{Sin}2\alpha_3\mathrm{Cos}\alpha_4}{\mathrm{Sin}(\alpha_4-\alpha_3)}\right] + I_3\sigma_2\left[\frac{\mathrm{Sin}2\alpha_4.\mathrm{Cos}\alpha_3}{\mathrm{Sin}(\alpha_4-\alpha_3)}\right]\} . \end{aligned}$$

$$F_1 = C_1 - \rho_{45} r_4 \sigma_3 \sigma_2 \left\{ \frac{2\sin^2\alpha_4 \cos(\alpha_4-2\alpha_3) - \sigma_3 \sin 2\alpha_3 \sin(2\alpha_4-\alpha_3)}{\sin(\alpha_4 - \alpha_3)} \right\}$$

$$+ \rho_{45} \left\{ I_4 \sigma_3 \sigma_2 \left[\frac{\sin 2\alpha_3 \sin\alpha_4}{\sin(\alpha_4 - \alpha_3)} \right] + I_3 \sigma_2 \left[\frac{\sin 2\alpha_4 \sin\alpha_3}{\sin(\alpha_4 - \alpha_3)} \right] \right\} .$$

$$G_1 = \frac{\rho_{45} \cdot I_3 \cdot \sigma_2}{\sigma_3} \left\{ -\cos^2\alpha_4 \cdot \frac{\cos(\alpha_4-\alpha_3)}{\cos\alpha_3} + \sigma_3 \cos(2\alpha_4-\alpha_3) \right\} .$$

$$\sin(\alpha_4 - \alpha_3)$$

$$HH_1 = \sigma_2 \left[\frac{I_4 \sigma_3 \cos\alpha_4 \sin\alpha_3 + I_3 \sin 2\alpha_4 - \frac{1}{2} r_4 \sigma_3 \sin 2\alpha_4 \frac{\cos(\alpha_4-2\alpha_3)}{\cos\alpha_3}}{\sin(\alpha_4 - \alpha_3)} \right.$$

$$\left. + \frac{r_4 \sigma_3^2 \cos\alpha_3 \sin(2\alpha_4-\alpha_3)}{\sin(\alpha_4 - \alpha_3)} \right] .$$

$$HH_2 = \left[\frac{-m_{r3}\cos^2\alpha_4\cos(\alpha_4-\alpha_3)+m_{r3}\sigma_3\cos\alpha_3\cos\alpha_4-I_4\sigma_2\sigma_3\cos\alpha_4\cos\alpha_3}{\sin(\alpha_4-\alpha_3)} \right.$$

$$\left. + \frac{-I_3\frac{\sigma_2}{\sigma_3}\cdot\frac{\cos^3\alpha_4}{\cos\alpha_3}+\frac{1}{2}\sigma_2\sigma_3 r_4\sin 2\alpha_4}{\sin(\alpha_4-\alpha_3)} \right] .$$

$$H_1 = -\rho_{45}\{ m_{r3}\cdot\frac{\cos^2\alpha_4}{\cos\alpha_3} + HH_1\cdot\cos\alpha_3 - HH_2\cdot\sin\alpha_3 \} .$$

$$P_1 = -\rho_{45}\{ HH_1\cdot\sin\alpha_3 + HH_2\cdot\cos\alpha_3 \} .$$

$$Q_1 = -\rho_{45}\sigma_2\{ I_3\frac{\cos\alpha_4}{\cos\alpha_3}\sin(\alpha_4-\alpha_3) + I_4\sigma_3^2\cos\alpha_3 + I_3\frac{\cos^2\alpha_4}{\cos\alpha_3} \} .$$

$$R_1 = \rho_{45}\sigma_3\{\sin(\alpha_4-\alpha_3)\left[\sigma_2\sigma_3 r_4\sin\alpha_4\cos\alpha_3-m_{r3}\sin\alpha_3\cos\alpha_4\right] \} .$$

$$S_1 = \rho_{45}\sigma_3\{\sin(\alpha_4-\alpha_3)\left[\sigma_2\sigma_3 r_4\sin\alpha_3\sin\alpha_4+m_{r3}\cos\alpha_3\cos\alpha_4\right] \}$$

4.3 Simplification of the Linearised Equations of Motion

The coefficients B_1, C_1, H_1, P_1, D_1, E_1 and F_1 are much smaller than those of A_1 and D_1 by at least a factor $\frac{1}{\sigma 2}$ in the worst cases. Therefore we may write :-

$$\frac{A_1}{D_1} = k_o\,, \quad \frac{B_1}{D_1} = k_1.\varepsilon, \quad \frac{C_1}{D_1} = k_2.\varepsilon$$

$$\frac{G_1}{D_1} = h_o\,, \quad \frac{H_1}{D_1} = k_3\varepsilon\,, \quad \frac{P_1}{D_1} = k_4\varepsilon$$

$$\frac{E_1}{D_1} = k_5.\varepsilon, \quad \frac{F_1}{D_1} = k_6.\varepsilon \qquad (4.22)$$

$$\frac{Q_1}{D_1} = g_o, \quad \frac{R_1}{D_1} = k_7\varepsilon\,, \quad \frac{S_1}{D_1} = k_8\varepsilon$$

where ε is a small parameter and h_o, $g_o << k_o$.

Let us now consider the damping term in equation (4.21). This may be written as :-

$$\lambda_c.\ (k_o + (k_1 Cos\theta + k_2 Sin\theta)\varepsilon)(1 + (k_5 Cos\theta + k_6 Sin\theta)\varepsilon)^{-1}\zeta'$$

By multiplying out, ignoring the terms in second and higher powers of ε and rearranging in an increasing powers of ε we obtain :-

$$\lambda_c.\ \{k_o + \left((k_1 - k_o k_5)Cos\theta + (k_2 - k_o k_6)Sin\theta\right)\varepsilon +$$

$$+ \left(k_o\ (k_5 Cos\theta + k_6 Sin\theta)^2 - (k_1 Cos\theta + k_2 Sin\theta)(k_5 Cos\theta + k_6 Sin\theta)\right)\varepsilon^2 + \ldots\}\,\zeta'$$

which, if terms in the order of third and higher powers of ε are ignored, may be written

$$\lambda_c\ \{k_o + (a_1 Cos\theta + b_1 Sin\theta)\varepsilon + (a_2 Cos2\theta + b_2 Sin2\theta)\varepsilon^2 + \ldots.\}\ \zeta' \qquad (4.23)$$

where

$$a_1 = k_1 - k_o k_5$$

$$b_1 = k_2 - k_o k_6 \qquad (4.24)$$

$$a_2 = \frac{1}{2}\{k_o(k^2_5 - k^2_6) - (k_1 k_5 - k_2 k_6)\}$$

$$b_2 = \frac{1}{2}\{2k_o k_5 k_6 - (k_1 k_6 + k_2 k_5)\}$$

Similarly the stiffness term may be written :-

$$\{\lambda^2_k \left(k_o + (a_1 \mathrm{Cos}\theta + b_1 \mathrm{Sin}\theta)\varepsilon + (a_2 \mathrm{Cos}2\theta + b_2 \mathrm{Sin}2\theta)\varepsilon^2 + \ldots\right) \qquad (4.25)$$

$$+ \left(h_o + (a_3 \mathrm{Cos}\theta + b_3 \mathrm{Sin}\theta)\varepsilon + (a_4 \mathrm{Cos}2\theta + b_4 \mathrm{Sin}\theta)\varepsilon^2 + \ldots\right) I\zeta$$

where

$$a_3 = k_3 - h_o k_5$$

$$b_3 = k_4 - h_o k_6 \qquad (4.26)$$

$$a_4 = \frac{1}{2}\{h_o(k^2_5 - k^2_6) - (k_3 k_5 - k_4 k_6)\}$$

$$b_4 = \frac{1}{2}\{2h_o k_5 k_6 - (k_3 k_6 + k_4 k_5)\}$$

In a similar manner the right hand side may be written :-

$$g_o + (a_5 \mathrm{Cos}\theta + b_5 \mathrm{Sin}\theta)\varepsilon + (a_6 \mathrm{Cos}2\theta + b_6 \mathrm{Sin}2\theta)\varepsilon^2 + \ldots \qquad (4.27)$$

where

$$a_5 = k_7 - g_o k_5$$

$$b_5 = k_8 - g_o k_6 \qquad (4.28)$$

$$a_6 = \frac{1}{2}\{g_o(k^2_5 - k^2_6) - (k_7 k_5 - k_8 k_6)\}$$

$$b_6 = \frac{1}{2}\{2g_o k_5 k_6 - (k_7 k_6 + k_8 k_5)\}$$

The equation of motion (3.21) may thus be written in its final form as

$$\zeta'' + \lambda_c \{k_o + (a_1\cos\theta + b_1\sin\theta)\varepsilon + (a_2\cos 2\theta + b_2\sin 2\theta)\varepsilon^2 + \ldots\} \zeta'$$

$$+ \{\lambda^2_k \begin{pmatrix} k_o + (a_1\cos\theta + b_1\sin\theta)\varepsilon + (a_2\cos 2\theta + b_2\sin 2\theta)\varepsilon^2 + \ldots \end{pmatrix}$$

$$+ \begin{pmatrix} h_o + (a_3\cos\theta + b_3\sin\theta)\varepsilon + (a_4\cos 2\theta + b_4\sin 2\theta)\varepsilon^2 + \ldots \end{pmatrix} \} \zeta$$

$$= g_o + (a_5\cos\theta + b_5\sin\theta)\varepsilon + (a_6\cos 2\theta + b_6\sin 2\theta)\varepsilon^2 + \ldots \qquad (4.29)$$

4.4 Resonance Analysis

4.4.1 No damping; $\lambda_c = 0$

Assume that ζ has a series periodic solution of the form

$$\zeta = \Sigma_{m=0}^{n} (X_m \cos m\,\omega t + Y_m \sin m\,\omega t). \qquad (4.30)$$

By substituting equation (4.30) into (4.29) and limiting the expansion of ζ to m = 2, then multiplying out and rearranging we obtain :-

$$- (X_1\cos\theta + Y_1\sin\theta + 4X_2\cos 2\theta + 4Y_2\sin 2\theta)$$

$$+ (\lambda_k^2 . k_o + h_o)\ (X_o + X_1\cos\theta + Y_1\sin\theta + X_2\cos 2\theta + Y_2\sin 2\theta)$$

$$+ X_o \begin{pmatrix} (\lambda_k^2 a'_1 + a'_3)\cos\theta + (\lambda_k^2 b'_1 + b'_3)\sin\theta + (\lambda_k^2 a'_2 + a'_4)\cos 2\theta \\ + (\lambda_k^2 . b'_2 + b'_4)\sin 2\theta \end{pmatrix}$$

$$+ X_1 \begin{pmatrix} (\lambda_k^2 a'_1 + a'_3)\left(\frac{1+\cos 2\theta}{2}\right) + (\lambda_k^2 b'_1 + b'_3)\frac{\sin 2\theta}{2} + (\lambda_k^2 a'_2 + a'_4)\left(\frac{\cos 3\theta + \cos\theta}{2}\right) \\ + (\lambda_k^2 b'_2 + b'_4)\left(\frac{\sin 3\theta + \sin\theta}{2}\right) \end{pmatrix}$$

$$+ Y_1 \begin{pmatrix} (\lambda_k^2 a'_1 + a'_3)\left(\frac{\sin 2\theta}{2}\right) + (\lambda_k^2 b'_1 + b'_3)\left(\frac{1-\cos 2\theta}{2}\right) + (\lambda_k^2 a'_2 + a'_4)\left(\frac{\sin 3\theta - \sin\theta}{2}\right) \\ + (\lambda_k^2 b'_2 + b'_4)\left(\frac{\cos\theta - \cos 3\theta}{2}\right) \end{pmatrix}$$

$$+ X_2\Big((\lambda_k^2 a'_1+a'_3)\left(\frac{\cos 3\theta+\cos\theta}{2}\right)+(\lambda_k^2 b'_1+b'_3)\left(\frac{\sin 3\theta-\sin\theta}{2}\right)+(\lambda_k^2 a'_2+a'_4)\Big)$$
$$\Big(\left(\frac{1+\cos 4\theta}{2}\right) + (\lambda_k^2 b'_2+b'_4)\frac{\sin 4\theta}{2}\Big)$$

$$+ Y_2\Big((\lambda_k^2 a'_1+a'_3)\left(\frac{\sin 3\theta+\sin\theta}{2}\right)+(\lambda_k^2 b'_1+b'_3)\left(\frac{\cos\theta-\cos 3\theta}{2}\right)\Big)$$
$$\Big(+ (\lambda_k^2 a'_2+a'_4)\frac{\sin 4\theta}{2} +(\lambda_k^2 b'_2+b'_4)\left(\frac{1-\cos 4\theta}{2}\right)\Big)$$

$$= g_o + a'_5\cos\theta + b'_5\sin\theta + a'_6\cos 2\theta + b'_6\sin 2\theta \qquad (4.31)$$

where a'_1, b'_1, a'_3, b'_3, a'_5, b'_5 are a_1, b_1, a_3, b_3, a_5 and b_5 multiplied by ε respectively and a'_2, b'_2, a'_4, b'_4, a'_6, and b'_6 are a_2, b_2, a_4, b_4, a_6 and b_6 multiplied by ε^2 respectively. Equating constant terms and coefficients of $\cos\theta$, $\sin\theta$, $\cos 2\theta$ and $\sin 2\theta$ on both sides of equation (4.31) we obtain the following recurrence relationships.

$$2(\lambda_k^2.k_o+h_o)X_o+ (\lambda_k^2\, a'_1+a'_3)X_1+ (\lambda_k^2\, b'_1+b'_3)\, Y_1$$
$$+ (\lambda_k^2\, a'_2+a'_4)X_2 + (\lambda_k^2\, b'_2+b'_4)\, Y_2 = 2g_o$$

$$2(\lambda_k^2\, a'_1+a'_3)X_o +(-2+2h_o+2\lambda_k^2.k_o+\lambda_k^2\, a'_2+a'_4)X_1 + (\lambda_k^2\, b'_2+b'_4)\, Y_1$$
$$+ (\lambda_k^2\, a'_1+a'_3)X_2 + (\lambda_k^2 b'_1+b'_3)\, Y_2 = 2a'_5$$

$$2(\lambda_k^2\, b'_1+b'_3)X_o + (\lambda_k^2\, b'_2+b'_4)X_1+ (-2+2h_o+2\lambda_k^2.k_o -\lambda_k^2\, a'_2-a'_4)\, Y_1 \qquad (4.32)$$
$$+ (-\lambda_k^2\, b'_1-b'_3)X_2+ (\lambda_k^2\, a'_1+a'_3)\, Y_2 = 2b'_5$$

$$2(\lambda_k^2\, a'_2+a'_4)X_o + (\lambda_k^2\, a'_1+a'_3)X_1 +(-\lambda_k^2\, b'_1-b'_3)\, Y_1$$
$$+ (-8 + 2h_o + 2\lambda_k^2.\, k_o)\, X_2 = 2a'_6$$

$$2(\lambda_k^2\, b'_2+b'_4)X_o + (\lambda_k^2 b'_1+b'_3)X_1 + (\lambda_k^2\, a'_1+a'_3)\, Y_1$$
$$+ (-8 + 2h_o+2\lambda_k^2.k_o)Y_2 = 2b'_6$$

The above relationships may be written as a matrix equation of the form

$$(A_{ij}) \cdot (W_j) = (B_i) \qquad (4.33)$$

where W_j is a column matrix $(X_o, X_1, Y_1, X_2, Y_2)$, A_{ij} is its square matrix of coefficients and B_i is the column matrix of the right hand side of (4.32). Equations (4.33) may be solved using a digital computer, thus yielding the values of the coefficients W_j.

4.4.2. Viscous damping; Coefficient of damping = μ

Assuming a solution of ζ as described in (4.30) and substituting it in equation (4.29), then multiplying and equating the coefficients of the trignometric functions of θ on both sides of that equation in a similar manner to the preceding section, we obtain the following recurrence relationships,

$$\left.\begin{aligned}
&2\,b_{oo}X_o + (b_{11}-d_{12})X_1 + (b_{12}+d_{11})Y_1 + (b_{13}-2d_{14})X_2 \\
&\qquad + (b_{14}+2d_{13})Y_2 = 2g_o
\end{aligned}\right)$$

$$\left.\begin{aligned}
&2\,b_{11}X_o + (-2+2b_{oo}+b_{13}-d_{14})X_1 + (2\lambda_c+b_{14}+d_{13})Y_1 \\
&\qquad + (b_{11}-2d_{12})X_2 + (b_{12}+2d_{11})Y_2 = 2a'_5
\end{aligned}\right)$$

$$\left.\begin{aligned}
&2\,b_{12}X_o + (-2\lambda_c+b_{14}+d_{13})X_1 + (-2+2b_{oo}-b_{13}+d_{14})Y_1 \\
&\qquad + (-b_{12}-2d_{11})X_2 + (b_{11}-2d_{12})Y_2 = 2b'_5
\end{aligned}\right)$$

$$2\,b_{13}X_o + (b_{11}+d_{12})X_1 + (-b_{12}+d_{11})Y_1 + (-8+2b_{oo})X_2 + 4\lambda_c Y_2 = 2a'_6$$

$$2\,b_{14}X_o + (b_{12}-d_{11})X_1 + (b_{11}+d_{12})Y_1 - 4\lambda_c X_2 + (-8+2b_{oo})Y_2 = 2b'_6 \qquad (4.34)$$

where,

$$b_{oo} = \lambda_k^2 . k_o + h_o$$

$$b_{11} = \lambda_k^2 . a'_1 + a'_3 \ , \ d_{11} = \lambda_c . \ a'_1$$

$$b_{12} = \lambda_k^2 . b'_1 + b'_3 \ , \ d_{12} = \lambda_c \ \ b'_1 \qquad (4.35)$$

$$b_{13} = \lambda_k^2 . a'_2 + a'_4 \ , \ d_{13} = \lambda_c . \ a'_2$$

$$b_{14} = \lambda_k^2 \ b'_2 + b'_4 \ , \ d_{14} = \lambda_c . \ b'_2 .$$

The above equations may be written in a matrix form similar to equation (3.33). A numerical solution may then be found for X_o, X_1, Y_1, X_2 and Y_2 and substituted in equation (3.30) to give a solution for the slider motion ζ.

4.5 Results

To illustrate the theory discussed earlier let us consider the linkage shown in fig. (4.2) and assume that :

(i) the mass and inertia of the coupler are negligible,

(ii) the centre of mass of the rocker lies on the centre line of the slider, and

(iii) the input data are (see equations 4.3b) and (4.14))

$$\omega_k^2 = 10^3, \ \rho_{45} = 0.2, \ \sigma_2 = 0.05, \ \ \sigma_3 = 1.$$

4.5.1. Resonance in The Absence of Damping

Figs. (4.3) and (4.4) show the amplitude curves of the first and second harmonics against the crank angular speed ω for three values of the inertia ratio I_4. These amplitudes correspond to $\sqrt{X_1^2 + Y_1^2}$ and $\sqrt{X_2^2 + Y_2^2}$ of equation (4.30) respectively. The figures show that resonance for the first harmonic occurs in the region of $(\omega_k - d) < \omega < \omega_k$ where $d \simeq 1$ rad./sec. These results are as would be expected and their deviation from the idealised spring-mass system accounts for

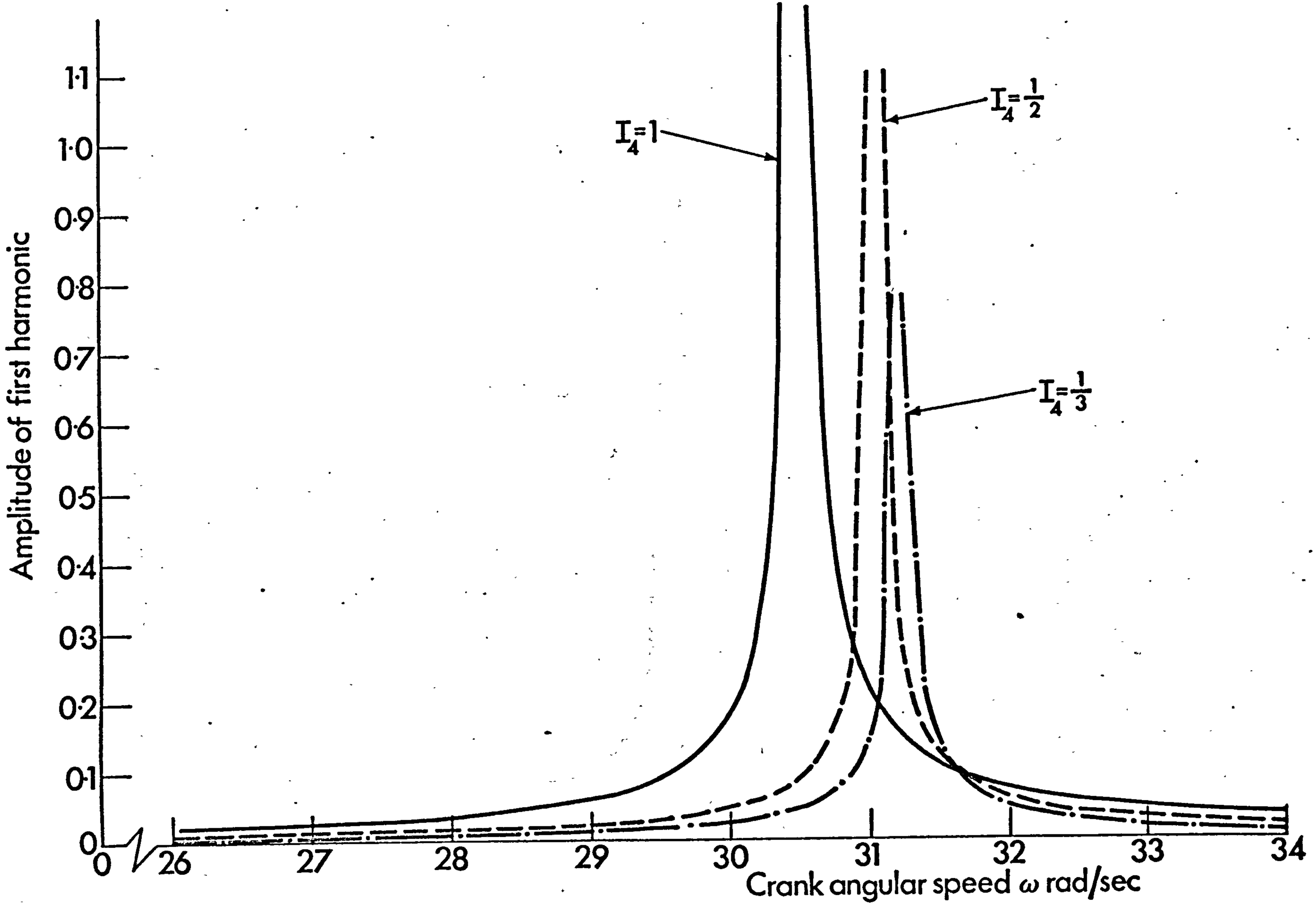

Fig(4.3): AMPLITUDE OF FIRST HARMONIC VERSUS CRANK ANGULAR SPEED

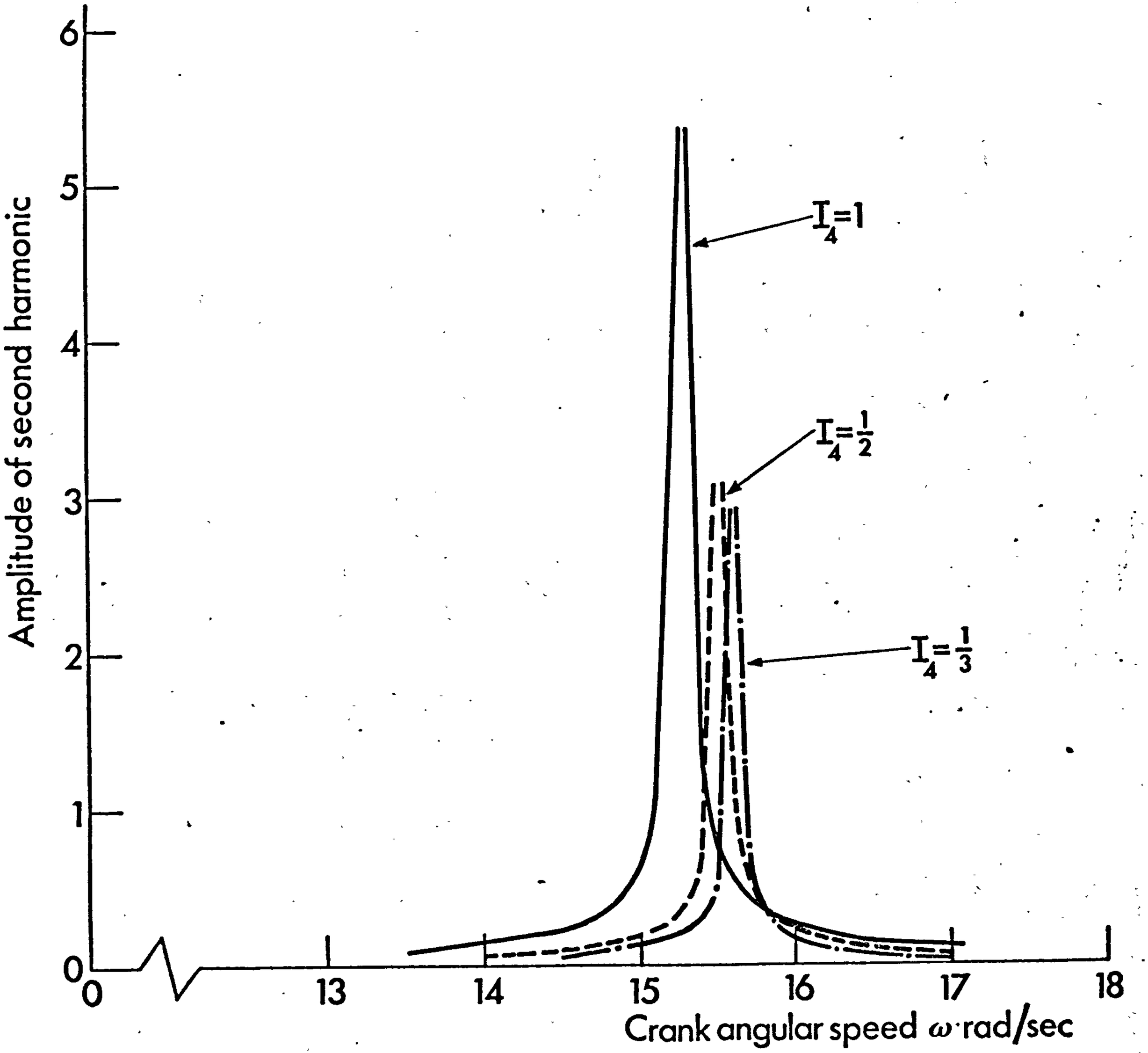

Fig(4.4): AMPLITUDE OF SECOND HARMONIC VERSUS CRANK ANGULAR SPEED ω

the oscillating inertia of the rocker. However, as shown in fig. (4.5), this deviation decreases linearly with decrease of inertia ratio I_4 and becomes zero when $I_4 = 0$. In fact for the case $I_4 = 0$ the equation of motion of the slider reduces to a second order linear differential equation describing an idealised spring-mass system. Fig. (4.3) and fig. (4.4) also show that the amplitude of oscillation decreases with decrease of I_4 and that as I_4 increases it widens the region of resonance. It is also clear by comparing the amplitude values in both figures that the first harmonic of the solution is dominant and the second harmonic may be neglected in comparison.

4.5.2 Resonance in the Presence of Damping

Figs. (4.6) and (4.7) show the effect of damping on the amplitude curves for the two values of $I_4 = 1$ and 0.5 respectively. The amplitude of oscillation is not affected, on the scale of the graph, outside the resonance region. The natural frequency decreases slightly with increase of damping. It also shows that a smaller value of damping eliminated resonance for the case of $I_4 = 0.5$ than that for $I_4 = 1$.

4.5.3 Remarks

a) Resonance occurs below the value of $\omega = \sqrt{\frac{k}{m_4+m_5}}$ and $\omega = \frac{1}{2}\sqrt{\frac{k}{m_4+m_5}}$. How much below depends on the value of I_4.

b) The increase in the inertia of the rocker widens the band of resonance and increases the amplitude of oscillation.

c) The viscous damping affects the solution only in the

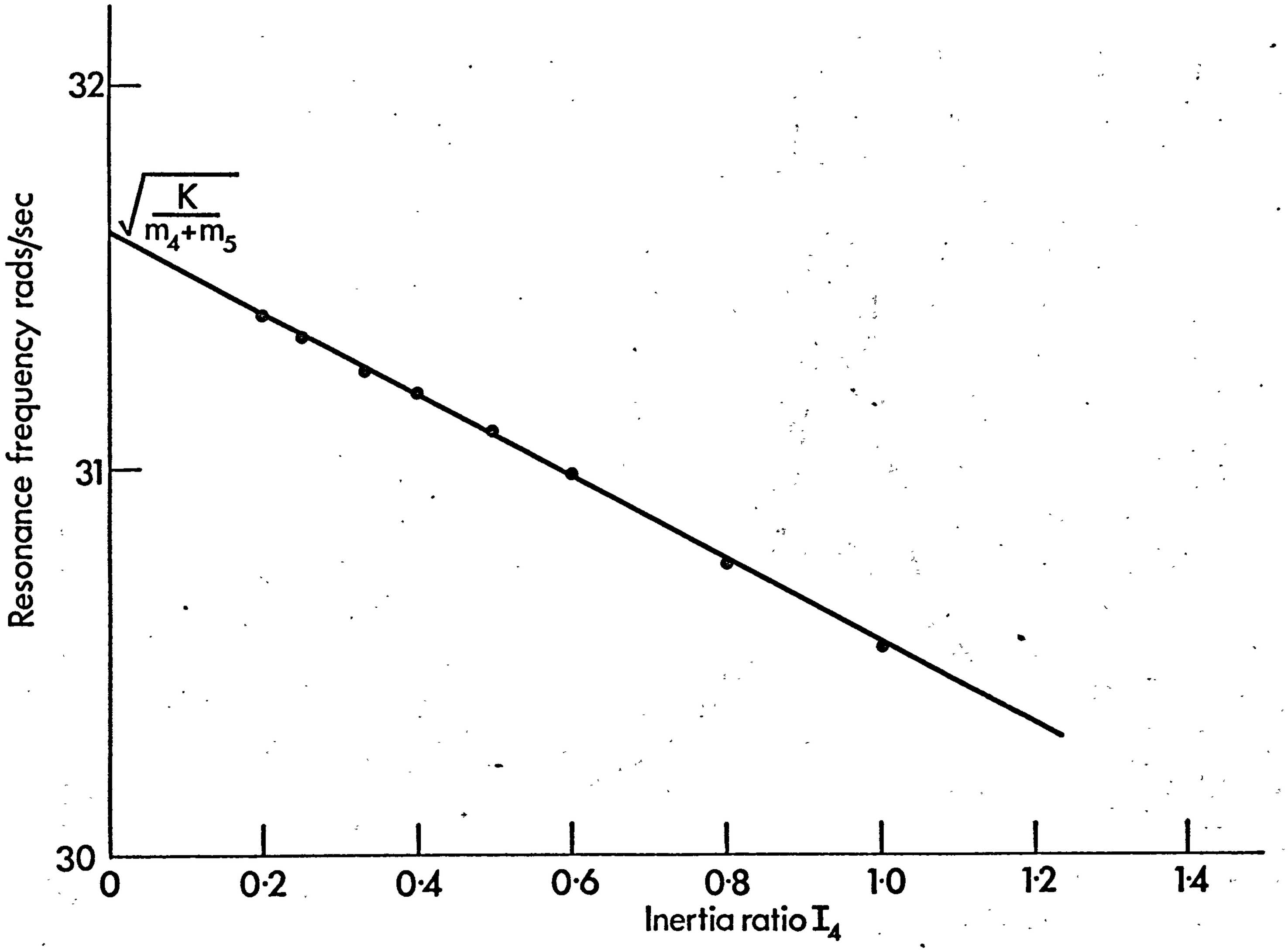

Fig(4.5); VARIATION OF RESONANCE FREQUENCY WITH INERTIA RATIO I_4

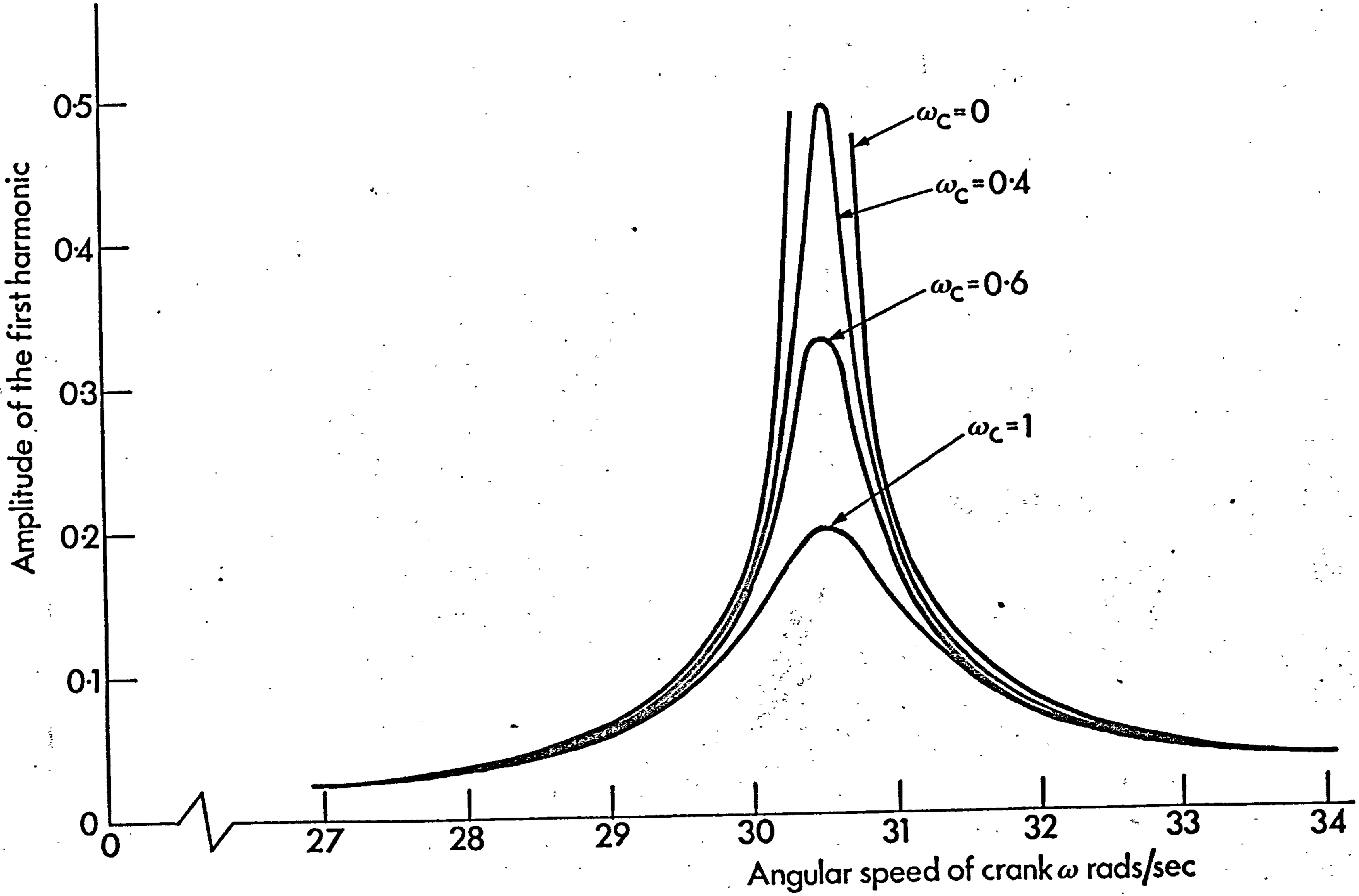

Fig(4.6); EFFECT OF DAMPING ON AMPLITUDE OF FIRST HARMONIC. $I_4=1$

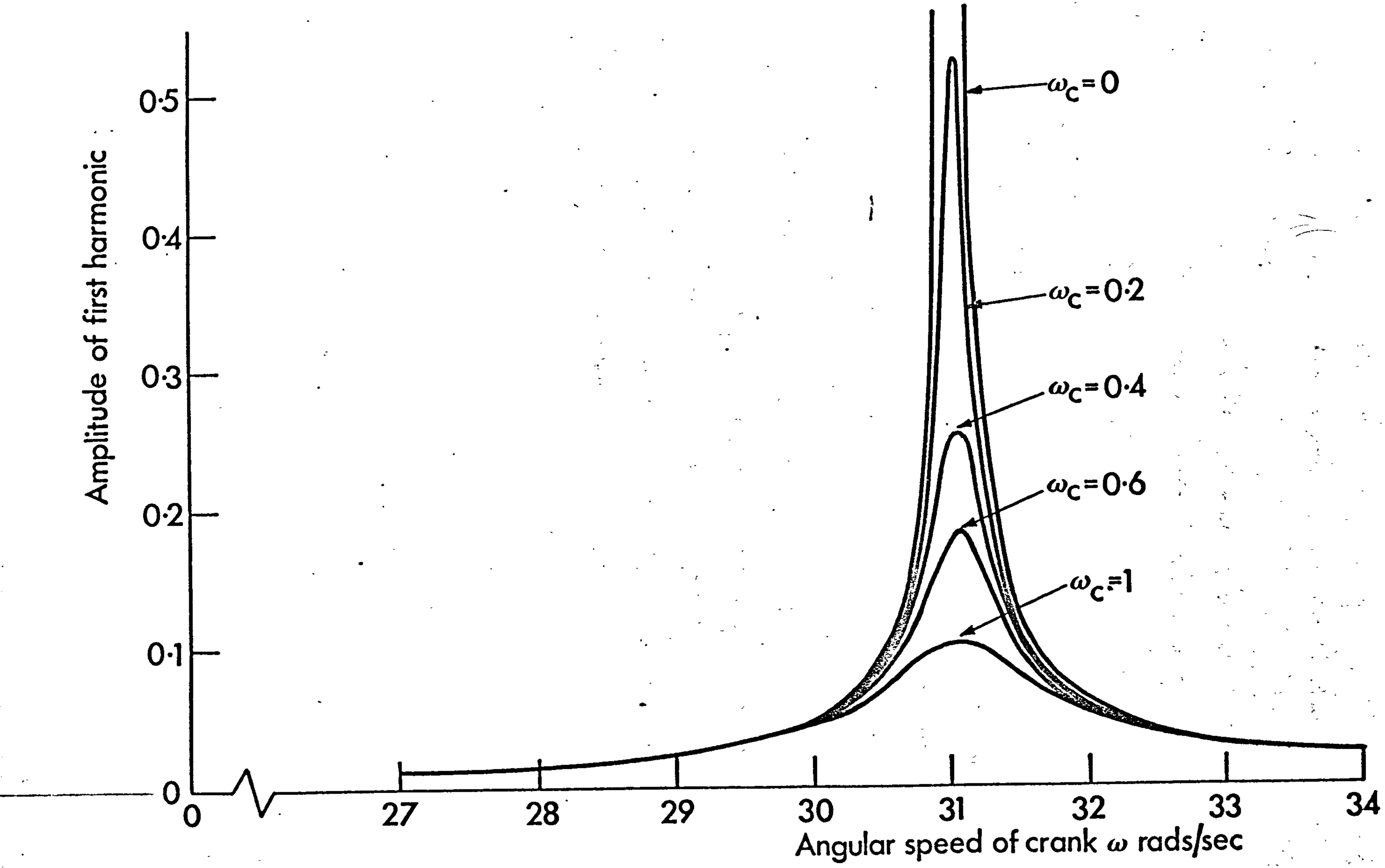

Fig(4.7): EFFECT OF DAMPING ON AMPLITUDE OF FIRST HARMONIC. I_4=0·5

vicinity of resonance.

d) The resonance curves are similar to a second order linear system

e) The dominant harmonic in the solution is the first, the second and higher harmonics are negligible in comparison.

4.6 Computer Programs

4.6.1 Brief Description

Two programs are written - the first deals with the case of no damping and the second with the damping case. Both follow similar steps. They start by calculating the elements of matrix A_{ij} of equation (4.33). They then use Gaussian elimination with error bounds correction to solve this equation for W_j. The crank speed is then incremented to a new value and the solution is repeated. Because of the similarities of the two programs only the second program dealing with the damping case is shown in Appendix 2.

Chapter V

STABILITY ANALYSIS

The stability problem is usually more difficult than the resonance. However there are vaious methods for dealing with it, the most commonly used are the perturbation methods. These methods can become very complex and involved especially when dealing with a large damping factor in the analysis.

We shall therefore study the stability of motion of the slider using a perturbation method for the case of no damping and a general solution substitution computer orientated method for the damping case. The latter will employ an optimisation routine to find the unstable boundaries.

5.1 STABILITY ANALYSIS BY A PERTURBATION METHOD

The stability of equation (4.29) may be investigated by considering the homogeneous part of it only.

5.1.1 No damping $\lambda_c = 0$

The equation of motion reduces to

$$\zeta'' + \{\lambda_1^2 + \lambda_2^2 [(a_1''\cos\theta + b_1''\sin\theta)\varepsilon + (a_2''\cos 2\theta + b_2''\sin 2\theta)\varepsilon^2 + \ldots]$$
$$+ [(a_3\cos\theta + b_3\sin\theta)\varepsilon + (a_4\cos 2\theta + b_4\sin 2\theta)\varepsilon^2 + \ldots]\} \zeta = 0 \quad (5.1)$$

where

$$\lambda_1^2 = \lambda_2^2 + h_o$$
$$\lambda_2^2 = \lambda_k^2 \cdot k_o \quad (5.2)$$

a_1'', b_1'', a_2'' and b_2'' are a_1, b_1, a_2 and b_2 divided by k_o and a_3, b_3, a_4 and b_4 are as defined in (4.26) exactly.

Assume that the solution ζ of (5.1) as well as λ_1^2 can be expanded in series of powers of ε as follows :

$$\zeta = \zeta_o + \varepsilon\zeta_1 + \varepsilon^2\zeta_2 + \ldots. \quad (5.3)$$

$$\lambda_1^2 = \frac{n^2}{4} + \varepsilon\delta_1 + \varepsilon^2\delta_2 + \ldots. \quad (5.4)$$

where λ_1^2 is expanded about the square of half integers i.e. solution is periodic in 2π if n is even and 4π if n is odd.

The quantities δ_1, δ_2, ... are constants and ζ_o, ζ_1, ζ_2, ... are unknown functions of θ to be determined such that there exists a periodic solution of ζ. Inserting equation (5.3) and (5.4) into (5.1) and assuming that the coefficients of all powers of ε vanish; we obtain the following relationships.

$$\zeta_o'' + \frac{n^2}{4}\zeta_o = 0 \tag{5.5}$$

$$\zeta_1'' + \frac{n^2}{4}\zeta_1 = -\{\delta_1 + (\frac{n^2}{4} - h_o)(a_1''\cos\theta + b_1''\sin\theta) + (a_3\cos\theta + b_3\sin\theta)\}\zeta_o \tag{5.6}$$

$$\begin{aligned}\zeta_2'' + \frac{n^2}{4}\zeta_2 = -\{ & [\delta_2 + \delta_1(a_1''\cos\theta + b_1''\sin\theta) + (\frac{n^2}{4} - h_o)(a_2''\cos\theta + b_2''\sin 2\theta) \\ & + (a_4\cos 2\theta + b_4\sin 2\theta)]\zeta_o \\ & + [\delta_1 + (\frac{n^2}{4} - h_o)(a_1''\cos\theta + b_1''\sin\theta) + (a_3\cos\theta + b_3\sin\theta)]\zeta_1\end{aligned} \tag{5.7}$$

from (5.5) it may be written

$$\zeta_o = \beta_o \cos\frac{n}{2}\theta + \gamma_o \sin\frac{\theta}{2} \tag{5.8}$$

where β_o and γ_o are arbitrary constants.

Substituting this equation in (5.6) and rearranging, we obtain,

$$\begin{aligned}\zeta_1'' + \frac{n^2}{4}\zeta_1 = & -\delta_1(\beta_o\cos\tfrac{n}{2}\theta + \gamma_o\sin\tfrac{n}{2}\theta) - \tfrac{1}{2}(\tfrac{n^2}{4} - h_o)\Big\{(a_1''\beta_o - b_1''\gamma_o)\cos(\tfrac{2+n}{2})\theta \\ & + (a_1''\beta_o + b_1''\gamma_o)\cos(\tfrac{2-n}{2})\theta + (a_1''\gamma_o + b_1''\beta_o)\sin(\tfrac{2+n}{2})\theta \\ & + (a_1''\gamma_o + b_1''\beta_o)\sin(\tfrac{2-n}{2})\theta\Big\} - \tfrac{1}{2}\Big\{(a_3\beta_o - b_3\gamma_o)\cos(\tfrac{2+n}{2})\theta \\ & + (a_3\beta_o + b_3\gamma_o)\cos(\tfrac{2-n}{2})\theta + (a_3\gamma_o + b_3\beta_o)\sin(\tfrac{2+n}{2})\theta \\ & + (-a_3\gamma_o + b_3\beta_o)\sin(\tfrac{2-n}{2})\theta\Big\}.\end{aligned} \tag{5.9}$$

In order that ζ_1 be periodic it is necessary that the coefficients of $\cos\frac{n}{2}\theta$ and $\sin\frac{n}{2}\theta$ vanish,

(a) <u>The case of n = 0 i.e. the zero region of instability.</u>

The solution of equation (5.5) may be written as

$$\zeta_o = \beta_o .$$

Since β_o is arbitrary we may write

$$\zeta_o = 1. \tag{5.10}$$

Substituting this equation in (5.6), then in order that ζ_1 be periodic we must have

$$\delta_1 = 0.$$

The corresponding solution of ζ_1 is then

$$\zeta_1 = (a_3 - h_o.a_1'')\cos\theta + (b_3 - h_o.b_1'')\sin\theta + (NI), \tag{5.11}$$

where (NI) is a constant.

Substituting (5.11) in (5.7), then in order that ζ_2 be periodic we must have

$$\delta_2 = (a_3 - h_o.a_1'')^2 + (b_3 - h_o b_1'')^2. \tag{5.12}$$

Therefore from (5.2), (5.4) and (5.12) we obtain

$$\lambda_k^2 = \frac{1}{k_o}\left(\left[(a_3 - h_o a_1'')^2 + (b_3 - h_o b_1'')^2\right]\varepsilon^2 - h_o \right) \tag{5.13}$$

Notice that (5.13) results from the second approximation i.e. from terms involving the second power of ε. Also notice that a region was not obtained but merely a boundary of two stable regions.

(b) <u>The case of n = 1 i.e. the first region of instability.</u>

Substituting (5.8) into (5.9), and applying the condition of periodicity, we obtain

$$\left[2\delta_1 + (\tfrac{1}{4} - h_o)a_1'' + a_3\right]\beta_o + \left[(\tfrac{1}{4} - h_o)b_1'' + b_3\right]\gamma_o = 0$$

and (5.14)

$$\left[(\tfrac{1}{4} - h_o)b_1'' + b_3\right]\beta_o + \left[2\delta_1 - (\tfrac{1}{4} - h_o)a_1'' - a_3\right]\gamma_o = 0.$$

Equating the determinant of the above system to zero, we obtain

$$\delta_1 = \pm\frac{1}{2}\left(\left[(\tfrac{1}{4} - h_o)a_1'' + a_3\right]^2 + \left[(\tfrac{1}{4} - h_o)b_1'' + b_3\right]^2 \right)^{1/2} \tag{5.15}$$

Therefore from (5.2), (5.4) and (5.15), a region for λ_k^2 may be defined by :

$$\frac{1}{k_o}\left\{\left(\frac{1}{4}-h_o\right)-\frac{\varepsilon}{2}\sqrt{\left[\left(\frac{1}{4}-h_o\right)a_1''+a_3\right]^2+\left[\left(\frac{1}{4}-h_o\right)b_1''+b_3\right]^2}\right\} \le \lambda_k^2 \le \frac{1}{k_o}\left\{\left(\frac{1}{4}-h_o\right)+\frac{\varepsilon}{2}\sqrt{\left[\left(\frac{1}{4}-h_o\right)a_1''+a_3\right]^2+\left[\left(\frac{1}{4}-h_o\right)b_1''+b_3\right]^2}\right\} \tag{5.16}$$

in which the system is unstable.

(c) <u>The case of n = 2 i.e. the second region of instability</u>.

Substituting equation (5.8) into (5.9) and demanding that ζ_1 be periodic we obtain

$$\delta_1 = 0, \tag{5.17}$$

and

$$\zeta_1''+\zeta_1 = -\frac{1}{2}\left\{(N_1\beta_o+N_2\gamma_o)+(N_1\beta_o-N_2\gamma_o)\cos 2\theta+(N_2\beta_o+N_1\gamma_o)\sin 2\theta\right\}, \tag{5.18}$$

where

$$N_1 = (1-h_o)a_1''+a_3 , \tag{5.19}$$

and

$$N_2 = (1-h_o)b_1''+b_3 .$$

Hence

$$\zeta_1 = -\frac{1}{2}(N_1\beta_o+N_2\gamma_o)+\frac{1}{6}\left\{(N_1\beta_o-N_2\gamma_o)\cos 2\theta+(N_2\beta_o+N_1\gamma_o)\sin 2\theta\right\} + \beta_1\cos\theta+\gamma_1\sin\theta . \tag{5.20}$$

Substituting equation (5.20) into (5.7) and applying the condition of periodicity on ζ_2, i.e. coefficients of $\cos\theta$ and $\sin\theta$ must vanish, we obtain :

$$\left[\delta_2 + \frac{N_2^2 - 5N_1^2}{12} + \frac{M1}{2}\right]\beta_o + \left[\frac{M2}{2} - \frac{N_1N_2}{2}\right]\gamma_o = 0,$$

and (5.21)

$$\left[\frac{M_2}{2} - \frac{N_1N_2}{2}\right]\beta_o + \left[\delta_2 + \frac{N_1^2 - 5N_2^2}{12} - \frac{M_1}{2}\right]\gamma_o = 0,$$

where $M_1 = (1-h_o)a_2'' + a_4$, (5.22)

and $M_2 = (1-h_o)b_2'' + b_4$.

Equations (5.21) may now be written as

$$[\delta_2 + P]\beta_o + [Q]\gamma_o = 0,$$

and (5.23)

$$[Q]\beta_o + [\delta_2 + R]\gamma_o = 0.$$

where,

$$P = \frac{N_2^2 - 5N_1^2}{12} + \frac{M_1}{2},$$

$$R = \frac{N_1^2 - 5N_2^2}{12} - \frac{M_1}{2} \quad \text{and} \quad Q = \frac{M_2}{2} - \frac{N_1N_2}{2}. \tag{5.24}$$

For non trivial solutions of (5.23) its determinant must vanish i.e.

$$(\delta_2 + P)(\delta_2 + R) - Q^2 = 0$$

which gives,

$$\delta_2 = -\frac{P+R}{2} \pm \frac{1}{2}\left[(P+R)^2 + 4Q^2\right]^{1/2}. \tag{5.25}$$

From equations (5.2), (5.4) and (5.25) the second region of instability may now be defined by :-

$$\frac{1}{k_o}\left[(1-h_o) - \varepsilon^2\left\{\frac{P+R}{2} + \frac{1}{2}\sqrt{(P+R)^2 + 4Q^2}\right\}\right] \leq \lambda_k^2 \leq$$

(5.26)

$$\frac{1}{k_o}\left[(1-k_o) - \varepsilon^2\left\{\frac{P+R}{2} - \frac{1}{2}\sqrt{(P+R)^2 + 4Q^2}\right\}\right]$$

5.2 Stability Analysis in the Presence of Damping.

5.2.1 Stability Analysis using a Substitution Method.

Equation (4.29) may be written in the form

$$\zeta'' + \psi_1(\theta)\zeta' + \psi_2(\theta)\zeta = 0, \tag{5.27}$$

where $\psi_1(\theta)$ and $\psi_2(\theta)$ are periodic functions of time.

Let

$$\zeta = \chi\, e^{-\frac{1}{2}\int \psi_1(\theta)\, d\theta} \tag{5.28}$$

Then by substituting (5.28) into (5.27) we obtain

$$\chi'' + \left(\psi_2 - \frac{1}{2}\frac{d\psi_1}{d\theta} - \frac{\psi_1^2}{4}\right)\chi = 0. \tag{5.29}$$

Equation (5.29) may now be expanded and written as :-

$$\chi'' + \left\{\left[\lambda_k^2.k_o + h_o - \frac{1}{4}k_o^2.\lambda_c^2\right] + \varepsilon\left[g_1(\theta)\right] + \varepsilon^2\left[g_2(\theta)\right] + \ldots\right\}\chi = 0. \tag{5.30}$$

It is clearly seen that regions of instability of the above system will resemble those obtained for the case of no damping but shifted by a small amount represented by the second order quantity of $\frac{1}{4}\lambda_c^2.k_o^2$ in (5.30). However, all solutions of this equation are multiplied by the factor $e^{-\frac{1}{2}\int \psi_1(\theta)d\theta}$ as shown in (5.28).

It may be appreciated by examining the above that an analysis to determine the regions of instabilities can become tedious. Therefore, we shall turn to a more sophisticated and computer oriented approach to analyse the stability when damping is present.

5.2.2 Stability Analysis using a Computer Orientated Method.

Let the solution of the characteristic equation (5.27) be expanded in a series such

$$\zeta = e.^{\lambda\theta} \sum_{m=o}^{n} \left[X_m.\mathrm{Cos}\tfrac{m}{2}\theta + Y_m\mathrm{Sin}\tfrac{m}{2}\theta\right] \tag{5.31}$$

where λ the characteristic component is complex, i.e.,

$$\lambda = s_1 + i\, s_2 \tag{5.32}$$

To investigate the stability of the solution it is enough to locate the boundaries between stable and unstable regions. At the boundary the value of the real part of λ i.e. s_1 is zero and therefore λ becomes

$$\lambda = i\, s_2 \tag{5.33}$$

By substituting this value of λ into (5.27) and equating the coefficients of the trignometric functions and the constant terms to zero, a system of equations may be obtained as follows:

$$\left[C_{ij}\right] \left[W_j\right] = 0. \tag{5.34}$$

where $\left[W_j\right]$ is a column vector $(X_o, X_1, Y_1, \ldots X_n, Y_n)$ and $\left[C_{ij}\right]$ is a square matrix of complex elements and is a function of s_2 and the crank speed ω.

If the system of equations (5.34) is to have a solution other than trivial the determinant of the matrix $\left[C_{ij}\right]$ must vanish, i.e.

$$\text{Det.} \quad \left[C_{ij}\right] = 0.$$

This means that

$$\begin{aligned} \text{Real} \quad & \{\det\left[C_{ij}\right]\} = 0 \\ \text{Imaginery} & \{\det\left[C_{ij}\right]\} = 0 \end{aligned} \tag{5.35}$$

The values of ω and s_2 that satisfy equations (5.35) determine the boundaries of the unstable regions. These values are obtained using "The Simplex"* ; which is an optimisation

* The details of the Simplex and its merits will be discussed in Chapter VI Section 6.2.1; see also Section 5.4 at the end of this chapter.

method that minimises in here the absolute values of the real and imaginery parts of the determinant. For a particular mechanism the method is capable of giving all the boundaries of the unstable regions without any extra work. This, if compared with the perturbation methods which require lengthy treatment for each region, is both useful and favourable.

5.3 RESULTS

To illustrate the theory discussed earlier, let us consider the linkage of fig. (4.2) and assume that;

(i) the mass and inertia of the coupler are negligible, and

(ii) the centre of gravity of the rocker lies on the centre line of the slider.

5.3.1 Stability in The Absence of Damping.

Fig. (5.1) shows the first region of instability in $\lambda_k^2 = \frac{\omega_k^2}{\omega^2}$ with varying I_4. The input data is

$$\rho_{45} = 0.2, \sigma_2 = 0.05, \sigma_3 = 1.$$

As is clearly seen the region is narrow and its width increases with increase of I_4. The region in λ_k^2 as a band also increases linearly with I_4 indicating that instability occurs when $\omega = A.\omega_k$ with $A = 2$ when $I_4 = 0$ and decreasing with increase of I_4.

Fig. (5.2) shows the first region of instability in λ_k^2 with varying σ_2. The input data is

$$\sigma_3 = 1, \ \rho_{45} = 0.2, \ I_4 = \frac{1}{2} .$$

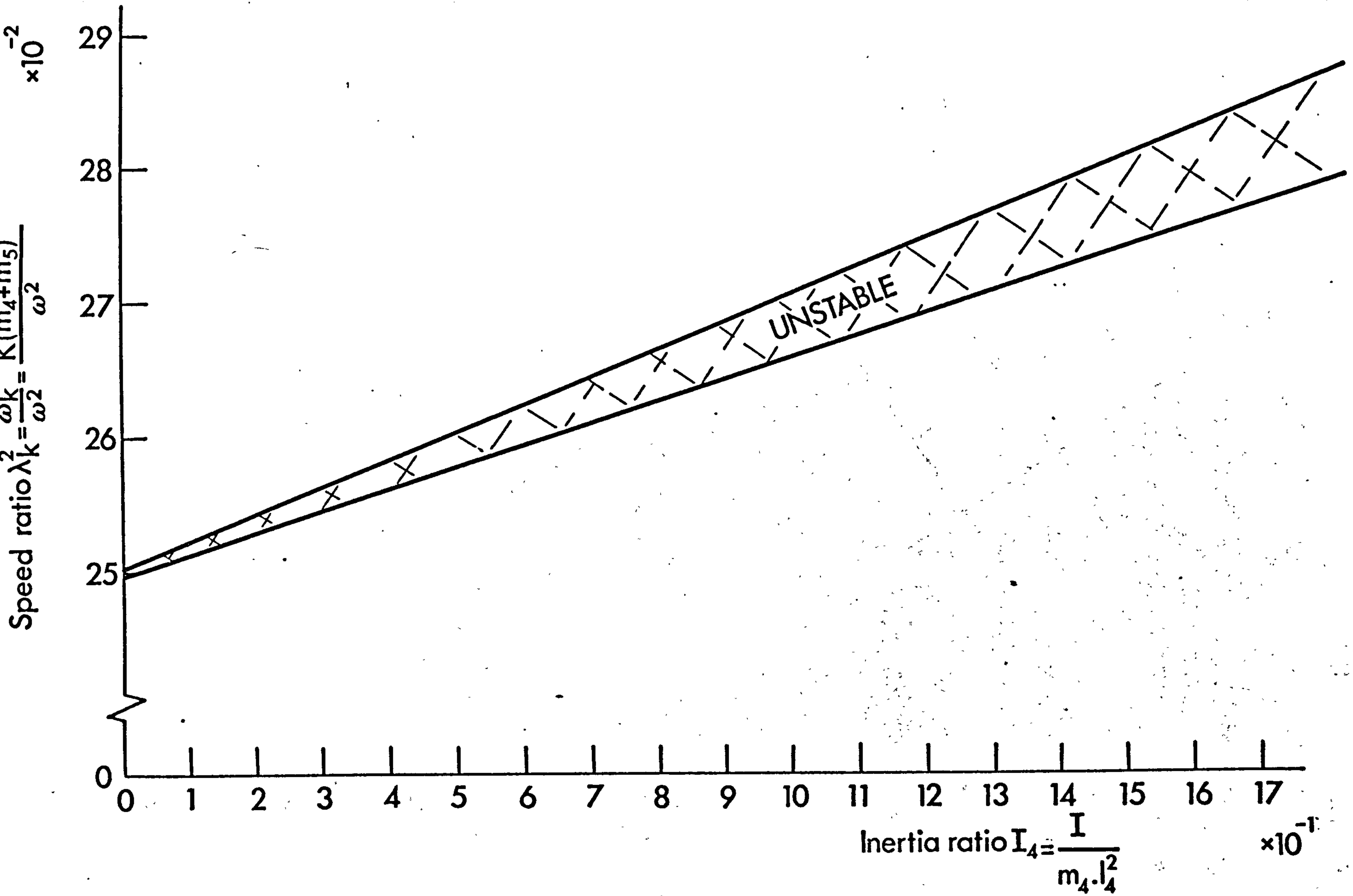

Fig(5.1); THE FIRST REGION OF INSTABILITY IN λ_k^2 VERSUS THE INERTIA RATIO I_4

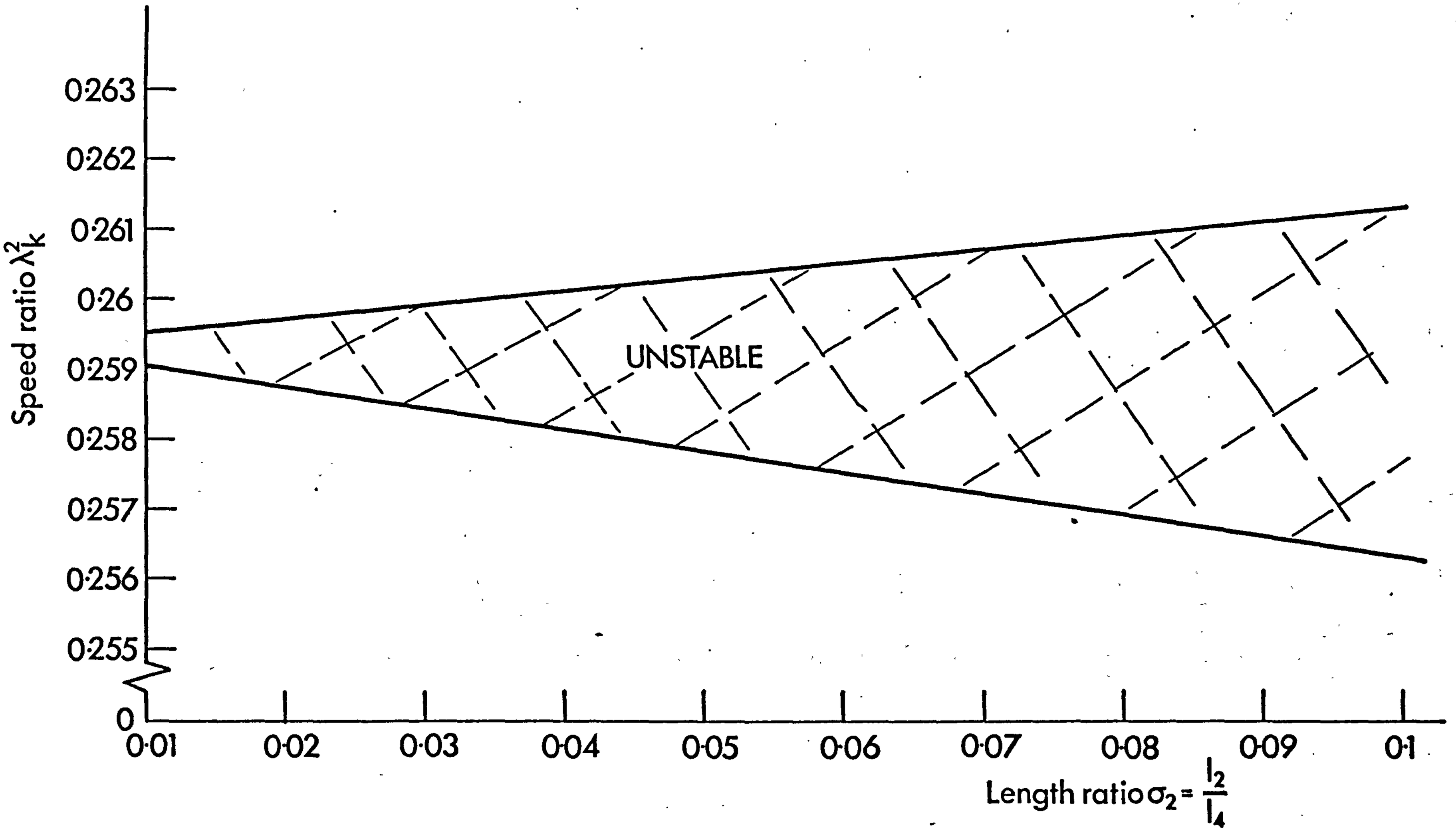

Fig(5.2); THE FIRST REGION OF INSTABILITY IN λ_k^2 VERSUS THE LENGTH RATIO σ_2

The width of the region increases with increase of σ_2. However the region diverges about an axis approximately given by $\omega = A.\omega_k$ where A = 1.968 when σ_2 = O.Ol and increasing very slightly with increase of σ_2. The region is narrower than that of Fig. (5.1).

Fig. (5.3) shows the first region of instability in λ_k^2 with varying σ_3. The input data is

$$\sigma_2 = 0.05,\ \rho_{45} = 0.2,\ I_4 = \frac{1}{2}$$

The width of the region decreases with increase of σ_3. It also converges about an axis given by $\omega = A.\omega_k$ where A = 1.96 when σ_3 = 0.8 and stays approximately constant with increase of σ_3. This region is narrower than both regions of Figs. (5.1 and (5.2).

In all the above examples the second region of instability was so small within the values of σ_2, σ_3 and I_4 it was negligible.

5.3.2 Stability in The Presence of Damping.

Fig. (5.4) shows the first region of instability in λ_k^2 versus the inertia ratio I_4 for different values of $\omega_c = \frac{\mu}{m_4 + m_5}$. As would be expected the region is decreased in width as ω_c is increased. It is also shifted to the right with increase of ω_c and is completely eliminated anywhere within I_4 = O to 1.5 for the value of ω_c = 0.45.

The instability regions shown in figs. (5.2) and (5.3) were also completely eliminated for the values of ω_c = 0.45 anywhere within σ_2 = 0.001 to 0.1 and σ_3 = 0.8 to 1.2 respectively.

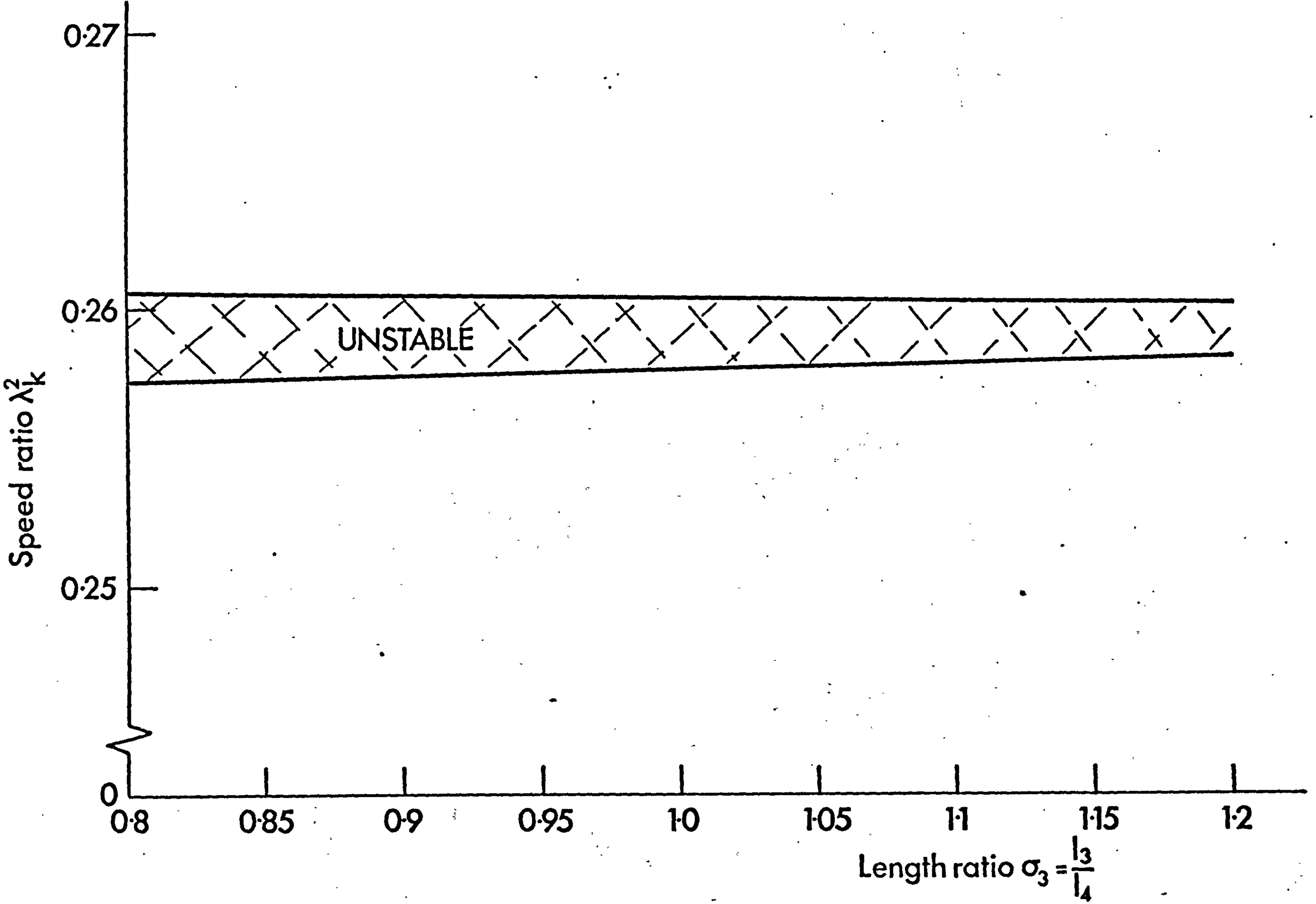

Fig(5.3); THE FIRST REGION OF INSTABILITY IN λ_k^2 VERSUS THE LENGTH RATIO σ_3

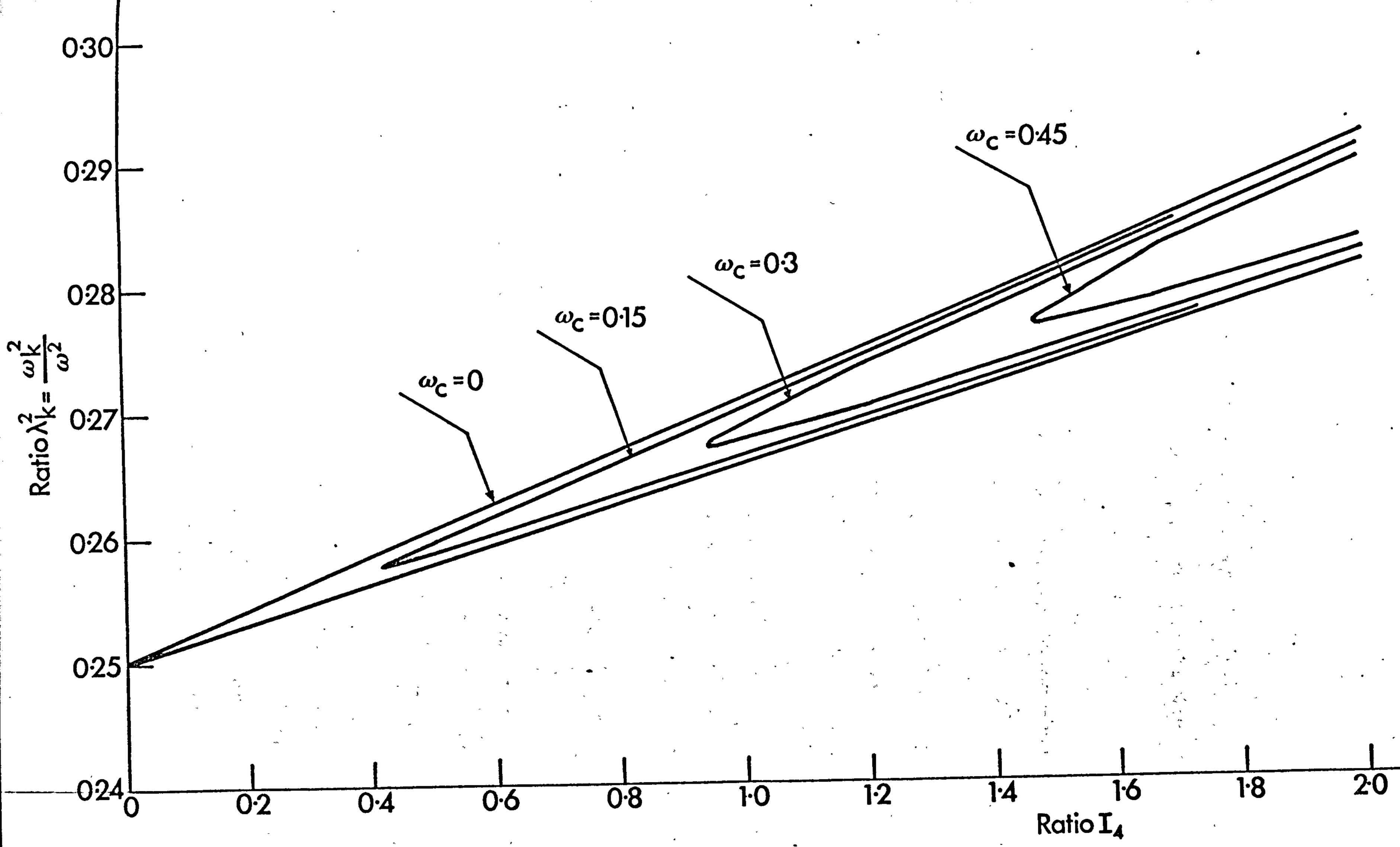

Fig(5·4); THE FIRST REGION OF INSTABILITY IN THE PRESENCE OF DAMPING

In all the above examples the solution for ζ described in equation (5.31) was truncated after the ninth term.

5.3.3. Remarks

a) The stability of the linkage under study increased with increase of the coupler length and decrease of the crank length and vice versa.

b) The stability decreased with increase of the rocker inertia. Also as this inertia was increased instability occurred further below the value of $\omega = 2\omega_n$.

c) Viscous damping had a stabilising effect. It was also possible to choose a value for this damping making the linkage under study completely stable for all ranges of speeds.

d) The computer orientated method provided a fast method for solving the stability problem.

e) The computer orientated method gave results which are in good agreement with the perturbation method; see the outer boundary of fig. (5.4) and fig. (5.1).

5.4 COMPUTER PROGRAMS

Two programs were written- the first dealing with the perturbation method without damping and the second dealing with damping using the computer orientated method. The first program, which is shown in Appendix 3, is relatively simple because it only evaluates the constant relationships described

in equations (5.16) and (5.26). However, the second program, which is shown in Appendix 4, is complex; it makes use of the Harwell library in order to evaluate the value of the complex determinant. It also uses the subroutine "simplx" which is fully explained and listed in Part III, Chapter VI.

The Harwell routines are not listed but may be obtained from the Harwell Atomic Energy Authority under the title "Harwell Subroutines Library". The routines employed are included in the call statement of subroutine NMA23CD.

Real double precision arithmetic was used throughout the perturbation method and complex double precision throughout the computer orientated method.

P A R T I I I

OPTIMISATION AND CONTROL

Chapter VI

PARAMETER OPTIMISATION

The versatility of introducing control principles into the study of mechanisms is enormous. However, in most cases, the practical applications become subject to the importance of the role played by the mechanism. It is feasible to introduce minor changes in the construction and mode of operation of mechanisms to give major versatility and adaptability. The extent of modifications that can be introduced to existent linkages may, in some ways, be limited while future ones may prove to be in demanding necessity for design and control different to what is classically acceptable.

In this part of the thesis we shall firstly establish a method for the optimisation of a mechanism parameters such as length and initial position, to achieve a desired output. This output will be assumed a path independent of or dependent on time. Secondly, we shall study ways of controlling the mechanism inputs in order to achieve an output.

6.1 STRATEGY

Optimisation techniques are widely used in control theory. Of these techniques, multivariable search methods are often employed in non-linear problems where the gradient of the objective or quality function is difficult to determine. In mechanisms it is often found that the kinematic analysis yields

a set of non-linear equations the solution of which may be obtained only by iteration or complicated mathematical analysis. The outputs are often required as functions of some of the variable parameters in the kinematic equations or independent of them as in position only dependent outputs. It is clear therefore that in the synthesis the quality function may take the form of an implicit function of the linkage parameters, which then makes the evaluation of its gradient complicated and hence makes the choice of multi-variable direct search methods most attractive.

Now we have determined the type of methods to be used we shall proceed to define the problem.

6.2 PROBLEM DEFINITION AND QUALITY FUNCTIONS

6.2.1 The desired output

Let us consider a desired output in the form

$$\underset{\sim}{\theta}_o^* = \phi(\underset{\sim}{\theta}_{in}) \qquad (6.1)$$

where $\underset{\sim}{\theta}_o^*$ is the desired output expressed as a function of inputs $\underset{\sim}{\theta}_{in}$. This may take several forms which include coupler curves; time dependent or independent and link angular rotations. In all the cases that follow we shall call the task of achieving a desired output dependent on time as function generation and that independent of time as path generation. In function generation the desired output may be stated as :-

$$\phi_1^* (x,y,t) = 0, \qquad (6.2)$$

while in path generation

$$\phi_2^* (x,y) = 0. \tag{6.3}$$

In both cases the coordinates (x,y) defining the actual output position in cartesian coordinates are functions of the controlling parameters. If the analytic relations for the desired output are not determinable equations (6.2) and (6.3) may be replaced by their equivalent numerical relations.
In the case of a desired angular rotation we shall consider function generation only; this may be written as

$$\phi_3^*(\theta,t) = 0. \tag{6.4}$$

where θ is the actual angular output.

6.2.2 The quality function

In function generation it is sufficient to consider the error as the summation of the squares or absolute values of the linear distances between desired and actual outputs over a discrete number of points N. These points are specified in both position and time within one output cycle. This may be stated in general as :

$$E_1 = \sum_{j=1}^{N} (\phi_j^* - \phi_j)^2 \tag{6.5}$$

$$\text{or} \qquad E_1^* = \sum_{j=1}^{N} \left|\phi_j^* - \phi_j\right|$$

where ϕ_j^* and ϕ_j are the desired and actual outputs at instance j respectively. In coupler curve generation the summation of the squares of the instantaneous positional error thus takes the form

$$E_{lp} = \sum_{j=1}^{N} \left[(x_j^* - x_j)^2 + (y_j^* - y_j)^2 \right] \qquad (6.6)$$

where (x_j^*, y_j^*) are values of (x,y) that satisfy equation (6.2) at instance j.

Similarly in angular function generation the same summation is expressed as

$$E_{la} = \sum_{j=1}^{N} (\theta_j^* - \theta_j)^2 \qquad (6.7)$$

where θ_j^* is the value of θ that satisfies equation (6.4) at instance j.

If the above quality functions are minimised they ensure that the mechanism will achieve the discrete desired output at the specified times with minimum positional error.

In path generation it is clear that minimisation of the above quality function would yield a minimum error. It does, however, impose the unnecessary condition that the mechanism pass the desired points at the specified times. This is no longer required and it is sufficient to minimise the area between the desired and actual output curves. This area may be stated as

$$E_2 = \sum_{i=1}^{q} \left| \int\int_{S_i} dA \right| \qquad (6.8)$$

where q is the numberof enclosed areas between the desired and actual outputs, S_i is the surface of one enclosure, i = 1, 2, ------q and dA is an element in the surface S_i. A finite approximation of this relation is obtained by taking a large and equal number of points on the desired and actual curves.

Triangular areas are then constructed using these points and the total area E_2 is taken as the summation of the absolute values of these areas.

A modified quality function may be formulated as a combination of (6.5) and (6.8). An approximation to the desired output may, therefore, be obtained by taking both function and path generation into consideration. Weighting functions may also be introduced permitting a more accurate generation of certain parts of the output at the expense of the rest.

6.2.3 The constraints

In linkages, the kinematic equations (loop closure) may be written as

$$f_i\ (\Theta_1, \ldots\ldots \Theta_n) = 0 \quad i = 1 \ldots\ldots s \leq n \tag{6.9}$$

which form a set of equality constraints implicit in time. Together with the external constraints imposed by the designer

$$h_i \leq P_i \leq H_i \qquad i = 1, \ldots . n \tag{6.10}$$

where P_i are the linkage parameters and h_i and H_i are their specified lower and upper bounds respectively, they form the complete set of constraints imposed on the problem.

The minimisation of the quality functions subject to the constraints stated above represent the complete constrained optimum problem. As will be seen the constraints have to be handled in a manner appropriate to the linkage in question. For instance, the constraints specified in (6.9) are dependent on time implicitly and thus may be satisfied at some instance in time while violated later. Therefore, when possible these

constraints should be transformed to equivalent forms that are time independent. This often saves tedious work and time in computer applications.

6.3 OPTIMISATION

6.3.1 Optimisation routine

The Simplex method as described in ref. (17) is chosen (ref. 18) and modified to accommodate the constraints. Essentially the method consists of constructing a geometric shape of (M + 1) apexes, where M is the number of parameters to be optimised. This shape, for example, is a triangle if M = 2 and a tetrahedron if M = 3. Initially, the method is provided with (M + 1) sets of values of the parameters to be optimised corresponding to (M + 1) apexes. It then evaluates the quality function for each of these apexes and reflects the apex with maximum quality function value through the centroid of the remaining apexes. This yields a new set of values for the parameters. The method continues in this manner halving or doubling the reflection action depending upon increase or decrease in quality function values. The method stops when a convergence criterion is satisfied and is said then to have located a minimum . It must be recognised, as in all optimisation methods, that this located minimum may not be a global minimum. It is therefore necessary to begin the optimisation from as many initial points as possible. The various minima thus located are compared and the best is taken as the "Best Located Optimum". In the proceeding work this will be called "The Global Optimum".

It is found that the global optimum is always reached quickly if some of the minima already located are included as initial values in a fresh optimisation cycle. It is also found that the number of minima of the quality function increases with the number of specified output points. A good technique is to find the optimum values of linkage parameters to yield a minimum error over a decreased number of specified output points. These values are then used again in the optimisation but this time taking all the specified output points into consideration. Another useful technique is to perform the optimisation for a decreased number of linkage parameters and to use the values obtained in the initial guesses of the complete optimisation programme. These techniques have, in all cases tried, located the global minimum quickly and efficiently.

In order to generate the different initial sets of parameter values to start the method, it is sufficient to supply one set only. This set must satisfy all the problem constraints. The remaining sets are then obtained using the following equation

$$P_i = h_i + \left[H_i - h_i\right] \cdot \mathrm{Sin}^2\lambda \qquad (6.11)$$

where P_i, h_i and H_i are as defined in equation (6.10) and λ is any real random number. This generates quickly and efficiently all the sets of required initial values and ensures that they satisfy all the explicit externally imposed constraints described in equation (6.10). Each new set obtained through this technique is then tested for violations of the constraint

equations (6.9) and if so, a new set is obtained by moving back quarter the distance towards the centroid of the sets already obtained.

6.3.2 Constraints

As mentioned previously, the constraints specified in equation (6.9) are usually time dependent. It is, therefore, necessary (a) to solve the kinematics for a complete cycle checking they are always satisfied, or (b) to transform these constraints into a more convenient form independent of time.

a) The improved set of linkage parameter values returned from the optimisation routine is used to evaluate the quality function. If at some point in the solution cycle the constraints are violated this improved set is rejected. The Simplex is then instructed to yield a set of values by moving back a quarter the distance between the rejected set (i.e., current set) and the set with maximum quality function value. The move is in a direction towards the centroid of the remaining sets in the current Simplex configuration. The kinematic solution is then restarted from time zero and the process is repeated until the constraints are satisfied.

b) In linkages, it is often possible to transform the time dependent constraints into a more convenient form for digital computer solution. For example, in the four bar link shown in fig. (6.1) the following term

$$c = 4\ell_4^2\ (\ell_1^2+\ell_2^2-2\ell_1\ell_2\cos\omega t)-(\ell_3^2-\ell_4^2-\ell_1^2-\ell_2^2+2\ell_1\ell_2\cos\omega t)^2 \qquad (6.12)$$

appears in the solution of equation (6.9) as a square root

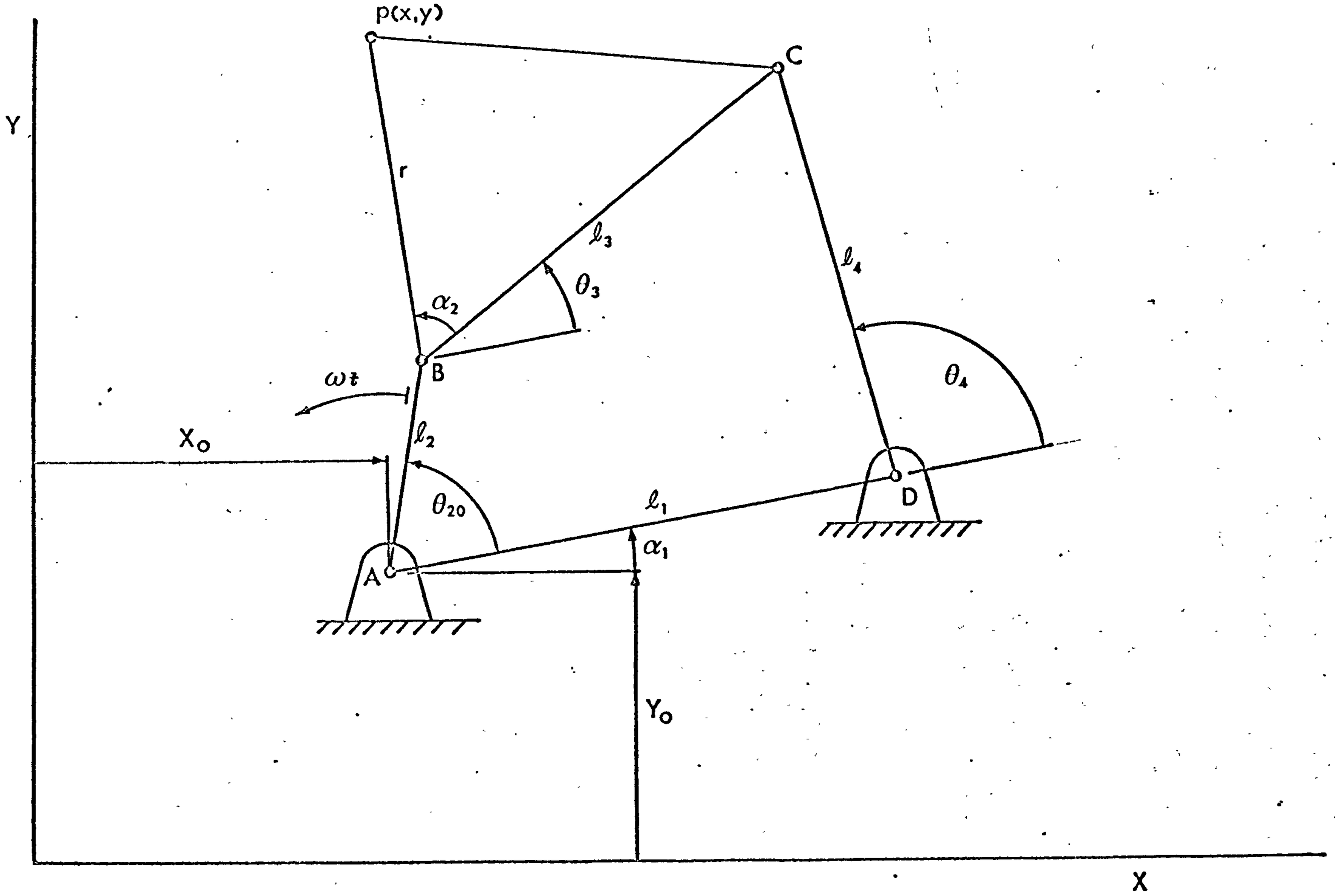

Fig. (6.1) General planar four bar linkage, A B C D.

argument. If this term, denoted by C, is positive or equal to zero, there always exists a solution, i.e., constraints are satisfied. The constraints may, therefore, be stated in the form

$$C \geq 0. \tag{6.13}$$

To check that this inequality is always satisfied it is sufficient to ensure that its minimum value is greater or equal to zero. However, the expression for C is quadratic in Cosωt and the coefficient of its square term is negative. This quadratic has, therefore, one stationary point always yielding a maximum value for C. The minimum occurs when either Cosωt = $\pm$ 1 whichever yields the least value, i.e., the constraints are satisfied when,

$$4\,\ell_4^2\,(\ell_1 \pm \ell_2)^2 - \left[\ell_3^2 - \ell_4^2 - (\ell_1 \pm \ell_2)^2\right]^2 \geq 0 \tag{6.14}$$

As the improved set of parameter values is returned from the simplex, only inequalities (6.10) and (6.14) have to be satisfied. If these inequalities are not satisfied a new set of parameter values is obtained as described previously and the process is repeated.

It is clear that when (a) is used time may be wasted in solving the system equations if the constraints are violated at later stages in the crank cycle. However, (b) is a straightforward evaluation of a constant relation and it is clearly preferable.

6.3.3 Flow chart of the Computer Algorithm

A flow chart of the computer algorithm, which is shown in Appendix 5, is shown in fig. (6.2). The input of the

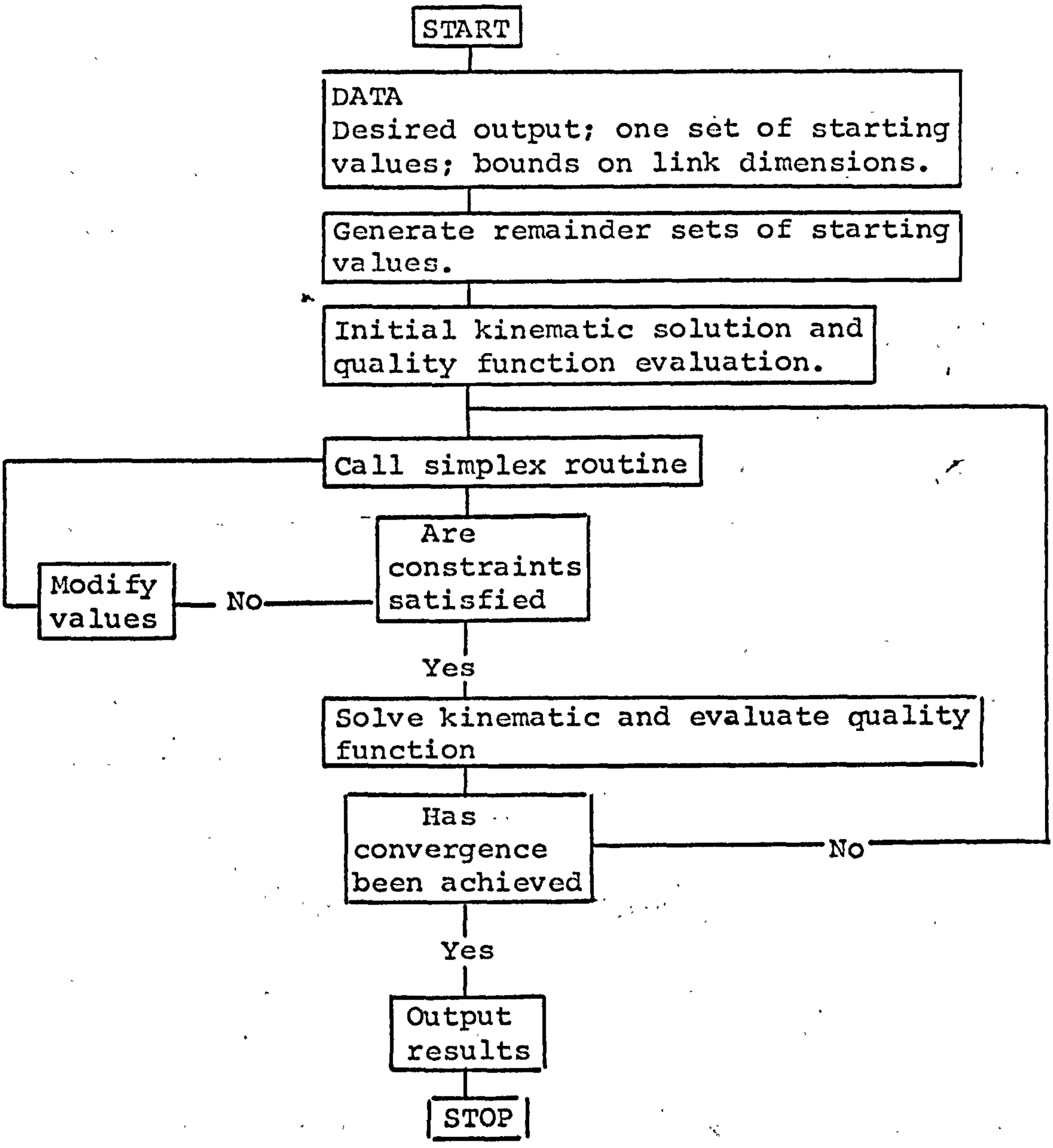

FIG. (6.2) FLOW CHART OF COMPUTER ALGORITHM.

algorithm consists of defined regions of acceptable linkage parameters, one initial guess and the desired output in analytic or numeric form. A subroutine to generate the remaining initial guesses is called and the quality function evaluated at each. The Simplex optimisation routine is then called and an improved set of linkage parameter values are obtained. This set is checked for violation of the constraints, and is modified as previously described. The system equations are then solved and the quality function evaluated. A convergence criterion is called and if it is satisfied the program returns the optimum linkage parameters and the value of the quality function; if not, the process is repeated from the stage of calling the Simplex routine. Convergence is satisfied only when both the quality function and parameter values satisfy the following relations

$$\left| E_{max} - E_{min} \right| \leq \left| \varepsilon . E_{min} \right| \tag{6.15}$$

and

$$\sum_{i=1}^{M+1} \left| P_i(max) - P_i(min) \right| \leq \sum_{i=1}^{M+1} \left| \varepsilon . P_i(min) \right|$$

where E_{max} and E_{min} are the maximum and minimum values of the quality function in the current Simplex, ε is a small error parameter and $P_i(max)$ and $P_i(min)$ are the parameters of the linkage corresponding to E_{max} and E_{min} respectively.

6.4 RESULTS

6.4.1 Consider the four bar linkage shown in fig. (6.1). Assuming rigid links, ideal pin joints and constant crank angular input speed ω the kinematic equations may be written as

$$\begin{aligned} \ell_2 \cos(\omega t+\theta_{2O}) + \ell_3\cos\theta_3 - \ell_4\cos\theta_4 - \ell_1 &= 0 \\ \ell_2 \sin(\omega t+\theta_{2O}) + \ell_3\sin\theta_3 - \ell_4\sin\theta_4 &= 0 \end{aligned} \qquad (6.16)$$

The error or quality function involved in coupler curve function generation from the above linkage may be written, by application of equation (6.6), as the summation

$$\begin{aligned} E_{1p} = \sum_{j=1}^{N} \{ &\left[x^* - (X_o + \ell_2\cos(\omega t+\theta_{2O}+\alpha_1) + r\cos(\alpha_2+\theta_3))\right]^2 \\ &+ \left[y^* - (Y_o + \ell_2\sin(\omega t+\theta_{2O}+\alpha_1) + r\sin(\alpha_2+\theta_3))\right]^2 \} \end{aligned} \qquad (6.17)$$

where N is the number of desired points. The sufficient linkage parameters for the minimisation of the above error are X_o, Y_o, ℓ_1, ℓ_2, ℓ_3, ℓ_4, r, α_1, θ_{2O} and α_2.

In path generation the error involved will be taken as the total area between the desired and actual curves as obtained by a finite approximation using triangular elements. In angular function generation from the rocker link ℓ_4 the error will be taken as the summation

$$E_{1a} = \sum_{j=1}^{N} (\theta_4^* - \theta_4)^2 \qquad (6.18)$$

where N is as defined earlier and θ_4^* and θ_4 are the desired and actual rocker angles in degrees, at point j, respectively. The linkage parameters sufficient for the optimisation in coupler path generation are the same as mentioned earlier for coupler function generation although the parameter θ_{2O} is redundant, in this case, it will be retained to maintain a consistency in presentation of results. The sufficient parameters for rocker

angular output generation are $\ell_1, \ell_2, \ell_3, \ell_4$ and θ_{20}.

In evaluating the quality function in path generation problems may arise in the method of evaluation stated earlier. These problems are best illustrated by the following example. Consider fig. (6.3a)where curve, A, and curve, B, are the desired and actual curves respectively. Let us also assume that the desired curve A is stored as N_1 points of (x,y) values in the order shown in the figure, i.e. clockwise.

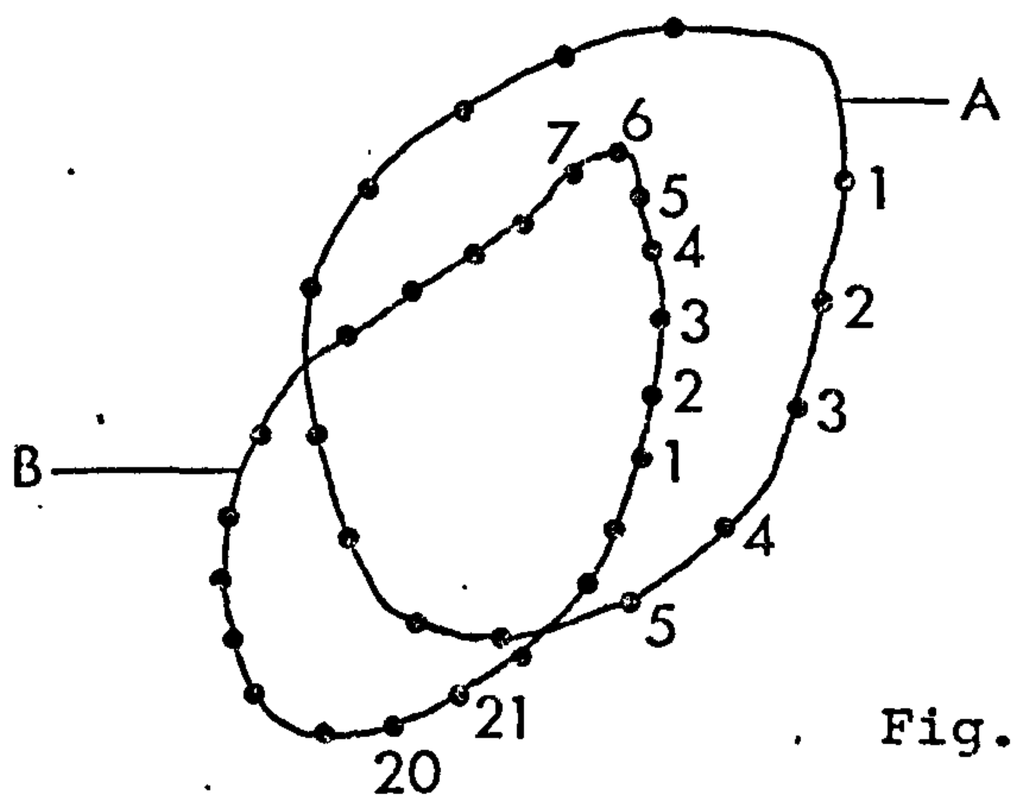

Fig.(6.3a)

Now since our objective is to find the minimum area error between curve A and curve B it is necessary to calculate the actual output at N_2 points where $N_2 >> N_1$. The first problem is that the first point, 1, evaluated on the actual curve may not be near point, 1, on the desired curve. The second problem is that the actual output may be stored in a counter rotational sense to that of the desired output as shown in the figure. And the third problem is that since $N_2 >> N_1$ we must choose N_1 points out of the N_2 points on the actual output in order that the triangular elements method of evaluation of area error may be applied. These points must be chosen such that the area is minimum.

The first problem is solved by scanning for the point on curve B that is nearest to point, 1, on curve A, and then reordering the actual points with this point as point, 1. The second problem is solved by evaluating the error firstly with the actual points stored as shown in the figure and secondly stored in the reverse order. The minimum of either is taken as the value of the quality function. The third problem is subtle and its solution requires a fair amount of curve fitting and logical checks. A detailed solution may be found in Appendix 6, in subroutine area. Briefly we set up a parameter Icp proportional to $\frac{N_2}{N_1}$ and the scatter of the desired points. Next we calculate the distances between Icp actual points, starting from actual point, 2, and the desired point, 2, and scan for the minimum distance. The actual point with minimum distance, which for instance may be point, 5, is then kept and stored in an array as actual point, 2, and paired with desired point, 2. The search is then started from point 5 on the actual curve to find actual point, 3, to be paired with desired point, 3. The process is continued until all the desired points are paired with suitable actual points, and the area error is then computed.

It must be appreciated that two different loop closures may be obtained from the four bar linkage, as shown in fig. (6.3b). Therefore in evaluating the quality function we must explore both closures and note the closure corresponding

to the minimum error in output generation.

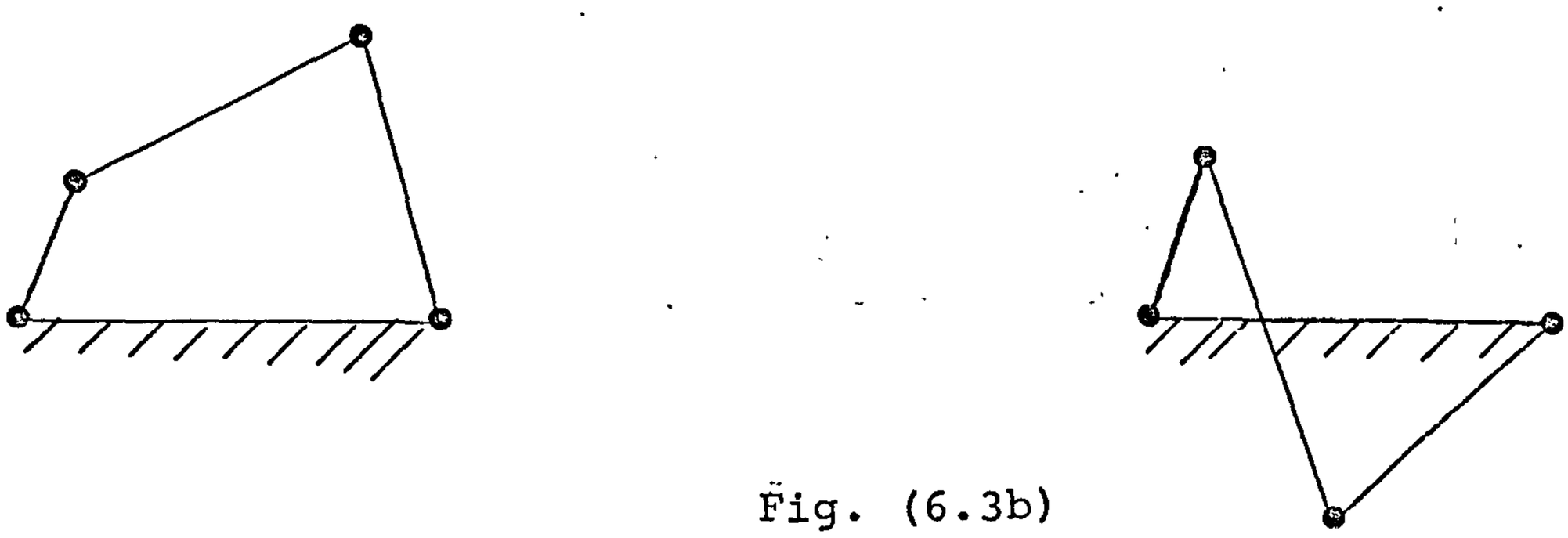

Fig. (6.3b)

In the results that follow all the curves, except those in fig. (6.11), are shown plotted at twenty degrees (20^{o}) intervals of crank angular rotation. The start of each output cycle is marked by $\omega t = 0^{o}$ and increases in an anti-clockwise direction. However, it is important to note that when the crank is at $\omega t = 0^{o}$ the angle between it and the fixed link is θ_{20}.

6.4.2 Function Generation

A) Let the desired output be of the type described in equation (6.2) and expressed as

$$x^* = \beta_1 + \beta_2 \cos\omega t$$
$$y^* = \beta_3 + \beta_4 \sin\omega t \qquad (6.19)$$

where β_1, β_2, β_3 and β_4 are constants. This output is required to be generated from point P(x,y) on the coupler link.

Starting the optimisation from different initial points, a best set of optimum values of the linkage parameters is obtained by comparing the various minima of the error

function E_{lp} shown in equation (6.17). Two example curves are generated here corresponding to

(a) $\beta_1 = 20, \quad \beta_2 = 10, \quad \beta_3 = 15, \quad \beta_4 = 5$

and

(b) $\beta_1 = 20, \quad \beta_2 = 15, \quad \beta_3 = 15, \quad \beta_4 = 5$

in units of cm. The optimisation is performed over 72 points on each of the curves at 5 degree intervals. Figs. (6.4) and (6.5) each show two curves, labelled 1 and 2 corresponding to the desired and actual outputs respectively. It may be seen from fig. (6.4) that the four bar output compares favourably with the desired output and in fact has an error value E_{lp} of 0.889 cm^2. However, as may be seen from fig. (6.5), the four bar is not able to produce output (b) to the same tolerances and has an error E_{lp} of 4.001 cm^2. This error is reduced further by releasing the rocker to ground joint and controlling it in a manner that will be explained in the following chapter. The optimum values of the linkage parameters, link lengths in cm. and angles in degrees are :

for curve 2 of fig. (6.4)

$$\ell_1 = 65.31, \quad \ell_2 = 5.04, \quad \ell_3 = 112.85, \quad \ell_4 = 104.34,$$
$$r = 63.26, \quad X_o = 16.48, \quad Y_o = -47.89, \quad \alpha_1 = -92.82,$$
$$\theta_{20} = 96.26, \quad \alpha_2 = 114.02$$

and for curve 2 of fig. (6.5)

$$\ell_1 = 165.65, \quad \ell_2 = 7.95, \quad \ell_3 = 179.09, \quad \ell_4 = 216.94,$$
$$r = 174.32, \quad X_o = -60.48, \quad Y_o = 169.45, \quad \alpha_1 = -3.44,$$
$$\theta_{20} = -27.05, \quad \alpha_2 = -136.94$$

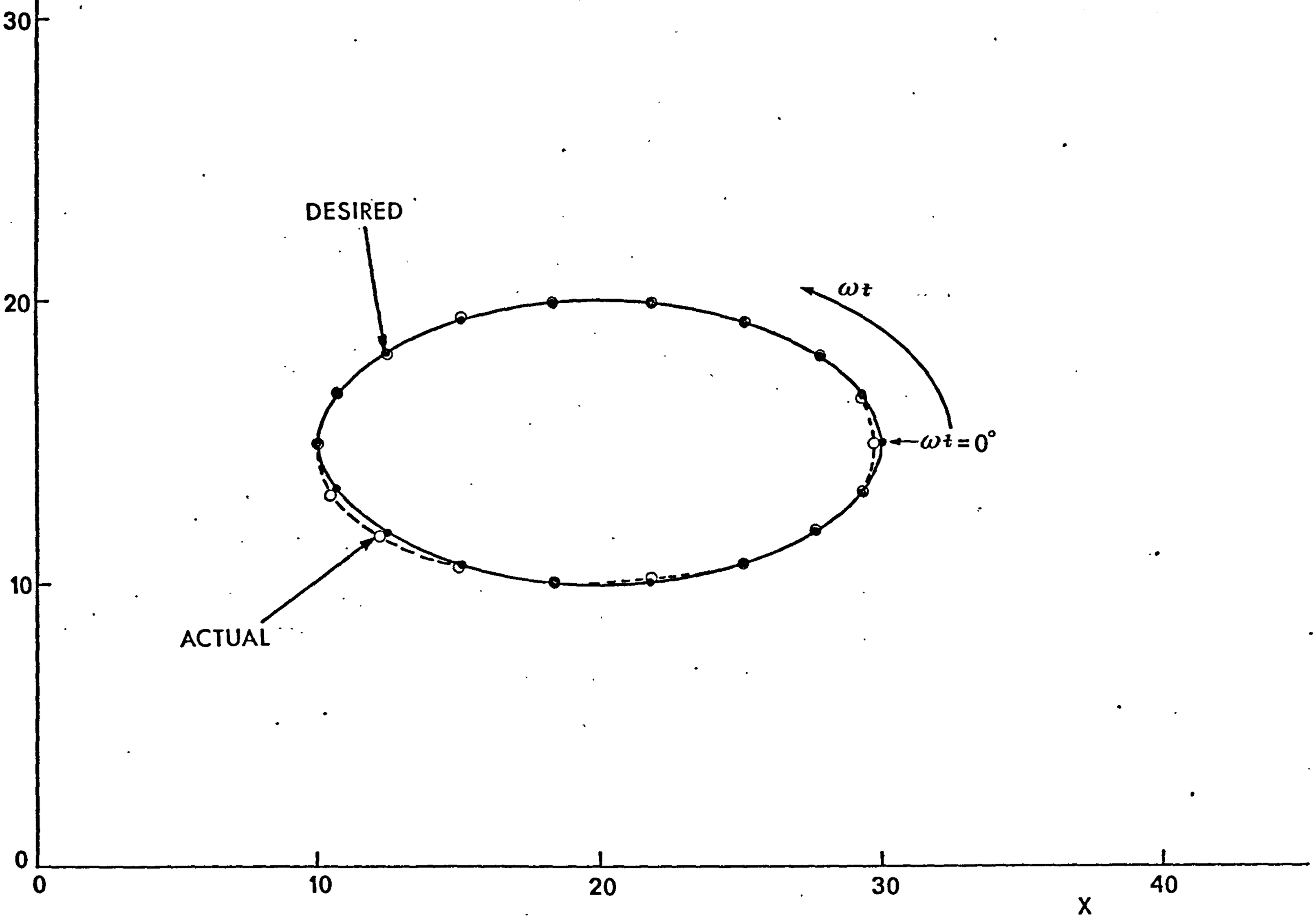

Fig (6·4) DESIRED AND ACTUAL COUPLER CURVES — FUNCTION GENERATION EXAMPLE (a)

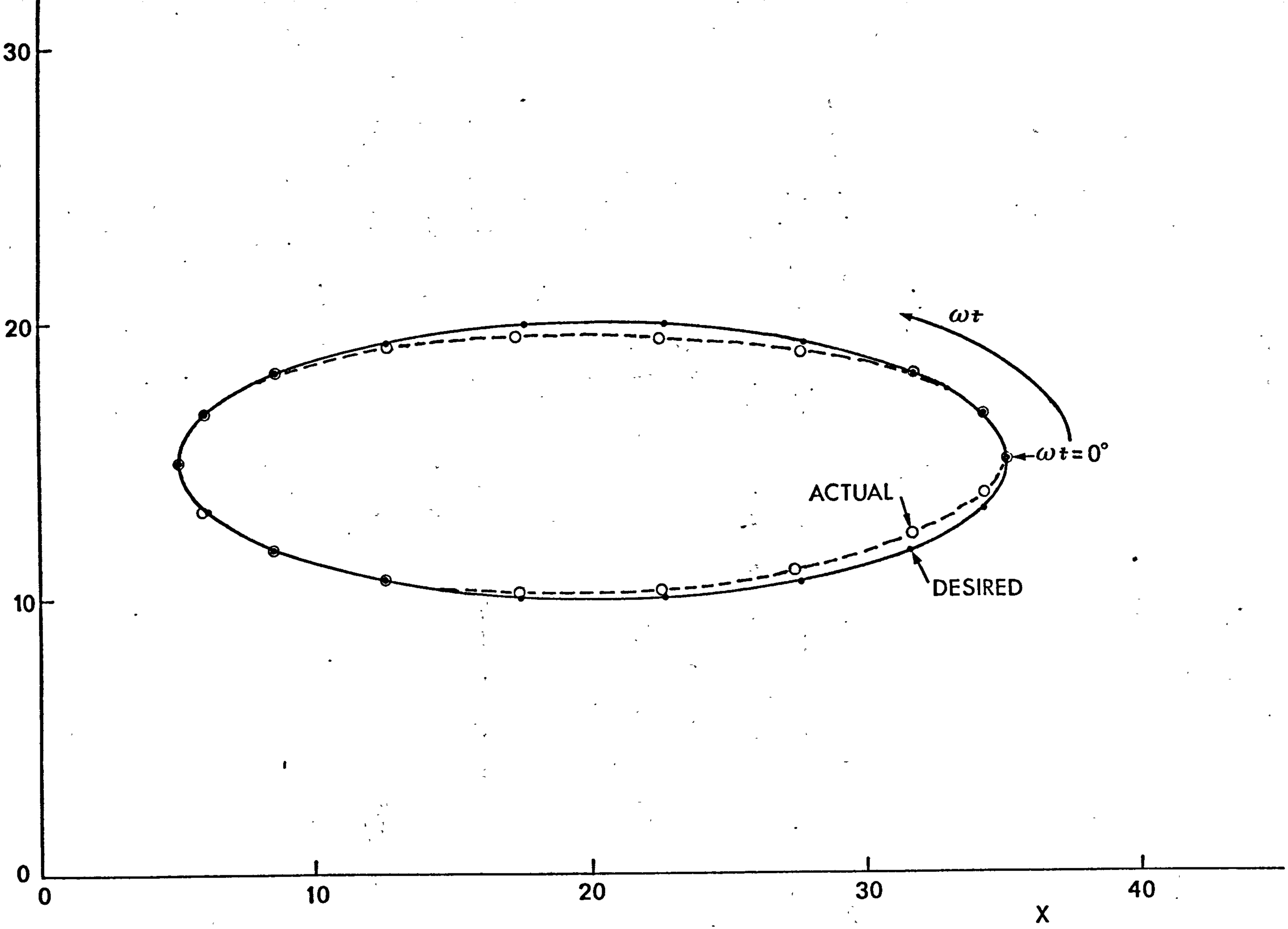

Fig(6·5) DESIRED AND ACTUAL COUPLER CURVES — FUNCTION GENERATION EXAMPLE (b)

The above outputs are obtained with no imposed constraints. If, however, the link dimensions are constrained to have values within a defined range a different linkage is obtained. Let us illustrate this by requiring that output (a) be generated from a four bar linkage with the following constraints

$$10 < \ell_1, \ell_3, \ell_4 < 30$$

$$4 < \ell_2 < 10$$

Fig. (6.6) shows the optimum linkage with its actual output and the desired output. The optimum values of the linkage parameters, link lengths in cm. and angles in degrees are now

$$\ell_1 = 16.4,\ \ell_2 = 5.01,\ \ell_3 = 26.5,\ \ell_4 = 22.0$$

$$r = 15.4,\ X_o = 19.6,\ Y_o = 0.03,\ \alpha_1 = 93.8^o,$$

$$\theta_{2O} = 93.2^o, \alpha_2 = 127.3^o$$

The resulting minimum error is now 53.6 cm^2 which when compared with the error resulting from the unconstrained case gives an increase of 52.7 cm^2.

B) Let the desired output be of the type described by equation (6.4) and expressed as

$$\theta_4^* = \beta_5 + \beta_6 . \left| \text{Sin} \ \frac{\omega t}{2} \right| . \qquad (6.20)$$

where β_5 and β_6 are constants in degrees and θ_4^* is the desired angular output in degrees to be produced from the rocker link ℓ_4. This output is firstly to be produced in whole with no weighting factors and secondly with a weighting factor equal to 1000

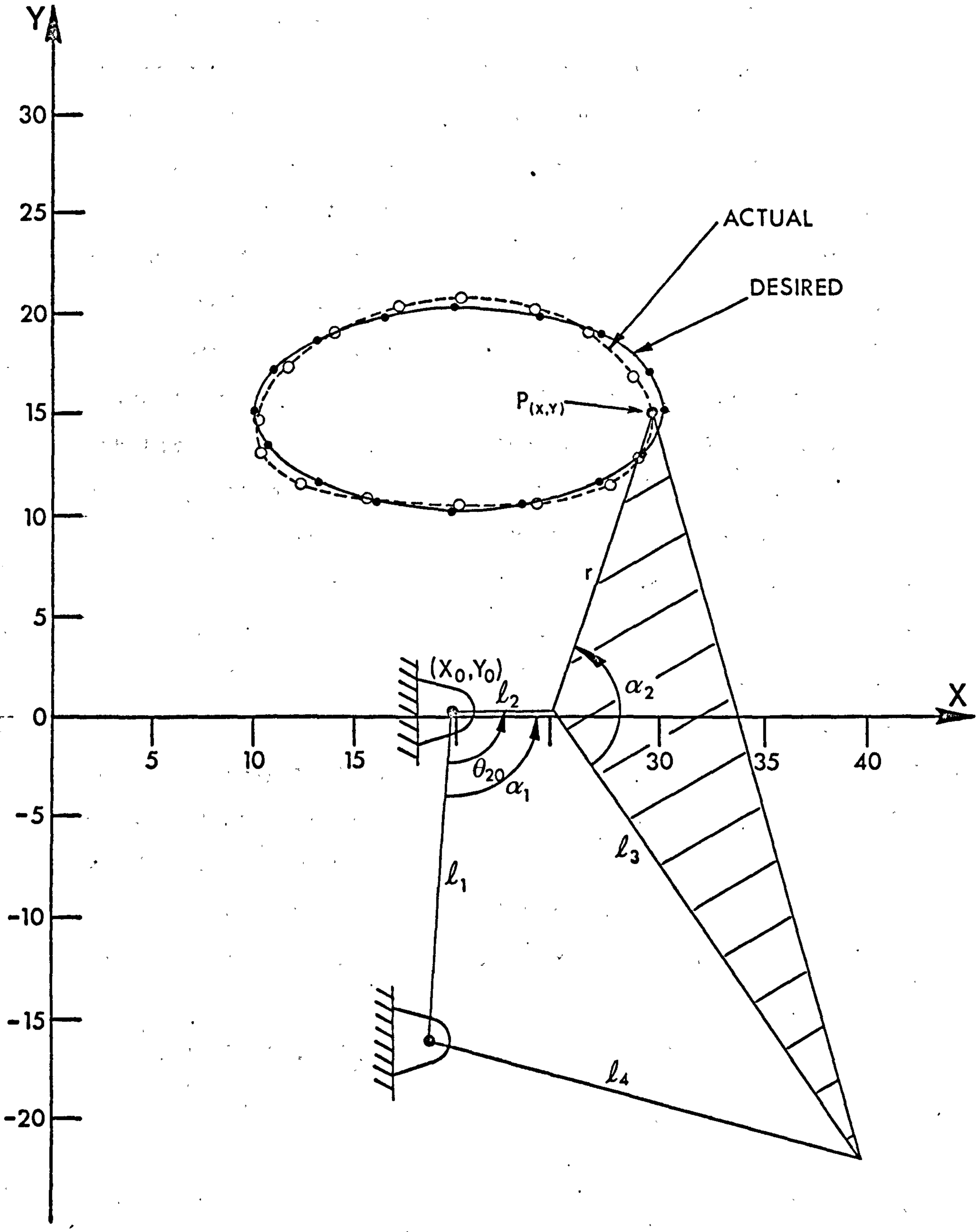

Fig(6·6) OPTIMUM LINKAGE AND DESIRED AND ACTUAL COUPLER CURVES.
FUNCTION GENERATION EXAMPLE (a) EXTERNAL CONSTRAINTS
$10 < \ell_1, \ell_3, \ell_4, < 30$ AND $4 < \ell_2 < 10$

applied on the portion of the output between $60^{o} < \omega t < 260^{o}$. The remaining portions of the output have a weighting factor equal to unity. The results are shown in figs. (6.7) and (6.8) respectively where the curves 1 and 2 describe the desired and actual outputs. The values of the constants β_4 and β_5 of the desired output are 70 and 100 degrees respectively. The values of the error function E_{1a} of equation (6.18) produced by the linkage in generating the unweighted and weighted outputs are 700.0 and 35.0 degree^2 respectively. These are further reduced by releasing and controlling the rocker to ground joint as will be seen in the following chapter. It is clearly seen from the figures that by weighting a portion of the output it is generated closely but at the expense of the remaining portions of the output. This is however acceptable since our interest lies in the weighted portion only. This procedure of weighting factors may be used when outputs in the form of straight lines are required by giving the straight line portion of the output a weighting of unity and the remainder a weighting of zero.

The optimum parameters of the four bar link to produce the unweighted output, link lengths in cms and angles in degrees, are;

$$\ell_1 = 5.083, \quad \ell_2 = 2.615, \ell_3 = 4.148, \ell_4 = 3.75$$

$$\Theta_{20} = 41.88$$

and to produce the weighted output

$$\ell_1 = 15.65, \quad \ell_2 = 6.91, \quad \ell_3 = 11.77, \quad \ell_4 = 11.56,$$

$$\Theta_{20} = 42.74$$

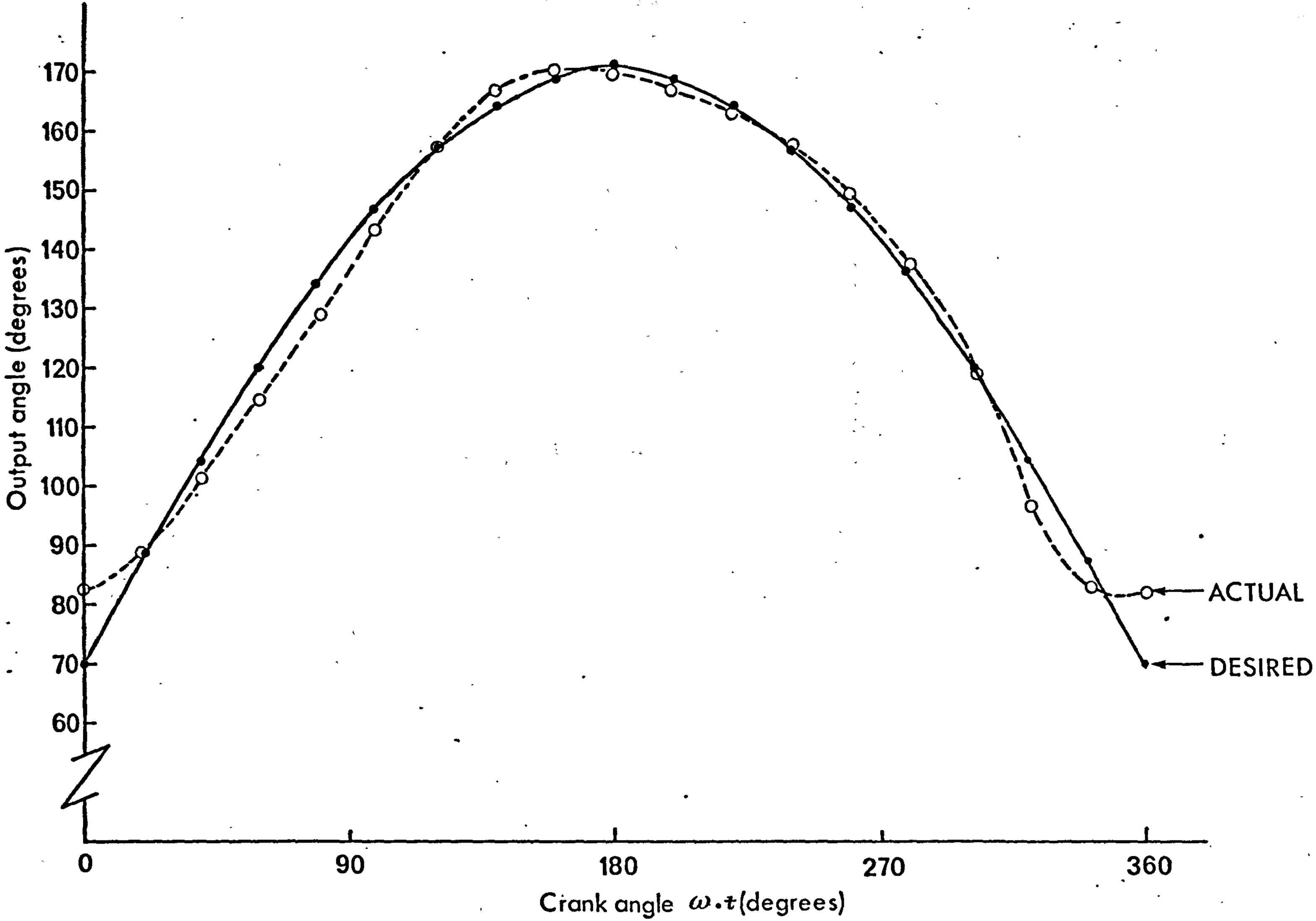

Fig(6·7) DESIRED AND ACTUAL ANGULAR OUTPUTS — FUNCTION GENERATION
UNWEIGHTED OUTPUT GENERATED FROM ROCKER LINK l_4

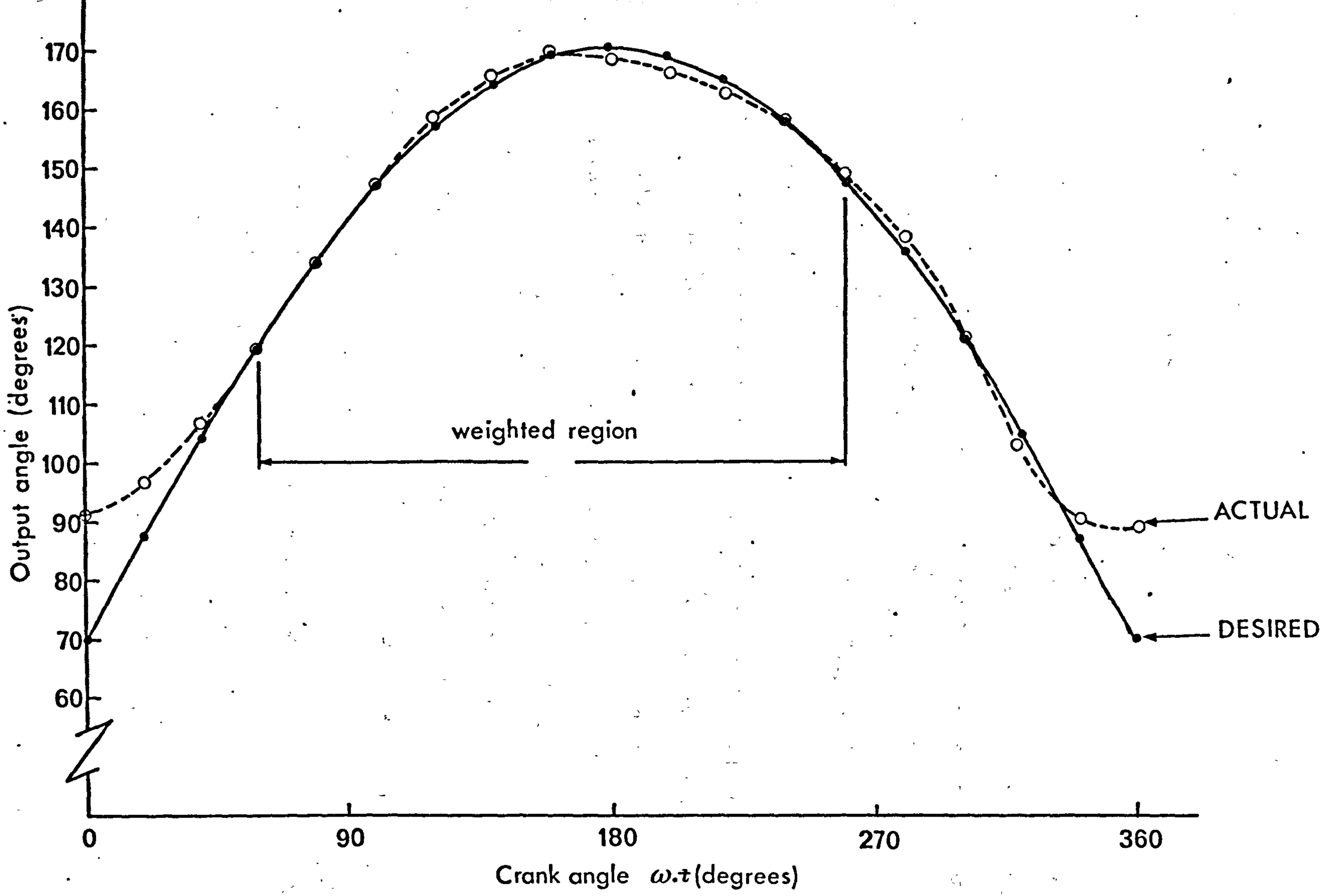

Fig(6·8) DESIRED AND ACTUAL ANGULAR OUTPUTS — FUNCTION GENERATION, WEIGHTED OUTPUT GENERATED BETWEEN 60 AND 260 DEGREES OF CRANK ANGLE ωt

6.4.3 Path Generation

Let the desired output be of the type described in equation (6.3) and expressed as

$$\left(\frac{x^* - \beta_7}{\beta_8}\right)^2 + \left(\frac{y^* - \beta_9}{\beta_{10}}\right)^2 = 1 \qquad (6.21)$$

where β_7, β_8, β_9, β_{10} are constants and x* and y* are the (X,Y) coordinates specifying the desired output. Two examples of this output are shown here corresponding to :

(a) $\beta_7 = 20$, $\beta_8 = 10$, $\beta_9 = 15$, $\beta_{10} = 5$

(b) $\beta_7 = 20$, $\beta_8 = 15$, $\beta_9 = 15$, $\beta_{10} = 5$

in cm units.

The area error between the desired and actual outputs is calculated over 360 points on each of the curves. The results are shown in figs. (6.9) and (6.10) where curves 1 and 2 correspond to the desired and actual outputs respectively. As shown in fig. (6.9) the four bar is able to generate the desired output (a) to within tolerable errors but as shown in fig. (6.10) it is unable to generate the desired output (b) as accurately. The error values involved in the output generation of outputs (a) and (b) are 2.3 and 12.6 cm.^{2} respectively. The optimum values of the four bar linkage parameters, link lengths in cms and angles in degrees, are;

for curve 2 of fig. (6.9)

$\ell_1 = 80.216$, $\ell_2 = 5.03$, $\ell_3 = 139.25$, $\ell_4 = 129.46$

$r = 77.75$, $X_o = 154.85$, $Y_o = -62.54$, $\alpha_1 = -93.22$,

$\theta_{2O} = 100.41$, $\alpha_2 = 113.83$

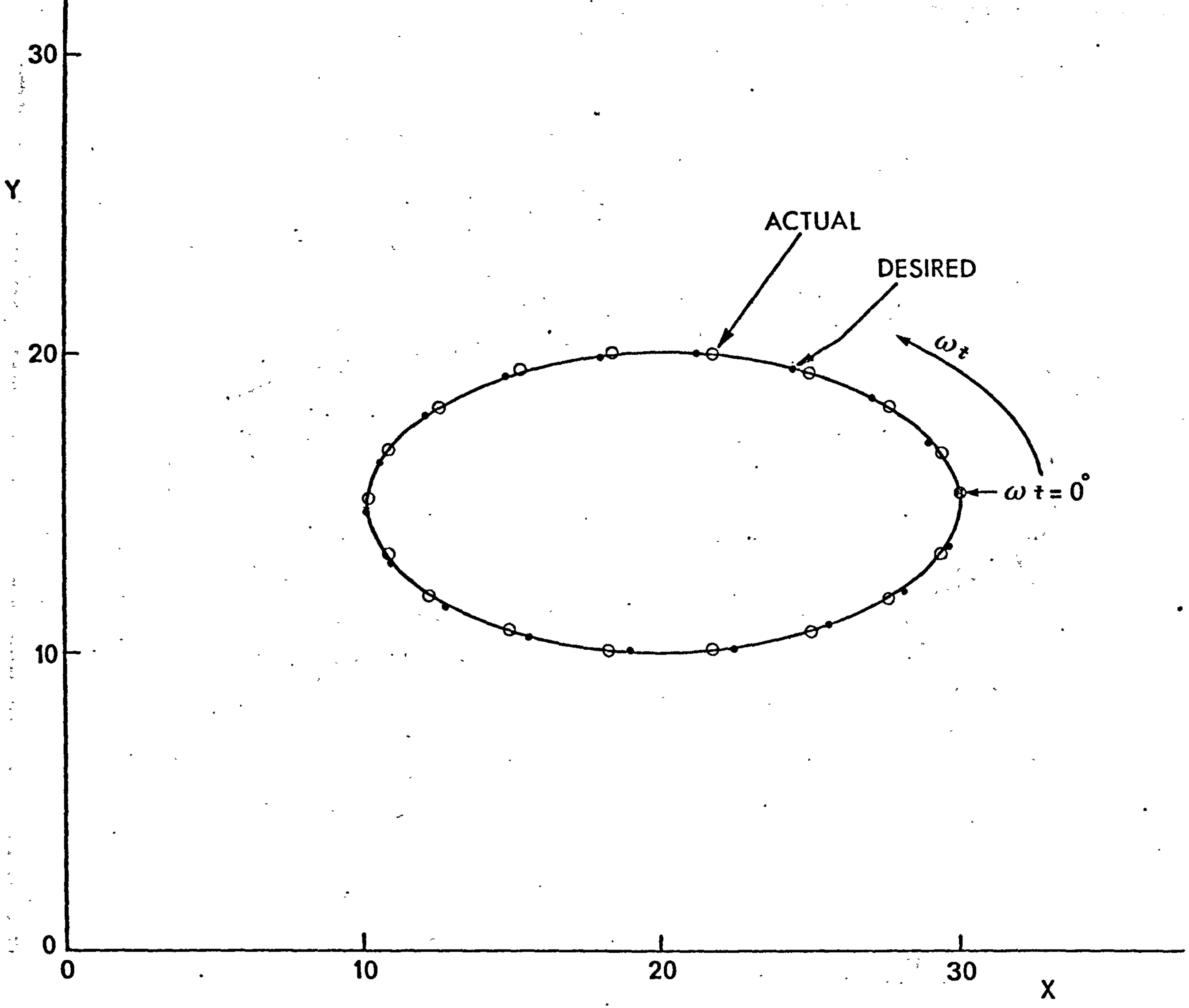

Fig (6·9) DESIRED AND ACTUAL COUPLER CURVES — PATH GENERATION EXAMPLE (a)

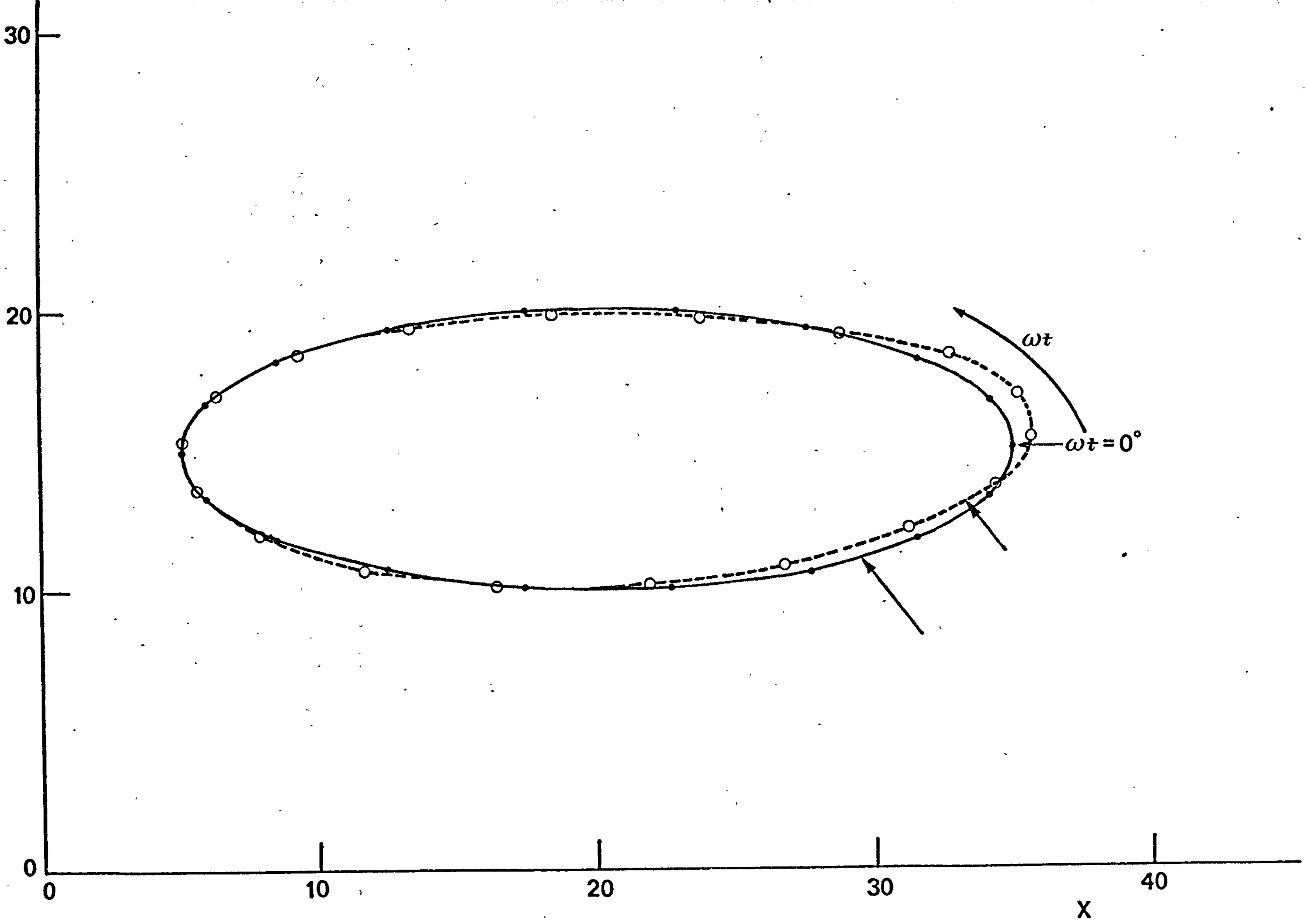

Fig (6·10) DESIRED AND ACTUAL COUPLER CURVES – PATH GENERATION EXAMPLE (b)

and for curve 2 of Fig. (6.10)

ℓ_1 = 142.576, ℓ_2 = 8.18, ℓ_3 = 152.743, ℓ_4 = 183.443,

r = 147.38, X_o = -49.13, Y_o = 144.98, α_1 = -3.062,

Θ_{20} = -31.19^o, α_2 = -136.04^o

A third example of path generation is a factual problem obtained from industry. A packaging machine in the form of a four bar is required to generate a path which is acceptable anywhere within the region bound by the dashed lines shown in Fig. (6.11a). The constraints are (1) the straight line travel AB should be achieved within the first 120^o rotation of the crank and (2) the crank shaft should be below the line of travel of the package.

Nineteen points are chosen on the desired path as shown by the "dots", (•), in Fig. (6.11a). Optimisation is then performed to find the optimum linkage from which 72 actual output points are calculated. The area error is computed by orientating the output specified by these 72 actual points to fit with the desired output specified by the nineteen points, as explained in (6.3.1). The optimum linkage obtained is shown in Fig. (6.11b), and has the following dimensions:

ℓ_1 = 137.54, ℓ_2 = 36.05, ℓ_3 = 134.05, ℓ_4 = 40.06

r = 435.15, X_o = 94.53, Y_o = -48.55, α_1 = 116.73^o

α_2 = 345.01^o.

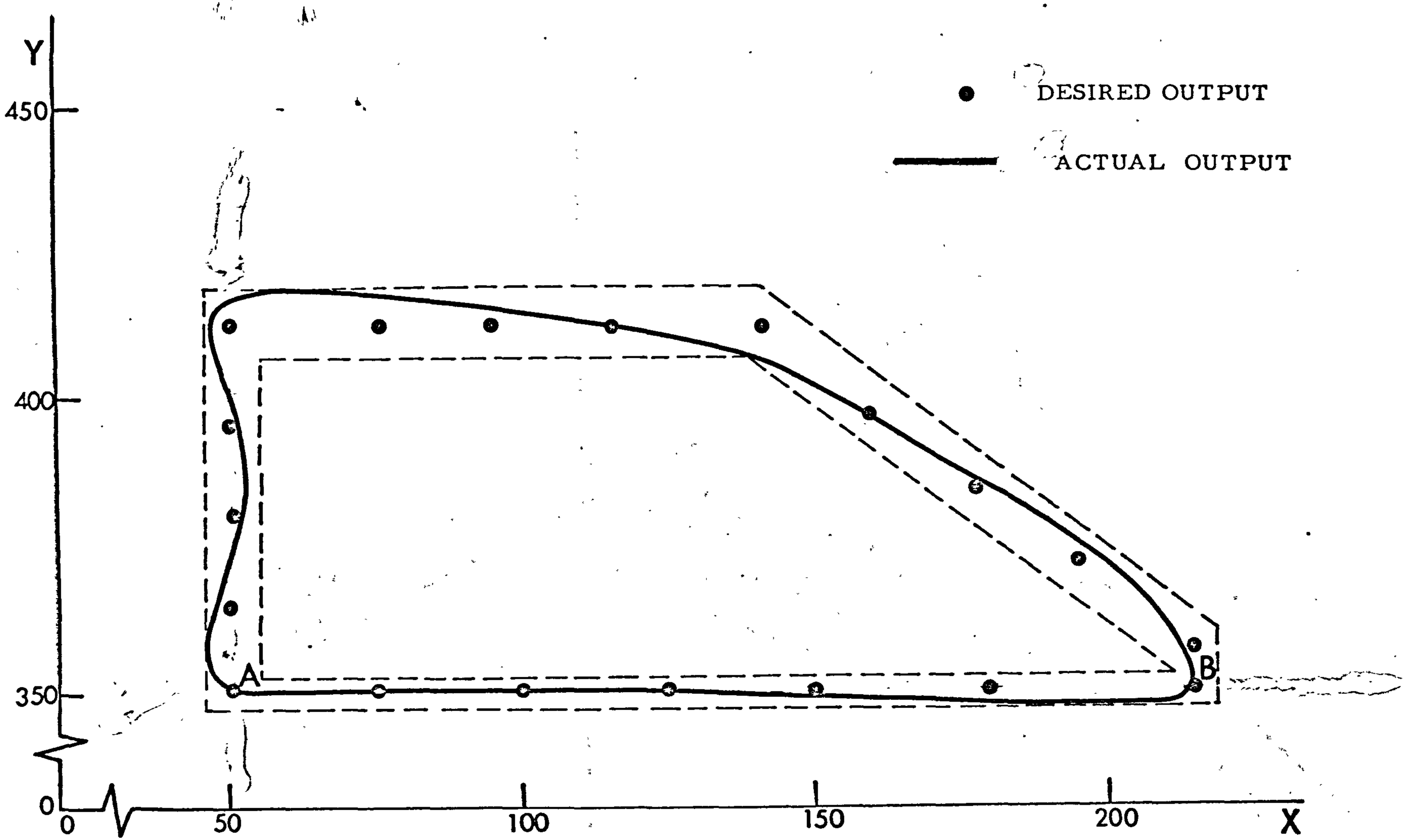

FIG.(C.11a) A PACKAGING MACHINE DESIRED AND ACTUAL PATHS.

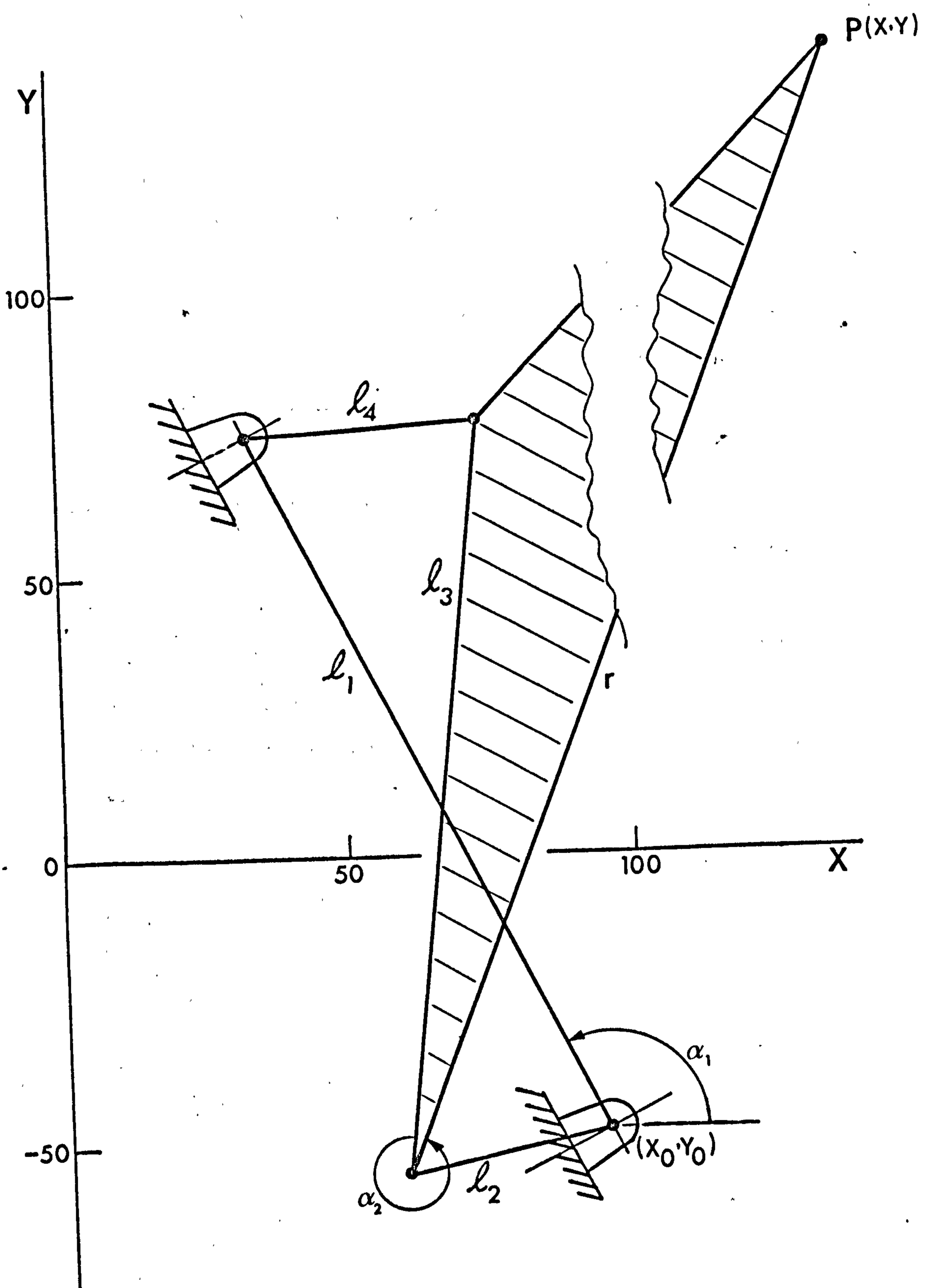

FIG.(6.11b) THE OPTIMUM FOUR-BAR LINKAGE PACKAGING MACHINE.

6.5 Further Remarks and Computer Programs.

The method described can find a planar linkage to generate a given output. It can deal with any type of planar linkage yielding in all cases a minimum. It can be made to follow a logical process in the choice of the type of linkage until it finds a satisfactory result.

The method is programmed using IBM Fortran IV language. The program, shown in Appendix 5, is conversational, adaptive and can deal with either function or path generation by setting a parameter denoted by Ipath to $\pm$ 1. Other features of its adaptability may be seen in the appendix.

The compilation time of the program is about 17 seconds and the running time depends on the form of the desired output and the quality of the initial guess of linkage parameters.

Chapter VII

CONTROL

7.0 INTRODUCTION

In many engineering applications the potential of controlling the input motion to achieve a specified output offers numerous attractive prospects. Many examples are readily seen; for instance, in many designs the output is required to prescribe a finite number of points often called precision points. In the past most of the analysis concerned setting up a number of equations, describing the kinematics of the mechanism, the number of which equals the number of precision points. These equations are then solved simultaneously for the kinematic parameters of the mechanism. It is readily understood that the number of precision points, hence the number of equations, cannot exceed the number of kinematic parameters sufficient to describe the mechanism. However, although the mechanism readily prescribes the precision points what happens in between is fixed. If the designer wishes to modify the motion in between he must perform a new analysis on an increased mobility mechanism. If, however, a second input is established to which a controller is attached the output may be modified, anywhere in an infinite variety, yet still prescribing the same originally desired precision points. To fix ideas, a particular mechanism, a simple planar linkage, ABCD is taken as an example (Fig. 7.1). The assumptions of rigidity, ideal pin-points and constant speed input are maintained, and attention is focused on the variations possible in coupler-point curves when a second input is provided by releasing the constraint of fixity at D.

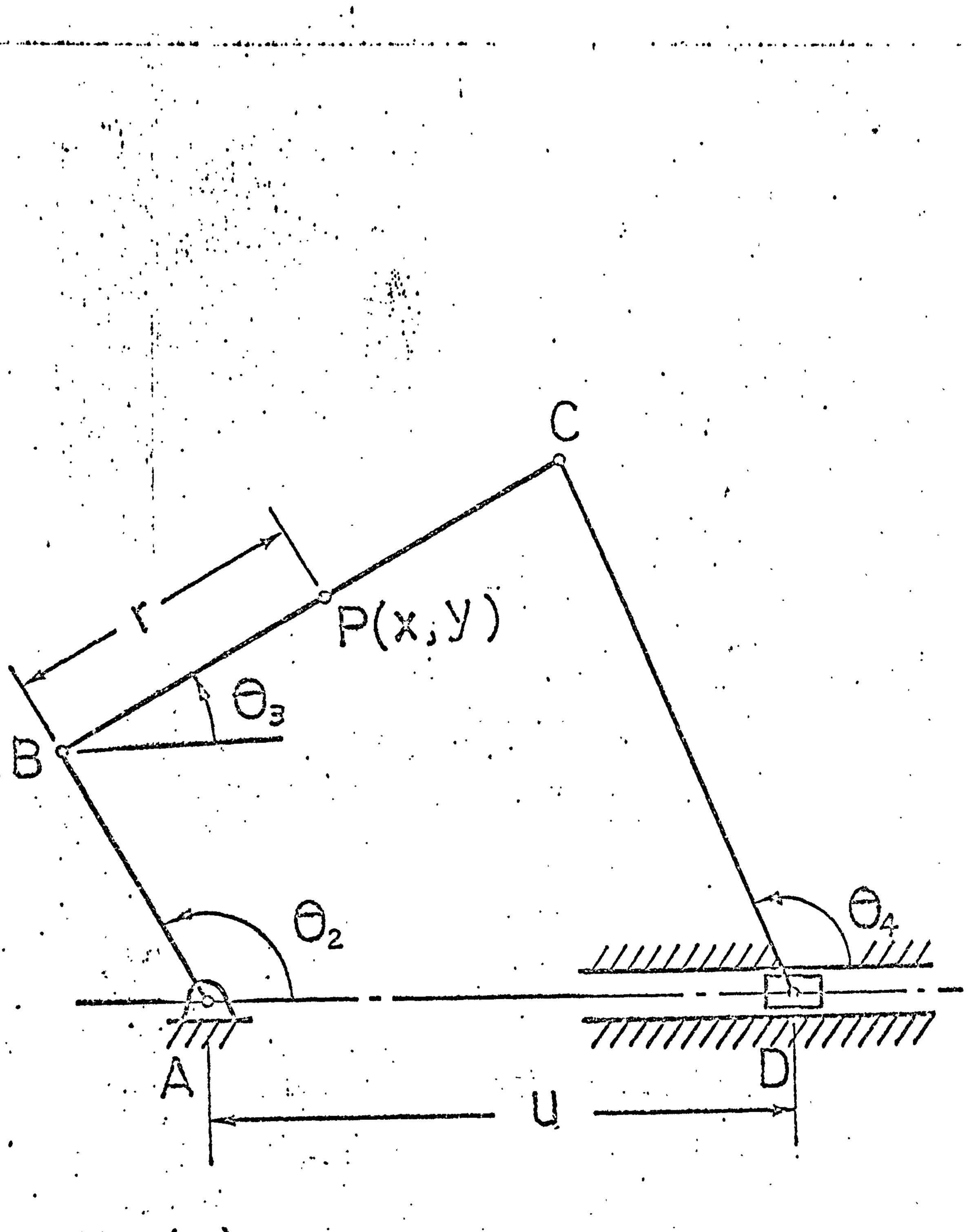

Fig.(7.1) Planar Linkage ABCD; AB=l_2
BC=l_3 , CD=l_4

Several alternative definitions of input and output are possible. For purposes of illustration we shall consider the crank-angle as the primary input, the length AD = U as the secondary or modifying input, and the two-dimensional path of a chosen point on the coupler as the output. Equally, the roles of the two inputs could be considered in reverse and/or the output to be the angular position of the link CD.

Fig. (7.2) shows a family of cyclic coupler-points paths, each drawn for a fixed value of U within chosen limits, the series of points marked on each path referring to an invariable set of consecutive crank-angle position. Two observations may be made from this presentation. First, any point lying on or within the outer boundaries of the family is accessible to the chosen coupler-point by suitable combination of θ_2 and U. Subject to the constraint that θ_2 increases at a constant rate, a coupler-point path may thus be achieved anywhere within this envelope, thereby permitting a closer approximation to a desired path by suitable control of U than could otherwise be obtained. Secondly, to take account of the assumed time-dependence of θ_2, a set of constant θ_2 curves may be constructed, as shown by the dotted lines. Such 'isochronous' curves, which are arcs of circles centred at the corresponding fixed position of B, can be regarded simply as a reference grid from which the resulting motion can be determined once a particular continuous variation of U is specified. Alternatively, they may be regarded as providing a starting point from which a desired variation in U may be deduced.

7.1 CONCEIVABLE CONTROL METHODS

Obviously, the envisaged system discussed earlier provides an enlarged versatility, albeit in some cases at the expense of

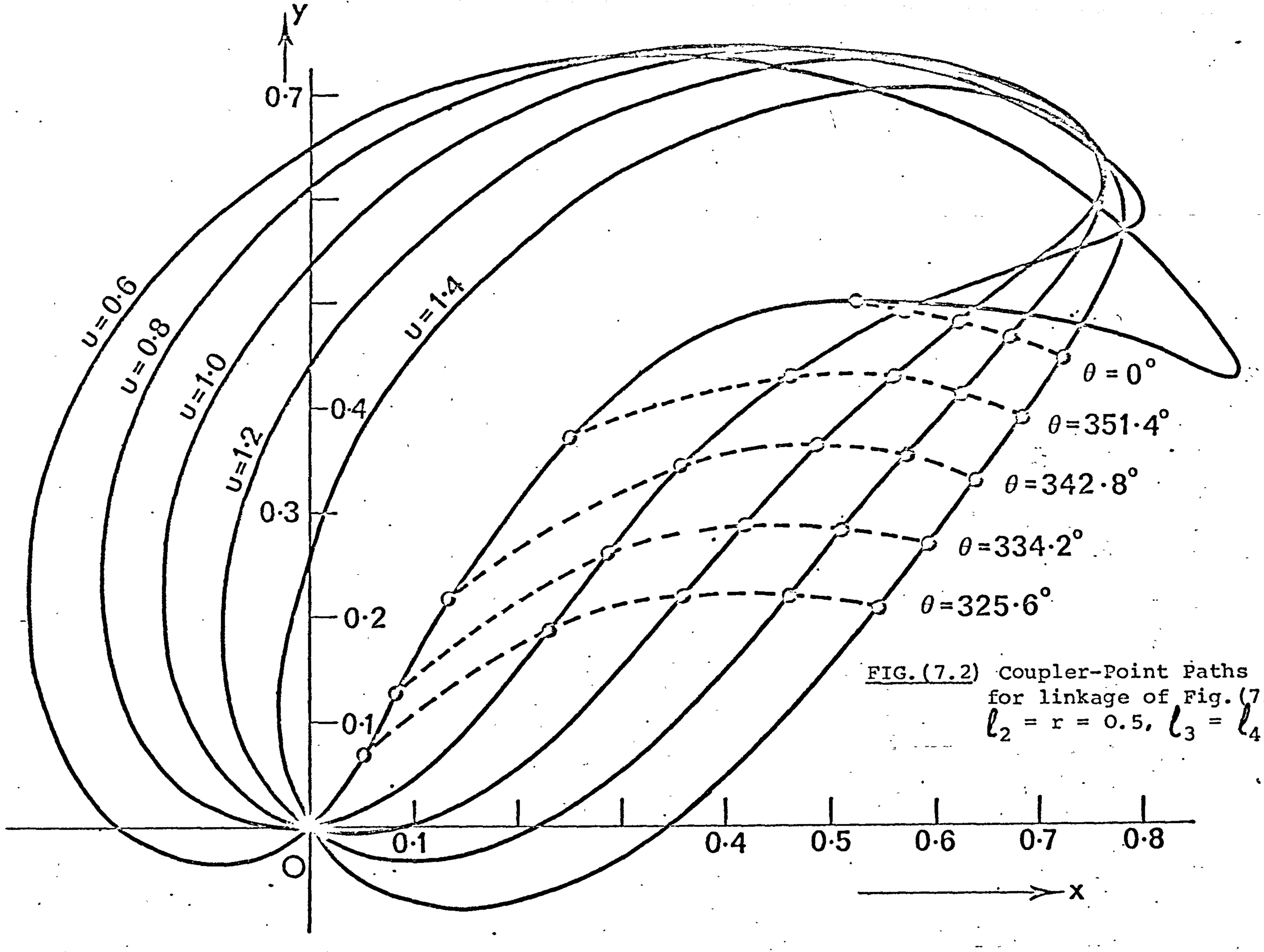

FIG.(7.2) Coupler-Point Paths for linkage of Fig.(7.1): $\ell_2 = r = 0.5$, $\ell_3 = \ell_4 = 1$.

mechanical complication. Its use must therefore be justified by the role of importance of the mechanism in the whole of the engineering plant. There are, however, certain alternatives. They vary from simple mechanical controls to advanced computer-based strategies, and their suitability will obviously relate to the nature of their application.

7.1.1 Off-Line Methods

The required motion of the secondary inputs are determined from the kinematics of the mechanism. A drive is then chosen to approximate as closely as possible to the requirement. At least three principal types of drive may be distinguished.

(a) An intermittent or continuous drive coupled to the primary input by means of direct mechanical connections, an arrangement that is simple in principle but suffers from the defects of limited adaptability and mechanical complications. Examples include secondary linkages, cams and latch mechanisms.

(b) A passive mechanical system embodying elements such as springs or latches whose operation depend on the pre-determined load or on inertia or other forces transmitted through the mechanism. The mode could be continuous or intermittent and its advantages and disadvantages are similar to the preceding option, and

(c) An independent drive of the appropriate periodic form maintained in correct phase with the primary input by non mechanical means, e.g. electrical signals: this offers considerable versatility although reproduction of a sufficiently accurate cyclic variation may be difficult.

There is no extrinsic feed back in these methods which may thus be regarded as open loop.

7.1.2 Partial-on-line Methods

The required motion of the input is determined as previously. This is stored as a reference model to which the actual motion is required to adhere by means of feedback. Measurement of the motion can be compared with the reference values and the corresponding independent drive can then be controlled by error signals. A variant of this arrangement is to take the mechanism manually through its correct path for the desired overall output and to record simultaneously and separately the values of the inputs. In practice this may be accomplished with primary input operating in its normal mode. This establishes inter alia, the necessary cyclic variation of the secondary input for reference model purposes, thus eliminating the prior calculation. Whichever the first stage may be, considerable demands will be placed on the drive to achieve the appropriate mechanical response, which clearly establishes a limit of the range of application.

7.1.3 Adaptive Methods

The same consideration of drive capacity applies to adaptive methods, in which the drive characteristics are adjustable. A reference model of the desired motion is established as in the preceding method and is used as a basis of comparison for the actual motion. Trial cycles may then be completed in which the adjustable parameters of the drive are progressively changed until a satisfactory correspondence is achieved. If the adjustments are made automatically on the basis of a defined error criterion, the mechanism becomes self adaptive to its reference, and is thus a self-learning device converging to the desired output.

Of these and other methods, the simplest and the most widely used is the mechanically coupled arrangement of type (7.1.1). The choice of either of the above methods depends on the accuracy required and the role of importance the mechanism plays in an overall plant.

7.2 ANALYSIS

7.2.1 Problem Definition

We suppose the desired path can be represented in an analytic form as

$$\phi_1 (x,y,t) = 0 \qquad (7.1)$$

if path is time dependent or as

$$\phi_2 (x,y) = 0 \qquad (7.2)$$

if it is not. In both cases the coordinates (x,y) defining the actual output position are functions of θ_2 and U, and θ_2 is a specified function of time. If the analytic functions are not determinable, equations (7.1) and (7.2) may be replaced by their equivalent numerical relations. The problem is to determine the variation of U which satisfies equations (7.1) or (7.2) as closely as possible subject to the constraint conditions of the mechanism

$$f_j (\theta_2, ...U) = 0 \ , \ j = 1, 2,...m \qquad (7.3)$$

A quality function is formulated as a positional error

$$E_1 = (x - x^*)^2 + (y - y^*)^2 \qquad (7.4)$$

where (x*, y*) are the values of (x,y) that satisfy equation (7.1) or equation (7.2) exactly, or as

$$E_2 = \Sigma_o^N E_1 \qquad (7.5)$$

where N is the number of desired points. The minimisation of the error described in equation (7.4) or (7.5) results in a solution to the problem.

Two methods will be attempted here namely (1) variational optimisation and (2) direct search optimisation.

7.2.2 Variational Method

A multiplier method is chosen here. The multipliers are introduced so that the constraints can be dealt with directly. The method is formulated by finding the stationary value of the quality function (i.e., error) subject to the constraints f_j. This may be expressed as follows :-

$$\frac{\partial E_1}{\partial q_i} + \sum_{j=1}^{m} \lambda_j \cdot \frac{\partial f_j}{\partial q_i} = 0 \qquad (7.6)$$

where q_i are the generalised coordinates i = 1,2,....n and λ_j are the multipliers.

Equation (7.6) gives n non-linear relations involving (n+m) unknowns. These may be solved simultaneously with the m relations expressed in (7.3) to give the q_i (i = 1,2,.....n) describing the mechanism.

There are two points to mention at this stage; a) the error used in the above analysis is that expressed in (7.4) and is time dependent. b) The optimisation is not carried out for all the n parameters of the mechanism but just for the controlling input ones. However, since our interest lies only in these controlling or secondary inputs, as will be called from now on, an explicit solution of the remaining ones is not required and they may be eliminated from the equations whenever possible.

7.2.3 Direct Search Methods

These consist of searching along a number of directions in parameter space. They require only the evaluation of the objective function for the whole cycle and thuse the second formulation of the error function, i.e., E_2 is suitable for use with these methods.

There are three types of these methods: Tabulation Methods; Sequential Methods, and Linear Methods. The first assumes the region in which the minimum lies is known. The region is divided into N sub regions and the objective function is evaluated at each. A table of these evaluations is then drawn from which the minimum is located by comparison. The second explores the behaviour of the objective function by using some form of a geometric shape. This geometric configuration is progressively modified and altered until finally it locates the optimum conditions. The third involves a search along n orthogonal vectors and as it progresses its direction is orientated towards the optimum.

A sequential method "the Simplex", which is described in the previous chapter, is used here to search for the optimum motion of the secondary inputs which in turn, as stated earlier, lead to achieving the desired output.

7.3 RESULTS

Let us consider the mechanism shown in Fig. (7.3). The constraints may be stated as follows:

$$f_1 = \ell_2 Cos\theta_2 + \ell_3 Cos\theta_3 - \ell_4 Cos(\theta_4+\nu) - u\ Cos\nu = 0$$
$$f_2 = \ell_2 Sin\theta_2 + \ell_3 Sin\theta_3 - \ell_4 Sin(\theta_4+\nu) - u\ Sin\nu = 0 \qquad (7.7)$$

where $\theta_2 = \theta_{20} + \omega t$

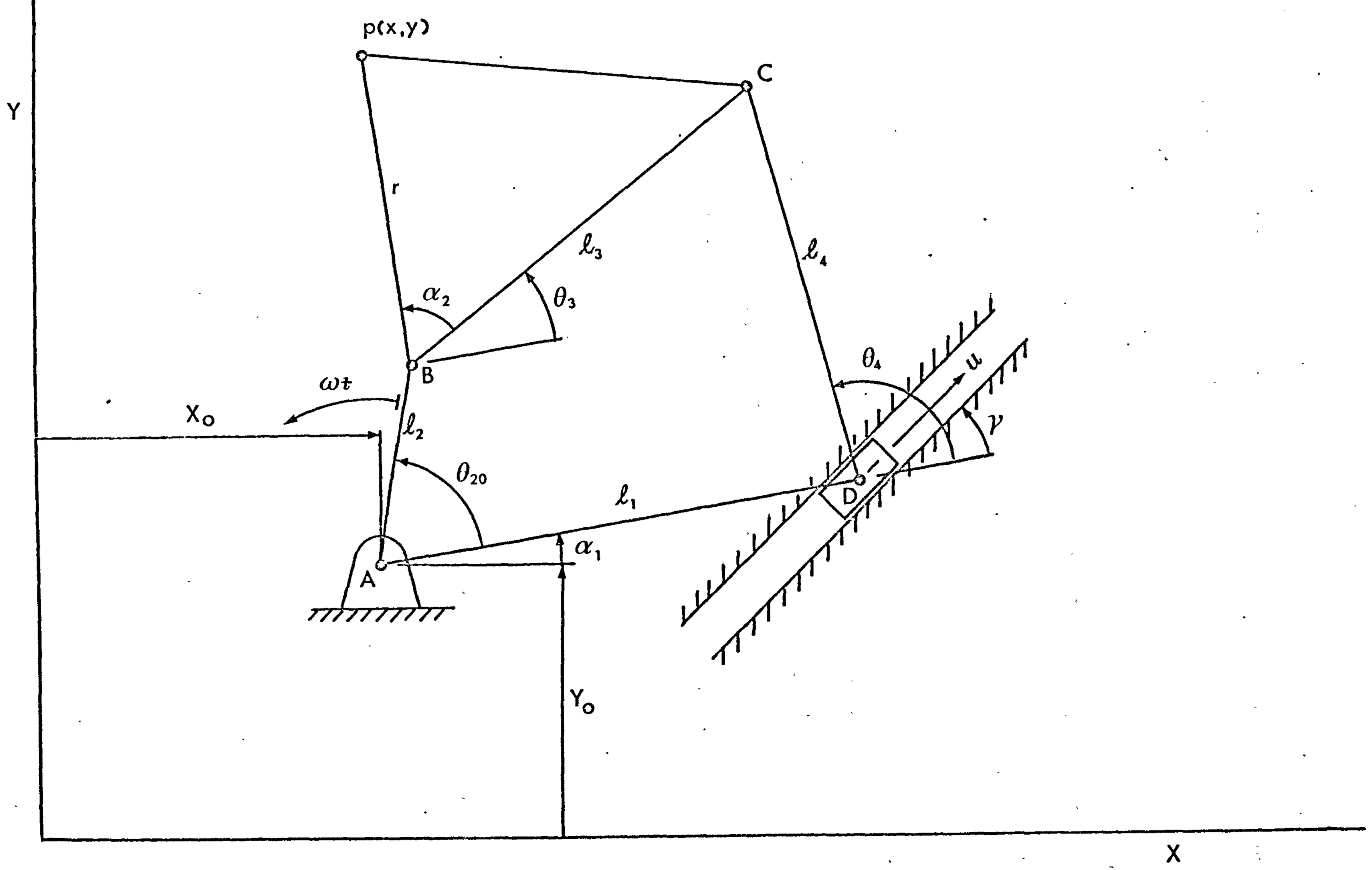

Fig.(7.3) General planar four bar linkage ABCD.
The rocker-to-ground joint is replaced by a slider and the output is generated from Coupler point p(x,y).

Let the output be generated from coupler point p(x,y) the positional error can then be given as

$$E_1 = \{ \left[(\ell_2 \text{Cos}(\Theta_2+\alpha_1)+r\text{Cos}(\Theta_3+\alpha_1+\alpha_2)\right] - x^*\}^2 + \{ \left[(\ell_2 \text{Sin}(\Theta_2+\alpha_1)+r\text{Sin}(\Theta_3+\alpha_1+\alpha_3)\right] - y^*\}^2 \quad (7.8)$$

The error E_2 is computed by summating the values of E_1 over the number of desired points.

7.3.1 Examples: Series 1

Let the desired output be numerically given as shown in Fig. (7.4). It is time dependent and is obtained from within the envelope shown in Fig. (7.2). Therefore, we could assume that $\alpha_1 = \alpha_2 = \nu = 0$ and let $U = u + \ell_1$, which in actual fact is Fig. (7.1).

Let us assume that the crank AB is rotating at constant angular speed ω, i.e.

$$\Theta_2 = \omega t \quad (7.9)$$

The goal is then to control the secondary input U so as to lead to close approximation of the desired function. The motion that U must perform may be obtained by the direct application of equation (7.6) to equations (7.7) and (7.8). This gives

$$-2r(\ell_2.\text{Cos}\Theta_2+r\ \text{Cos}\Theta_3-x^*)\text{Sin}\Theta_3 + 2r(\ell_2\text{Sin}\Theta_2+r\ \text{Sin}\Theta_3-y^*)\text{Cos}\Theta_3 - \lambda_1(\ell_3\text{Sin}\Theta_3)+\lambda_2(\ell_3\text{Cos}\Theta_3) = 0 \quad (a)$$

$$\lambda_1(\ell_4\text{Sin}\Theta_4) -\lambda_2(\ell_4\ \text{Cos}\Theta_4) = 0 \quad (b) \quad (7.10)$$

$$\lambda_1 = 0. \quad (c)$$

and as explained earlier these equations are solved simultaneously with equations (7.7) to yield the optimum U.

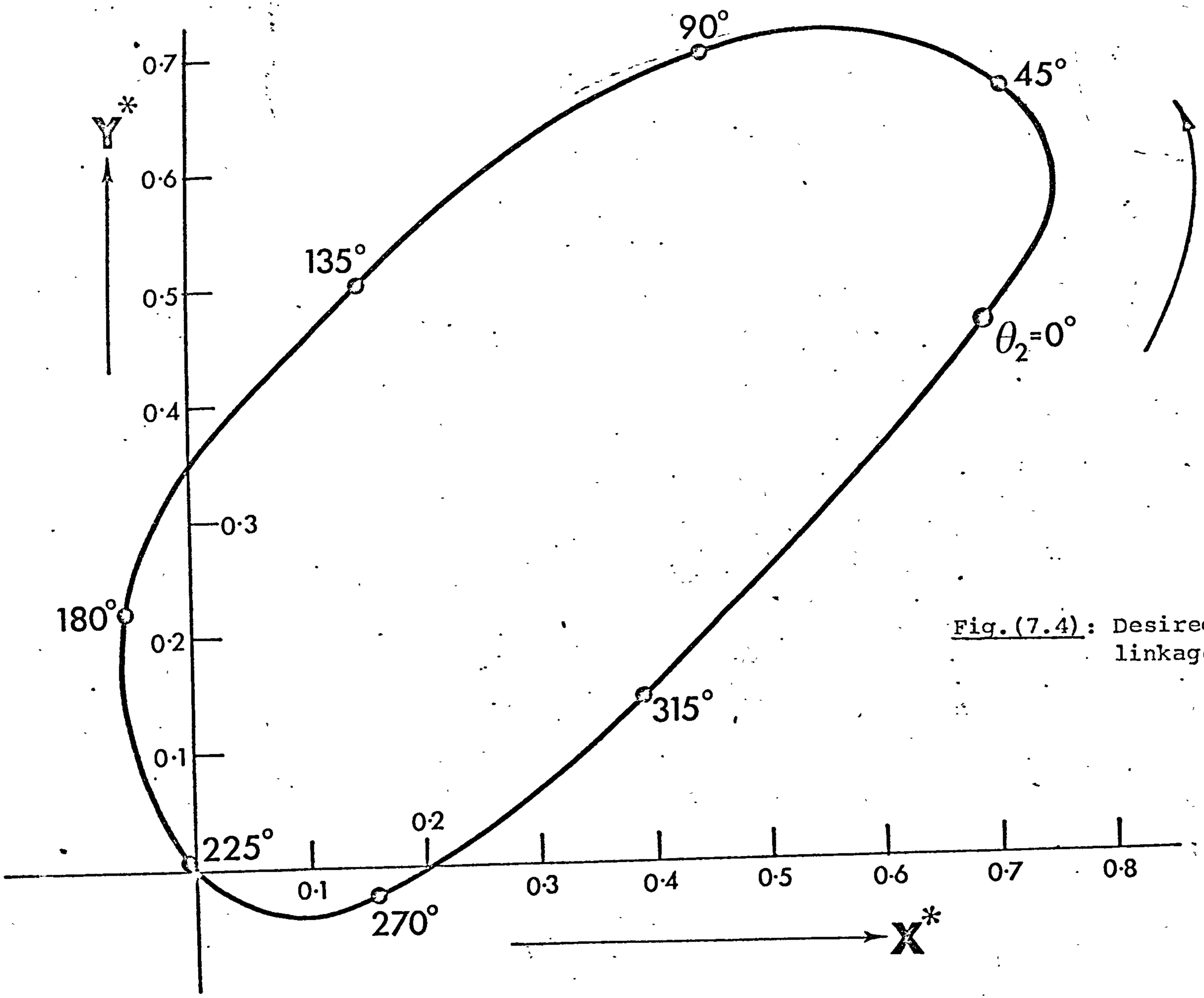

Fig.(7.4): Desired Coupler-Path for linkage of Fig.(7.1).

Now from (7.10c) and (7.10b)

$$\lambda_2 = 0 \qquad \text{(a)}$$

or (7.11)

$$\text{Cos}\Theta_4 = 0 \qquad \text{(b)}$$

Taking the first solution, i.e. (7.11a) and substituting in (7.10a) we obtain

$$\Theta_3 = \tan^{-1}\left(\frac{y^* - \ell_2\ \text{Sin}\Theta_2}{x^* - \ell_2\ \text{Cos}\Theta_2}\right) \qquad (7.12)$$

or $\Theta_3 = \tan^{-1}(A)$ where A corresponds with (7.12).

This corresponds to the relation that for minimum error the coupler takes the position of a straight line with the point p(x*, y*). However, we may now solve equations (7.7) to give:-

$$U^2 - 2(\ell_2\text{Cos}\Theta_2+\ell_3\text{Cos}\Theta_3)U+ \left[(\ell_2{}^2+\ell_3{}^2-\ell_4{}^2)+2\ell_2\ell_3\text{Cos}(\Theta_2-\Theta_3)\right] = 0 \qquad (7.13)$$

Equation (7.12) may be substituted in (7.13) to give a solution for U, i.e.

$$U_{1,2} = \left[\ell_2\text{Cos}\Theta_2+\ell_3\text{Cos}(\tan^{-1}(A))\right] \pm \{\left[\ell_2\text{Cos}\Theta_2+\ell_3\text{Cos}(\tan^{-1}(A))\right]^2 - \left[(\ell_2^2+\ell_3{}^2-\ell_4{}^2)+2\ell_2\ell_3\text{Cos}(\Theta_2-\tan^{-1}(A))\right]\}^{1/2} \qquad (7.14)$$

i.e. two solutions corresponding to two positions of the rocker CD as shown in Fig. (7.5)

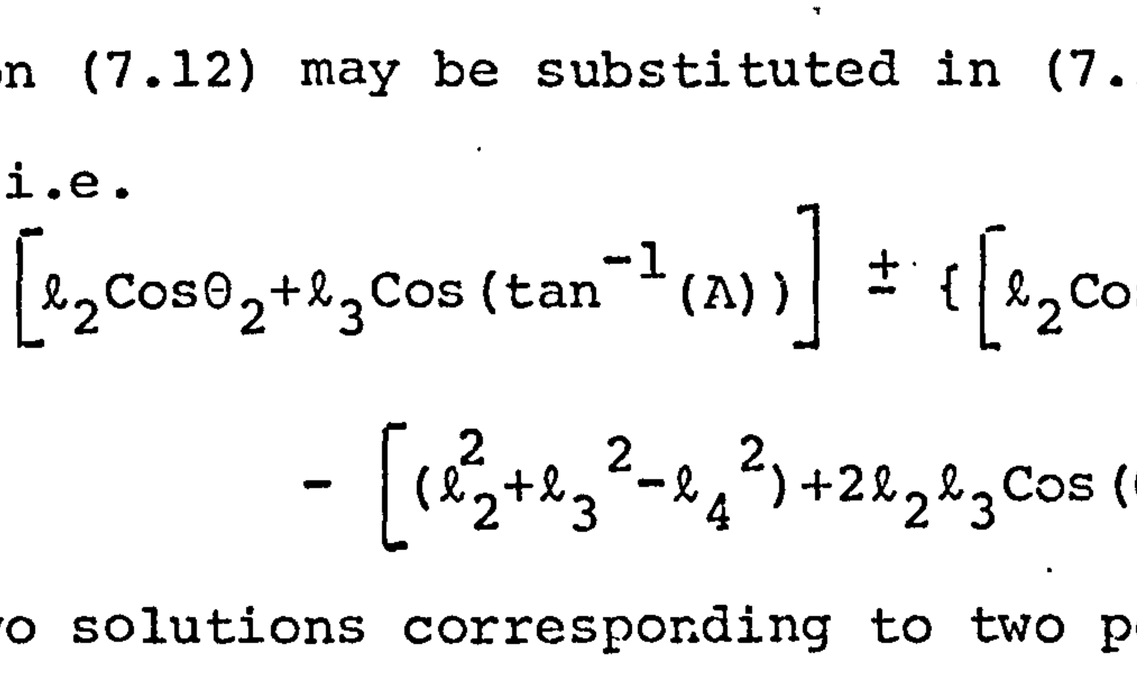

Fig. (7.5)

If the argument of the square root term in (7.14) is negative then (7.11a) is not true and (7.11b) is the correct solution of (7.10b). In physical reality this is equivalent to the coupler being in a straight line with the desired point, then no matter how the rocker CD is positioned, point D never lies on U. In these circumstances the optimum condition must surely be when the rocker CD is upright, i.e. $\theta_4 = \frac{\pi}{2}$ and the value of U is recomputed from (7.7) to give:-

$$U_{1,2} = \ell_2 \cos\theta_2 \pm \{\left[\ell_2 \cos\theta_2\right]^2 - \left[(\ell_2^2+\ell_4^2-\ell_3^2)-2\ell_2\ell_4\cos(\theta_2-\theta_4)\right]\}^{1/2} \quad (7.15)$$

(B) Direct Search Solution

The same assumptions are made as stated in the previous method. A periodic solution which appears here in the form of a Fourier series is initially assumed for U i.e.

$$U = A_o + \sum_{n=1}^{\infty} \left[A_n \cos n\omega t + B_n \sin n\omega t\right] \quad (7.16)$$

where A_o, A_n and B_n are constant coefficients taking different values in different iterations. The optimisation is proceeded according to the simplex method until finally A_o, ..., A_n, B_n take up values that give optimum motion of U.

(C) Results: Series 1

The input data is

$$\ell_2 = r = 0.5$$

$$\ell_3 = \ell_4 = 1$$

and the initial value of $\theta_2 = 0$.

Fig. (7.6) shows the motion that U must trace to result in minimum output error. The positional error E_1 is shown in

FIG (7.6) OPTIMUM MOTION OF U

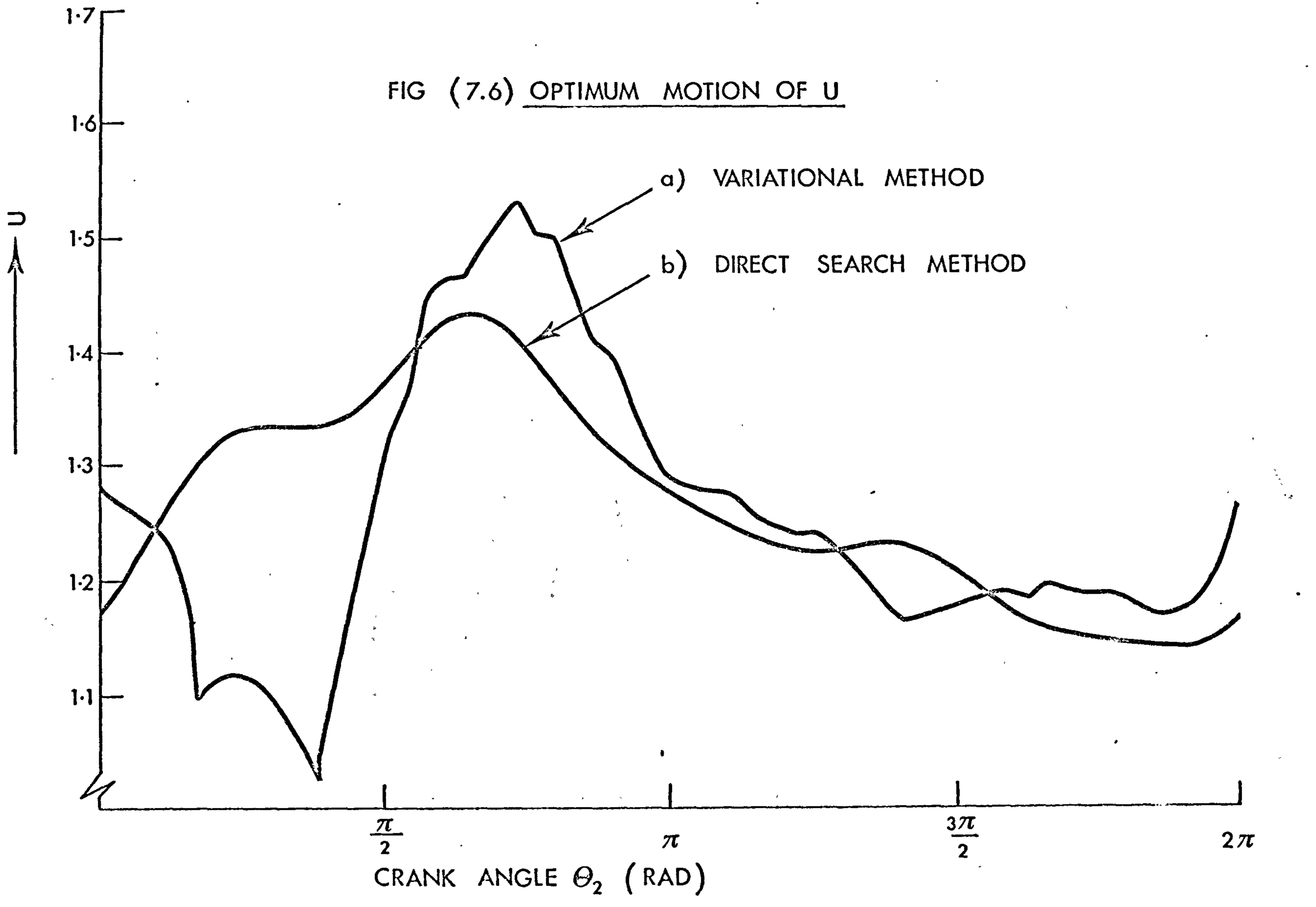

FIG (7.7) THE POSITIONAL ERROR E_1

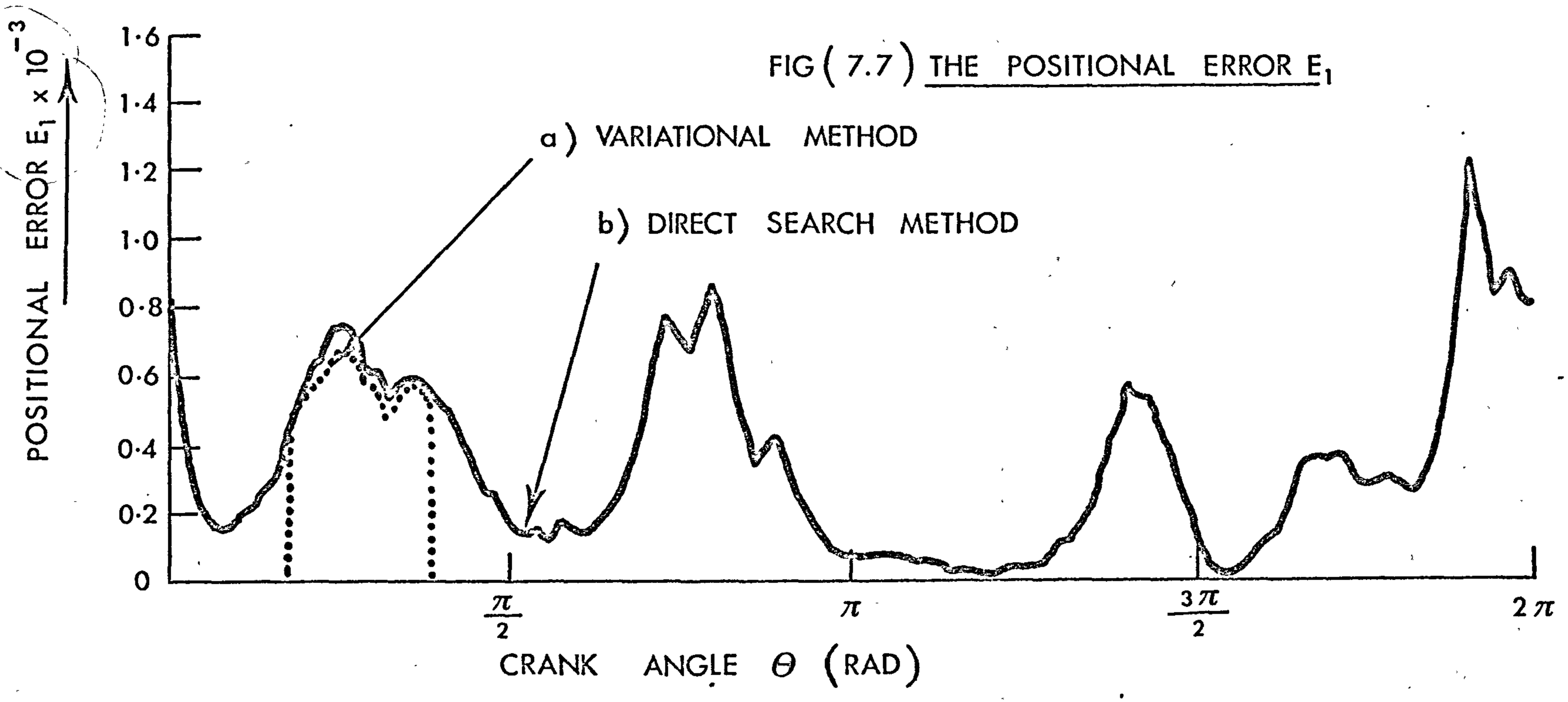

Fig. (7.7). The curves (a) and (b) in both figures represent the results obtained from the variational and direct search methods respectively. Fig. (7.8) shows the actual output curves obtained from both methods superimposed on the desired curve of Fig. (7.4).

In the direct search solution the Fourier series was truncated to eleven terms, the initial values of their coefficients were guessed at random. Different initial guesses of the coefficients produced different optima. This suggested the presence of a number of stationary value points of the objective function. Of all these stationary values one must be the global optimum while the rest are all local. In an effort to locate the global optimum a number of various starting conditions were tried. The one that generated least error was taken finally to represent the global optimum, results of which were those shown in Figs. (7.6), (7.7) and (7.8).

The variational method located the true global optimum which the direct search located as best as an eleven-term Fourier series could provide. If an infinite number of terms were used the direct search would have led to the variational results. Now since a true global optimum may be found readily at first trial from the variational method, one may argue the philosophy behind the use of any other method. Fortunately, there are several reasons that justify the use of alternative methods:

1) The global optimum is not always the prime interest as such but in many cases a smooth and slowly varying controller action. This is so that the controller can smoothly and easily

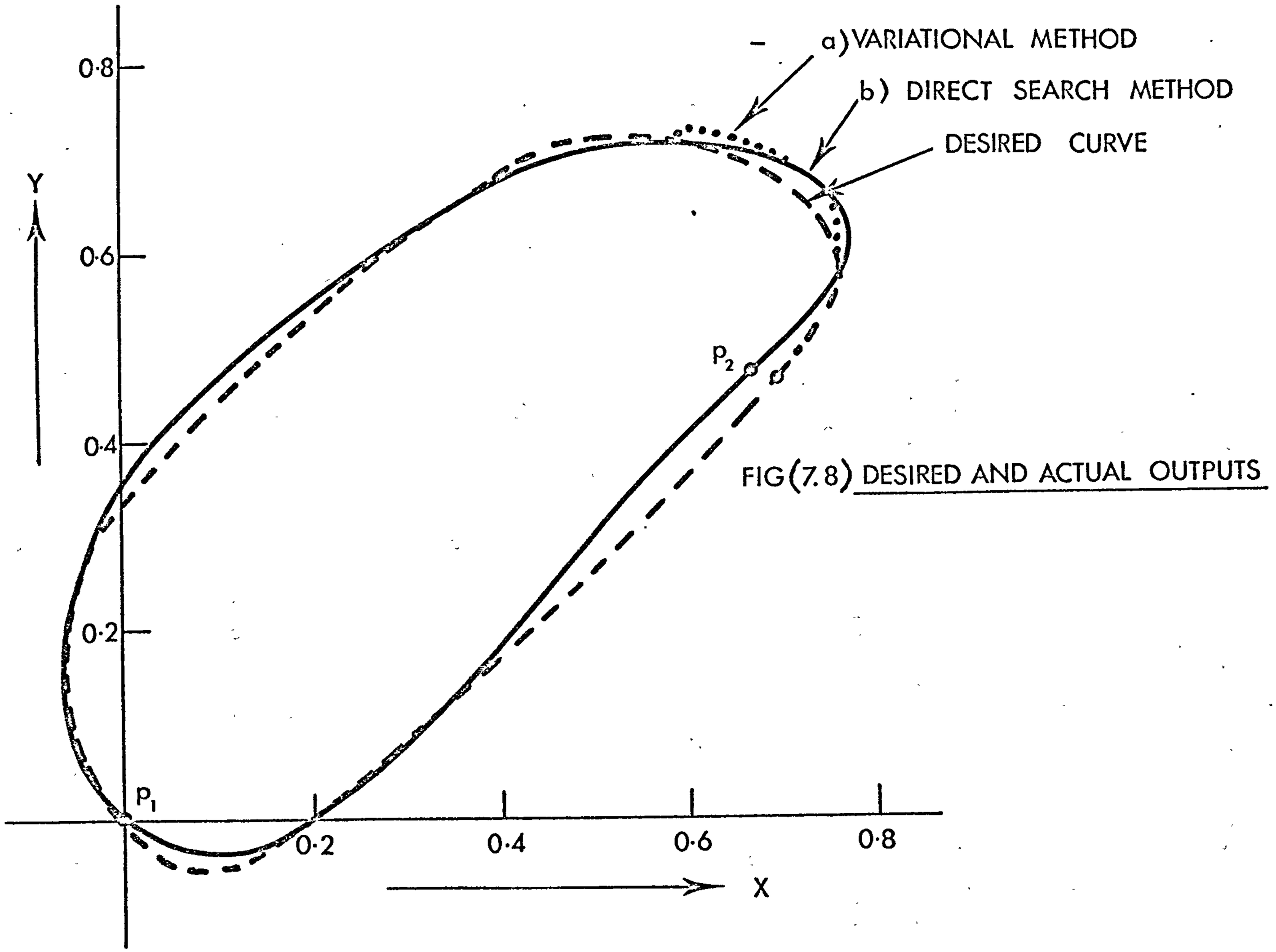

FIG (7.8) DESIRED AND ACTUAL OUTPUTS

cope with its task and thus eliminate undesirable and complicated dynamic situations. By studying curve (a) of Fig. (7.6) we find it very difficult, if not impossible, to accomplish at high speeds while curve (b) of the same figure is a more feasible task.

2) The direct search permits an easier use of stricter error conditions or constraints at some portion of a desired function. Thus provisions may be incorporated to cater for cases where for instance certain priorities or weighting functions are added to certain parts of an output. As an example, let the portions p_1p_2 of Fig. (7.8) be generated as closely as possible while the rest is not so rigorously required. Let us assume weighting functions w_1, w_2 where w_1 is used within the range P_1P_2 and w_2 without. Now let:

$$w_1 = 5w_2$$

and

$$w_2 = 1$$

Then the error E_2 may be formulated thus:

$$E_2 = W_2 \sum_{O}^{N_1} E_1 + w_1 \sum_{N_1}^{N_2} E_1 + w_2 \sum_{N_2}^{N} E_1 \qquad (7.17)$$

where N_1 and N_2 are the number of desired points up to p_1 and p_2 respectively. The required motion U of the controller for this case is then shown in Fig. (7.9) and the actual output curve is shown in Fig. (7.10) superimposed on the desired one. It is clearly seen from Fig. (7.10) how a close generation of range p_1p_2 is accomplished while larger errors are tolerated outside it. Another interesting point is that if the

FIG (7.9) OPTIMUM MOTION OF U

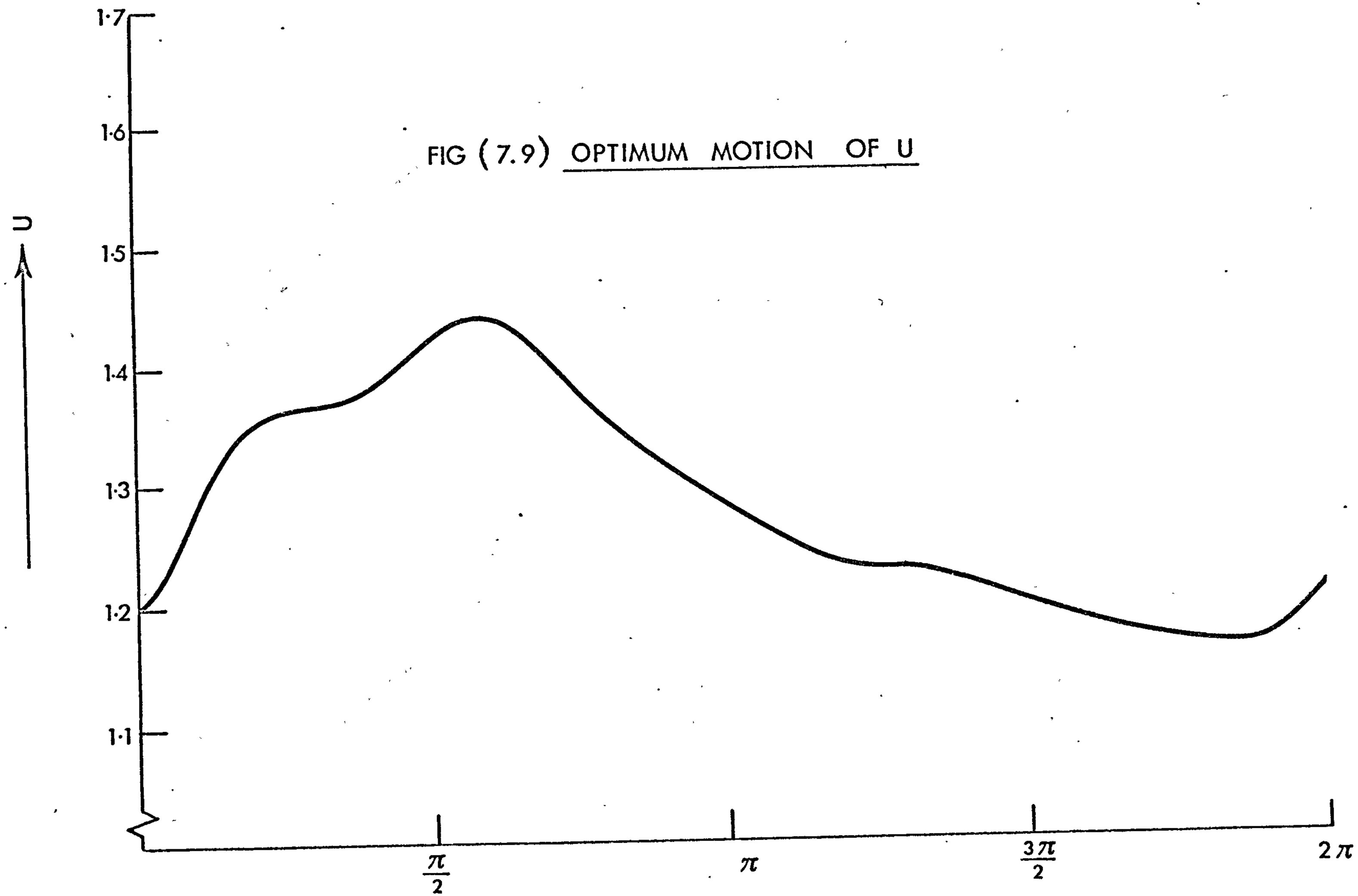

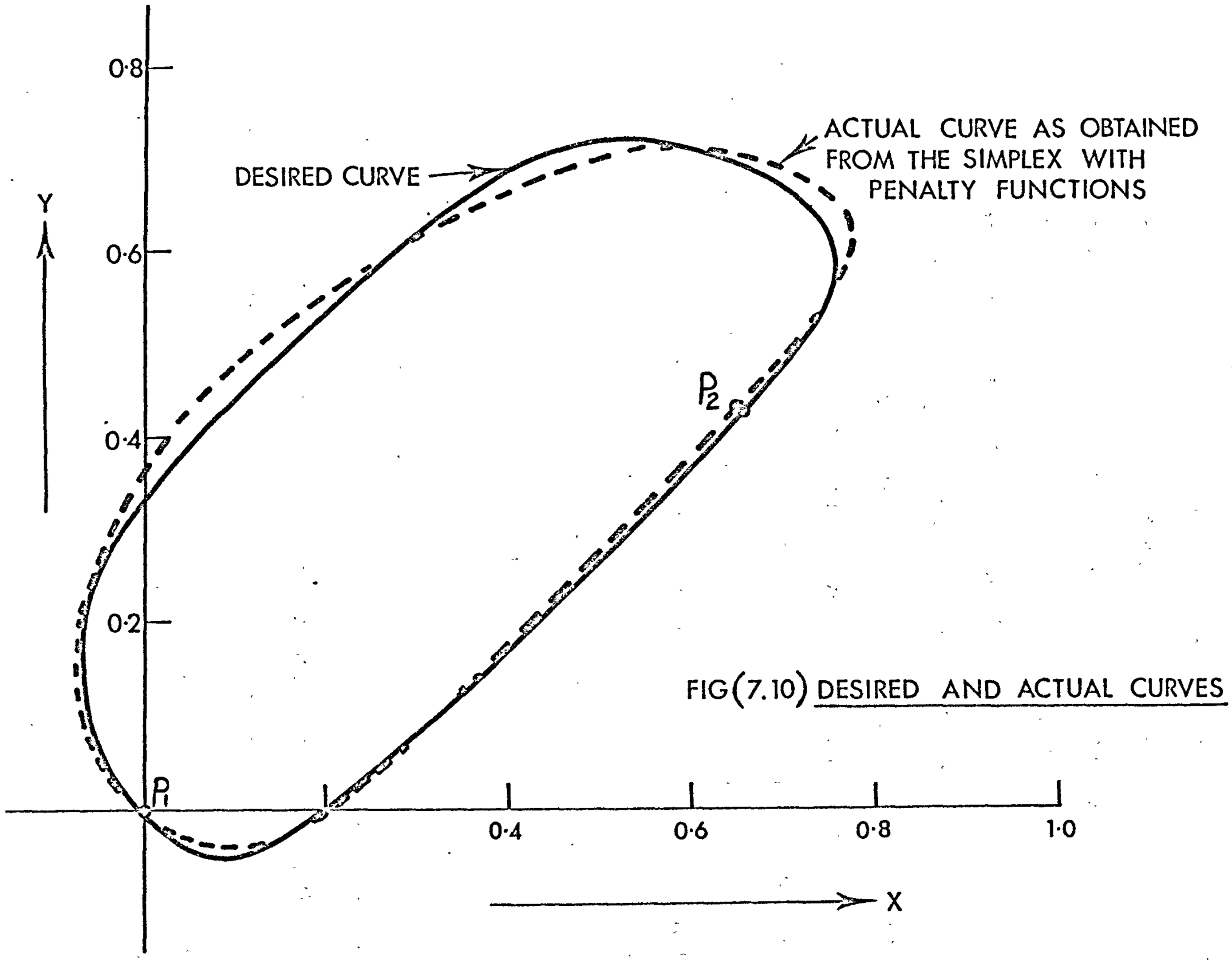

FIG(7.10) DESIRED AND ACTUAL CURVES

requirements outside p_1p_2 are very relaxed the controller motion U involved there, may be modified further to give a more favourable dynamic condition.

3) With reference to secton 7.1, the two methods cater for two distinct control applications, the variational method is used off line to precompute the would-be required controller motion of U. The controller is assumed to be able to produce this motion despite the dynamic problems that may arise. The direct search method, however, may be used "on-line" and accommodate the dynamic considerations into its structure. This is done by monitoring the error over one cycle with the actual mechanism operating. The controller is then asked to vary its motion according to the optimisation routine. The error incurred is monitored again and further modifications in U by the controller are performed. Thus as can be seen from this procedure the dynamics are automatically taken into consideration.

4) With the variational method, any change in the operating conditions require a recalculation of optimum conditions. The direct search merely experiments with a number of cycles, after which the controller adjusts itself, in an optimum manner, to the changes. Thus for automation purposes a heavy swing in favour of the direct search method is justified.

5) The variational method requires the solution of (n+m) non-linear equations. In many cases this entails a far greater effort than would otherwise be needed with a direct search. In fact, in some cases, the direct search method is required to solve these equations.

Finally, it may be summarised that the choice of the method depends upon the complexity of the problem and the type of application required.

7.3.2 Examples; Series 2

In this series of examples we show how the errors obtained in the previous chapter are further reduced by increasing the mobility of the optimised four bar by replacing the rocker-to-ground joint by a slider and controlling it to prescribe a motion described by the following equation.

$$u = \sum_{n=0}^{\infty} (A_n \text{ Cos } n\omega t + B_n \text{ Sin } n\omega t) \qquad (7.18)$$

Since we specify the general form of motion of the slider the variational method fails and therefore only the direct search method "the simplex" will be considered here. The link dimensions obtained from the optimisation in the previous chapter are retained. The new optimisation parameters are obtained by limiting n to the value of 3 in equation (7.18). The parameters are thus A_o, A_1, A_2, B_2 and the angle ν between the slider line of travel and the ground link. The reason for choosing n = 3 is to reduce the mechanical complications involved in producing the controlled motion of the slider.

All the examples discussed in the previous chapter have been tried and in all cases the errors were reduced. However, only two of the examples will be discussed here.

1) The desired output is to be generated from the rocker link ℓ_4 of Fig. (7.4) as an angular function

$$\Theta_4 = \beta_5 + \beta_6 \left| \text{Sin } \frac{\omega t}{2} \right|$$

where β_5 and β_6 have the same values as in chapter 6, section 6.4.2, sub-section B. The output is to be given a weighting

factor of 1000 in the range $60^{o} < \omega t < 260^{o}$ and the remainder a weighting factor of unity.

The optimisation produced the following optimum values :

$A_o = 1.46$, $A_1 = -0.425$, $B_1 = -0.256$, $A_2 = -0.855$,

$B_2 = 0.569$, $\nu = -41^{o}$.

The optimum output curve, 2, is shown together with the desired output curve, 1, in Fig. (7.11). The figure shows that the weighted portion is generated very closely. In fact the error involved is 4.8 degrees^2 as compared with 35.0 degrees^2 in chapter 2. This presents an enormous reduction which would have been even more if terms in equation (7.19) were considered.

2) The desired output is to be generated from coupler point p (x,y) of Fig. (7.4) as a path

$$\frac{(x^* - \beta_7)^2}{\beta_8} + \frac{(y^* - \beta_9)^2}{\beta_{10}} = 1$$

where β_7, β_8, β_9 and β_{10} have the same values as in chapter 6, section 6.4.3, example (b)

The optimisation produced the following optimum values

$A_o = 3.1$, $A_1 = 0.772$, $B_1 = -0.34$, $A_2 = 0.568$

$B_2 = -0.136$, $\nu = -0.9^{o}$

The optimum output curve, 2, together with the desired output curve 1, are shown in Fig. (7.12). The error is 4.3 cm^2 as compared with 12.6 cm^2 in chapter 6.

7. 4 A Strategy in Search for the Optimum Linkage

Based on the work described in chapters 6 and 7 a strategy for the search of an optimum linkage may be formulated.

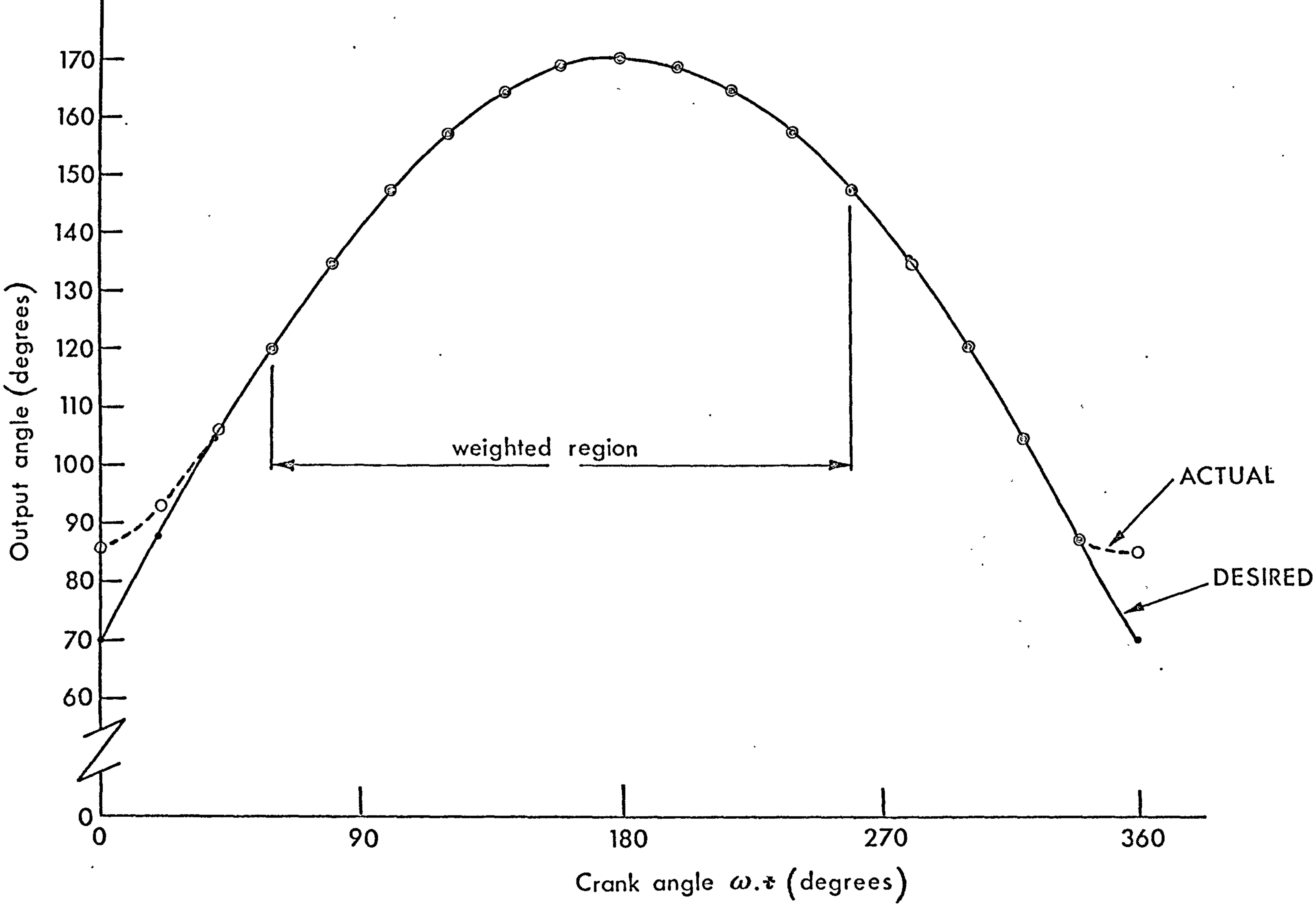

Fig (7·11) DESIRED AND ACTUAL ANGULAR OUTPUT — FUNCTION GENERATION WEIGHTED OUTPUT GENERATED BETWEEN 60 AND 260 DEGREES OF CRANK ANGLE ωt

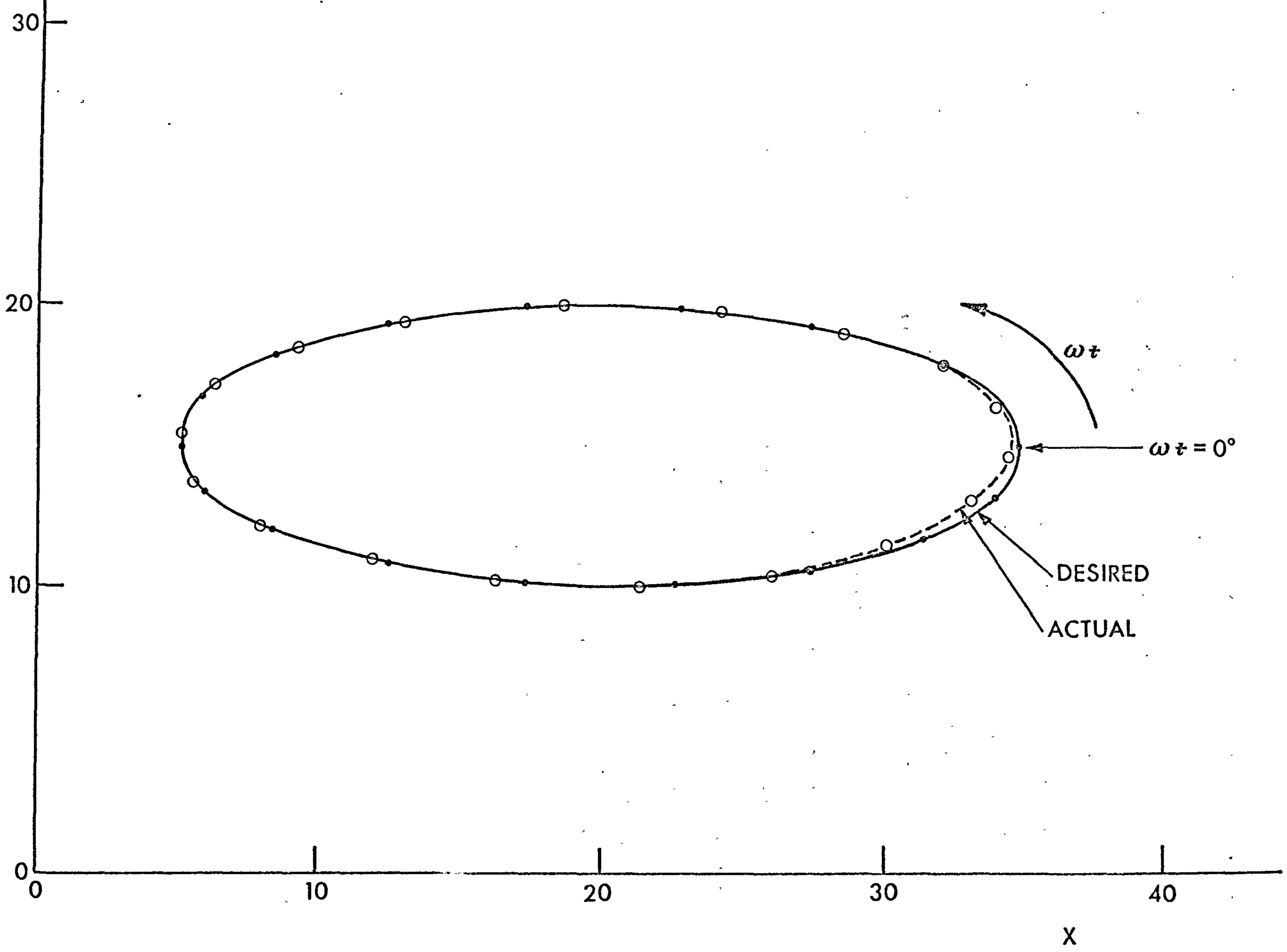

Fig (7·12) DESIRED AND ACTUAL COUPLER CURVES – FUNCTION GENERATION EXAMPLE (b)

Firstly, we start with the simple four bar linkage and optimise its link dimensions so as to lead to minimum error in output generation. Secondly, if unacceptable errors occur in the output we increase the mobility of the four bar by introducing a second input and control its motion in an optimum manner so as to lead to acceptable errors. The second input could be a slider as discussed in this chapter or could be another link resulting in a five bar loop. This fifth link can be driven by the crank via gears or may be independently driven. If unacceptable errors still occur we could continue introducing further inputs or indeed building a chain of linkages.

The computer program shown in Appendix, 5, can cope with the above defined strategy producing optimum results in each case. Obviously, the fortran function "error" shown in the program of the above appendix should in every case contain the kinematic equations of the type of linkage being treated.

P A R T I V

EXPERIMENT & CONCLUSIONS

CHAPTER VIII

EXPERIMENTAL INVESTIGATIONS AND DISCUSSION OF RESULTS

8.0 AIMS OF EXPERIMENT

The theoretical investigations in this thesis concerned two aspects of mechanism study. The first dealt with the dynamics of a five bar linkage with a sliding joint. The response of this mechanism has been analyzed using results obtained mainly from computer solutions. A linearised analysis has also been performed to study the resonance and stability of the mechanism. The resonance analysis showed a behaviour similar to a second order system while the stability analysis showed instability in the second region, i.e. in the vicinity of twice the natural frequency only. The instability, however, disappeared completely by addition of a small value of damping. The second aspect of the study dealt with the optimisation of the linkage kinematic parameters and also the control of its inputs to achieve a desired output.

The theoretical investigations considered two types of inputs, (a) a constant speed input and (b) a torque input. In this experimental work we shall consider a constant speed input only, applied to the crank.

The main aims of the experiment are :-

1) To investigate the motion of the slider with different input speeds and springs and also to compare the experimental and theoretical results.

2) To investigate the resonance of the slider when the ratio of crank length to other links is small. This, if in good agreement with the theoretical results, sukports the analysis described in Chapter IV.

8.1 APPARATUS

Two experimental apparatus were built. The first, which will be referred to as Experimental Rig 1, was used to achieve the first aim of the experiment set out above. The second apparatus, which will be referred to as Experimental Rig 2, was used to achieve the second aim of the experiment also set out above. The first apparatus operates in the vertical plane and the second in the horizontal plane.

8.2 DESCRIPTION OF APPARATUS

8.2.1 Experimental Rig 1

8.2.1.1 Mechanical Components

Fig. (8.1) shows a view of the apparatus with one side plate of the slider guide removed to show the slider and spring arrangement. Fig. (8.2) shows a top view of the linkage showing the coupling arrangement to the motor and also the slider and its guide in more detail. Figs. (8.3a) and (8.3b) show exploded views of the various components of the linkage and the slider guide respectively.

The apparatus, including the motor, is mounted on a pedestal which is bolted to a block. The crank or input link is a fly-wheel (1) mounted on an input shaft via a taper lock. The input shaft (2) (see Fig. (8.2)) is located in two pedestal bearings (3) and connected to the motor via a coupling. A further fly-wheel (4) is mounted on the shaft to ensure constant speed input.

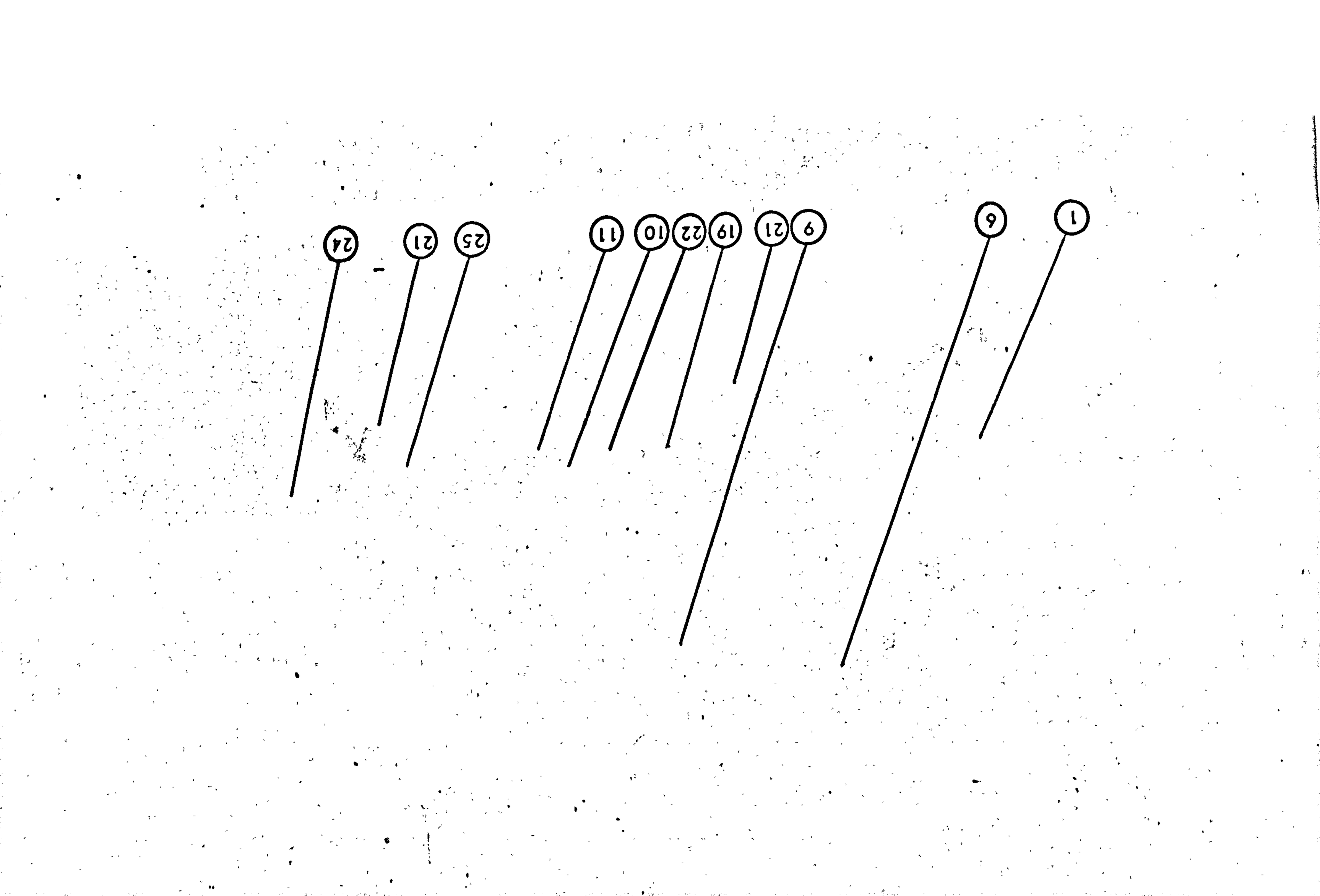
24
21
25
11
10
22
19
21
9
6
1

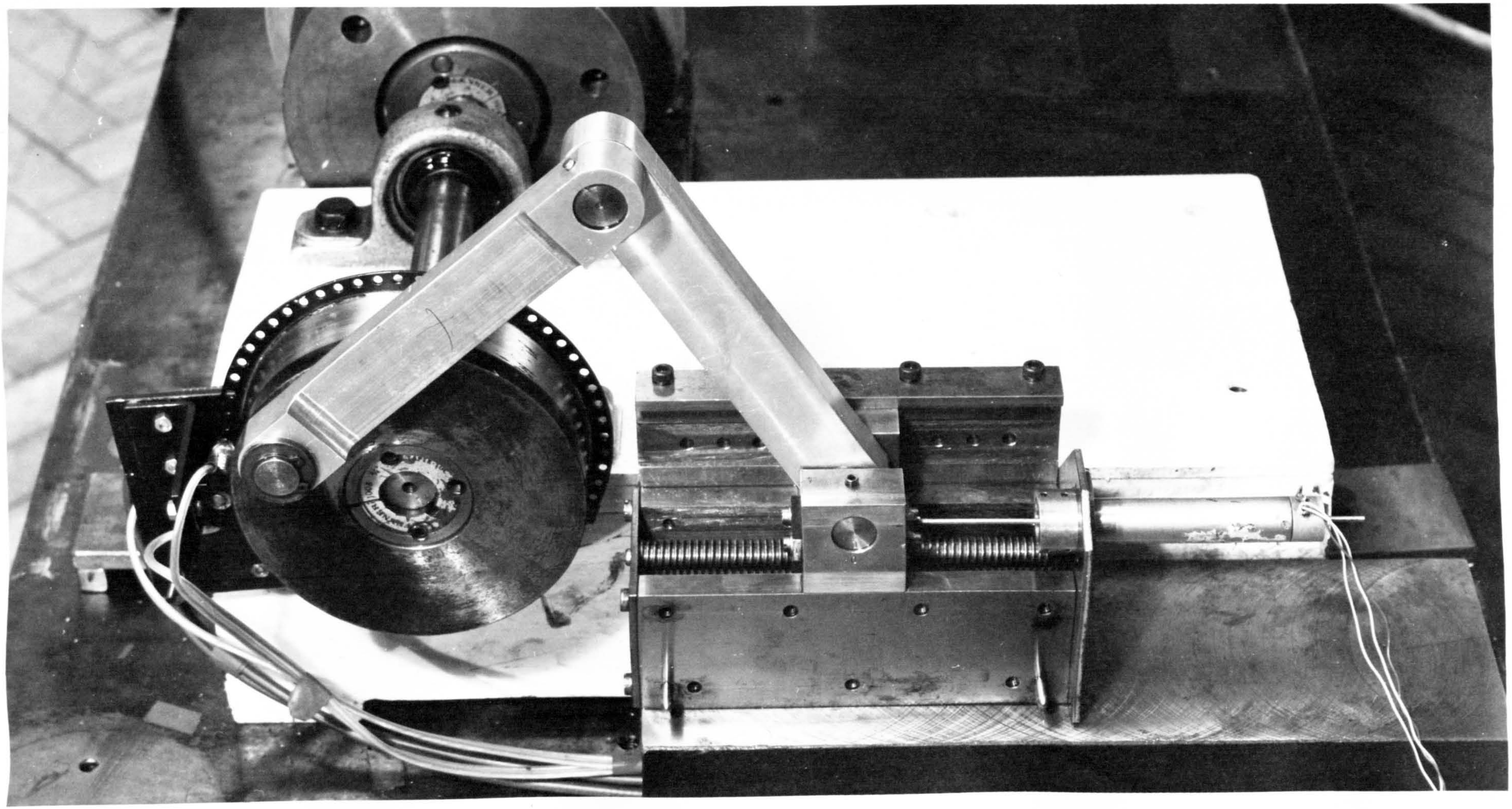

FIG. (8.1) A FRONT VIEW OF EXPERIMENTAL RIG 1.

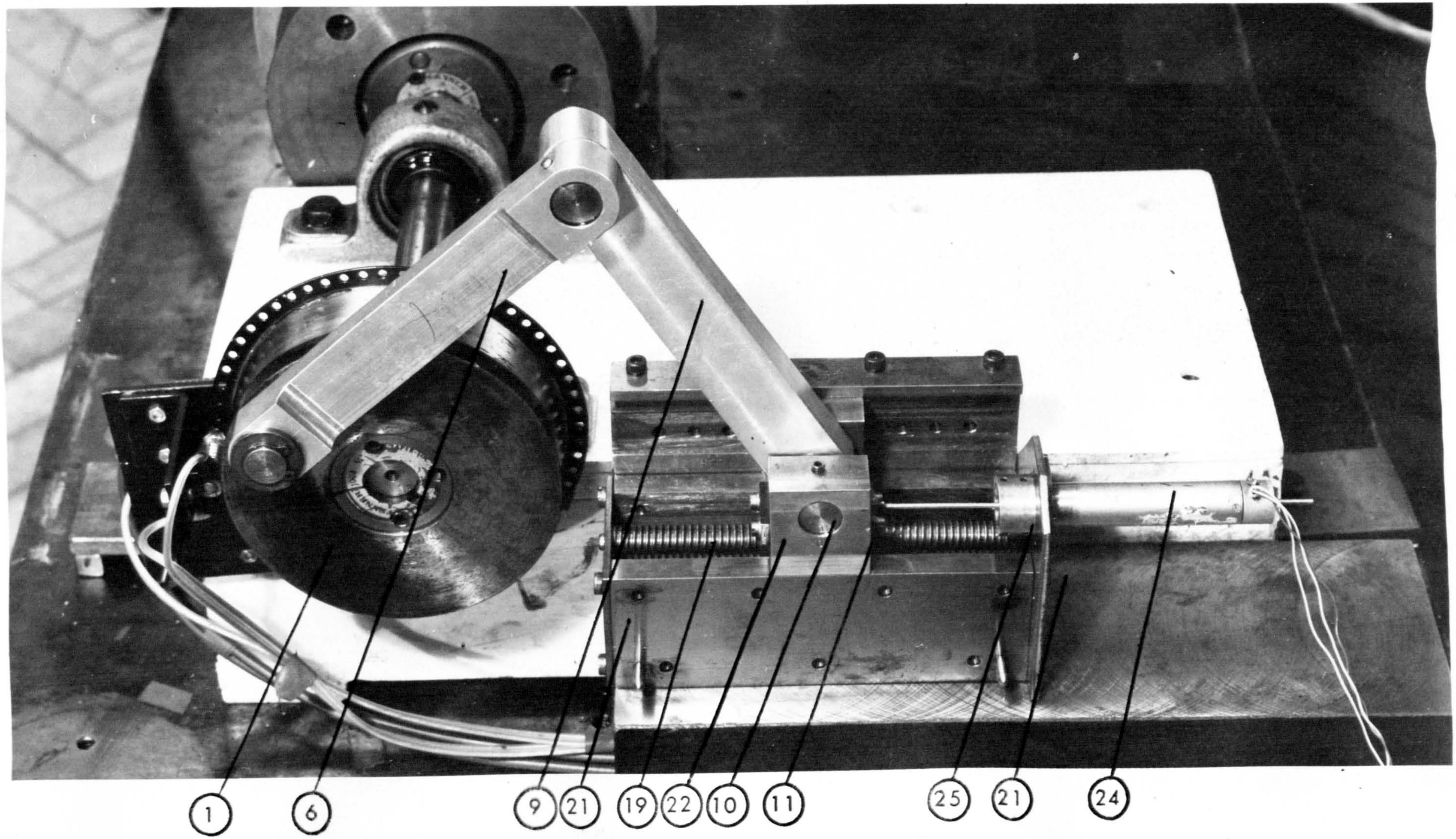

FIG. (8.1) A FRONT VIEW OF EXPERIMENTAL RIG 1.

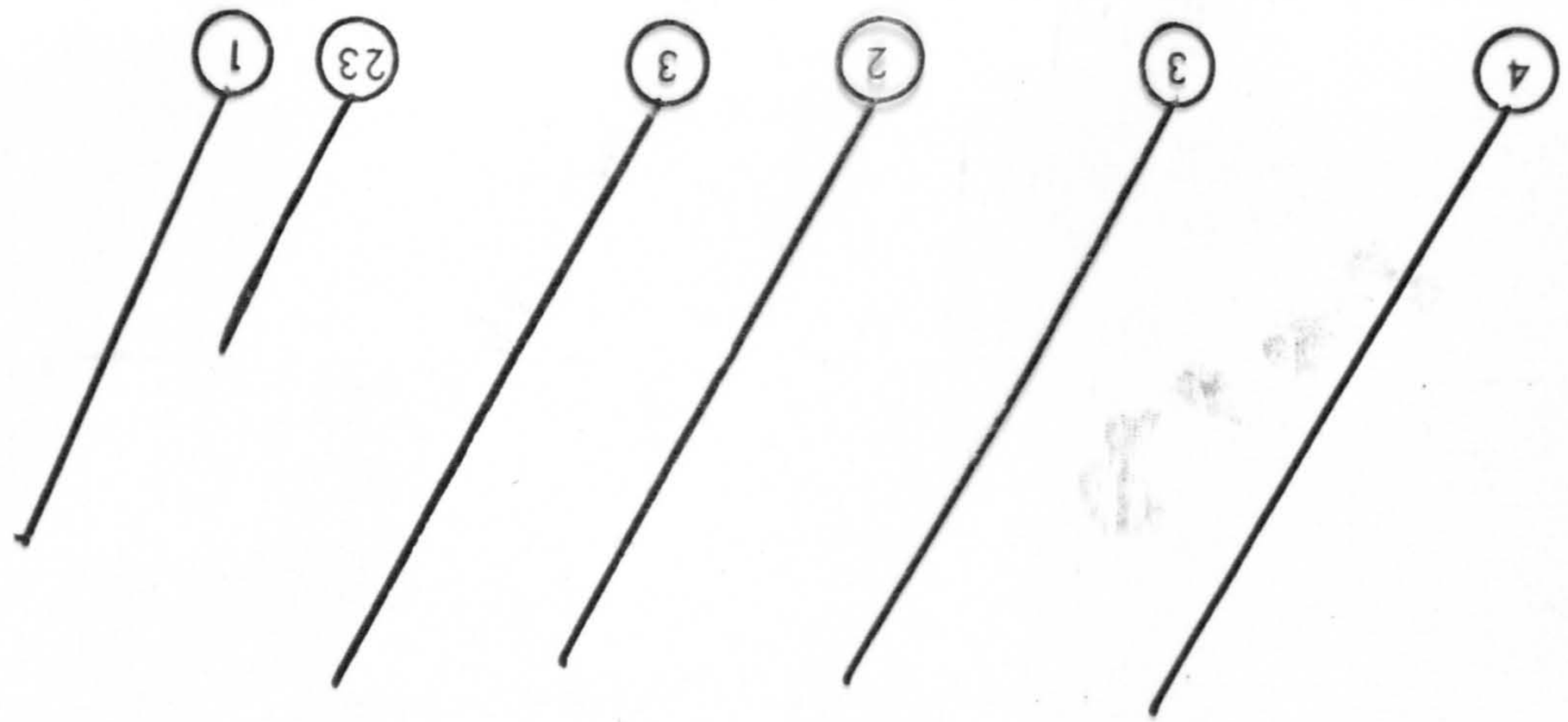
1
23
3
2
3
4

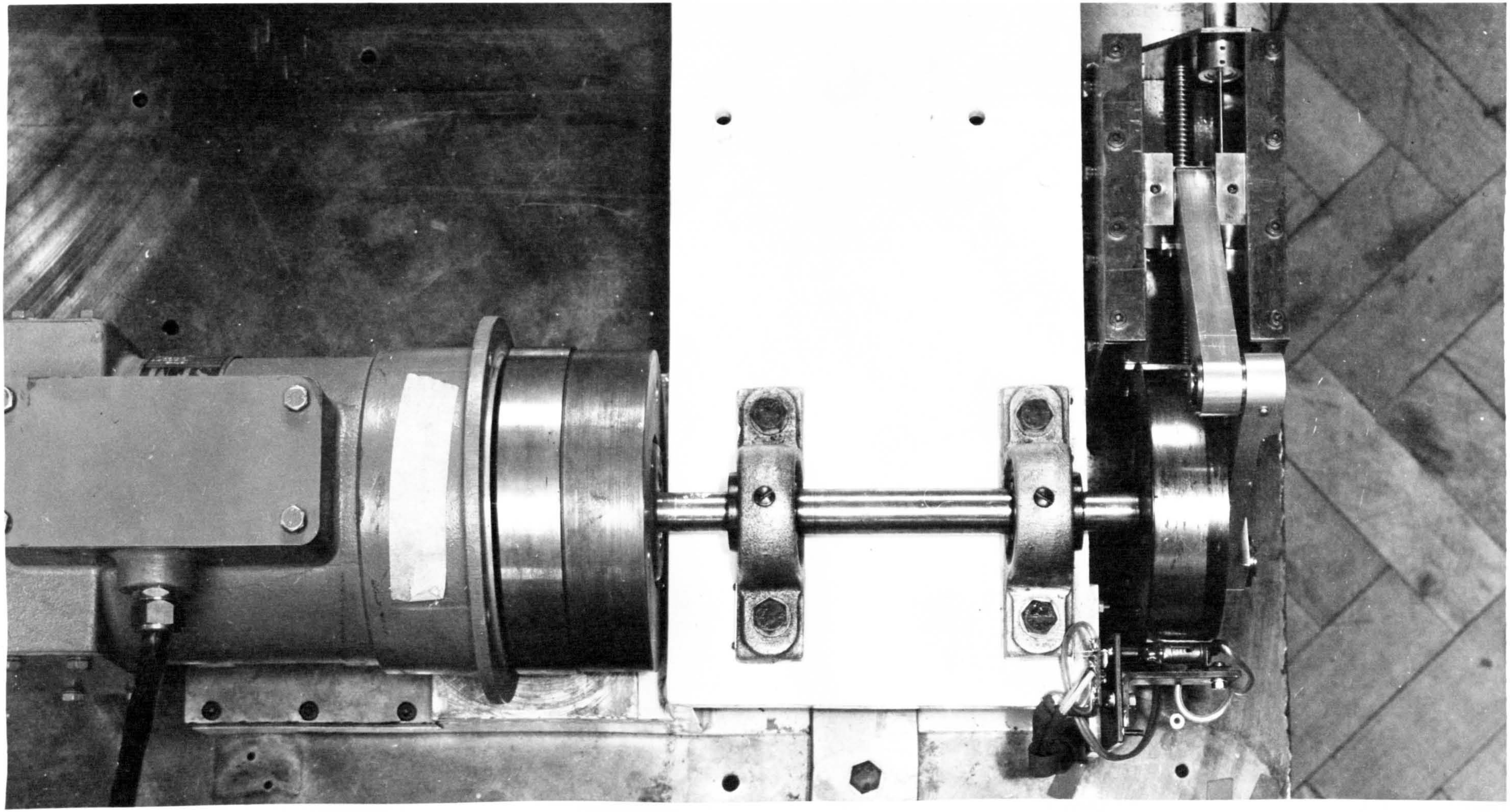

FIG. (8.2) A TOP VIEW OF EXPERIMENTAL RIG 1.

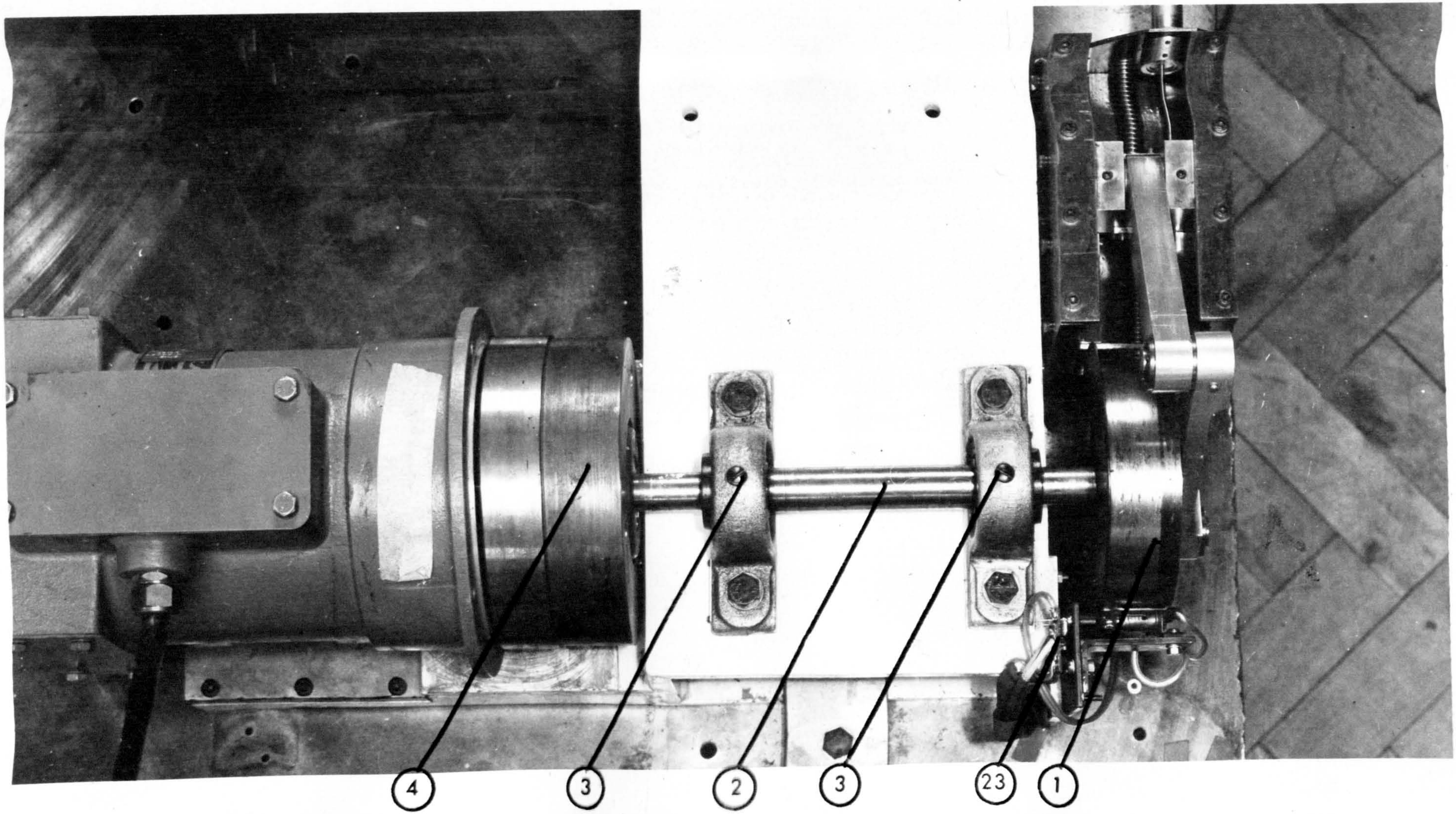

FIG. (8.2) A TOP VIEW OF EXPERIMENTAL RIG 1.

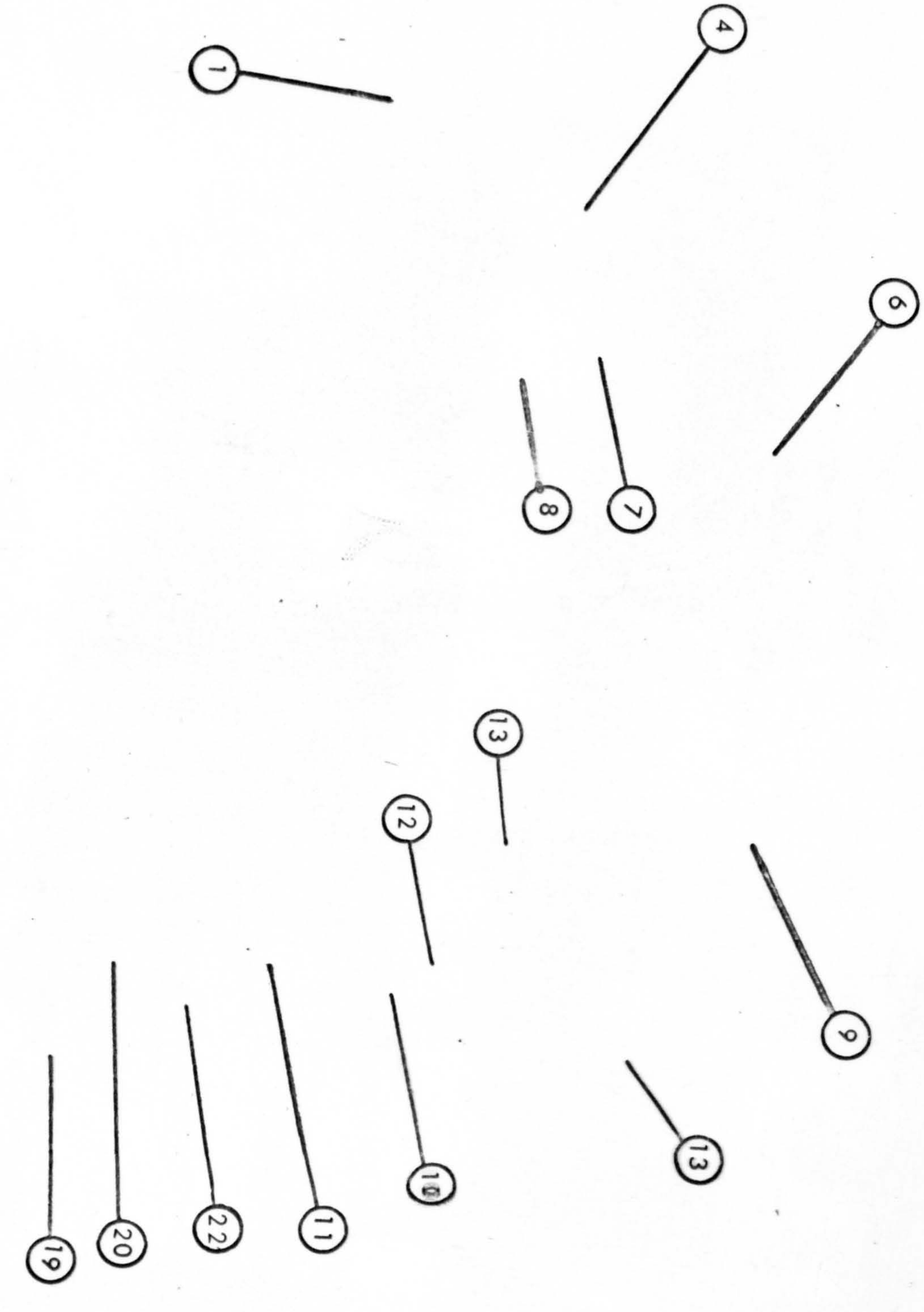
1
4
9
8
7
13
12
10
11
22
20
19

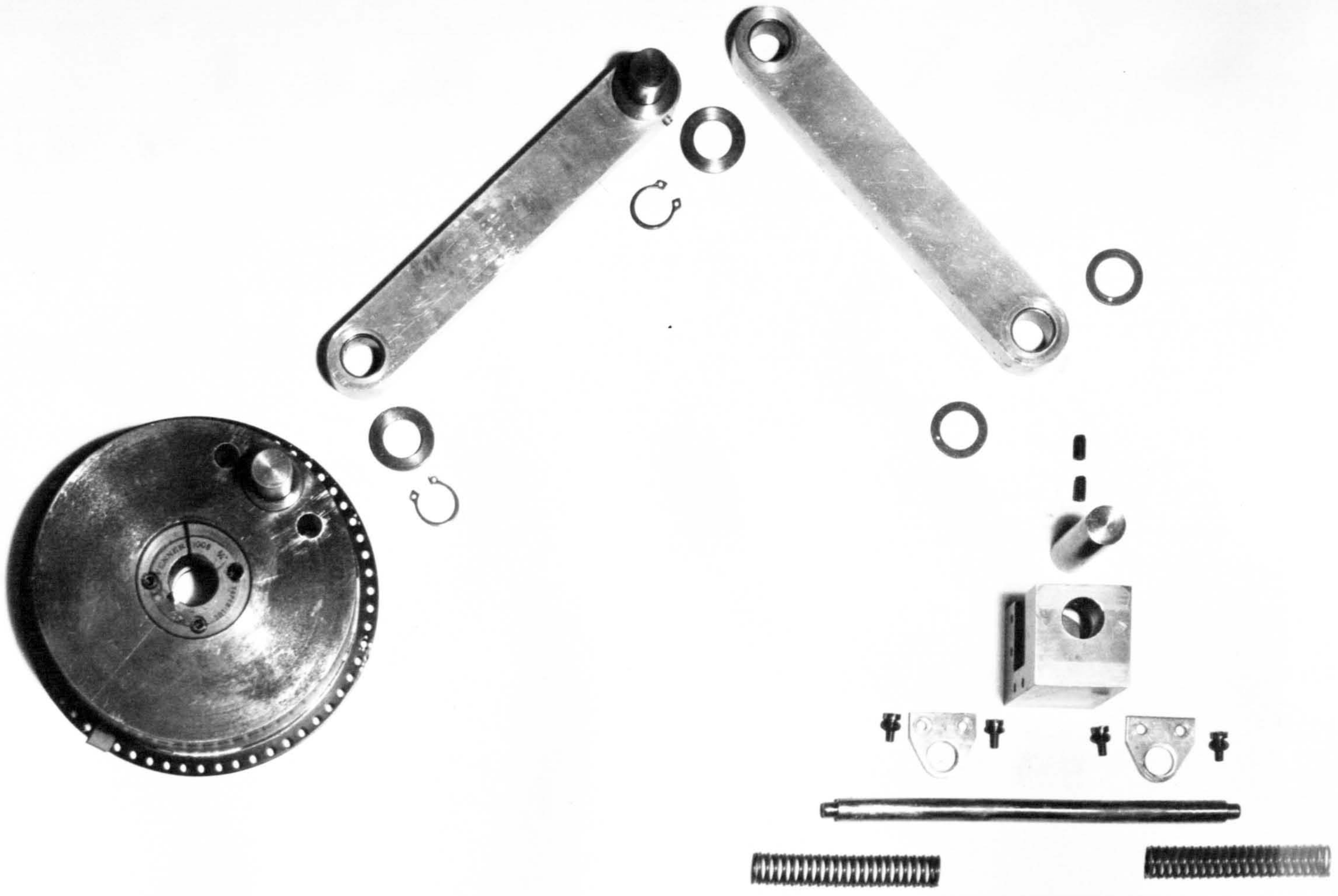

FIG. (8.3a) AN EXPLODED VIEW OF THE LINKAGE OF EXPERIMENTAL RIG 1.

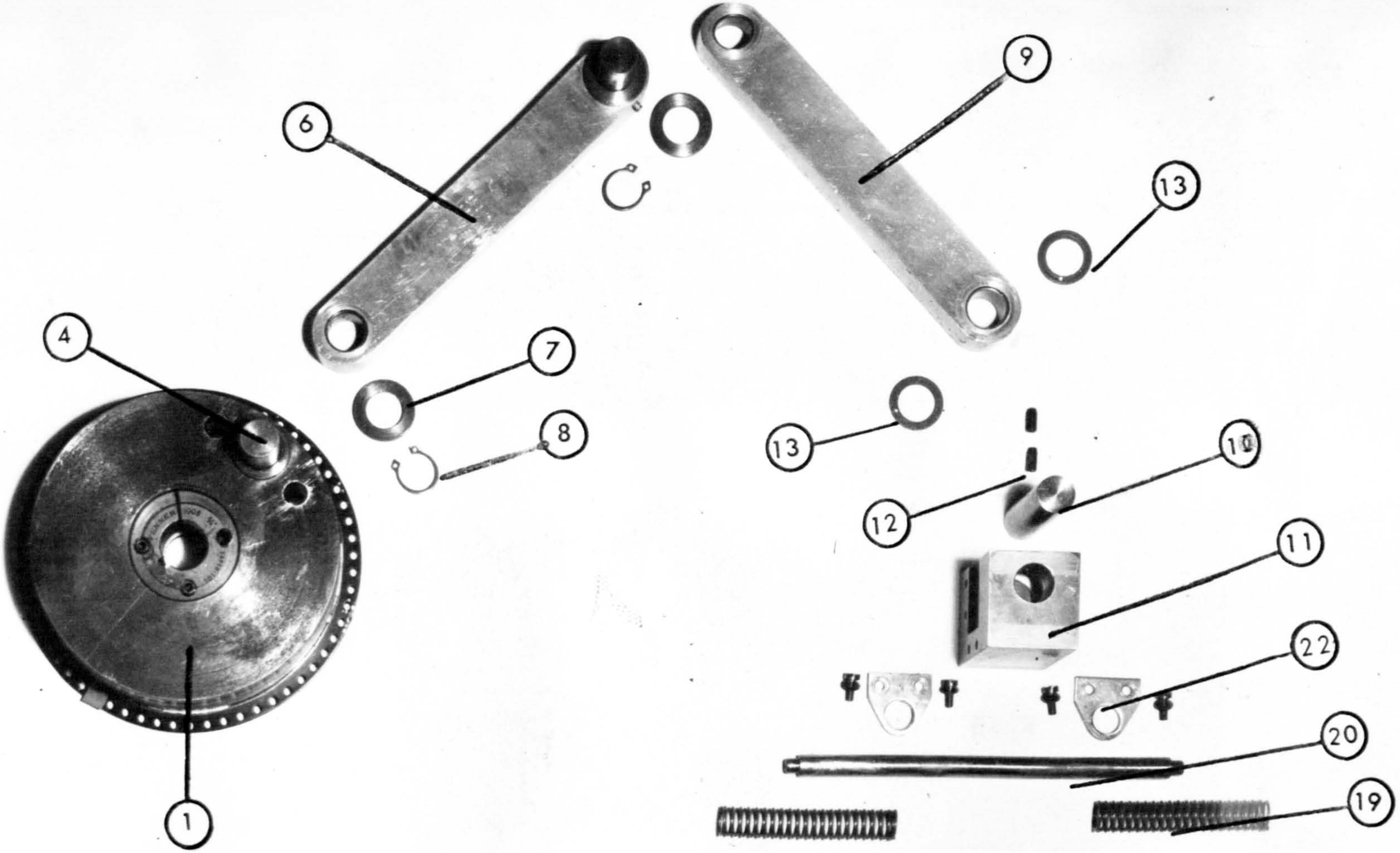

FIG. (8.3a) AN EXPLODED VIEW OF THE LINKAGE OF EXPERIMENTAL RIG 1.


21


16


16

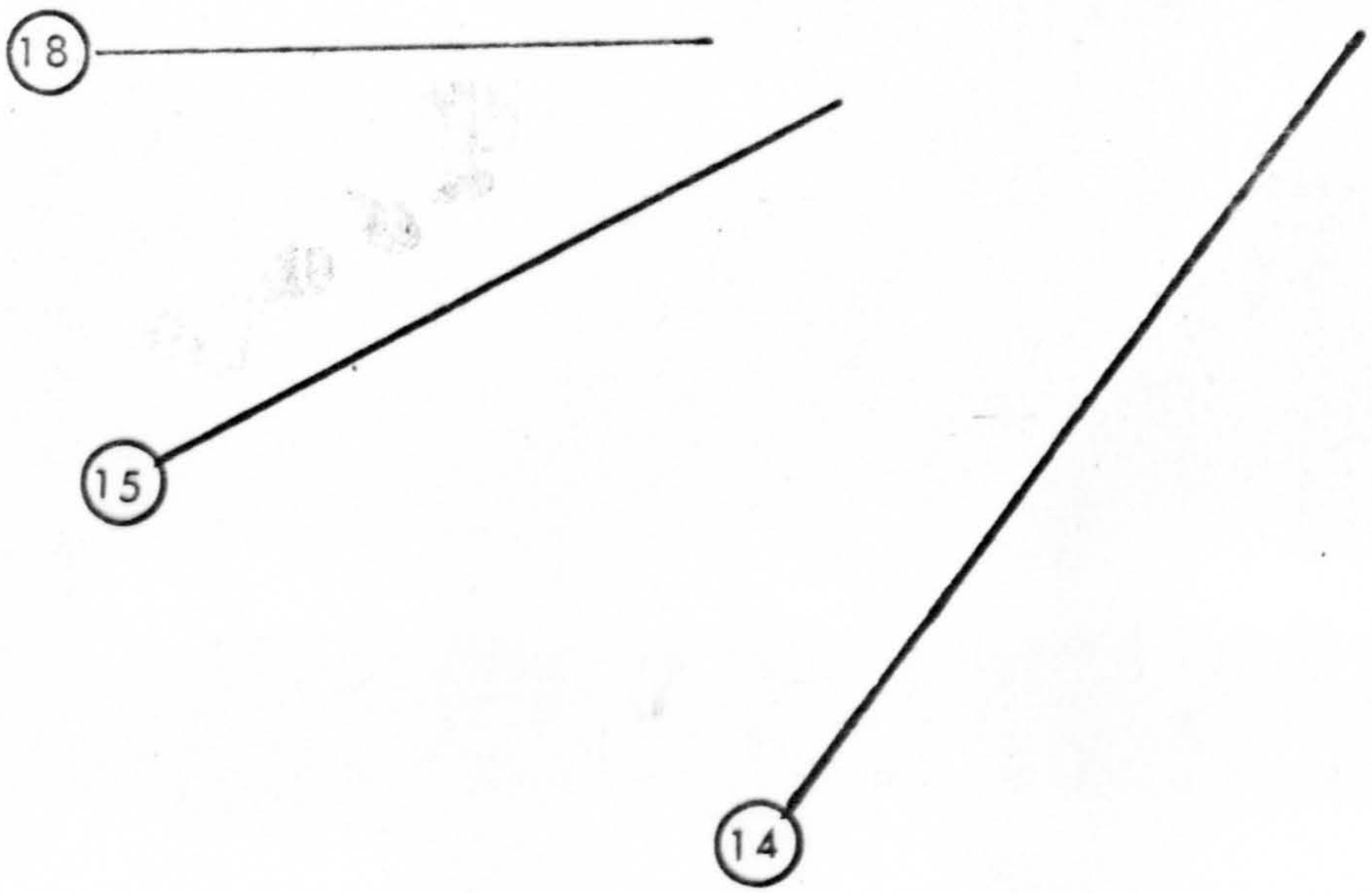
18
15
14

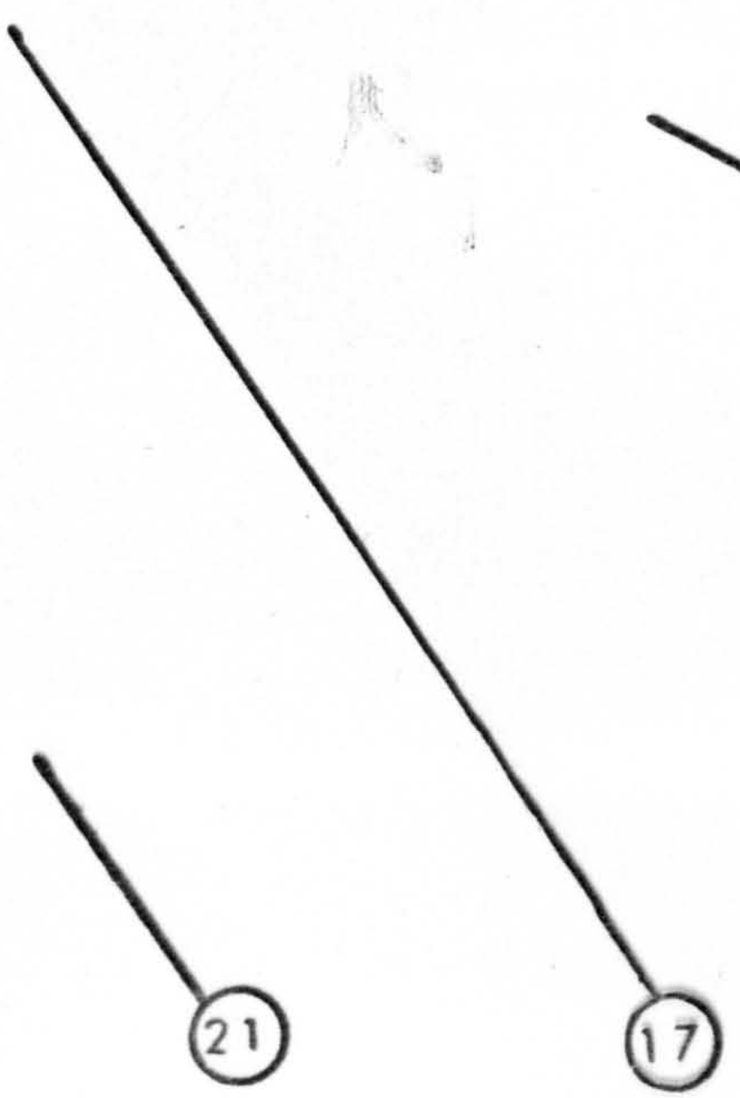
21
17

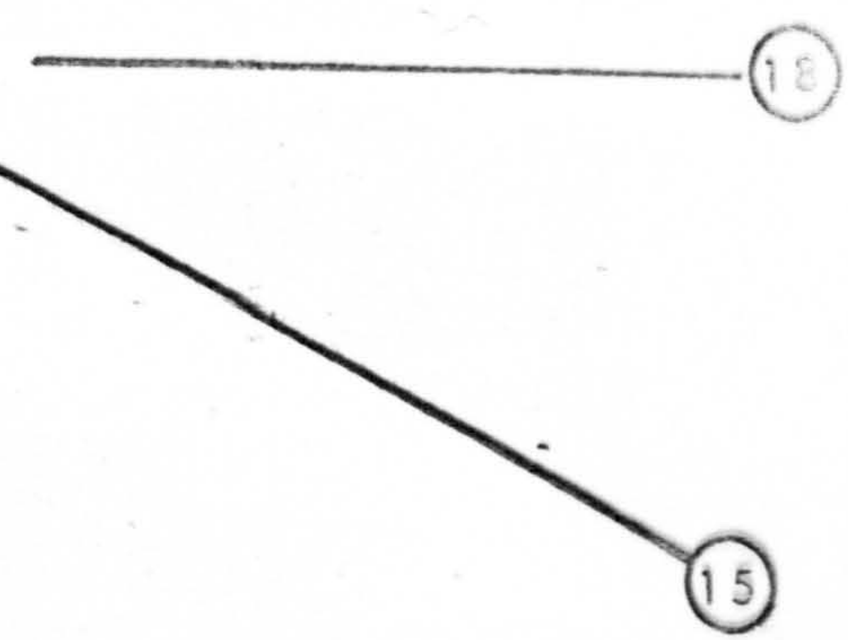
18
15

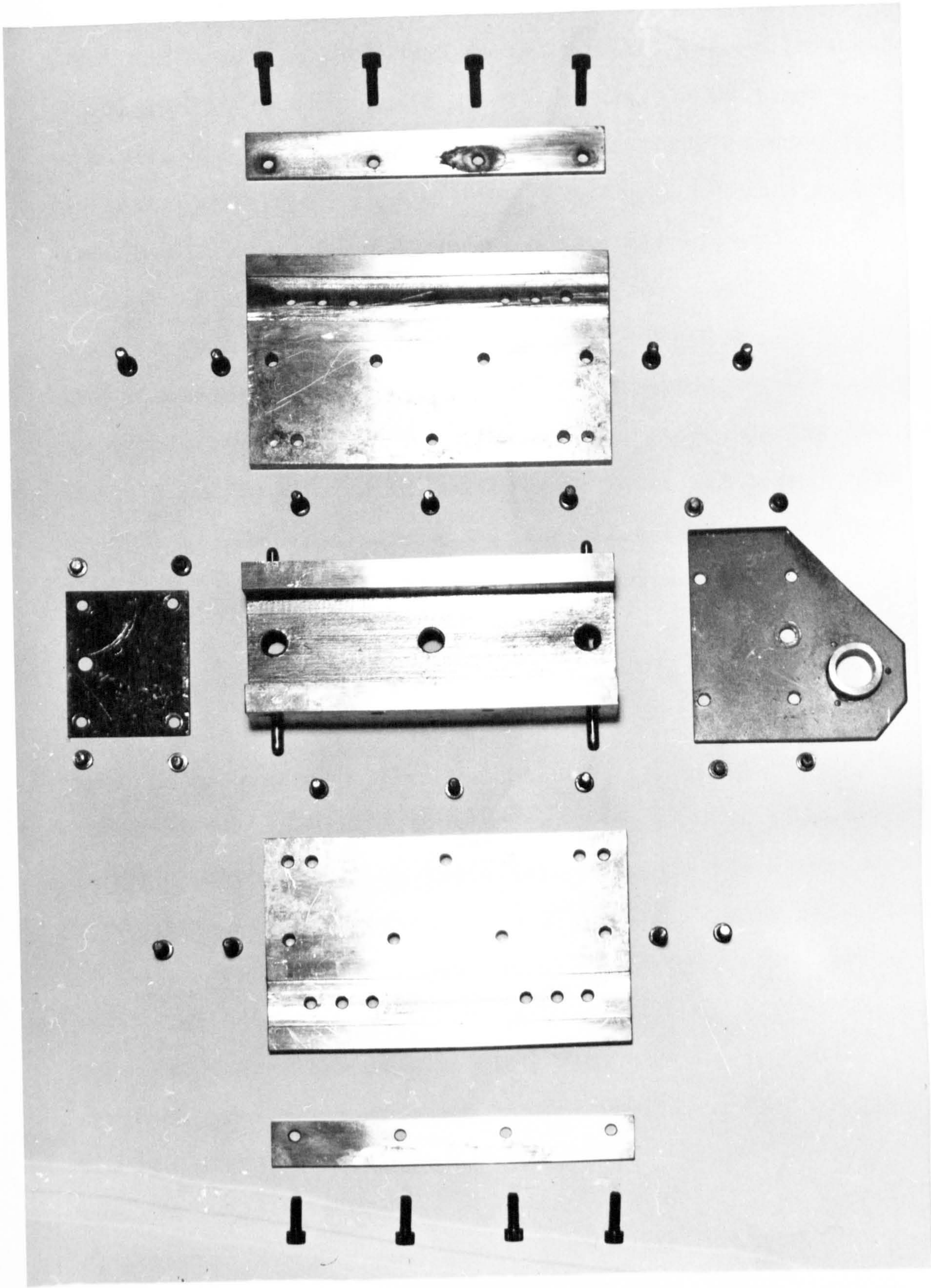

FIG. (8.3b) AN EXPLODED VIEW OF THE SLIDER GUIDE OF EXPERIMENTAL RIG 1.

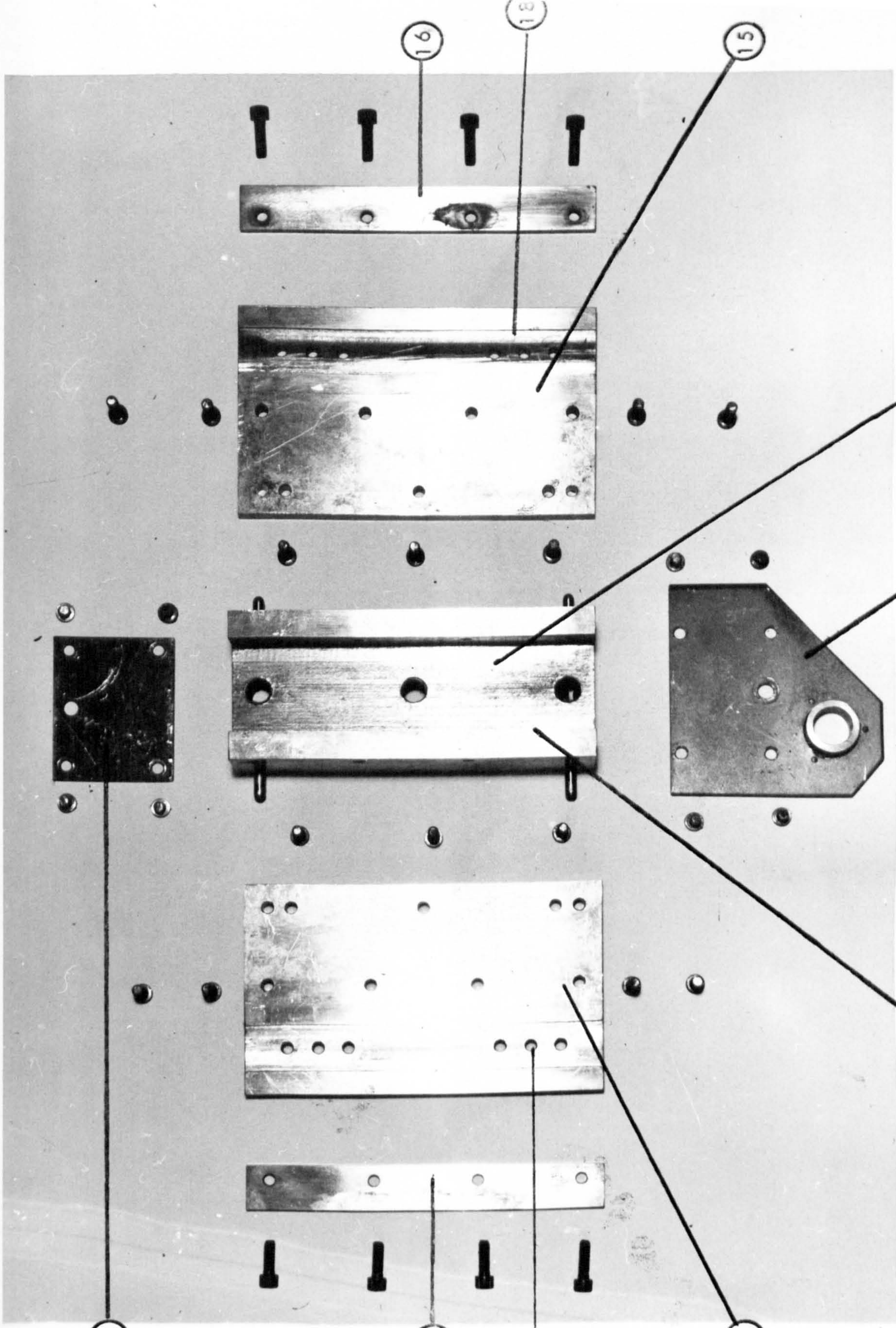

FIG. (8.3b) AN EXPLODED VIEW OF THE SLIDER GUIDE OF EXPERIMENTAL RIG 1.

The crank is connected to the coupler via a stainless steel pin (4) (see Fig. (8.3a)). This pin is fixed to the crank with a tight fit and runs in a dry PTFE bearing (5) housed in the coupler (6). The pin joint assembly is held together by a spacer (7) retained by a cir-clip (8). The coupler is connected to the rocker (9) via a similar assembly with the pin fixed to the coupler. The rocker oscillates on the slider about a pin (10) rigidly connected to the slider (11) by grub screws (12). Two PTFE spacers (13) separate the rocker sides from the slider in order to minimise friction. The slider is made of bronze and its sliding surfaces are ground on a surface grinder to a high surface finish.

The slider oscillates in a guide made of stainless steel and composed of a bed plate (14), (see Fig. (8.3b)), two side plates (15) and two retaining plates (16). The sliding surface area is reduced by milling a channel (17) in the bed plate and a longitudinal channel (18) ⅛" deep along each of the side plates. In addition to reducing the sliding surface the longitudinal channels serve to lubricate the sliding area more effectively. In manufacturing and assembling the sliding guide extreme care was taken to ensure that opposite sliding surfaces are parallel to within close tolerances. In fact all the mating and sliding surfaces are ground on a surface grinder to a high surface finish. The bed plate of the guide is bolted to the main bed plate and located on it by dowels. The positioning is such that when the slider runs its pin moves along a line collinear with the crank shaft. The side plates are doweled to the bed plate and fixed to it by a series of Allen screws. The retaining plates on the

top of the guide are fixed to the side plates by Allen screws. All mating surfaces are marked and doweled to facilitate dismantling and assembly.

The slider is constrained by two springs (19), (see Fig. (8.1) and also (8.3a)), one at each side, of equal stiffness and which, to prevent buckling, run on a silver steel shaft (20). The shaft is held in place by two plates (21) fixed to the end of the guide. The springs are constrained by the end plates and two brass rings (22) fixed to the slider by slot screws.

8.2.1.2 Electrical Components

The linkage is driven by a 0.5 H.P. Servomex variable speed motor. The motor control unit is of type MC47 Servomex Control Ltd., displaying the speed in R.P.M. In addition to the speed display on the control unit the input speed is measured by a photocell arrangement (23), (see Fig. (8.2)). This arrangement consists of a disc mounted concentrically on the crank with 60, ⅛ inch diameter, holes drilled equally spaced on a circumference of a circle having a ½ inch diameter larger than that of the crank. A light source directs a beam of light on the photocell which is behind the crank and mounted on a bracket fixed to the linkage pedestal. The cell receives the light when a hole is in line with both the beam and the cell. As the crank is rotated the reception of light by the cell is interrupted and thus a series of pulse signals, each corresponding to a hole, are generated. The circuit associated with the photocell is shown in Fig. (8.4a) and has two outputs; one is fed to a pulse counter or an oscilloscope, and the other

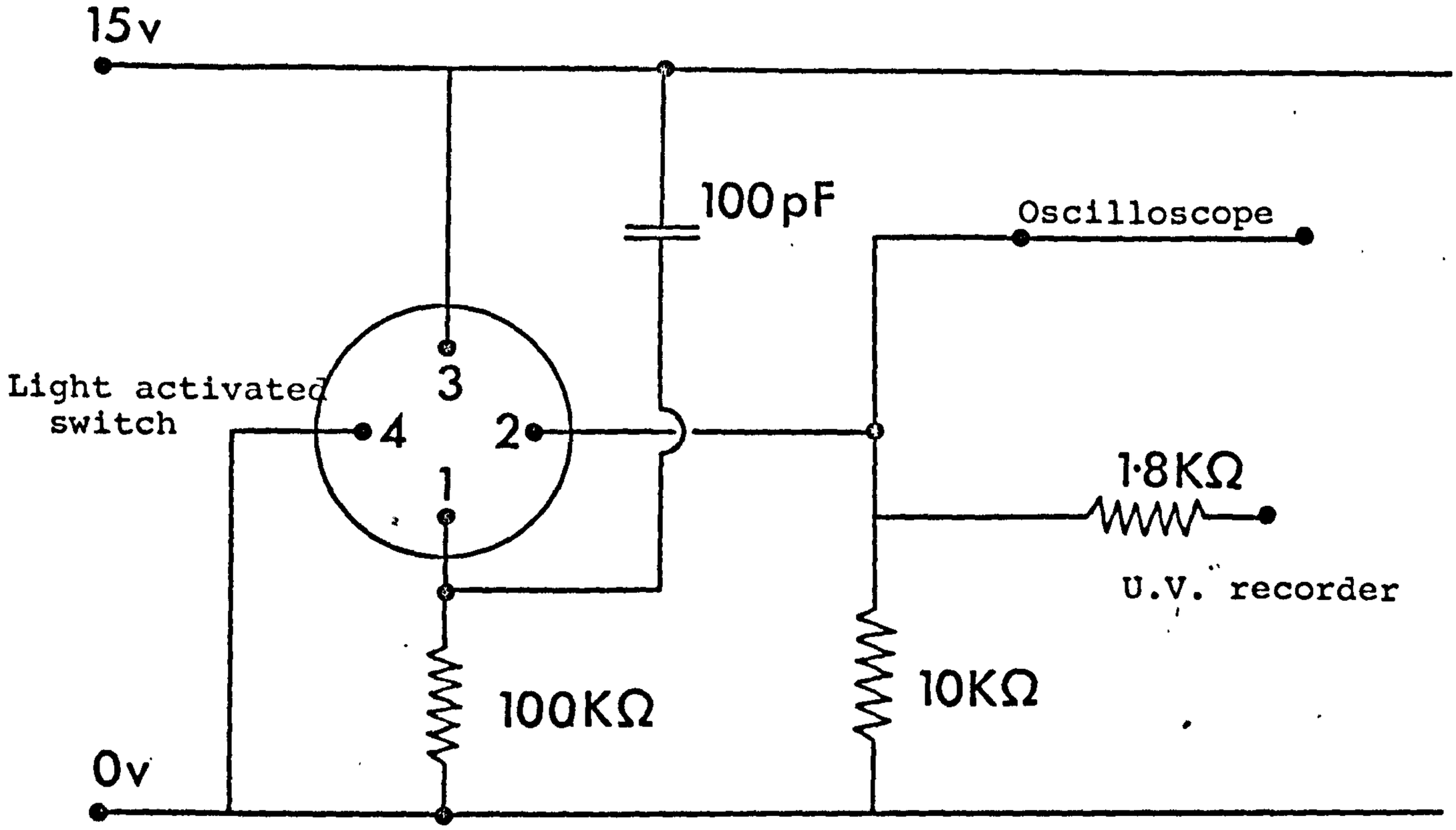

FIG. (8.4a) PHOTO CELL CIRCUIT.

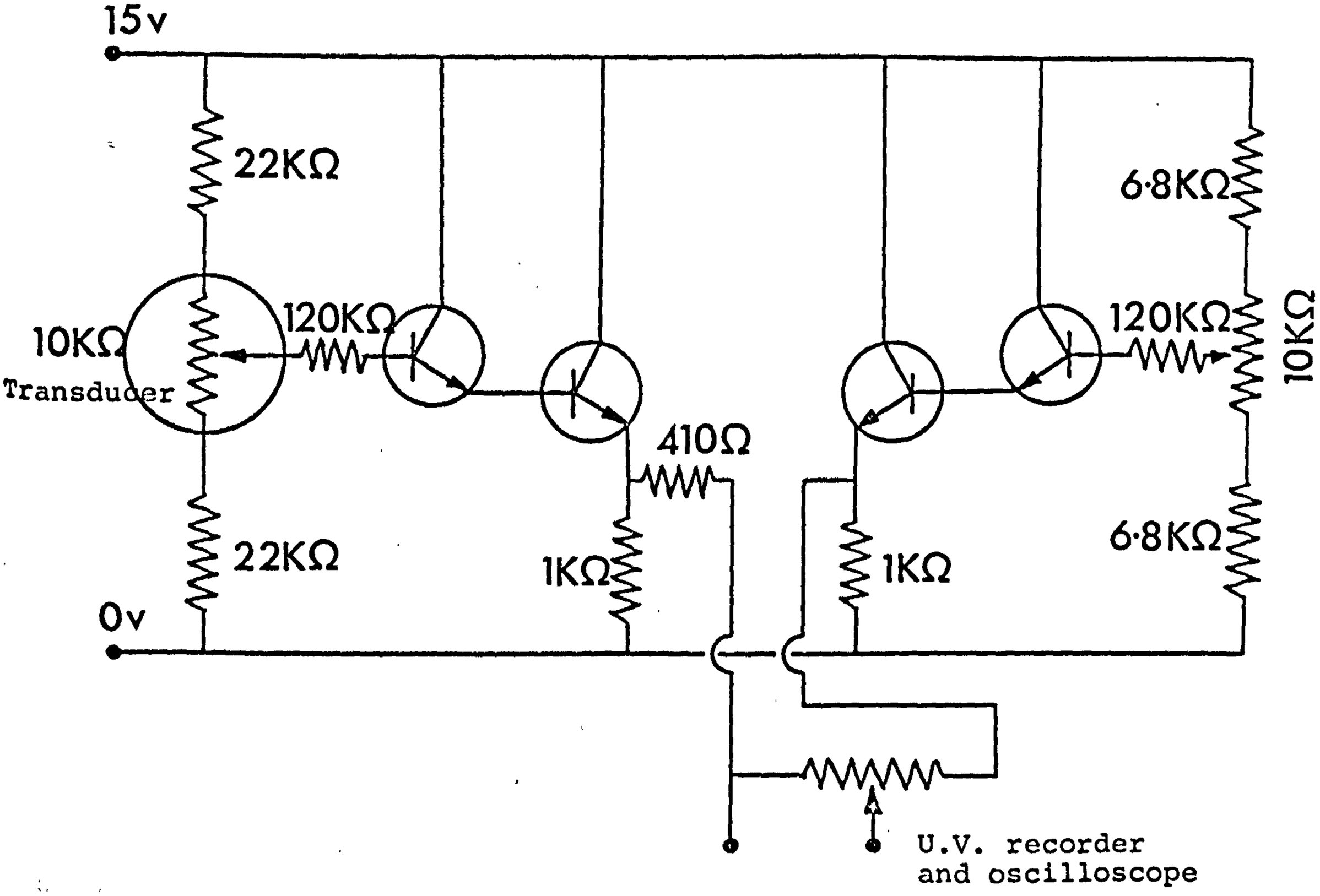

FIG. (8.4b) TRANSDUCER DIFFERENTIAL AMPLIFIER CIRCUIT.

to a U.V. recorder. The counter displays the speed in R.P.M. and the oscilloscope and U.V. recorder display the pulsating signals. Since each pulse corresponds to a hole a comparison of the width of each shows whether the speed varies within the crank cycle. The crank speed may also be obtained from the width of the pulses and the speed of paper in the U.V. recorder or the time base of the scope.

The slider movement is measured by a displacement transducer (24), (see Fig. (8.1)), type PD13, rectilinear transducer made by "ETHER Ltd.". It is mounted on three pairs of Grub screws, 120^{o} apart, in a collar (25) mounted on the end plate (21). The moving element of the transducer is fixed to the slider by a screw and thread arrangement. The output of the transducer is fed to an oscilloscope and a U.V. recorder. The input to the U.V. recorder is fed through a differential amplifier circuit shown in Fig. (8.4b). The differential amplifier was necessary to ensure linear deflection on either side of the datum position. The need arose because of the galvanometer loading on the transducer.

8.2.2 Experimental Rig 2*

A photograph of this apparatus is shown in Fig. (8.5). Its purpose is to investigate the slider resonance when the crank length is small compared with other links. One of its main features is that the slider runs on two linear bearings on two parallel shafts fixed to a solid frame, thus minimising the frictional forces opposing the slider motion.

The instrumentation involved with this apparatus is similar to the instrumentation of Experimental Rig 1.

* This rig was the subject of an M.Sc. dissertation. Full description and detailed photographs may be found in reference (53).

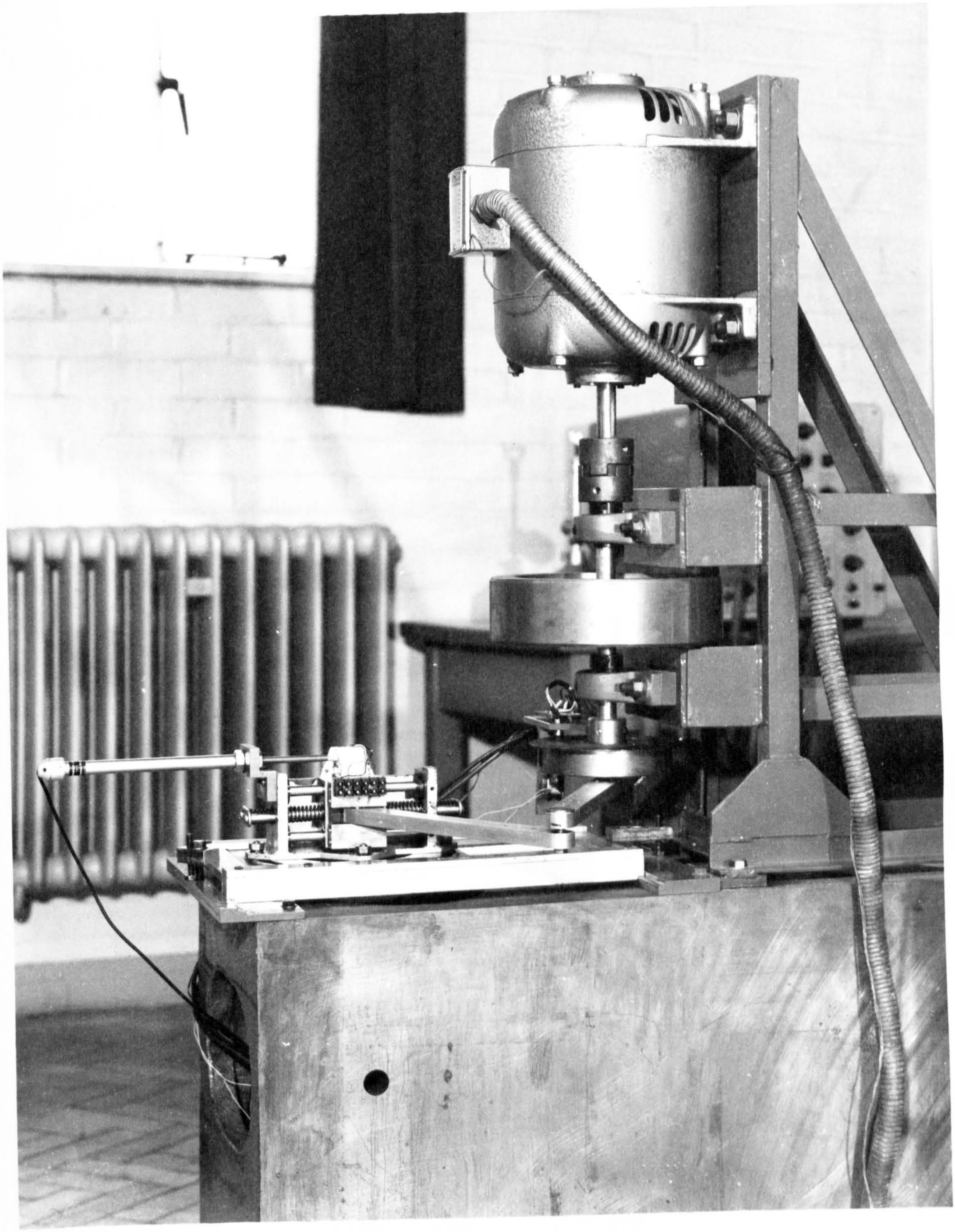

FIG. (8.5) A GENERAL VIEW OF EXPERIMENTAL RIG 2.

8.3 CALIBRATION

8.3.1 Linkages Input Parameters

The coupler, the rocker and the slider were weighed and their masses recorded in gms. The inertias of the coupler and rocker about their centres of gravity were measured using laboratory experiments namely the compound and bifiliar pendumum. The lengths of the links were measured between the centres of the pin joints at either end. The crank length was measured between the crank shaft and the crank pin. The following tables show the measured parameters of the two apparatus used.

Item	Crank	Coupler	Rocker	Slider
Length (cm)	5	15	15	-
C.G. (cm)	O	To crank pin 9.55	To slider pin 7.5	To crank shaft 15.37
Mass (gm)	-	222	206	600
Inertia about C.G. ($gm.cm^2$)	-	7064	4797	-

Table (8.1). Data for Experimental Rig 1.

Item	Crank	Coupler	Rocker	Slider
Length (cm)	1.27	25.4	25.4	-
C.G. (cm)	O	To crank pin 14.2	To slider pin 12.7	To crank shaft 25.4
Mass (gm)	-	324	264	856
Inertia about C.G. ($gm.cm^2$)	-	23784	15100	-

Table (8.2). Data for Experimental Rig 2.

8.3.2 Spring Stiffness

The stiffnesses of the springs were measured using "J. Bantham" (spring manufacturers) calibration apparatus. Theoretical calculations of the stiffness, based on the number of coils, the wire and mean coil diameters and the modulus of rigidity of the material gave good agreement with the experimentally determined values.

8.3.3 Damping Coefficient

The damping coefficient was estimated by observing the response to the slider, when disconnected from the linkage, to an impulse input. A typical response is shown in Fig. (8.6). The coefficient is estimated from measurement of the logarithmic decrement. Average values of the coefficient were found to be 9×10^3 dyne.Sec/cm. for Experimental Rig 1 and 5.5×10^3 dyne. Sec/cm. for Experimental Rig 2 (linearised rig).

8.3.4 The Slider Displacement

The slider movement was calibrated using slip gauges and noting the deflection of the galvanometer signal of the U.V. recorder.

8.4 RESULTS

8.4.1 Experimental Rig 1

In this section the steady state oscillations of the slider are investigated when the mechanism is driven at different constant input speeds. Two cases are studied corresponding to two springs constraining the slider in its line of travel. The first case corresponds to a spring stiffness of 3×10^6 dyne/cm.

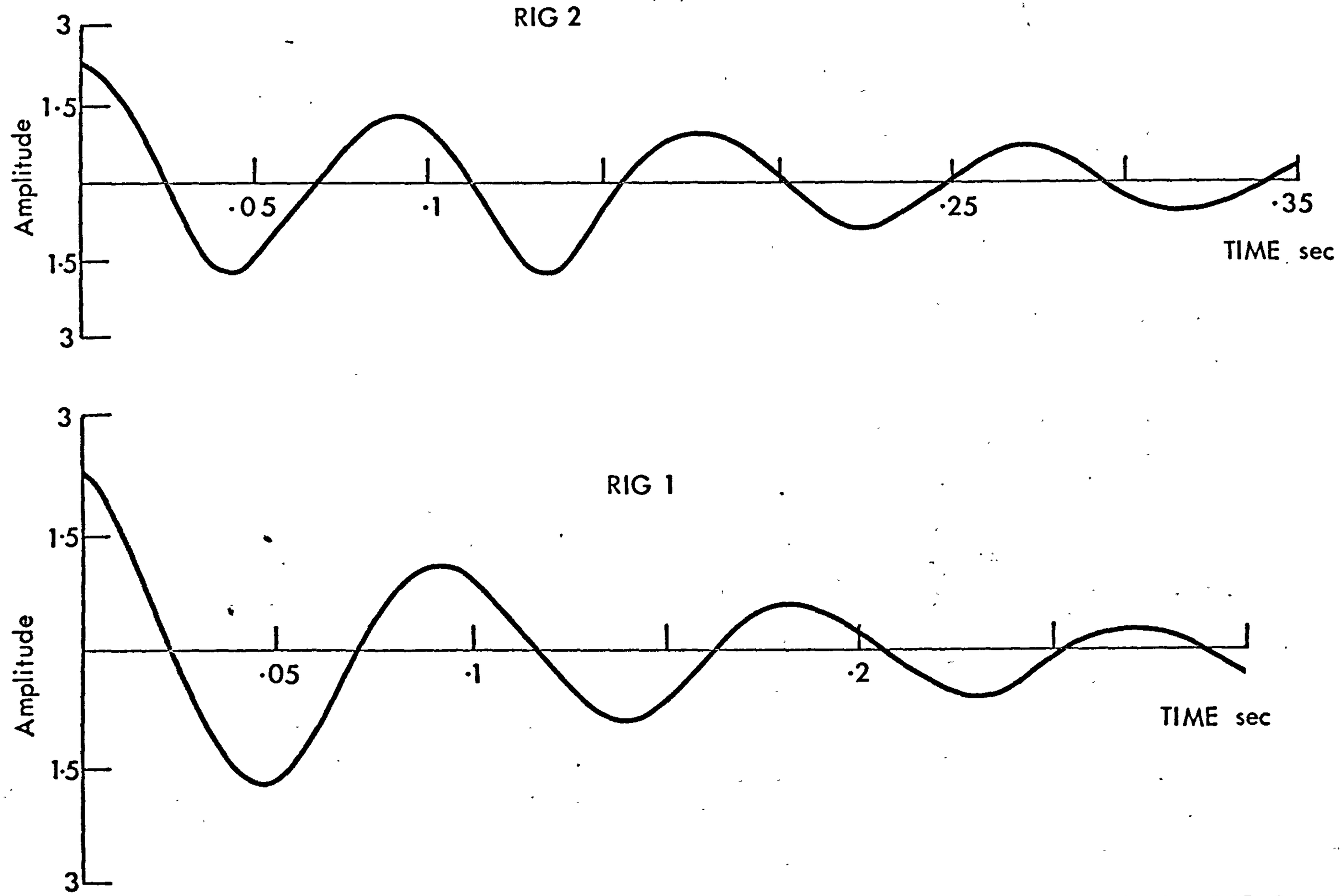

FIG. (8.6) DECAY OF SLIDER OSCILLATIONS; ESTIMATION OF DAMPING COEFFICIENT

and the second to a stiffness of 11 x 10^6 dyne/cm. The first spring will be referred to as spring A and the second as spring B. The results are compared with those obtained using the theory developed in Chapters II and III.

8.4.1.1 Comparison of Experimental and Theoretical Results

The theory predicts the steady state slider motion to be oscillatory and periodic with one crank cycle. This is verified experimentally as shown in Fig. (8.7) in which a typical experimentally observed steady state motion of the slider is shown against the crank angle. The particular motion shown in this figure is obtained with spring A and a constant crank speed of 360 RPM. However, for all other speeds, using this spring and also spring B, the motion was always periodic with one crank cycle.

In order to investigate the agreement between the experimental and theoretical results the slider experimental steady state motion was recorded, at a number of speeds below the natural frequency, with both springs A and B and compared with the theoretical motion. For illustration purposes the comparison shown in here is at a selection of these speeds only. These are 390, 420 and 450 RPM with spring A and 600, 660 and 720 RPM with spring B. The choice of these speeds was arbitrary and only one slider oscillation corresponding to one crank cycle is shown at each speed. The results with spring A are shown in Figs. (8.8), (8.9) and (8.10) and with spring B in Figs. (8.11), (8.12) and (8.13).

As may be seen from Figs. (8.8), (8.9) and (8.10) the theoretical and experimental results are in good agreement in

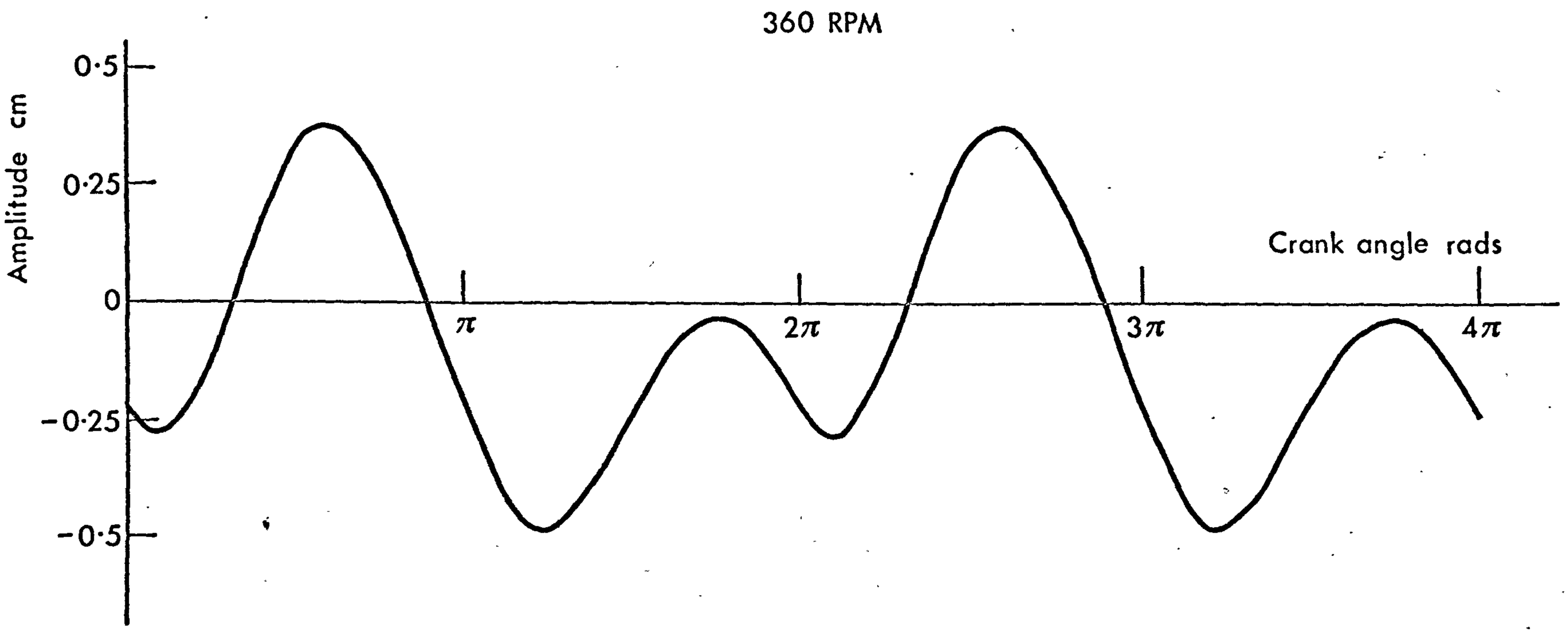

FIG. (8.7) A TYPICAL STEADY STATE SLIDER MOTION OBTAINED FROM RIG 1.

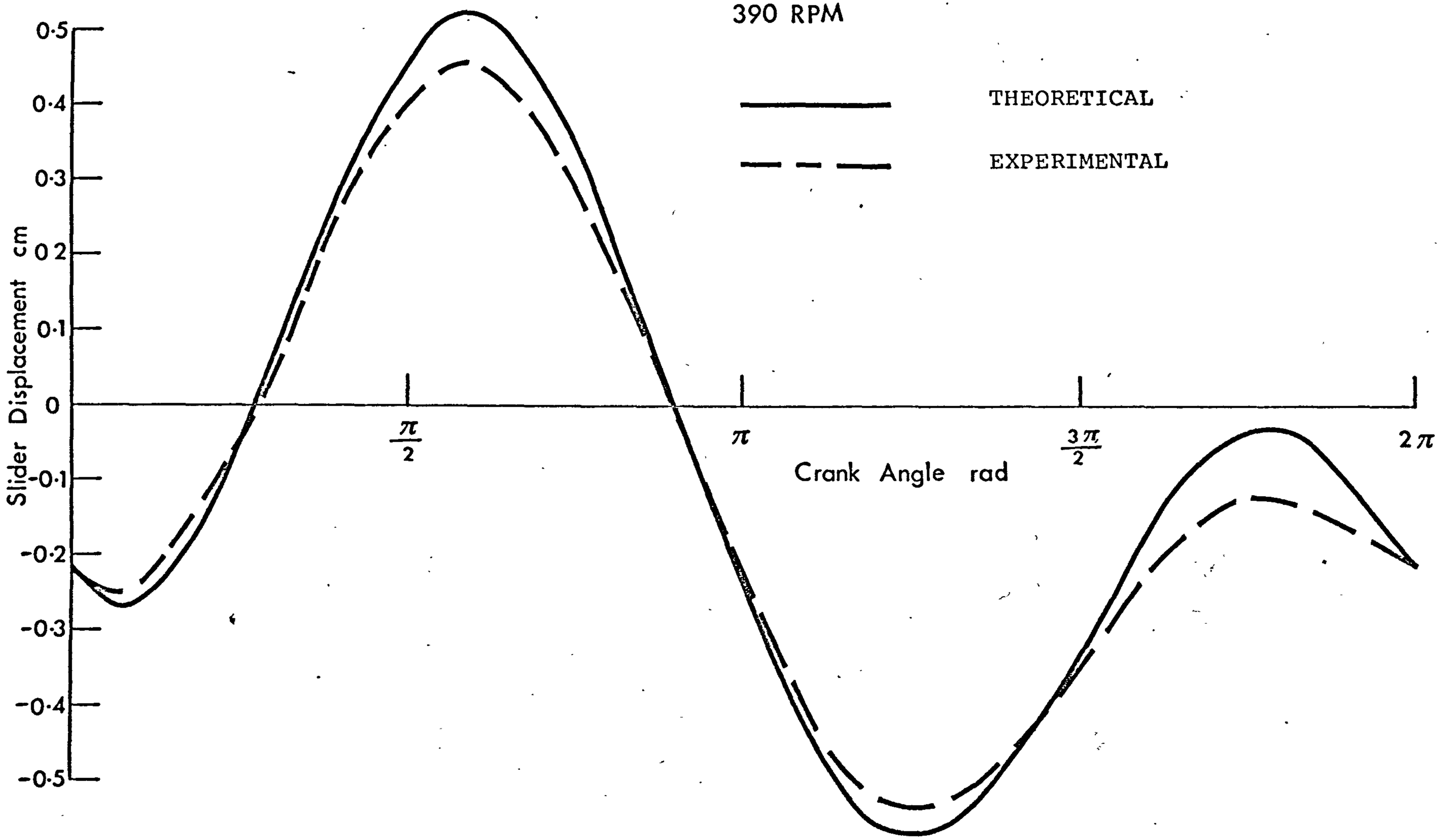

FIG. (8.8) SLIDER MOTION FOR ONE CRANK CYCLE WITH SPRING A AND CONSTANT CRANK SPEED OF 390 RPM.

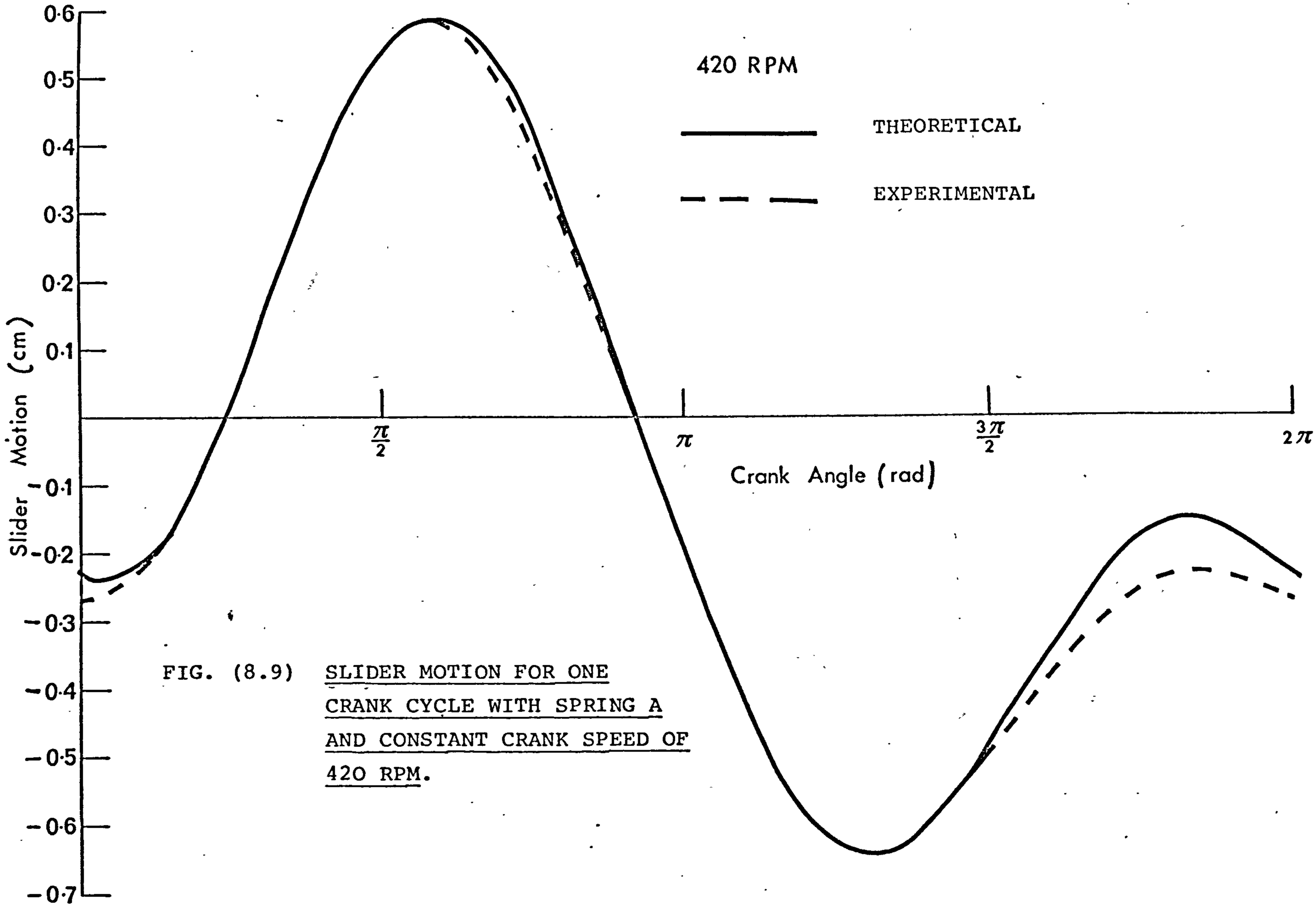

FIG. (8.9) SLIDER MOTION FOR ONE CRANK CYCLE WITH SPRING A AND CONSTANT CRANK SPEED OF 420 RPM.

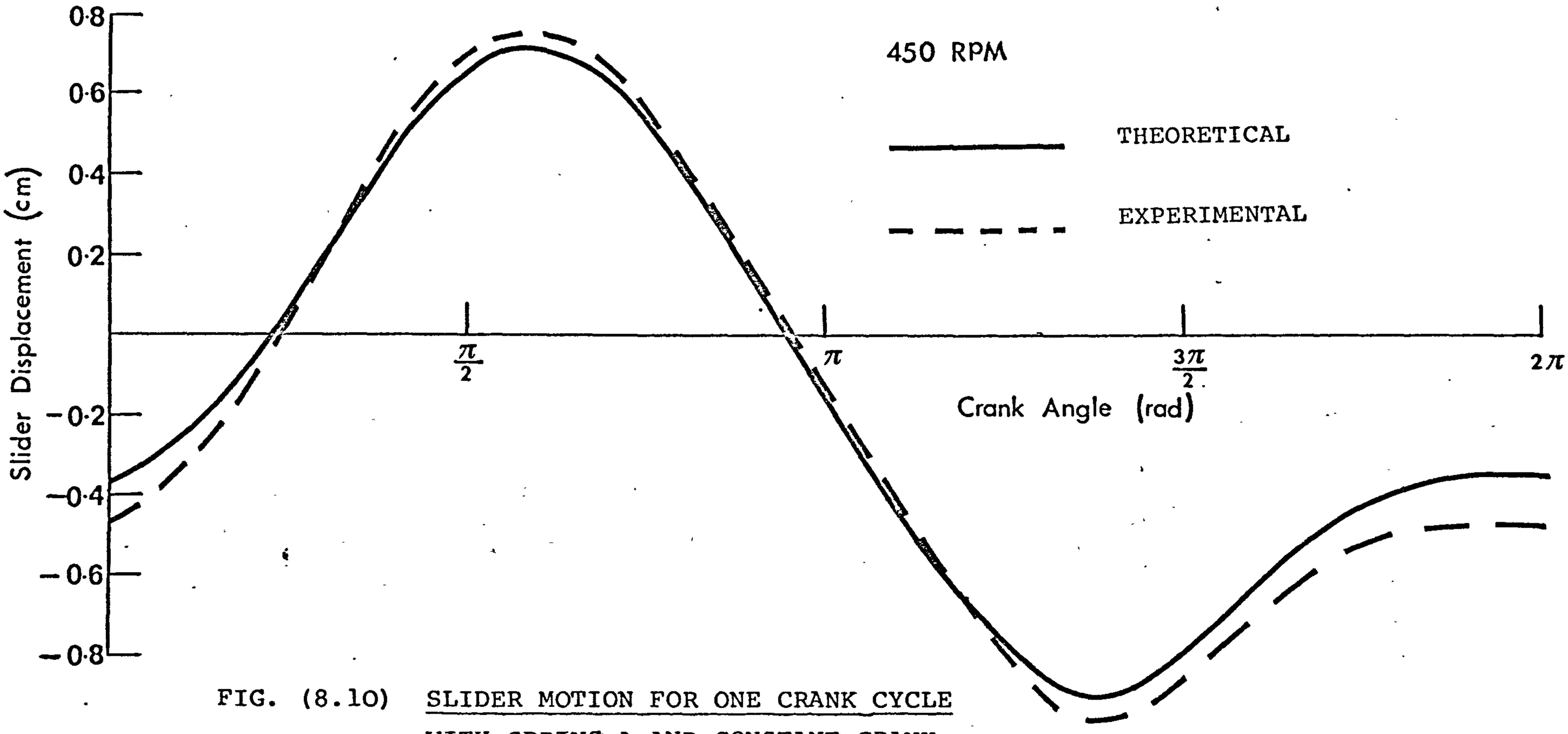

FIG. (8.10) SLIDER MOTION FOR ONE CRANK CYCLE WITH SPRING A AND CONSTANT CRANK SPEED OF 450 RPM.

both phase and amplitude. It can however be observed that while the phase is almost in total agreement the amplitude shows slight variations. This may be explained by the fact that the frictional forces opposing the slider motion are considered solely viscous in the theory. However in practice these frictional forces are a combination of viscous and Coloumb friction forces, although in this experiment the viscous forces are dominant. Because a Coloumb friction force varies with the normal force and since in this experiment this normal force, which is the vertical force in the rocker-slider joint, varies with crank speed and also within a crank cycle, this explains the difference in amplitude between the theoretical and experimental motions with variation of crank speed and also within one crank cycle. Other factors contributing to the difference are (a) only an average estimation of the damping coefficient is considered in the theory and (b) the friction in the pin joints of the linkage is also ignored in the theory.

Figs. (8.11), (8.12) and (8.13) show the selection of experimentally observed slider oscillations compared with corresponding theoretical results obtained with spring B and corresponding to crank speeds of 600, 660 and 720 RPM respectively. As may be seen the theoretical and experimental results are almost in total agreement in phase. The agreement in amplitude is, however, not as good but nevertheless reasonable. The differences may be attributed to the same factors as previously described with spring A.

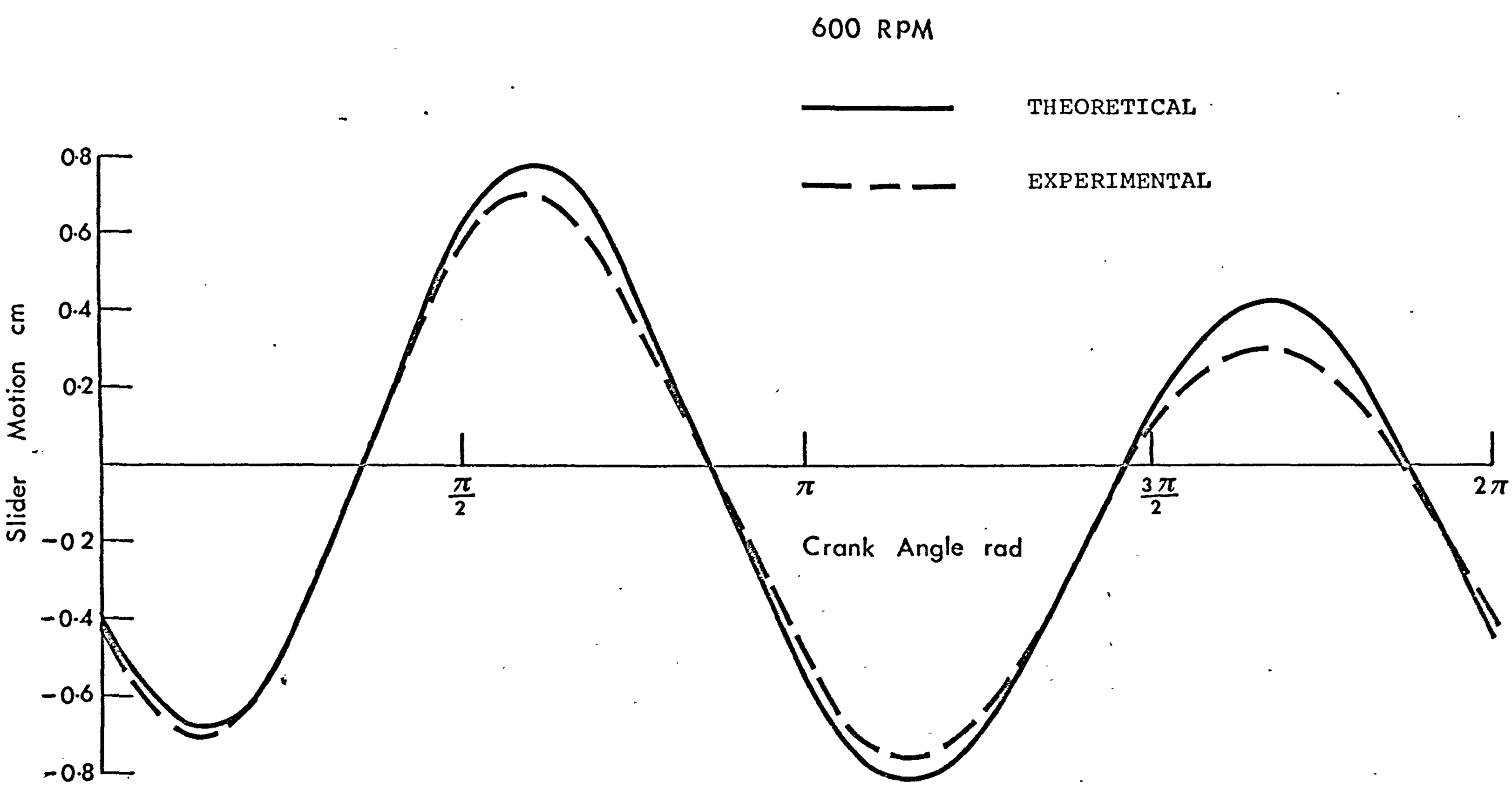

FIG. (8.11) SLIDER MOTION FOR ONE CRANK CYCLE WITH SPRING B AND CONSTANT CRANK SPEED OF 600 RPM.

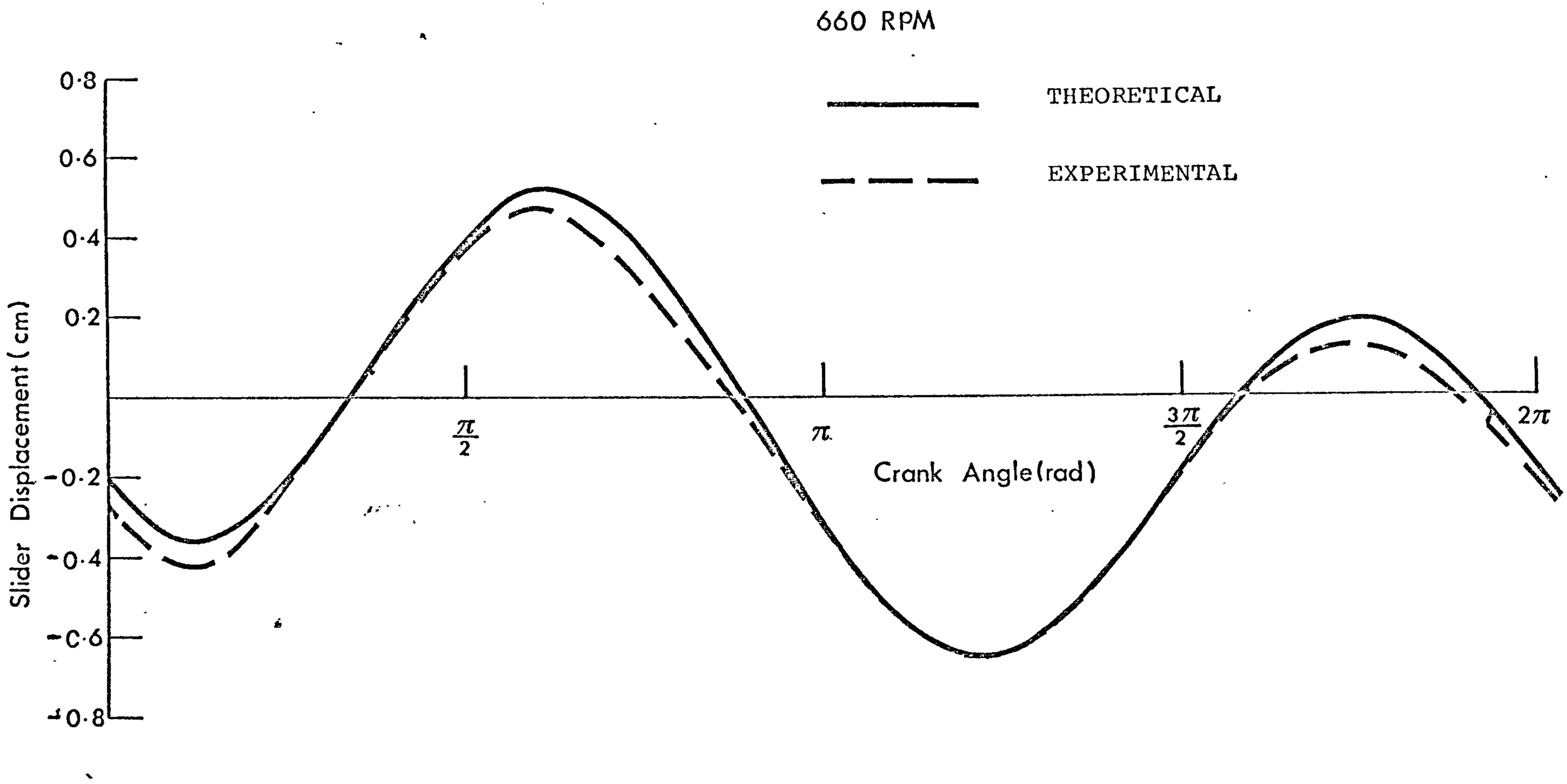

FIG. (8.12) SLIDER MOTION FOR ONE CRANK CYCLE WITH SPRING B AND CONSTANT CRANK SPEED OF 660 RPM.

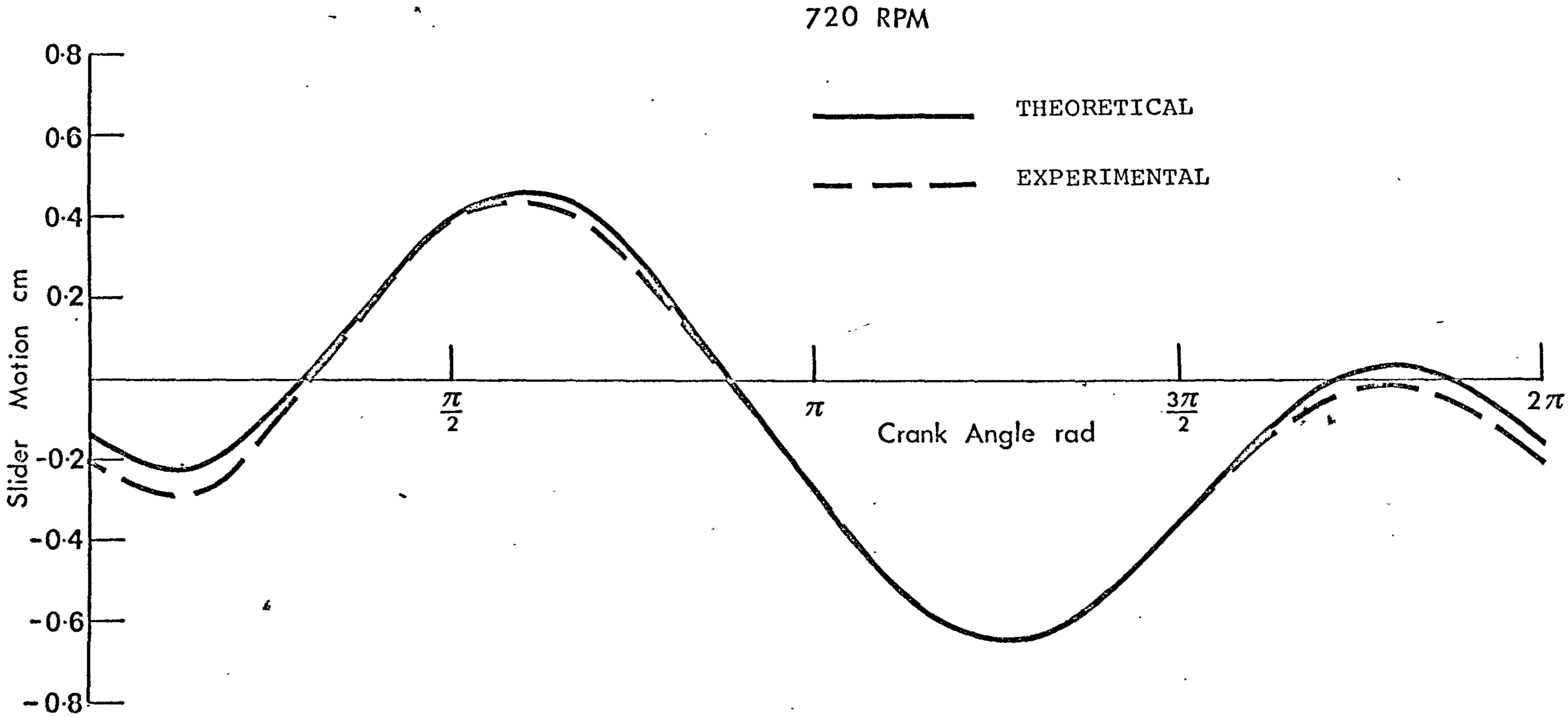

FIG. (8.13) SLIDER MOTION FOR ONE CRANK CYCLE WITH SPRING B AND CONSTANT CRANK SPEED OF 720 RPM.

The experimental and theoretical results were compared for a number of other speeds below the natural frequencies with both springs A and B and in all cases the agreement in phase was good and in amplitude reasonable.

8.4.1.2 Variation of the Slider Oscillations with Crank Speed

Due to practical difficulties, namely the large amplitudes of oscillations near the natural frequencies, resonance curves could not be obtained using this apparatus. However, these resonance curves are obtained from the Experimental Rig 2 as will be seen in the next section. Theoretical calculations give the natural frequency with spring A to be in the region of 580 RPM and with spring B in the region of 1160 RPM. However when the speed was increased to 500 RPM with spring A and 800 RPM with spring B the amplitude of slider oscillations was so large that the slider guide could not accommodate it. This was unfortunate but it did not, however, prevent an investigation of the oscillations up to 500 and 800 RPM with springs A and B respectively.

Figs. (8.14) and (8.15) show a number of slider oscillations for one crank cycle with spring A. The oscillations correspond to constant crank speeds of 240, 260, 280, 300, 360 and 500 RPM. These figures together with Figs. (8.8) to (8.10) show how a slider oscillation corresponding to one crank cycle varies with input speed. They also show that a typical oscillation has four peaks indicating that, since the oscillations are periodic in the crank cycle, more than one harmonic is present in the solution.

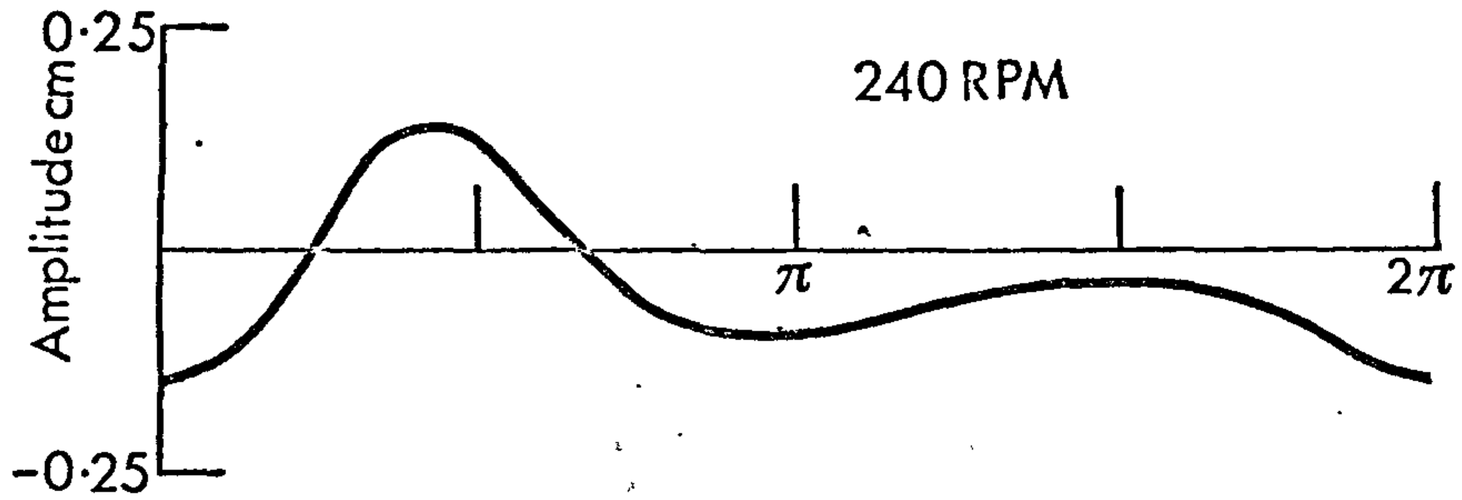

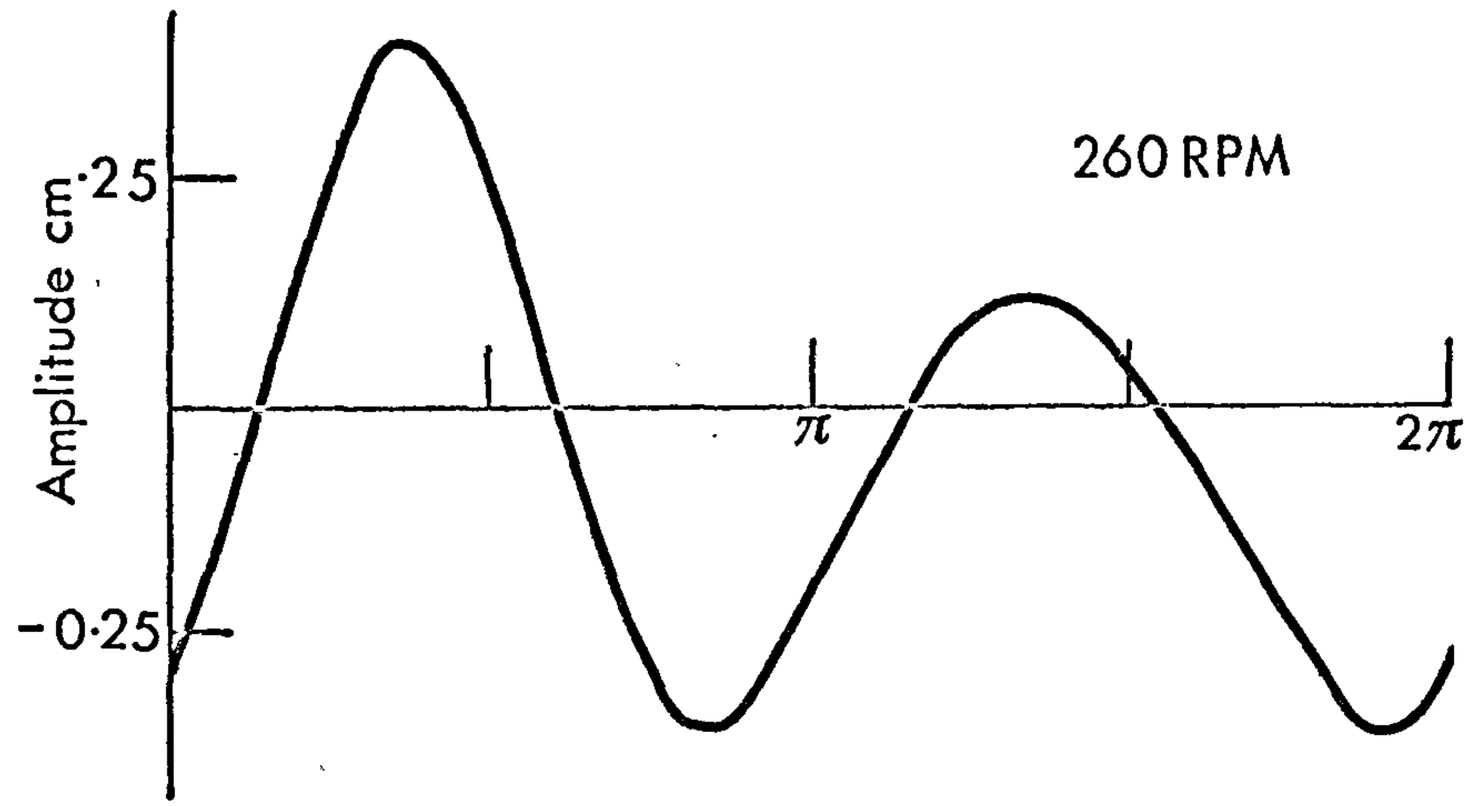

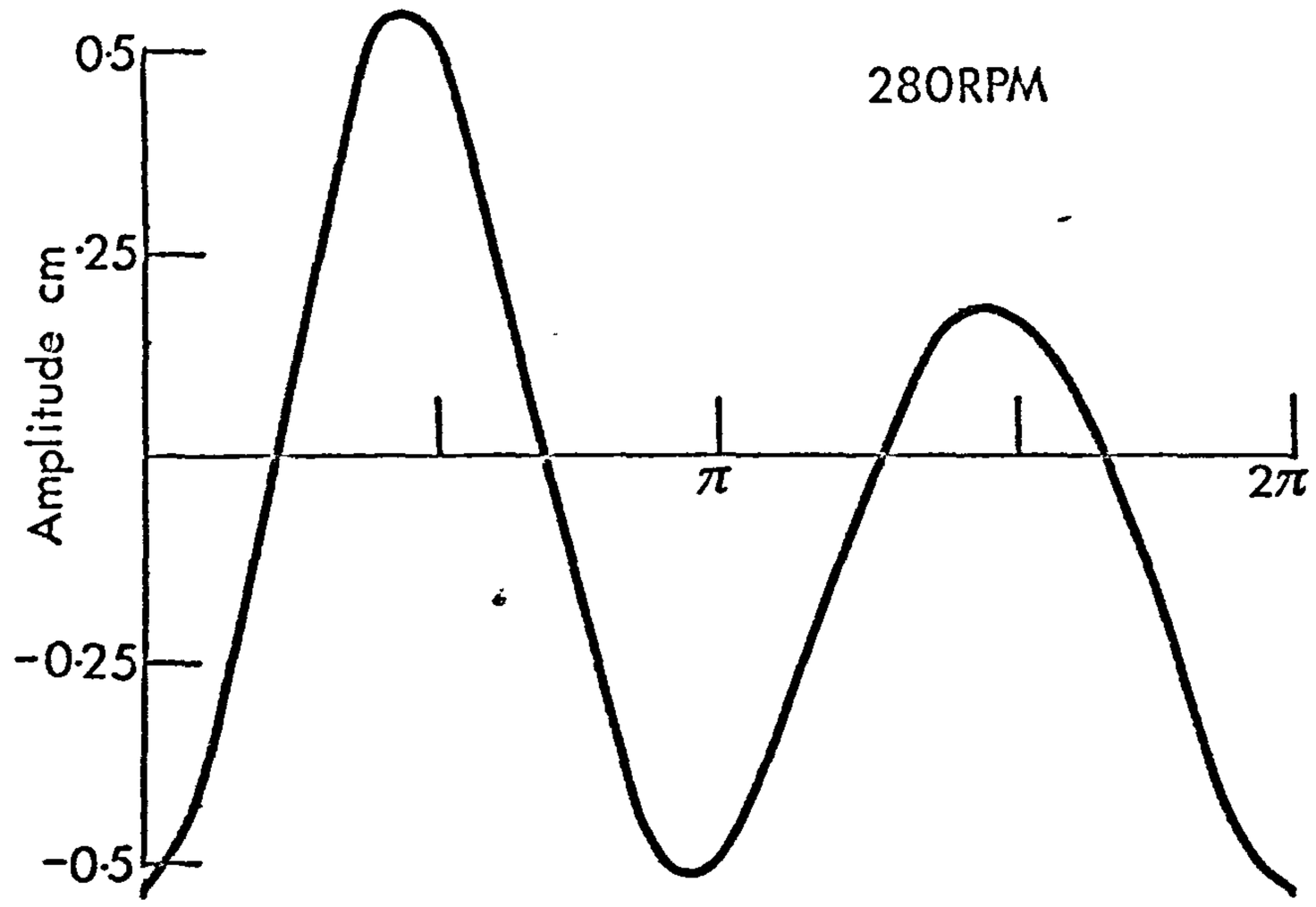

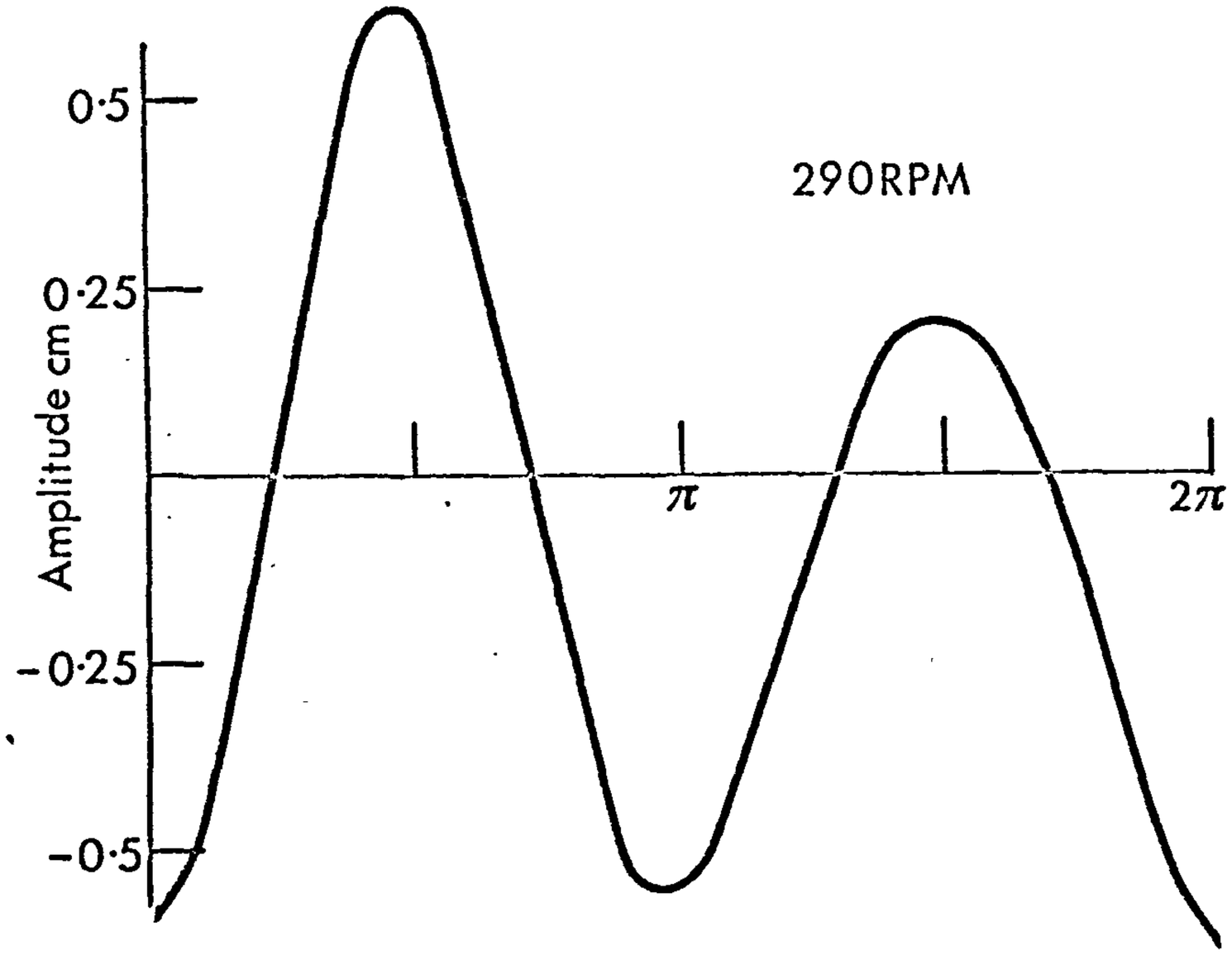

FIG. (8.14) VARIATION OF SLIDER MOTION WITH CRANK SPEED FOR ONE CRANK CYCLE; SPRING A.

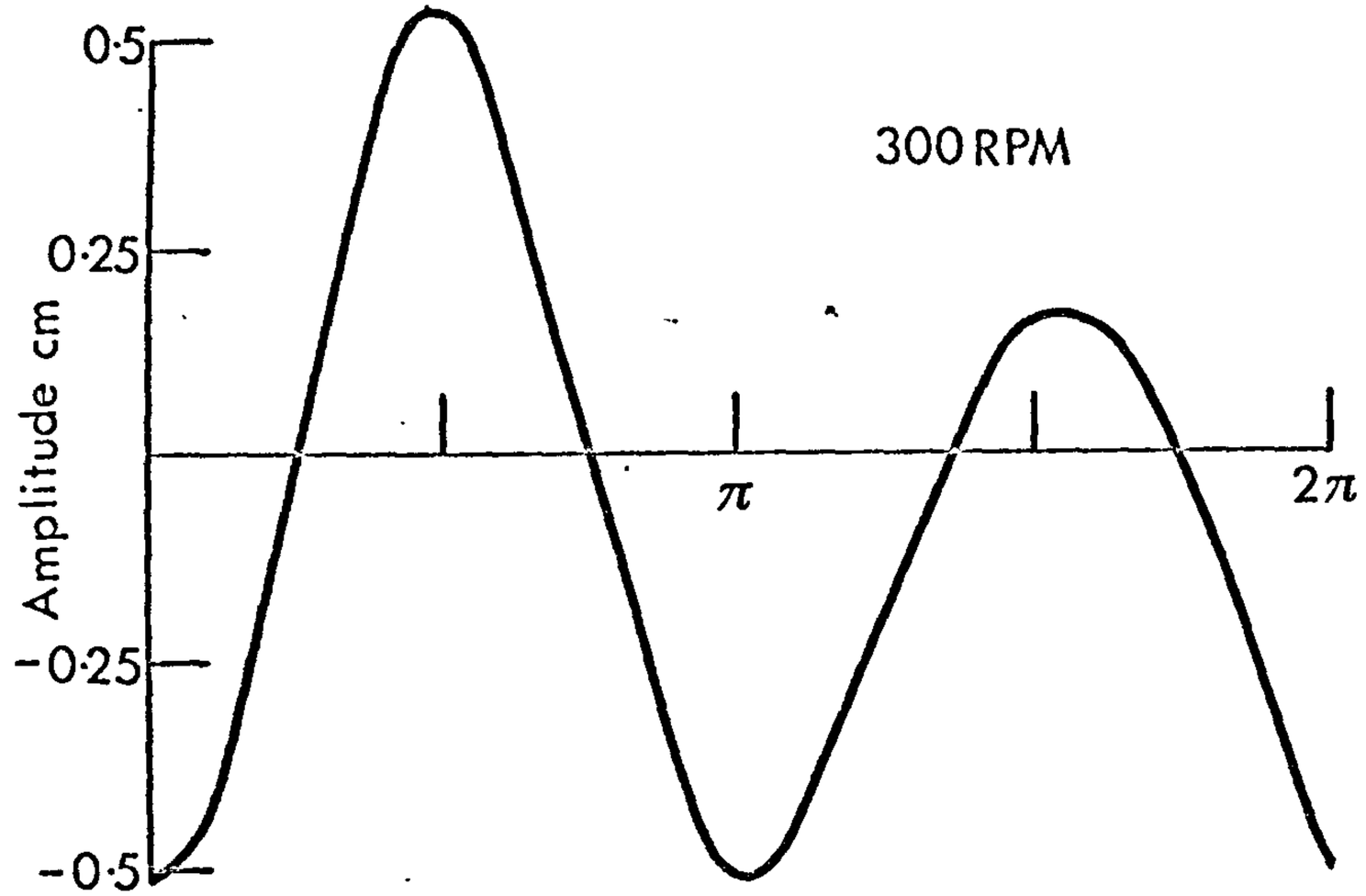

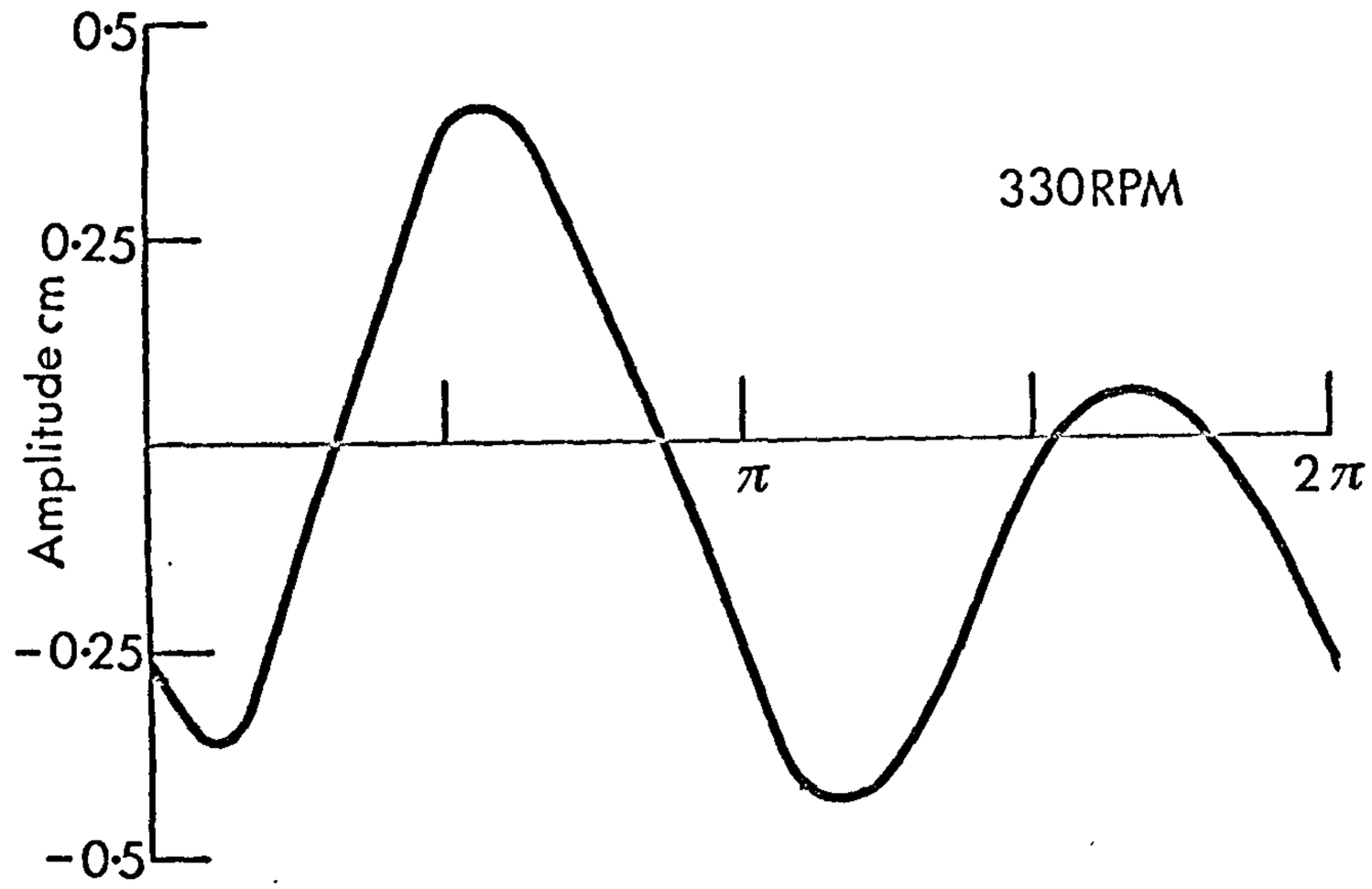

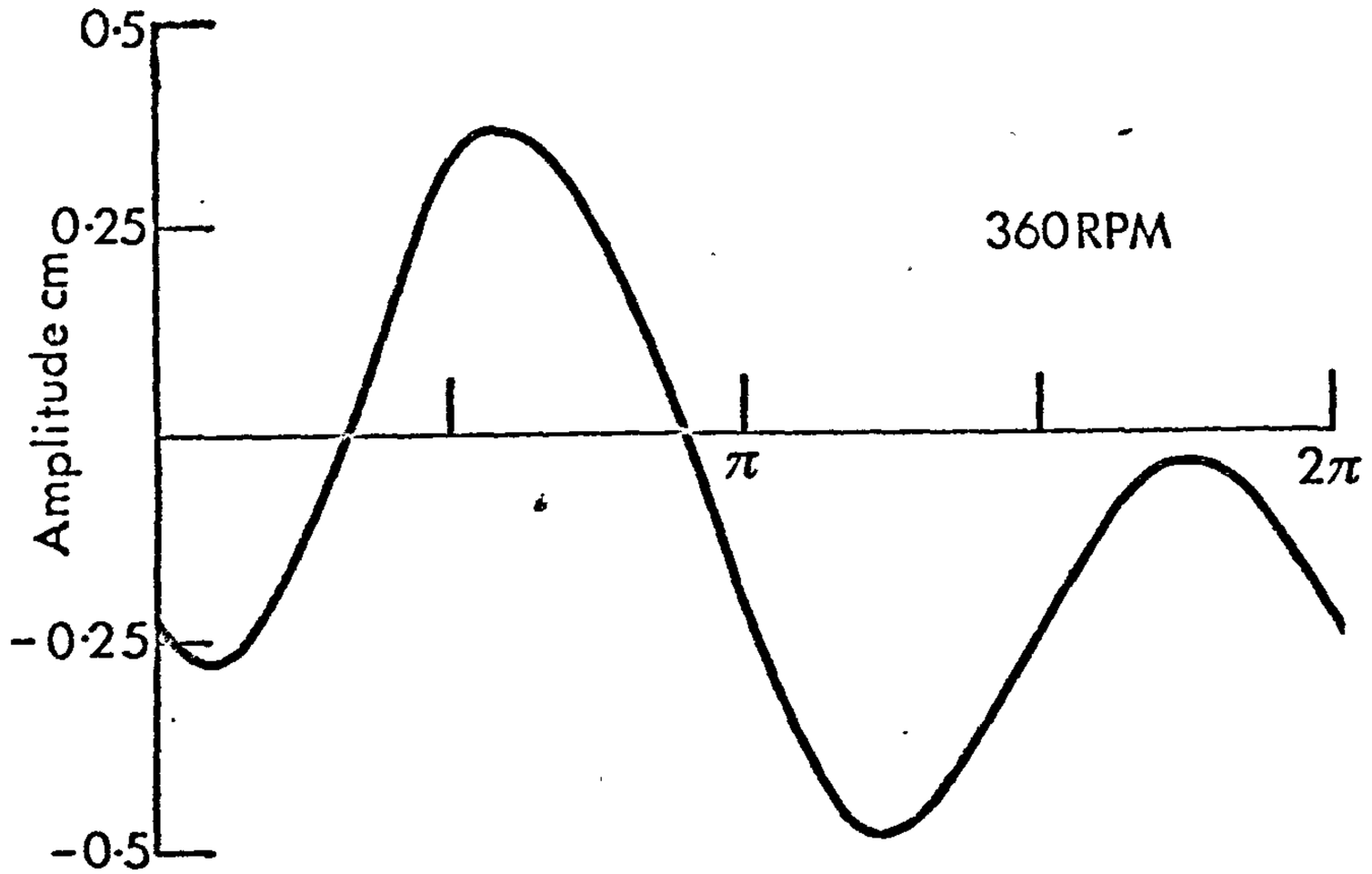

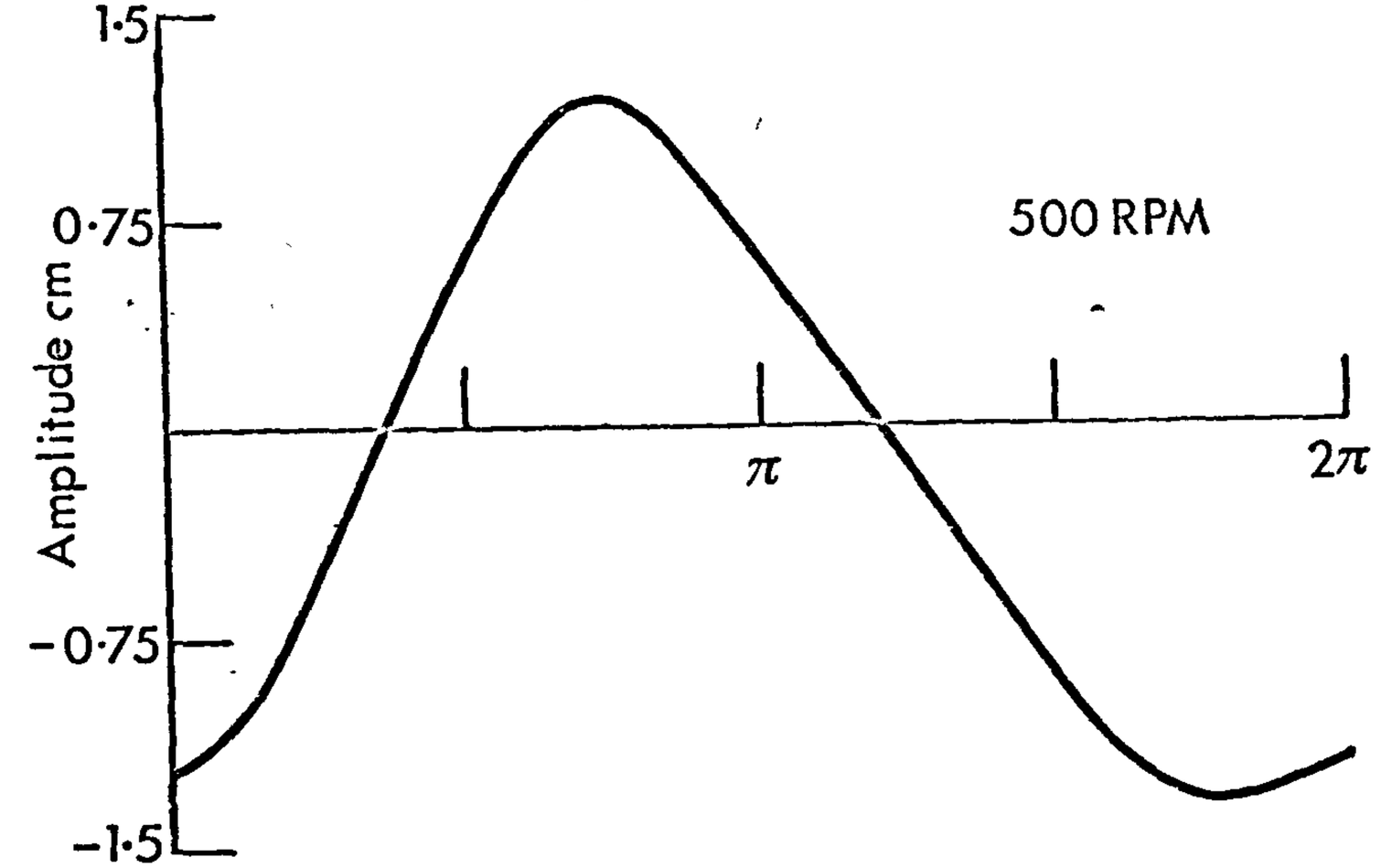

FIG. (8.15) VARIATION OF SLIDER MOTION WITH CRANK SPEED FOR ONE CRANK CYCLE; SPRING A.

At 240 RPM the slider oscillation has four peaks; however when the speed is 450 RPM the first and last peaks coincide and become an inflection point and as the speed is increased further this inflection point coincides with the third peak, thus resulting in a sinusoidal type oscillation as shown in the case of 500 RPM. The amplitude of oscillations increases as the speed increases up to 290 RPM, i.e. half the natural frequency, where it reaches a maximum after which the amplitude decreases with increase of speed up to 345 RPM beyond which it increases with increase of speed.

Figs. (8.16) and (8.17) show a number of slider oscillations with spring B corresponding to one crank cycle and constant crank speeds of 500, 540, 580, 620, 680 and 780 RPM respectively. As in the case of spring A the oscillations are periodic and each oscillation has four peaks. The amplitude of oscillations increases with speed up to 580 RPM, i.e. half the natural frequency, where it reaches a maximum after which the amplitude decreases and then increases with increase of speed. The four peaks in the oscillations show the same tendency as for spring A, i.e. the first and last peaks coinciding and becoming an inflection point. Although it is not possible to show these peaks coinciding in this case the tendency may be predicted from Figs. (8.11) to (8.13) and (8.16) to (8.17).

In both cases of springs A and B it was noticed that no noticeable effects on the amplitude of vibrations were observed at $\omega \simeq \frac{\omega_n}{4}, \frac{\omega_n}{3}$, where ω_n is the natural frequency. This suggested a slider solution based on the first and second harmonics, and that the third and higher harmonics are small in comparison.

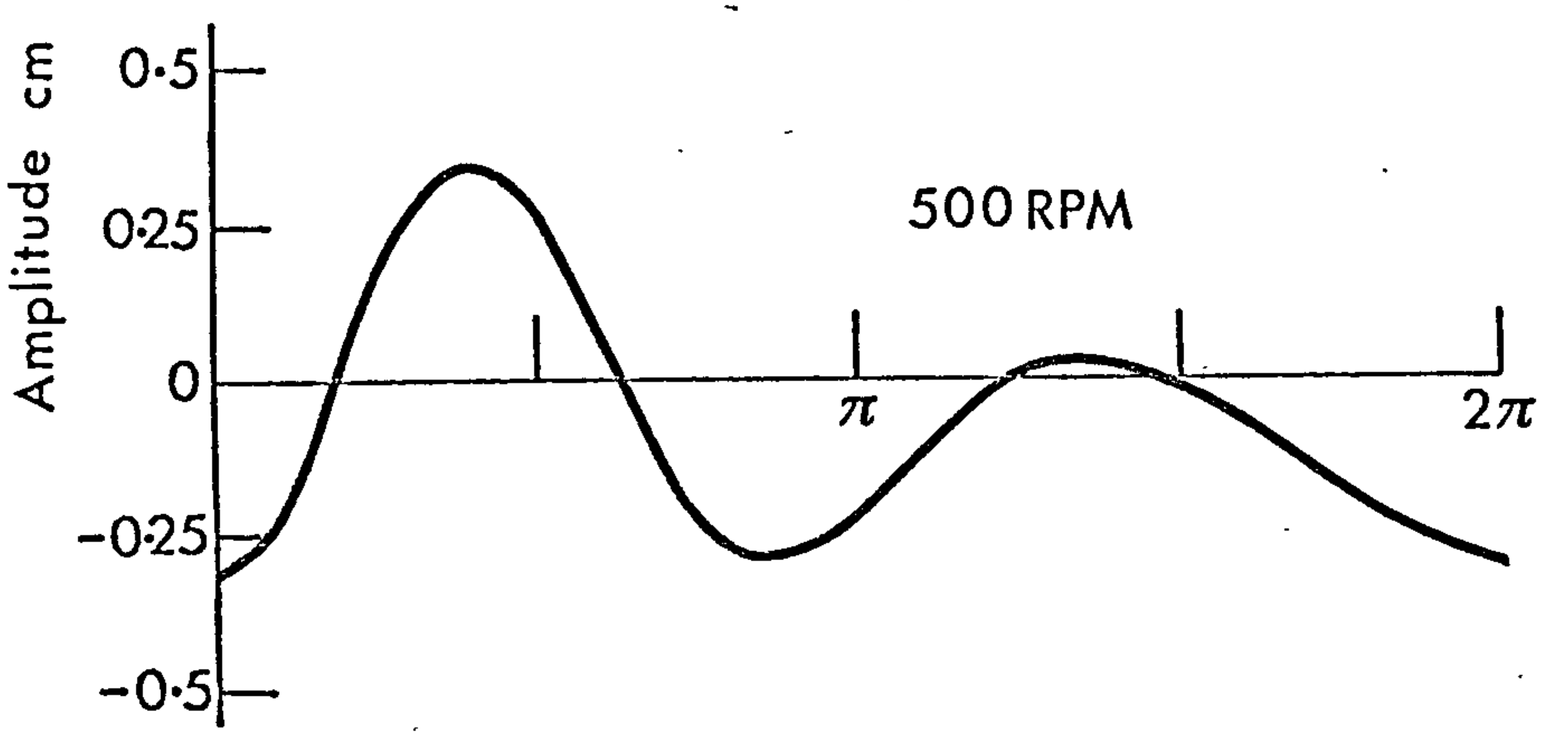

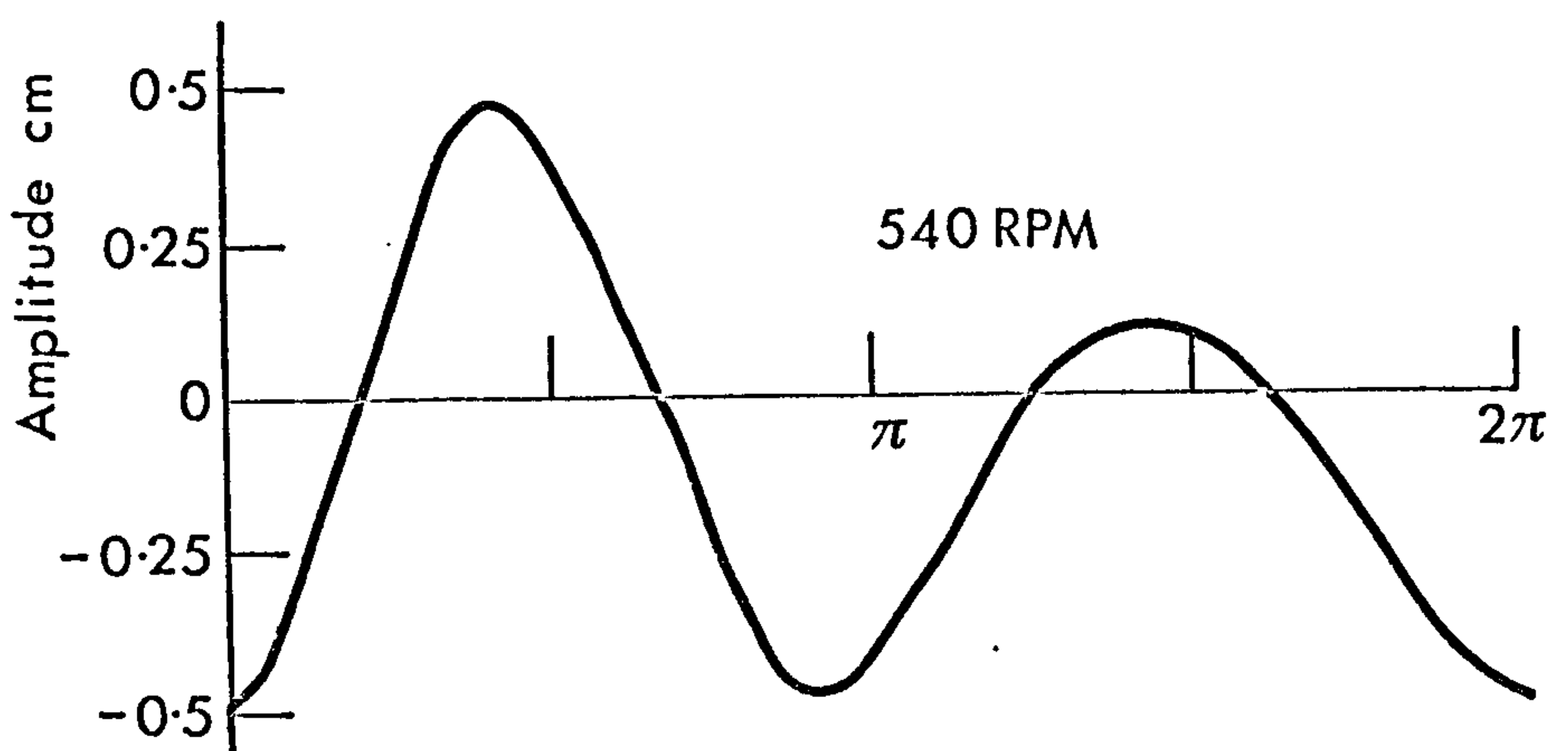

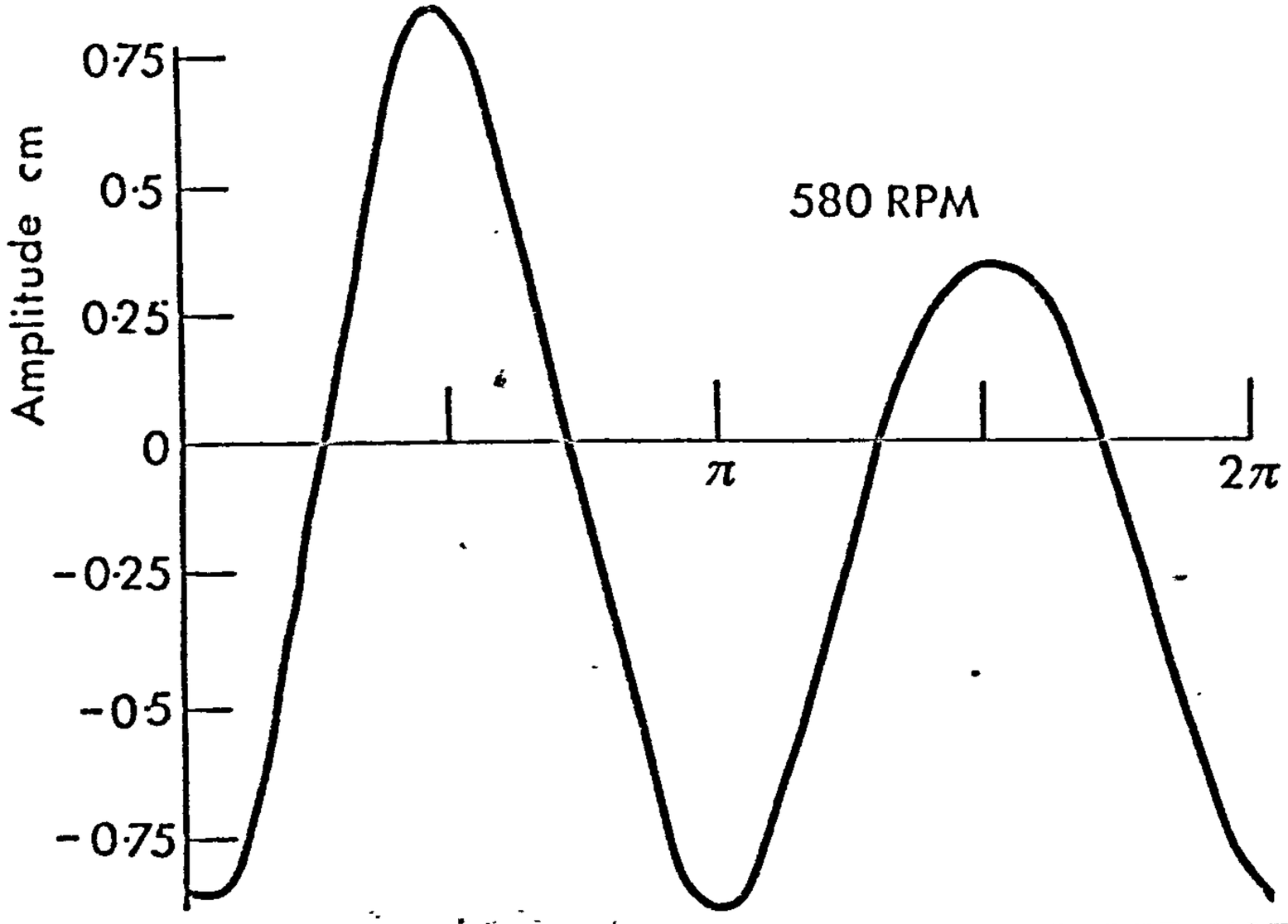

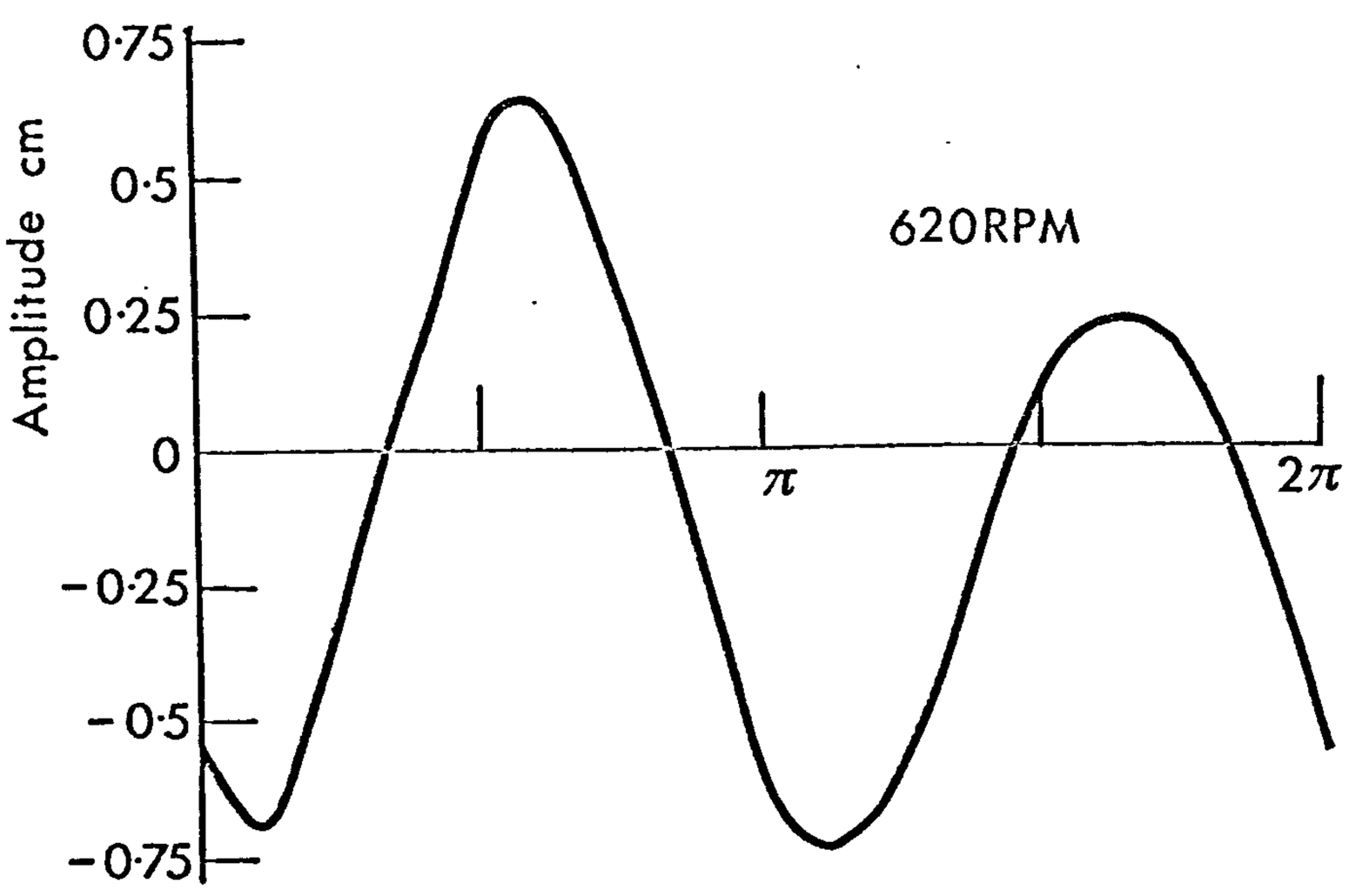

FIG. (8.16) VARIATION OF SLIDER MOTION WITH CRANK SPEED FOR ONE CRANK CYCLE; SPRING B.

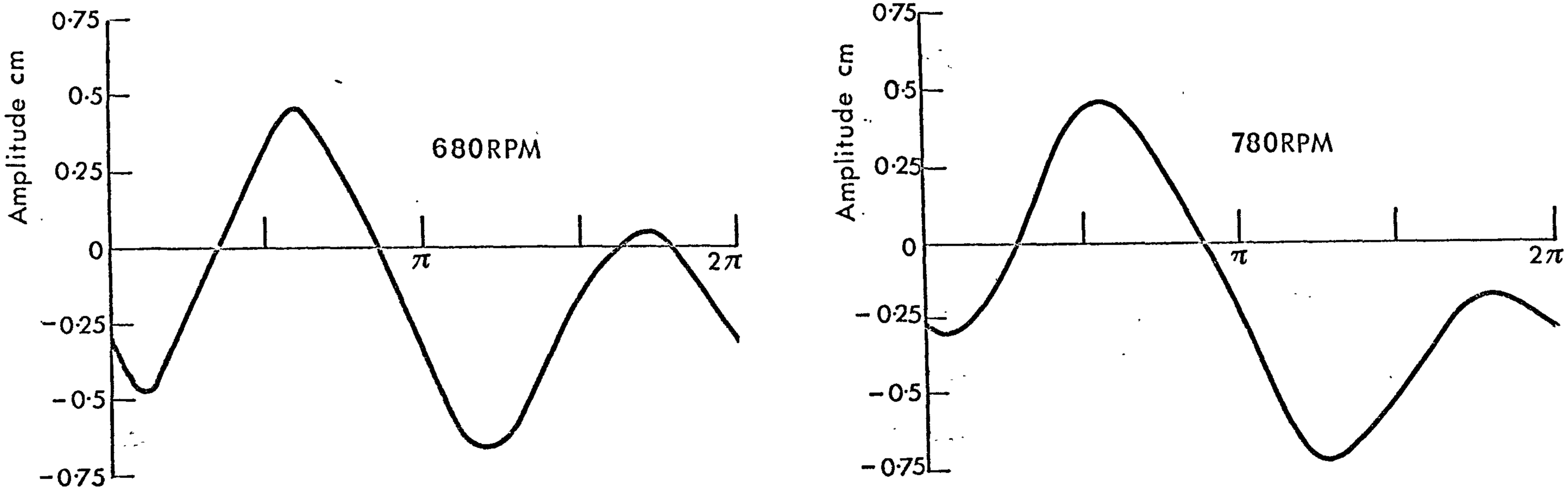

FIG. (8.17) VARIATION OF SLIDER MOTION WITH CRANK SPEED FOR ONE CRANK CYCLE; SPRING B.

8.4.2 Experimental Rig 2 (Linearised Rig)

In this section a comparison of the experimental results with the theoretical results, obtained using the linearised theory discussed in Chapter IV, is performed. The main points to show are (1) the assumption in the theory, that the third and higher harmonics in the slider displacement may be ignored, is valid experimentally and (2) experimentally obtained resonance curves are in good agreement with the theoretical curves.

Two springs are used in this experiment - spring C of stiffness 4 x 10^6 dyn./cm. and spring D of stiffness 8 x 10^6 dyn./cm.

8.4.2.1 Slider Oscillation

Typical experimentally observed slider oscillations are shown in Fig. (8.18) which exhibit an almost sinusoidal behaviour with a phase shift and also periodic in one crank cycle. Other results show that the sinusoidal behaviour is maintained throughout the range of speeds performed in this experiment, i.e. a range of 300 to 1000 RPM, and the phase shift varies with speed. This indicates that the basic and dominant harmonic in the slider motion is the first; the second is very small in comparison and no evidence of the third and higher harmonics exists. It also indicates that the steady state behaviour is similar to a second order demped mass-spring system described by

$$m\ddot{x} + \mu\dot{x} + kx = F_o \sin(\omega t+\phi).$$

8.4.2.2 Resonance Curves

Figs. (8.19) and (8.20) show the experimental and theoretical resonance curves of the slider with the two springs C and D respectively. These are plots of the slider amplitude

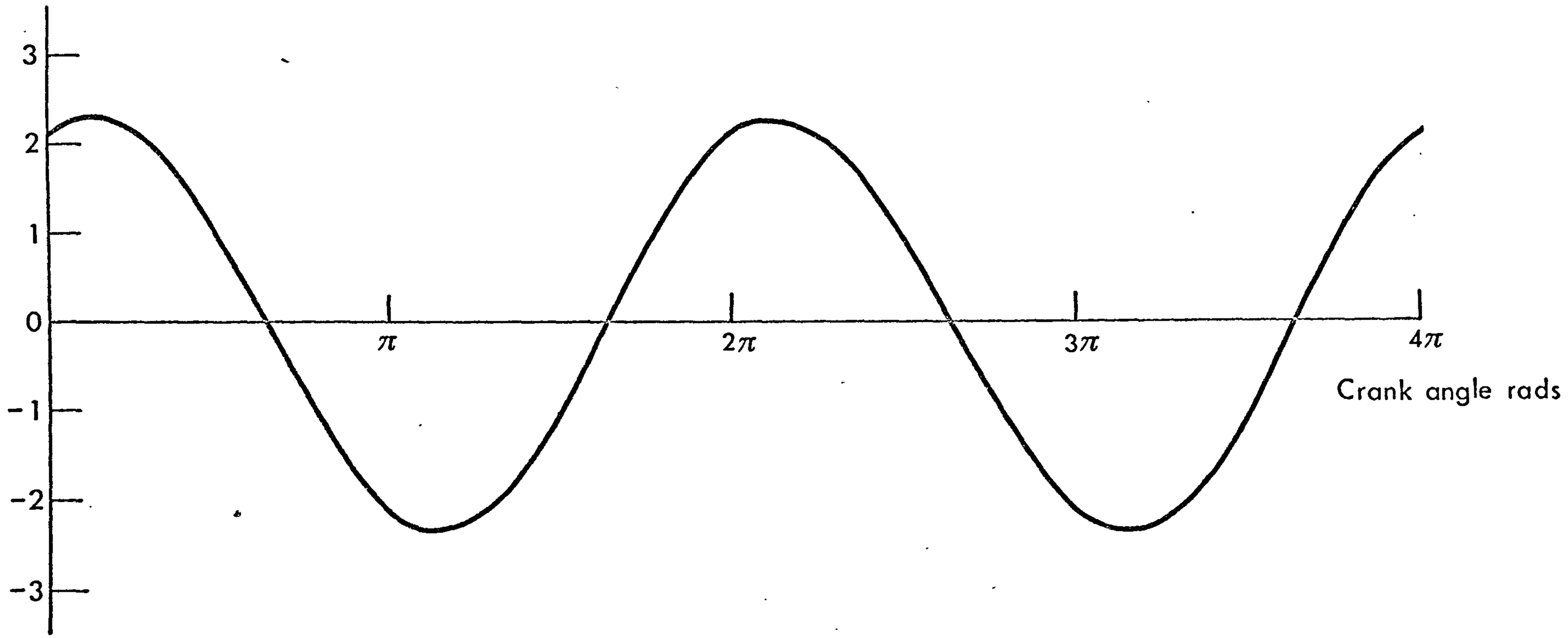

FIG. (8.18) A TYPICAL STEADY STATE SLIDER MOTION OBTAINED FROM RIG 2.

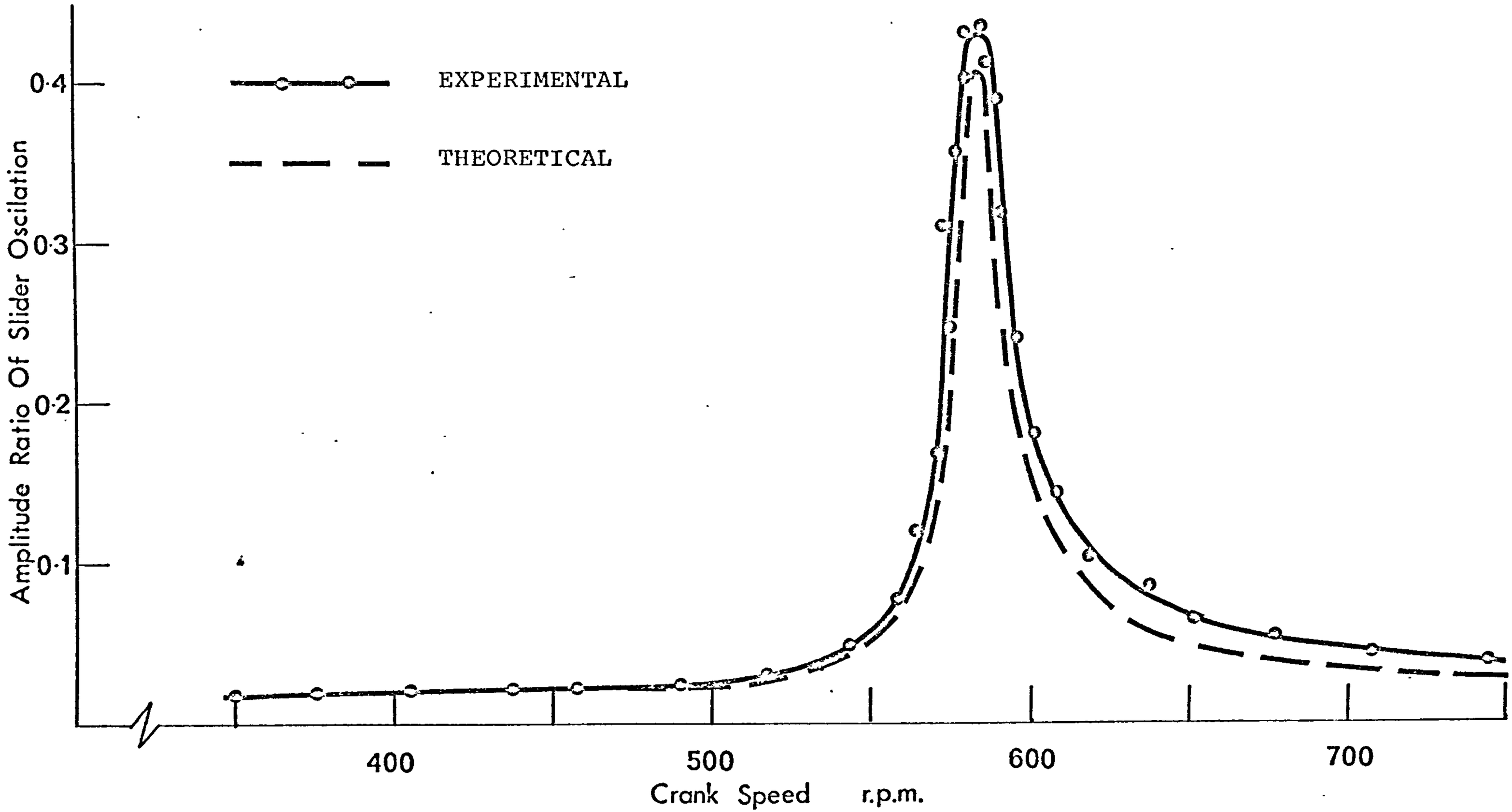

FIG. (8.19) RESONANCE CURVES WITH SPRING C.

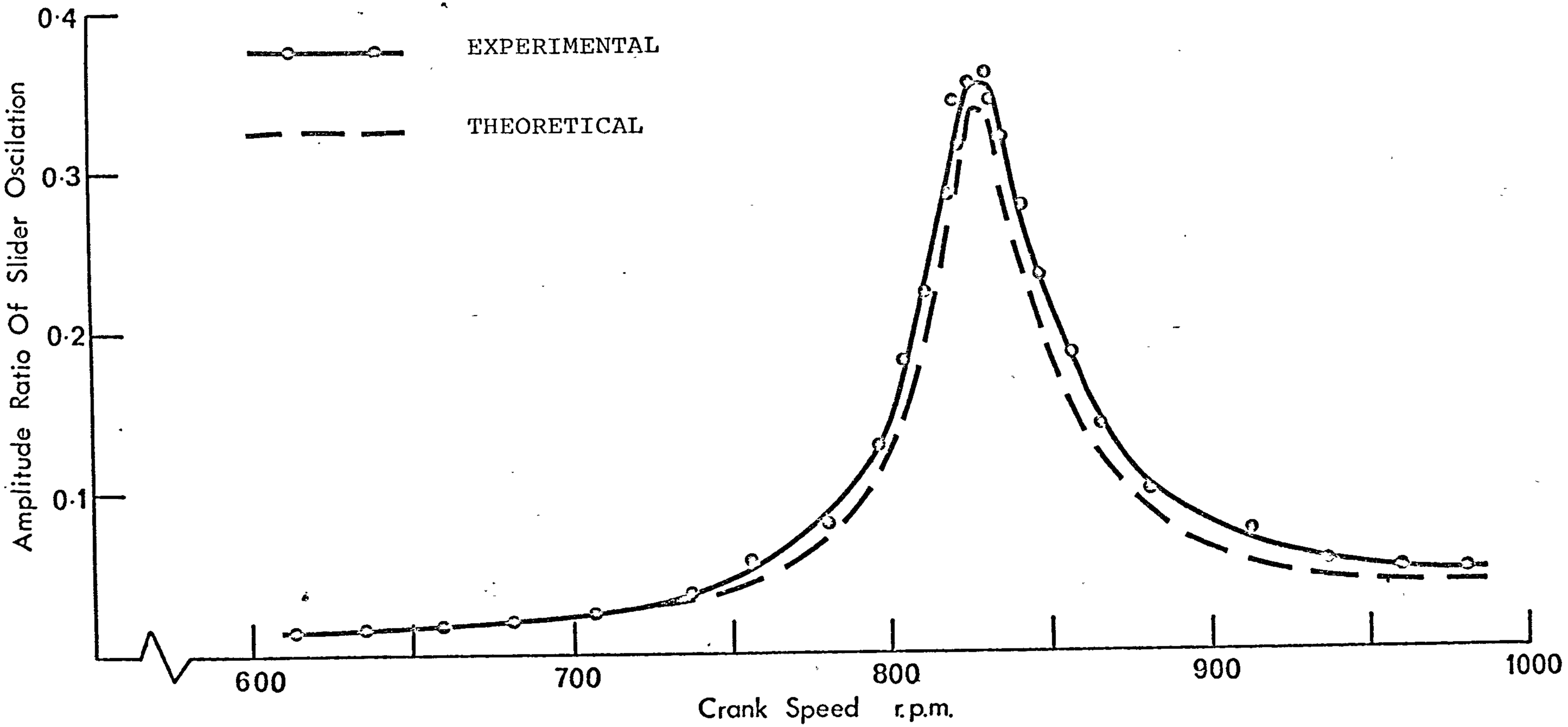

FIG. (8.20) RESONANCE CURVES WITH SPRING D.

ratio, i.e. the amplitude divided by the length of the rocker, versus the crank speed. The experimental and theoretical curves agree in the region of speed leading up to resonance at $\omega = \omega_n$. However the width of the resonance region and the amplitude of vibration beyond resonance obtained from the theory is smaller than that of the experiment but, nevertheless, a reasonable agreement is evident. These differences may however be attributed to the fact that quantities involving the second and higher orders of ζ_3, ζ_4, ζ and σ_2, and their derivatives are ignored in the theory. Other factors contributing to the differences may, as before, be attributed to the presence of Coloumb friction in the guide and pin joints and to the fact that only an average value of the damping is considered in the theory.

Figs. (8.19) and (8.20) also show a natural frequency in the region of 585 RPM with spring C and in the region of 825 RPM with spring D. These are in good agreement with theoretical calculations based on the equivalent mass of the linkage which are 582 and 829 for springs C and D respectively.

There were no experimentally observable changes in the amplitude of oscillations at quarter, third and half the natural frequency, which again indicated a slider motion based on the first harmonic. The theoretical resonance curves corresponding to the second harmonic for both springs C and D are shown in Fig. (8.21). These are smaller than those corresponding to the first harmonic by a factor in magnitude of 50 and hence are in agreement with the experiment.

The above results stated in (8.4.2.1) and (8.4.2.2) support the theoretical analysis performed in Chapter IV. This support may be deduced from the following points which are mainly :

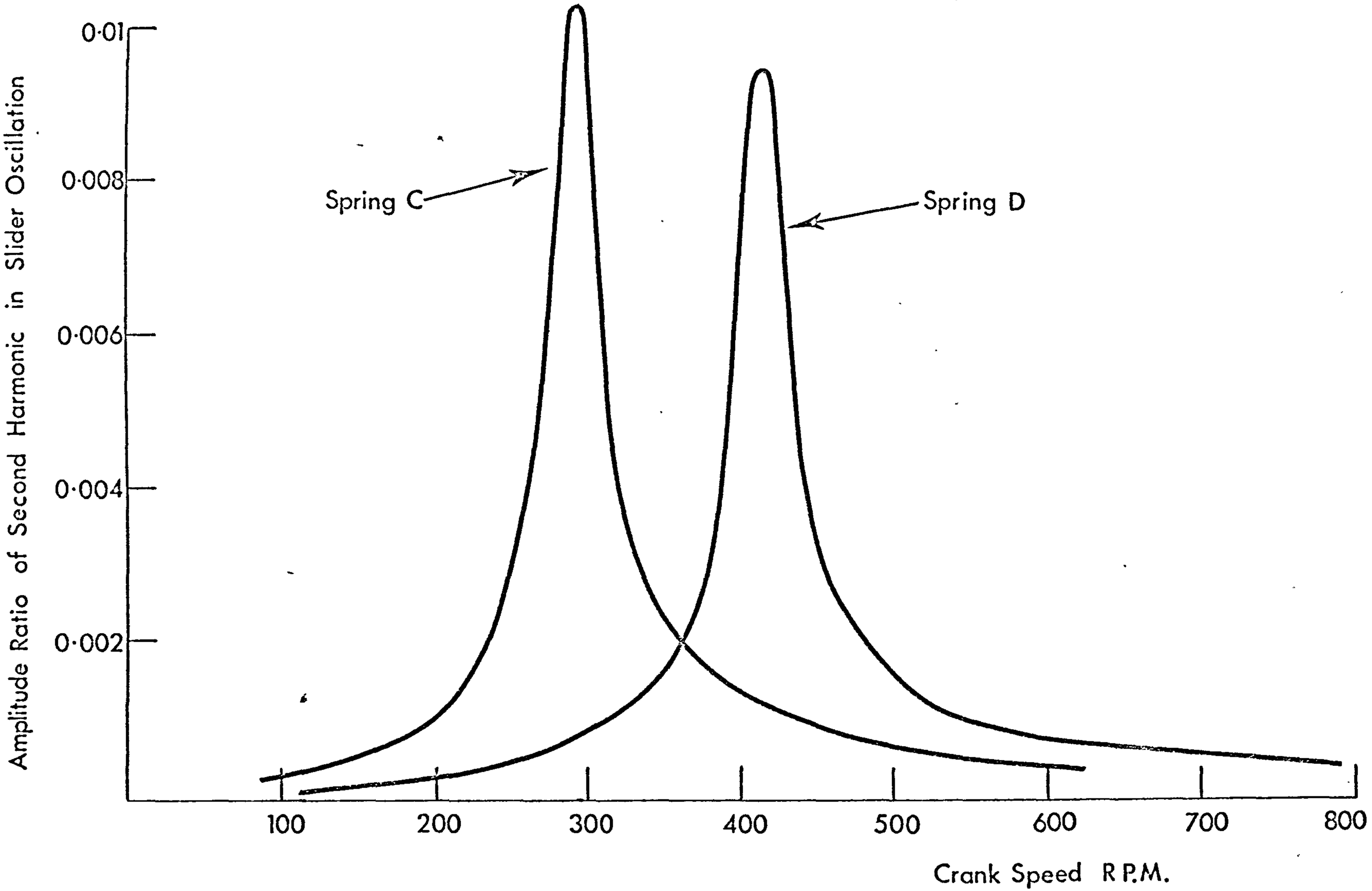

FIG. (8.21) THEORETICAL RESONANCE CURVES OBTAINED FROM THE AMPLITUDE OF THE SECOND HARMONIC IN THE SLIDER MOTION.

(1) The third and higher harmonics in the slider displacement are negligible; the second is very small. (2) The resonance and steady state behaviour is similar to a linear second order damped mass-spring system and (3) the theoretical and experimental resonance curves are in good agreement indicating that the assumption in the theory that the second and higher orders of ζ_3 and ζ_4 and their derivatives are negligible is a reasonable assumption.

CHAPTER IX

CONCLUSIONS

AND

RECOMMENDATIONS FOR FURTHER WORK

9.1 CONCLUDING REMARKS

The releasing of some constraints in linkage mechanisms and treating them as inputs that may be controlled yield versatile and powerful mechanisms. For example the introduction of a second input to a four bar linkage gives a variety of outputs thus making the linkage a multipurpose mechanism which may be adapted to generate a family of cutput motions.

A four bar linkage with the rocker to ground joint replaced by a slider has been used throughout the analysis to illustrate the results. A proper control of the slider enabled modifications and more accurate generation of outputs than could otherwise be obtained. However, the control of this second input produced changes that were limited by an envelope dictated by the linkage kinematics. Therefore it was logical firstly to find the linkage that would approximately generate the desired output and then secondly to introduce a second input and control it for more accurate generation. As a result an optimisation method was developed, the output of which gave a planar linkage that minimised the errors involved in function or path generation. The method could be applied to any planar linkage and was implemented as a package of subroutines for general use. The package was also made conversational to facilitate usage.

The optimisation method was applied to a variety of examples and in most cases produced satisfactory results. Recommendations on its use and various techniques relating to finding the best solution were also discussed.

The dynamics of the mechanism were studied by developing the equations of motion using the Lagrangian multipliers method. The multipliers were associated with the pin forces and suitable methods of solution of the equations of motion were discussed. It was found that, when performing the numerical integrations, it was better if all the derivatives of the generalised coordinates used in the multipliers method were integrated.

The response of the above linkage with the slider constrained by a spring and opposed by viscous friction was studied for a variety of cases. Inputs to the crank included a torsion bar type input and a constant-speed input. It was found that the spring stiffness had little effect on the torque required to drive the mechanism. It was also found that when the slider was opposed by both spring and viscous damping its motion was a transient followed by periodic oscillations of period 2π of the crank angle. However, when the spring was eliminated the slider moved with periodic oscillations superimposed on a linear shift in its position thus making the linkage fall into a collinear configuration. For a forced input (torsion bar input applied to the crank) it was found that the linkage accelerated until the input torque became smaller than the load offered by the linkage after which the

slider executed periodic oscillations in 2π of the crank angle. The oscillations, however, decayed due to the viscous dissipation of energy in the slider guide.

A linearised analysis of the equations of motion was developed and conditions of resonance and stability of the slider were studied.

Results for a short crank showed similarity to a damped second order linear system behaviour. The major harmonic in the solution was the first harmonic; the remaining ones were almost negligible. Resonance curves were obtained varying the rocker inertia and the coefficient of damping. It was found that the increase in the rocker inertia decreased the natural frequency linearly, increased the amplitude of vibrations and widened the region of resonance. The stability analysis showed a narrow region of instability in the viscinity of $\omega = 2\omega_n$ only, where ω_n is the natural frequency. Instability of the slider motion was shown to increase with increase of crank length, decrease of coupler length and increase of output inertia.

The experimental investigations were conducted on two experimental rigs. The first rig was used to compare the results of the numerical solutions obtained in Chapter III with the experimental results. It was found that good agreement existed between the two in both phase and amplitude. The rig was also used to study the variation of slider displacement with different crank input speeds. The second rig was used to validate the assumptions made mainly in Chapter IV and also to study the resonance curves of the slider and compare them with

the results obtained from the linearised theory. The assumptions were found to be reasonable and good agreement between theory and experiment was found in the resonance behaviour.

9.2 RECOMMENDATIONS FOR FURTHER WORK

The investigation relating to optimisation and control discussed in this thesis is based mainly on a kinematic treatment. However, the dynamic effects have an appreciable influence on the motion. Such influence is manifested in the forces and moments which lead to wear causing a change in the kinematic conditions or producing undesirable effects. Therefore, as a part of the search for an optimum linkage for a desired output it is recommended that in addition to finding the kinematic requirements a parallel study involving the optimisation of dynamic parameters, such as masses and inertias, should be carried out. It would be useful to have such a work in the form of a well documented package of computer programs available to industrial and research establishments.

In this thesis we discussed ways of controlling a second input in order to achieve a better approximation of a desired output. Illustrative examples were shown in which it was assumed that a suitable controller able to produce the required input motion may be found. However although constraints were incorporated, these concerned only the position and length of links, it would be very useful to extend the work to examples in which constraints are applied on the dynamic characteristics of the controller.

A number of the control methods mentioned in Chapter VII were off line passive methods involving continuous or intermittent motion and relying on mechanical elements such as springs and latches for their operation. These are attractive, basically for their relative low cost compared with other sophisticated methods. It is therefore recommended that an optimisation study involving the finding of optimum values of such parameters as mass, position and release and hold times of latches and other dynamic parameters is performed. The study should incorporate the optimisation of masses and inertias of the mechanism components such that the controller experiences desirable dynamic characteristics. For example, in the linkage considered in the theory the slider may be controlled by latches which are released and held at appropriate times in the crank cycle. The inertias and masses of the links may be optimised such that when the latches, for example, are released the forces transmitted to the slider by the linkage would cause it to move in a desirable manner.

It would be useful to study the practical problem involved in the adaptive control of mechanisms. This would consist of measuring the errors, experimentally on line, in the output and processing them by a digital computer, also on line, using some optimisation technique. The digital computer would be interfaced with the controller which would provide the optimum input motion. Such work would take into account both kinematic and dynamic requirements simultaneously.

In many industrial examples it is found that when designers are confronted with a complex motion they tend to think of complex multi-link mechanisms which are not necessarily of more than one degree of freedom. We have shown that in a four bar linkage the releasing of one constraint and replacing it by an input makes any point within an output area accessible by a suitable control of this input. Therefore, rather than using a series of four bar linkages coupled in some manner to produce some complex motion it is recommended that the basic four bar is looked into more deeply by releasing some of its constraints and replacing them by controlled inputs.

Finally, it would be interesting to see the linearised theory developed in Chapters IV and V extended to mechanisms flexibly supported at the slider and crank shaft ends. It would also be interesting to see the theory and programs developed in Chapter V cn finding the unstable regions by a computer applied optimisation method, on a variety of problems such as transverse and longitudinal flexibility in the links of a four bar linkage and also flexibility in its input and output shafts.

P A R T V

REFERENCES & APPENDICES

References

1. HIRSCHHORN, J., "Kinematics and dynamics of plane mechanisms", McGraw-Hill Book Company, New York, 1962.

2. HARTENBURG, R.S. & DENAVIT, J., "Kinematic synthesis of linkages", McGraw-Hill Book Company, New York, 1964.

3. HALL, A.S. "Kinematics and Linkage design", Prentice-Hall, 1961.

4. FREUDENSTEIN, F. & SANDOR, G., "Synthesis of path generating mechanisms by means of a programmed digital computer", Journal of Engineering for Industry, Trans. ASME, Series B, Vol. 81, 1959, pp 159-168.

5. FREUDENSTEIN, F. & SANDOR, G., "Structural error analysis in plane kinematic synthesis", Journal of Engineering for Industry, Trans. ASME, Series B, Vol. 81, 1959, pp 159-168.

6. ROTH, B. & FREUDENSTEIN, F., "Synthesis of path generating mechanisms by numerical methods", Journal of Engineering for Industry, Trans. ASME, Series B, Vol. 85, 1963, pp 298-306.

7. PHILIPP, R.E. & FREUDENSTEIN, F., "Synthesis of two degree of freedom linkages - a feasibility study of numerical methods of synthesis of bivariate function generators", Journal of Mechanisms, Vol. 1, 1966, pp 9 - 21.

8. WILSON, J.T., "Analytical kinematic synthesis by finite displacements", Journal of Engineering for Industry", Trans. ASME, Series B, Vol. 87, 1965, pp 161-169.

9. McLARNAN, C.W., "Synthesis of six-link plane mechanisms by numerical analysis", Journal of Engineering for Industry, Trans. ASME, Series B, Vol. 85, 1963, pp 5 - 11.

10. McLARNAN, C.W., "On linkage synthesis with minimum error", Journal of Mechanisms, Vol. 3, 1968, pp 101 - 105.

11. NOLLE, H. & HUNT, K.H., "Optimum synthesis of planar linkages to generate coupler curves", Journal of Mechanisms, Vol. 6, 1971, pp 267,287.

12. SUH, C.H. & RADCLIFFE, C.N., "Synthesis of plane linkages with use of the displacement matrix", Journal of Engineering for Industry, Trans. ASME, Series B, Vol. 89, 1967, pp 206-214.

13. BUSSELL, W.H. & MARTIN, G.H., "An analytical method for synthesizing mechanisms based on Roulette theory", Journal of Engineering for Industry, Vol. 89, 1967, pp 77-83.

14. WORTHLEY, W.W. & HINKLE, R.T., "Four-bar linkages - approximate synthesis", Journal of Engineering for Industry, Trans. ASME, Vol. 81, 1959, pp 293-300.

15. ALLEN, C.W., "The design of linkages to generate functions of two variables", Journal of Engineering for Industry, Trans. ASME, Vol. 8, 1959, pp 23-29.

16. DUKSMAN, E.A., "How to compare mechanisms with parallel moving bars (with application on a level-buffing jib-crane consisting of a four-bar linkage and exploiting a coupler-point curve), EUROMECH 22, Newcastle upon Tyne University, 1971.

17. BOX, SWAN & DAVIES, "Nonlinear optimisation", ICI Monograph, Oliver and Boyd, 1969.

18. FLETCHER, R. "Methods of solution of Optimisation problems", Computer physics.

19. FIACO & McCORMICK, "Nonlinear programming: sequential unconstrained minimisation techniques", John Wiley & Sons, 1968.

20. POLLAK, E. "Computational Methods in Optimisation", Academic Press, 1971.

21. FLETCHER, R., "Optimisation", Academic Press, 1969.

22. FLETCHER, R.& POWELL, M.J.D., "A rapidly convergent descent method for minimisation", The Computer Journal, Vol. 6, 1963, pp 163-168.

23. YOUSSEF, A.H. & MAUNDER, L. "Motion of a two degree of freedom mechanism", Institution of Mechanical Engineers, Conference of Mechanisms, 1972.

24. YOUSSEF, A.H., "Optimisation of mechanisms for path and function generation", Institution of Mechanical Engineers, Conference on Mechanisms, 1973.

25. MUELLER, G.S. & OSMAN, M.O.M., "Multivariable search for optimum synthesis of planar mechanisms", Institution of Mechanical Engineers, Conference on Mechanisms, 1972.

26. OSMAN, M.O.M. & MANSOOR, W.M., "A computer-orientated numerical approach to the kinematic analysis and synthesis of mechanisms", Proceedings of the Third World Congress on Theory of Machines & Mechanisms, Vol. 14, 1971, pp 299-309.

27. FOX, R.L. & WILLMERT, K.D., "Optimum design of curve generating linkages with inequality constraints", Journal of Engineering for Industry, Trans. ASME, Series B, Vol. 89, 1967, pp 144-152.

28. HAN, C.Y. "A general method for the optimum design of mechanisms", Journal of Mechanisms, Vol. 1, 1966, pp 301-313.

29. JONES, J.R. & ROONEY, G.T., "Motional Analysis of rigid-link mechanisms by gradial-optimisation on an analogue computer", Journal of Mechanisms, Vol. 5, 1970, pp 191-201.

30. GOLINSKI, J., "Optimum synthesis problems solved by means of nonlinear programming and random methods", Journal of Mechanisms, Vol. 5, 1970, pp 287-309.

31. BONA, C. & AGNESOD, R., "An experiment of dimensional synthesis using nonlinear programming techniques", EUROMECH 22 - Dynamics of Mechanisms, 1970.

32. TIMM, R.F., "Analogue simulation of rigid-link mechanisms", Journal of Engineering for Industry, Trans. ASME, Series B, Vol.89, 1967, pp 199-205

33. CHACE, M.A., "Vector analysis of linkages", Journal of Engineering for Industry, Trans. ASME, Series B, Vol. 85, 1963, pp 289-297.

34. POLLIT, E.P., "Five bar linkages with two drive cranks", Machine Design, Vol. 34, No. 2, 1962, pp 168-179.

35. FREUDENSTEIN, F., "Harmonic analysis of crank-and-rocker mechanisms with application", Journal of Applied Mechanics, Trans. ASME, 1959, pp 673 - 675

36. MARES, D. & ORLANDEA, N.,"The kinematics of the plane mechanisms with a certain number of motive elements", Mathematic Vol. 9 (32), 1, 1967, pp91-100.

37. BOGDAN, R.C.& HUNCHER, T.V., "General systemisation and unified calculation of five and four bar plane basic mechanisms", Journal of Engineering for Industry, Trans. ASME, Series B, Vol. 89, No. 2, 1967, pp 189-198.

38. CHI-YEH, H., "A general method of kinematic analysis of mechanisms using variable parameters", Journal of Mechanisms, Vol. 1, 1966, pp 185 -201

39. MARKUS, L., "A general method for the kinematic analysis of planar mechanisms by the computer", ASME Conference on Mechanisms and International Symposium on bearing and transmissions", Trans. ASME, 72 - MECH -58, 1972.

40. BOGDAN, R.C., "General study of five bar mechanisms with the aid of complex harmonic series", Studii si cercchariде mecanica applicatii, Acad. F.P.R., Vol. 15, No. 2, 1964, pp 851-868.

41. SMITH, M.R. & MAUNDER, L., "Inertia forces in a four bar linkage", JMES, Vol. 9, No. 3, 1967.

42. PORTER, B. & SANGER, D.J., "Synthesis of dynamically optimal four bar linkages", Institution of Mechanical Engineers, Conference on Mechanisms, 1972.

43. MAUNDER, L., "The balancing of elastically coupled mechanisms", Proceedings of the Third World Congress for the Theory of Machines & Mechanisms, Vol. B, 1971, pp 103-114.

44. BERKOF, R.S., "Complete force and moment balancing of inline four bar linkages", Journal of Mechanisms, Vol. 8, 1973, pp 397-410.

45. SMITH, M.R., & MAUNDER, L., "Stability of a four bar linkage with flexible coupler", JMES, Vol. 13, No. 4, 1971, pp 237-242.

46. BARR,A.D.S.n "Some general aspects of the analysis of the vibration and stability of mechanisms", EUROMECH 22, Dynamics of Mechanisms, 1970.

47. VISCOM, B.V. & AYRE, R.S., "Nonlinear dynamic response of elastic slider-crank mechanism", Journal of Engineering for Industry, Trans. ASME, Vol. 93, No. 1, 1971, pp 251-262.

48. SEEVERS, J.A. & YANA, A.T., "Dynamic stability analysis of linkages with elastic members via analogue simulations", ASME, paper 70 - MECH - 48, 1970.

49. SMITH, M.R., "The dynamics of rigid and flexible four bar linkage mechanisms", Ph.D. Thesis, University of Newcastle upon Tyne, 1972.

50. MEYER ZUR CAPELLEN, W., "Torsional vibrations in the shafts of linkage mechanisms", Journal of Engineering for Industry, Trans. ASME, Series B., Vol. 89, 1967, pp 126-136.

51. MEYER ZUR CAPELLEN, W., "Oscillation of an elastically suspended coupler of a four bar linkage", Journal of Mechanisms, Vol. 6, 1971, pp 351 - 365.

52. YOUSSEF, A.H., "A study in resonance and stability of special five bar linkage", Internal Report No. , Department of Mechanical Engineering, University of Newcastle upon Tyne.

53. ILEY, L., "An investigation into a special two degree of freedom mechanism", M.Sc. dissertation, University of Newcastle upon Tyne, 1973.

54. LAKSHMINARAYANA, K. & DIZIOGLUE, B, "Synthesis of spring constrained mechanisms for amplitude independent natural frequency of oscillation", Mechanisms and Machine Theory, Vol. 7, 1972, pp 167 - 190.

55. CHACE, M.A., "Analysis of the time dependence of multi-freedom mechanical systems in relative coordinates", Journal of Engineering for Industry, Trans. ASME, 1967, pp 119-125.

56. BENEDICT, C.E. & TESAR, D., "Dynamic response analysis of quasi-rigid mechanical systems using kinematic influence coefficients", Journal of Mechanisms, Vol. 6, 1971, pp 383 - 403.

57. TIMM, R.F. & ELLIS, J.R., "The use of digital simulation languages in mechanism study", Private communications.

58. KOZEVNIKOV, S.N., "Dynamics of mechanisms with two degree of freedom", Sovrem. Prob. l. Teorri Mashin, I. Mekhanzmove, Moscow, Nanka.

59. SKREINER, M., "Dynamic Analysis used to complete the design of a mechanism", Journal of Mechanisms, Vol. 5, 1970, pp 105 - 119.

60. SKREINER, M. & ROBERTS, B.W., "The dynamics of hydraulically actuated linkage mechanisms", The Institution of Engineers, Australia, Mechanical and Chemical Engineering Transaction, 1967, pp 207 - 215.

61. STEWART, D., "A platform with six degrees of freedom", Proceedings of the Institution of Mechanical Engineers, Vol. 180, Part 1, No. 15, 1965, pp 371 - 386.

62. SONI, A.H., "Design of the crank-rocker mechanism with unit time ratio", Journal of Mechanisms, Vol. 5, 1970, pp 1 - 4.

63. PEARCE, G.F., "Dynamic Characteristics of mechanisms using linear independence", Journal of Mechanisms, Vol. 5, 1970, pp 351-355.

64. MACLEOD, I.N., "The dynamic behaviour of two degree of freedom linkage mechanisms", Ph.D. Thesis, Liverpool Polytechnic, 1970.

65. WILSON, R. & FAWCETT, J.N., "The dynamics of piston slap", ASME, paper 72 - MECH - 63, 1972.

66. FAWCETT, J.N. & BURDESS, J.S., "Effects of bearing clearance in a four bar linkage", Proceedings of the Third World Congress for the Theory of Machines & Mechanisms", Vol. C, paper C-9, 1971, pp 111-126.

67. EARLES, S.W.E. & WU, C.L.S., "Motion analysis of a rigid-link mechanism with clearance at a bearing using Lagrangian mechanics and digital computation", Institution of Mechanical Engineers Conference on Mechanisms, 1972.

68. GRANT, S. & FAWCETT, J.N., "Research colloquium on clearance of mechanisms and also private communications", Department of Mechanical Engineering, Newcastle University.

69. DUBOWSKY, S, "On predicting the dynamic effects of clearances in planar mechanisms", ASME publication, paper 72 - Mech. 91, 1972.

70. ROSE, S.E., "Five bar loop synthesis", Machine design, Vol. 33, No. 21, 1961, pp 189-195.

71. LANCOZ, C., "Variational principles of mechanics", University of Toronto Press, 1964.

72. WELLS, D.A., "Theory and problems of Lagrangian dynamics", Schaum Publishing Co., 1967.

73. GOLDSTEIN, H., "Classical Mechanics", Addison-Wesley Publishing Co., 1964.

74. McLACHLAN, N.W., "Theory and Application of functions", Dover Publication, 1964.

75. STOKER, J.J., "Nonlinear Vibrations", Interscience Publishers, 1950.

76. MALKIN, I.G., "On the stability of Motion", Moscow-Leningrad, Translation by U.S. Atomic Energy Commission, Office of Technical Information, 1952.

77. MALKIN, I.G., "Some problems in the theory of non-linear oscillations", Volumes 1 & 2, The state publishing house of technical and theoretical literature, Moscow, Translation by U.S. Atomic Energy Commission, 1956.

78. KOBRINSKII, A.E., "Dynamics of Mechanisms with elastic connections and impact systems", ILIFFE Books Ltd., 1969.

79. RAYEVSKII, N.P., "The measurement of mechanical parameters in machines", Pergamon Press, 1965.

80. HILDEBRAND, F.B. "Methods of Applied Mathematics", Prentice-Hall, 1963.

81. BUTLER, R. & KERR, E., "An introduction to numerical methods", Sci. Isaac Pitman, 1962.

82. REDISH, K.A., "An Introduction to computational methods", The English Universities Press, 1961.

83. I.B.M., "IBM System 360, Fortran IV Language Manual", IBM Systems Reference Library.

84. HOPPER, M.J., "Harwell subroutine library", U.K. Atomic Energy Authority, 1971.

A P P E N D I X 1

```
£CO MCE1:SCL-2D-FORT
      IMPLICIT REAL*8(A-H,O-Z)
      DIMENSION Y(2),DY(2),PR(5),AUX(16,2)
      EXTERNAL GAUSS,OUTP
      COMMON /FIRST/ AR3,R3,R4,STIF,VISC,G,AL1,AL2,AL3,AL4
      COMMON /INMAS/ AIG3,AIG4,AM3,AM4,AM5
      COMMON /SECOND/ EPS1,TD,NLMD
      COMMON /THIRD/ FCTR,SP,NSP
      COMMON /FOURTH/ A26,A35,A44
      COMMON /FIFTH/ STD,PI
      COMMON /SIXTH/ S1,S2,Q1,Q2
      COMMON /FORCE/ FX43,FY43,U2DOT,TORQ,T2D4,T2D3
      T=0.DO
      RPM=450.DO
      NDIM=2
      PR(1)=0.DO
      PR(2)=1.DO
      PR(3)=1.D-03
      PR(4)=1.D-06
      PR(5)=0.DO
      SP=5.DO*PR(3)
  100 FORMAT(9D12.4)
  101 FORMAT(5D12.4)
  102 FORMAT(4D12.4,2I5)
  103 FORMAT(5D12.4)
      WRITE(6,100)AL1,AL2,AL3,AL4,AM3,AM4,AM5,AIG3,AIG4
      WRITE(6,101)R3,R4,STIF,VISC,G
      WRITE(6,102)RPM,T,EPS1,EPS2,NLMD,NDIM
      WRITE(6,103)(PR(I),I=1,5)
      WRITE(6,104)
  104 FORMAT('TIME',11X,'ANG2',11X,'U',14X,'UDOT',9X,'TORQ',9X,'CHEKX'
     1,9X,'CHEKY')
      DO 1 I=1,NDIM
      Y(I)=0.DO
    1 DY(I)=0.5DO
      PI=4.DO*DATAN(1.DO)
      FCTR=180.DO/PI
      S1=AL4**2-AL3**2-AL2**2
      S2=2.DO*AL2*AL3
      Q1=AL3**2-AL4**2-AL2**2
      Q2=2.DO*AL2*AL4
      TD=RPM/30.DO*PI
      STD=TD
C       CONSTANT ELEMENTS OF ARRAY A(I,J)
      A26=AIG3+AM3*R3**2
      A35=AIG4+AM4*R4**2
      A44=AM4+AM5
      CALL KINE(Y,T,ST,CT,ST3,CT3,ST4,CT4,TD3,TD4,T3,T4)
      CALL DHAM(PR,Y,DY,NDIM,IHLF,GAUSS,OUTP,AUX)
      STOP
      END
      SUBROUTINE DHAM(PRMT,Y,DERY,NDIM,IHLF,FCT,OUTP,AUX)
      DIMENSION PRMT(1),Y(1),DERY(1),AUX(16,1)
      DOUBLE PRECISION Y,DERY,AUX,PRMT,X,H,Z,DELT
      EXTERNAL KINE
      N=1
      IHLF=0
      X=PRMT(1)
      H=PRMT(3)
```

```
      PRMT(5)=0.D0
      DO 1 I=1,NDIM
      AUX(16,I)=0.D0
      AUX(15,I)=DERY(I)
    1 AUX(1,I)=Y(I)
      IF(H*(PRMT(2)-X))3,2,4
C      ERROR RETURNS
    2 IHLF=12
      GOTO 4
    3 IHLF=13
C      COMPUTATION OF DERY FOR STARTING VALUES
    4 CALL FCT(X,Y,DERY)
C      RECORDING OF STARTING VALUES
      CALL OUTP(X,Y,DERY,IHLF,NDIM,PRMT)
      IF(PRMT(5))6,5,6
    5 IF(IHLF)7,7,6
    6 RETURN
    7 DO 8 I=1,NDIM
    8 AUX(8,I)=DERY(I)
C      COMPUTATION OF AUX(2,I)
      ISW=1
      GOTO 100
    9 X=X+H
      DO 10 I=1,NDIM
   10 AUX(2,I)=Y(I)
C      INCREMENT H IS TESTED BY MEANS OF BISECTION
   11 IHLF=IHLF+1
      X=X-H
      DO 12 I=1,NDIM
   12 AUX(4,I)=AUX(2,I)
      H=.5D0*H
      N=1
      ISW=2
      GOTO 100
   13 X=X+H
      CALL FCT(X,Y,DERY)
      N=2
      DO 14 I=1,NDIM
      AUX(2,I)=Y(I)
   14 AUX(9,I)=DERY(I)
      ISW=3
      GOTO 100
C      COMPUTATION OF TEST VALUE DELT
   15 DELT=0.D0
      DO 16 I=1,NDIM
   16 DELT=DELT+AUX(15,I)*DABS(Y(I)-AUX(4,I))
      DELT=.0666666666666667D0*DELT
      IF(DELT-PRMT(4))19,19,17
   17 IF(IHLF-10)11,18,18
C      NO SATISFACTORY ACCURACY AFTER 10 BISECTIONS. ERROR MESSAGE.
   18 IHLF=11
      X=X+H
      GOTO 4
C      THERE IS SATISFACTORY ACCURACY AFTER LESS THAN 11 BISECTIONS.
   19 X=X+H
      CALL FCT(X,Y,DERY)
      DO 20 I=1,NDIM
      AUX(3,I)=Y(I)
   20 AUX(10,I)=DERY(I)
      N=3
```

```
      ISW=4
      GOTO 100
   21 N=1
      X=X+H
      CALL FCT(X,Y,DERY)
      X=PRMT(1)
      DO 22 I=1,NDIM
      AUX(11,I)=DERY(I)
  220Y(I)=AUX(1,I)+H*(.375D0*AUX(8,I)+.791666666666667D0*AUX(9,I)
     1-.208333333333333D0*AUX(10,I)+.041666666666666667D0*DERY(I))
   23 X=X+H
      N=N+1
      CALL FCT(X,Y,DERY)
      CALL OUTP(X,Y,DERY,IHLF,NDIM,PRMT)
      IF(PRMT(5))6,24,6
   24 IF(N-4)25,200,200
   25 DO 26 I=1,NDIM
      AUX(N,I)=Y(I)
   26 AUX(N+7,I)=DERY(I)
      IF(N-3)27,29,200
   27 DO 28 I=1,NDIM
      DELT=AUX(9,I)+AUX(9,I)
      DELT=DELT+DELT
   28 Y(I)=AUX(1,I)+.333333333333333D0*H*(AUX(8,I)+DELT+AUX(10,I))
      GOTO 23
   29 DO 30 I=1,NDIM
      DELT=AUX(9,I)+AUX(10,I)
      DELT=DELT+DELT+DELT
   30 Y(I)=AUX(1,I)+.375D0*H*(AUX(8,I)+DELT+AUX(11,I))
      GOTO 23
C       THE FOLLOWING PART OF SUBROUTINE DHAM COMPUTES BY MEANS OF
C       RUNGE-KUTTA METHOD STARTING VALUES FOR THE NOT SELF-STARTING
C       PREDICTOR-CORRECTOR METHOD.
  100 DO 101 I=1,NDIM
      Z=H*AUX(N+7,I)
      AUX(5,I)=Z
  101 Y(I)=AUX(N,I)+.4D0*Z
C       Z IS AN AUXILIARY STORAGE LOCATION
      Z=X+.4D0*H
      CALL FCT(Z,Y,DERY)
      DO 102 I=1,NDIM
      Z=H*DERY(I)
      AUX(6,I)=Z
  102 Y(I)=AUX(N,I)+.296977609247753 60D0*AUX(5,I)+.158759644971035 83D0*Z
      Z=X+.455737254218789 43D0*H
      CALL FCT(Z,Y,DERY)
      DO 103 I=1,NDIM
      Z=H*DERY(I)
      AUX(7,I)=Z
  103 Y(I)=AUX(N,I)+.218100388225920 47D0*AUX(5,I)-3.050965148692930 8D0*
     1AUX(6,I)+3.832864760467010 3D0*Z
      Z=X+H
      CALL FCT(Z,Y,DERY)
      DO 104 I=1,NDIM
 1040Y(I)=AUX(N,I)+.174760282262690 37D0*AUX(5,I)-.551480662878732 94D0*
     1AUX(6,I)+1.205535599396523 5D0*AUX(7,I)+.171184781219519 03D0*
     2H*DERY(I)
      GOTO(9,13,15,21),ISW
C       POSSIBLE BREAK-POINT FOR LINKAGE
C       STARTING VALUES ARE COMPUTED.
```

```
C       NOW START HAMMINGS MODIFIED PREDICTOR-CORRECTOR METHOD.
  200 ISTEP=3
  201 IF(N-8)204,202,204
C       N=8 CAUSES THE ROWS OF AUX TO CHANGE THEIR STORAGE LOCATIONS
  202 DO 203 N=2,7
      DO 203 I=1,NDIM
      AUX(N-1,I)=AUX(N,I)
  203 AUX(N+6,I)=AUX(N+7,I)
      N=7
C       N LESS THAN 8 CAUSES N+1 TO GET N
  204 N=N+1
C       COMPUTATION OF NEXT VECTOR Y
      DO 205 I=1,NDIM
      AUX(N-1,I)=Y(I)
  205 AUX(N+6,I)=DERY(I)
      X=X+H
  206 ISTEP=ISTEP+1
      DO 207 I=1,NDIM
     ODELT=AUX(N-4,I)+1.33333333333333D0*H*(AUX(N+6,I)+AUX(N+6,I)-
     1AUX(N+5,I)+AUX(N+4,I)+AUX(N+4,I))
      Y(I)=DELT-.925619834710743800*AUX(16,I)
  207 AUX(16,I)=DELT
C       PREDICTOR IS NOW GENERATED IN ROW 16 OF AUX, MODIFIED PREDICTOR
C       IS GENERATED IN Y. DELT MEANS AN AUXILIARY STORAGE.
      CALL FCT(X,Y,DERY)
C       DERIVATIVE OF MODIFIED PREDICTOR IS GENERATED IN DERY
      DO 208 I=1,NDIM
     ODELT=.125D0*(9.D0*AUX(N-1,I)-AUX(N-3,I)+3.D0*H*(DERY(I)+AUX(N+6,I)
     1+AUX(N+6,I)-AUX(N+5,I)))
      AUX(16,I)=AUX(16,I)-DELT
  208 Y(I)=DELT+.074380165289256200*AUX(16,I)
C       TEST WHETHER H MUST BE HALVED OR DOUBLED
      DELT=0.D0
      DO 209 I=1,NDIM
  209 DELT=DELT+AUX(15,I)*DABS(AUX(16,I))
      IF(DELT-PRMT(4))210,222,222
C       H MUST NOT BE HALVED. THAT MEANS Y(I) ARE GOOD.
  210 CALL FCT(X,Y,DERY)
      CALL OUTP(X,Y,DERY,IHLF,NDIM,PRMT)
      IF(PRMT(5))212,211,212
  211 IF(IHLF-21)213,212,212
  212 RETURN
  213 IF(H*(X-PRMT(2)))214,212,212
  214 IF(DABS(X-PRMT(2))-.1D0*DABS(H))212,215,215
  215 IF(DELT-.02D0*PRMT(4))216,216,201
C       H COULD BE DOUBLED IF ALL NECESSARY PRECEEDING VALUES ARE
C       AVAILABLE
  216 IF(IHLF)201,201,217
  217 IF(N-7)201,218,218
  218 IF(ISTEP-4)201,219,219
  219 IMOD=ISTEP/2
      IF(ISTEP-IMOD-IMOD)201,220,201
  220 H=H+H
      IHLF=IHLF-1
      ISTEP=0
      DO 221 I=1,NDIM
      AUX(N-1,I)=AUX(N-2,I)
      AUX(N-2,I)=AUX(N-4,I)
      AUX(N-3,I)=AUX(N-6,I)
      AUX(N+6,I)=AUX(N+5,I)
```

```
      AUX(N+5,I)=AUX(N+3,I)
      AUX(N+4,I)=AUX(N+1,I)
      DELT=AUX(N+6,I)+AUX(N+5,I)
      DELT=DELT+DELT+DELT
 2210 AUX(16,I)=8.9629629629629D0*(Y(I)-AUX(N-3,I))
     1-3.3611111111111111D0*H*(DERY(I)+DELT+AUX(N+4,I))
      GOTO 201
C       H MUST BE HALVED
  222 IHLF=IHLF+1
      IF(IHLF-20)223,223,210
  223 H=.5D0*H
      ISTEP=0
      DO 224 I=1,NDIM
     0Y(I)=.390625D-2*(8.D1*AUX(N-1,I)+135.D0*AUX(N-2,I)+4.D1*AUX(N-3,I)
     1+AUX(N-4,I))-.1171875D0*(AUX(N+6,I)-6.D0*AUX(N+5,I)-AUX(N+4,I))*H
     0AUX(N-4,I)=.390625D-2*(12.D0*AUX(N-1,I)+135.D0*AUX(N-2,I)+
     1108.D0*AUX(N-3,I)+AUX(N-4,I))-.0234375D0*(AUX(N+6,I)+
     218.D0*AUX(N+5,I)-9.D0*AUX(N+4,I))*H
      AUX(N-3,I)=AUX(N-2,I)
  224 AUX(N+4,I)=AUX(N+5,I)
      X=X-H
      DELT=X-(H+H)
      CALL FCT(DELT,Y,DERY)
      DO 225 I=1,NDIM
      AUX(N-2,I)=Y(I)
      AUX(N+5,I)=DERY(I)
  225 Y(I)=AUX(N-4,I)
      DELT=DELT-(H+H)
      CALL FCT(DELT,Y,DERY)
      DO 226 I=1,NDIM
      DELT=AUX(N+5,I)+AUX(N+4,I)
      DELT=DELT+DELT+DELT
     0AUX(16,I)=8.9629629629629D0*(AUX(N-1,I)-Y(I))
     1-3.3611111111111111D0*H*(AUX(N+6,I)+DELT+DERY(I))
  226 AUX(N+3,I)=DERY(I)
      GOTO 206
      END
      SUBROUTINE GAUSS(TIME,Y,DY)
      IMPLICIT REAL*8(A-H,O-Z)
      DIMENSION W(6),DW(6),A(6,6),B(6),TEMPA(6,6),
     1TEMPB(6),DWO(6),BO(6),ALMD(3),Y(2),DY(2)
      COMMON /FIRST/ AR3,R3,R4,STIF,VISC,G,AL1,AL2,AL3,AL4
      COMMON /INMAS/ AIG3,AIG4,AM3,AM4,AM5
      COMMON /SECOND/ EPS1,TD,NLMD
      COMMON /FOURTH/ A26,A35,A44
      COMMON /FORCE/ FX43,FY43,U2DOT,TORQ,T2D4,T2D3
      T=TD*TIME
      CALL KINE(Y,T,ST,CT,ST3,CT3,ST4,CT4,TD3,TD4,T3,T4)
      EPS3=0.D0
      NFLAG1=-1
      NCOUNT=0
C       COMPUTATION OF ARRAY A(I,J) ELEMENTS
      DO 1 I=1,6
      DO 1 J=1,6
    1 A(I,J)=0.D0
      A(1,6)=AM3*AL2*R3*(CT*CT3+ST*ST3)
      A(1,3)=AL2*ST
      A(1,2)=-AL2*CT
      A(1,1)=-1.D0
      B(1)=AM3*G*A(1,2)-AM3*AL2*R3*(ST*CT3-CT*ST3)*TD3**2
```

```
      A(2,3)=AL3*ST3
      A(2,2)=-AL3*CT3
      A(2,6)=A26
      B(2)=-AM3*G*R3*CT3+AM3*AL2*R3*(ST*CT3-CT*ST3)*TD**2
      A(3,4)=-AM4*R4*ST4
      A(3,3)=-AL4*ST4
      A(3,2)=AL4*CT4
      A(3,5)=A35
      B(3)=-AM4*G*R4*CT4
      A(4,3)=1.DO
      A(4,4)=A44
      A(4,5)=A(3,4)
      B(4)=-VISC*Y(1)-STIF*Y(2)+AM4*R4*CT4*TD4**2
      A(5,4)=1.DO
      A(5,6)=A(2,3)
      A(5,5)=A(3,3)
      B(5)=A(3,2)*TD4**2+A(2,2)*TD3**2+A(1,2)*TD**2
      A(6,6)=-A(2,2)
      A(6,5)=-A(3,2)
      B(6)=A(1,3)*TD**2+A(2,3)*TD3**2+A(3,3)*TD4**2
C       SET MATRICES A(I,J) AND B(I) TO DUMMY MATRICES
      DO 10 I=1,6
      DO 16 J=1,6
   16 TEMPA(I,J)=A(I,J)
   10 TEMPB(I)=B(I)
C       START GAUSS ELEMINATION METHD
   12 DO 2 K=1,5
      L=K+1
C       REARRANGE ROWS SO THAT PIVOT ELEMENT A(K,K) HAS THE GREATEST
C       ABSOLUTE VALUE IN IT'S COLCUMN
      M=K
      DO 6 I=L,6
    6 IF(DABS(A(I,K)).GT.DABS(A(M,K)))M=I
      IF(M.EQ.K)GO TO 7
      DO 8 J=K,6
      TEMP=A(K,J)
      A(K,J)=A(M,J)
    8 A(M,J)=TEMP
      TEMP=B(K)
      B(K)=B(M)
      B(M)=TEMP
C       FORWARD ELEMINATION
    7 DO 2 I=L,6
      FACTOR=A(I,K)/A(K,K)
      DO 3 J=L,6
    3 A(I,J)=A(I,J)-FACTOR*A(K,J)
    2 B(I)=B(I)-FACTOR*B(K)
C       BACK SUBSTITUTION
      DW(6)=B(6)/A(6,6)
      I=5
    4 L=I+1
      SUM=0.DO
      DO 5 J=L,6
    5 SUM=SUM+A(I,J)*DW(J)
      DW(I)=(B(I)-SUM)/A(I,I)
      I=I-1
      IF(I.GE.1)GO TO 4
C       CHECK ON ERROR BOUNDS IF BELOW A SPECIFIED MIN. ERROR THEN
C       DO GAUSS ELEMINATION ONCE MORE,COMPUTING ERRORS AND ADDING
C       THEM TO THE PREVIOUSLY CALCULATED VALUES OF DW(J)
```

```
      IF(NFLAG1.LT.0)GO TO 13
      NCOUNT=NCOUNT+1
      DO 14  I=1,6
      IF(DABS(DW(I)).GT.EPS1)EPS3=DW(I)
   14 DW(I)=DWO(I)+DW(I)
      IF(EPS3.LT.1.1D-10)GO TO 15
      IF(NCOUNT.GE.4)GO TO 15
   13 NFLAG1=1
      DO 11  I=1,6
      DWO(I)=DW(I)
      SUM1=0.DO
      DO 9  J=1,6
      A(I,J)=TEMPA(I,J)
      BO(I)=A(I,J)*DW(J)+SUM1
    9 SUM1=BO(I)
   11 B(I)=TEMPB(I)-BO(I)
      GO TO 12
C       THE VECTOR OF 2ND. ORDER QUANTS. (TORQ,FY43,FX43,U2DOT,T2D4,T2D3)
   15 DO 20  I=1,NLMD
   20 ALMD(I)=DW(I)
      DY(1)=DW(4)
      DY(2)=Y(1)
      TORQ=DW(1)
      FY43=DW(2)
      FX43=DW(3)
      U2DOT=DW(4)
      T2D4=DW(5)
      T2D3=DW(6)
      RETURN
      END
      SUBROUTINE CUTP(TIME,Y,DY,IHLF,NDIM,PR)
      IMPLICIT REAL*8(A-H,O-Z)
      DIMENSION Y(2),DY(2),PR(5)
      COMMON /FIRST/ AR3,R3,R4,STIF,VISC,G,AL1,AL2,AL3,AL4
      COMMON /INMAS/ AIG3,AIG4,AM3,AM4,AM5
      COMMON /THIRD/ FCTR,SP,NSP
      COMMON /FIFTH/ STD,PI
      COMMON /FORCE/ FX43,FY43,U2DOT,TORQ,T2D4,T2D3
      IF(IHLF-20)6,1,1
    6 INT=TIME/SP
      IF(INT-NSP)3,2,2
    2 NSP=NSP+1
    1 T=STD*TIME
      CALL KINE(Y,T,ST,CT,ST3,CT3,ST4,CT4,TD3,TD4,T3,T4)
      CHEKX=AL2*CT+AL3*CT3-AL4*CT4-(Y(2)+AL1)
      CHEKY=AL2*ST+AL3*ST3-AL4*ST4
      XACT=AL2*CT+AR3*CT3
      YACT=AL2*ST+AR3*ST3
      ANG2=T*FCTR
      IANG2=ANG2/360.DO
      ANG2=ANG2-IANG2*360.DO
      ANG3=T3*FCTR
      ANG4=T4*FCTR
C       FORCES ON SLIDER:SUFFICES X @ Y DENOTE X@Y DIRECTIONS£
      FX45=AM4*R4*(TD4**2*CT4+T2D4*ST4)-FX43-AM4*U2DOT
      FY45=AM4*R4*(TD4**2*ST4-T2D4*CT4)-FY43+AM4*G
      FORCE4=DSQRT(FX45**2+FY45**2)
      PHASE=45.DO/DATAN(1.DO)*DATAN(FY45/FX45)
      UDOT=Y(1)
      U=Y(2)
```

```
      WRITE(6,100)TIME,ANG2,U,UDOT,TORQ,CHEKX,CHEKY
C      WRITE(3,100)TIME,ANG2,U,UDOT,TORQ,FX45,FY45
  100 FORMAT(2D14.6,5D13.5)
  101 FORMAT(7D15.7)
    3 CONTINUE
      RETURN
      END
      SUBROUTINE KINE(Y,T,ST,CT,ST3,CT3,ST4,CT4,TD3,TD4,T3,T4)
      IMPLICIT REAL*8(A-H,O-Z)
      DIMENSION Y(2)
      COMMON /FIRST/ AR3,R3,R4,STIF,VISC,G,AL1,AL2,AL3,AL4
      COMMON /INMAS/ AIG3,AIG4,AM3,AM4,AM5
      COMMON /FIFTH/ STD,PI
      COMMON /SIXTH/ S1,S2,Q1,Q2
      ST=DSIN(T)
      CT=DCOS(T)
      C1=2.DO*AL4*((Y(2)+AL1)-AL2*CT)
      C2=Q2*ST
      C3=Q1+2.DO*AL2*(Y(2)+AL1)*CT-(Y(2)+AL1)**2
      ST4=(-C2*C3+DSQRT((C1**2-C3**2)*C1**2+(C1*C2)**2))/(C1**2+C2**2)
      CT4=(C3+C2*ST4)/C1
      ST3=(AL4*ST4-AL2*ST)/AL3
      CT3=((Y(2)+AL1)+AL4*CT4-AL2*CT)/AL3
      IF(CT4.EQ.0.DO.AND.ST4.GT.0.DO)T4=PI/2.DO
      IF(CT4.EQ.0.DO.AND.ST4.LT.0.DO)T4=-PI/2.DO
      IF(CT4.EQ.0.DO)GO TO 19
      T4=DATAN(ST4/CT4)
      IF(CT4.LT.0.DO)T4=T4+PI
   19 CONTINUE
      IF(CT3.EQ.0.DO.AND.ST3.GT.0.DO)T3=PI/2.DO
      IF(CT3.EQ.0.DO.AND.ST3.LT.0.DO)T3=-PI/2.DO
      IF(CT3.EQ.0.DO)GO TO 18
      T3=DATAN(ST3/CT3)
      IF(CT3.LT.0.DO)T3=T3+PI
   18 CONTINUE
      TD3=(AL2*DSIN(T-T4)*STD+DCOS(T4)*Y(1))/(AL3*DSIN(T4-T3))
      TD4=(AL2*DSIN(T-T3)*STD+DCOS(T3)*Y(1))/(AL4*DSIN(T4-T3))
   17 CONTINUE
      RETURN
      END
      BLOCK DATA
      IMPLICIT REAL*8(A-H,O-Z)
      COMMON /FIRST/ AR3,R3,R4,STIF,VISC,G,AL1,AL2,AL3,AL4
      COMMON /INMAS/ AIG3,AIG4,AM3,AM4,AM5
      COMMON /SECOND/ EPS1,TD,NLMD
      COMMON /THIRD/ FCTR,SP,NSP
      COMMON /FOURTH/ A26,A35,A44
      COMMON /FIFTH/ STD,PI
      COMMON /SIXTH/ S1,S2,Q1,Q2
      COMMON /FORCE/ FX43,FY43,U2DOT,TORQ,T2D4,T2D3
      DATA AL1,AL2,AL3,AL4/15.35DO,5.DO,15.DO,15.DO/
     1,AM3,AM4,AM5/209.DO,206.DO,590.DO/
     2,AIG3,AIG4/5250.DO,3863.DO/,STIF,VISC,G/1.5D 06,2.8D 04
     3,981.DO/,EPS1/1.D-10/,NSP,NLMD/0,3/
     4,AR3,R3,R4/22.5DO,9.82DO,7.5DO/
      END
```

APPENDIX 2

```
£CO MCE1:RSN-DMP-TRM5
      IMPLICIT REAL*8(A-H,O-Z)
C
C     THIS PROG. INVISTIGATES RESONANCE IN PRESENCE OF DAMPING
C
      DIMENSION A(5,5),B(5),Y(5),TEMPB(5),TEMPA(5,5),YO(5),BO(5)
C       DATA OF MECHANISM
      DATA S2,S3,AM4,AM5,AK,P45/0.05,1.,200.,800.,1.D 06,0.2/
     1,ALF,ALF3,ALF4,OMGAO,N1,N2/149.,57.,120.,9.,5,4/
C       INITIALISATION OF PARAMETERS AND INITIAL CALCULATIONS
      TIME=0.1DO
      AG=1.DO
      VISC=0.DO
      NMR=0
      PI=4.DO*DATAN(1.DO)
      FCTR=PI/180.DO
      F=ALF*FCTR
      F3=ALF3*FCTR
      F4=ALF4*FCTR
      SF3=DSIN(F3)
      CF3=DCOS(F3)
      SF4=DSIN(F4)
      CF4=DCOS(F4)
      SF43=DSIN(F4-F3)
      CF43=DCOS(F4-F3)
      CF04=DCOS(F-F4)
      CF03=DCOS(F-F3)
C       LOOP OPTIONAL FOR VARYING INETIAS,MASSES,OR LENGTHS
   17 C=-SF43**2+S2*CF43*(-CF03+CF04/S3)
      AA=-AG*CF3**2+AG*S2/S3*(SF3*CF3*CF04)/SF43
      G1=AG*S2/S3*SF3*CF3/SF43
      G2=S2*CF43
      H2=AG*S2/S3*SF3*CF4/SF43
      BB=G2*CF3-G2/S3*CF4
      CC=G2*SF3-G2/S3*SF4
      D=P45*H2*CF3
      E=P45*H2*SF3
      P=C+P45*AA
      Q=G2*CF3-(G2/S3+P45*G1)*CF4
      R=G2*SF3-(G2/S3+P45*G1)*SF4
      A0=C/P
      A1=(BB-A0*Q)/C
      B1=(CC-A0*R)/C
      A2=0.5DO*((Q**2-R**2)/P**2-(BB*Q-CC*R)/(C*P))
      B2=Q*R/P**2-(BB*R+CC*Q)/(2.DO*C*P)
      A3=D/P
      B3=E/P
      A4=0.5DO*(E*R-D*Q)/P**2
      B4=-0.5DO*(D*R+E*Q)/P**2
      U=P45*AG*S2*CF3**2
      V=P45*AG*S2*SF3*CF3
      A5=U/P
      B5=V/P
      A6=0.5DO*(R*V-Q*U)/P**2
      B6=-0.5DO*(R*U+Q*V)/P**2
      AB0=(0.25D0+0.125D0*(A1**2+B1**2))*A0**2
      WRITE(6,101)
  101 FORMAT('PARAMETERS ARE:OMGA,Y(1),Y(2),Y(3),Y(4),Y(5),Z1,Z2')
```

```
C       START OF DYNAMIC SECTION
        OMGA=OMGA0
      1 OMGA=OMGA+TIME
        ALC=(VISC/(AM4+AM5))/OMGA
        ALM=(AK/(AM4+AM5))/OMGA**2
        FW1=ALM*A1+A3
        FW2=ALM*B1+B3
        FW3=ALM*A2+A4
        FW4=ALM*B2+B4
        FZ1=ALC*A1
        FZ2=ALC*B1
        FZ3=ALC*A2
        FZ4=ALC*B2
        FK0=2.D0*ALM*A0
C       INITIALISATION OF MATRIX EQUATION'S COEFFECIENTS
        A(1,1)=FK0
        A(1,2)=FW1-FZ2
        A(1,3)=FW2+FZ1
        A(1,4)=FW3-2.D0*FZ4
        A(1,5)=FW4+2.D0*FZ3
        A(2,1)=2.D0*FW1
        A(2,2)=-2.D0+FK0+FW3-FZ4
        A(2,3)=FW4+FZ3+2.D0*ALC
        A(2,4)=FW1-2.D0*FZ2
        A(2,5)=FW2+2.D0*FZ1
        A(3,1)=2.D0*FW2
        A(3,2)=FW4+FZ3-2.D0*ALC
        A(3,3)=-2.D0+FK0-FW3+FZ4
        A(3,4)=-A(2,5)
        A(3,5)=A(2,4)
        A(4,1)=2.D0*FW3
        A(4,2)=FW1+FZ2
        A(4,3)=-FW2+FZ1
        A(4,4)=-8.D0+FK0
        A(4,5)=4.D0*ALC
        A(5,1)=2.D0*FW4
        A(5,2)=-A(4,3)
        A(5,3)=A(4,2)
        A(5,4)=-A(4,5)
        A(5,5)=A(4,4)
        B(1)=0.D0
        B(2)=2.D0*A5
        B(3)=2.D0*B5
        B(4)=2.D0*A6
        B(5)=2.D0*B6
C
C       SET MATRICES A(I,J) AND B(I) TO DUMMY MATRICES
        DO 10 I=1,N1
        DO 16 J=1,N1
       16 TEMPA(I,J)=A(I,J)
       10 TEMPB(I)=B(I)
C       START GAUSS ELEMINATION METHD
       12 DO 2 K=1,N2
        L=K+1
C       REARRANGE ROWS SO THAT PIVOT ELEMENT A(K,K) HAS THE GREATEST
C       ABSOLUTE VALUE IN IT'S COLOUMN
        M=K
        DO 6 I=L,N1
        6 IF(DABS(A(I,K)).GT.DABS(A(M,K)))M=I
        IF(M.EQ.K)GO TO 7
```

```
      DO 8 J=K,N1
      TEMP=A(K,J)
      A(K,J)=A(M,J)
    8 A(M,J)=TEMP
      TEMP=B(K)
      B(K)=B(M)
      B(M)=TEMP
C       FORWARD ELEMINATION
    7 DO 2 I=L,N1
      FACTOR=A(I,K)/A(K,K)
      DO 3 J=L,N1
    3 A(I,J)=A(I,J)-FACTOR*A(K,J)
    2 B(I)=B(I)-FACTOR*B(K)
C       BACK SUBSTITUTION
      Y(N1)=B(N1)/A(N1,N1)
      I=N2
    4 L=I+1
      SUM=0.
      DO 5 J=L,N1
    5 SUM=SUM+A(I,J)*Y(J)
      Y(I)=(B(I)-SUM)/A(I,I)
      I=I-1
      IF(I.GE.1)GO TO 4
C       CHECK ON ERROR BOUNDS IF BELOW A SPECIFIED MIN. ERROR THEN
C       DO GAUSS ELEMINATION ONCE MORE,COMPUTING ERRORS AND ADDING
C       THEM TO THE PREVIOUSLY CALCULATED VALUES OF Y(J)
      IF(FLAG1.LT.0.)GO TO 13
      AMINER=1.D-10
      COUNT=COUNT+1.
      DO 14 I=1,N1
      IF(Y(I).GT.AMINER)AMINER=Y(I)
   14 Y(I)=YO(I)+Y(I)
      IF(AMINER.LT.1.1D-10)GO TO 15
      IF(COUNT.GE.4.DO)GO TO 15
   13 FLAG1=1.DO
      DO 11 I=1,N1
      YO(I)=Y(I)
      SUM1=0.DO
      DO 9 J=1,N1
      A(I,J)=TEMPA(I,J)
      BO(I)=A(I,J)*Y(J)+SUM1
    9 SUM1=BO(I)
   11 B(I)=TEMPB(I)-BO(I)
      GO TO 12
   15 Z1=DSQRT(Y(2)**2+Y(3)**2)
      Z2=DSQRT(Y(4)**2+Y(5)**2)
C       OUTPUT FORMATS
      WRITE(6,100)OMGA,Y(1),Y(2),Y(3),Y(4),Y(5),Z1,Z2
  100 FORMAT(8D12.4)
C       LOGIC TO END PROG. OR RECYCLE DEPENDING UPON CONDITIONS
      IF(OMGA.LE.40.DO)GO TO 1
      VISC=VISC+2.D 02
      WRITE(6,102)VISC
  102 FORMAT('DAMPING COEFFECIENT....',/D20.5)
      NMR=NMR+1
      IF(NMR.LE.6)GO TO 17
      STOP
      END
```

A P P E N D I X 3

```
£CO MCE1:STB-PER-REG1
      IMPLICIT REAL*8(A-H,O-Z)
C      ..................................................
C      THIS PROG. INVISTIGATES STABILITY IN ABSENCE OF DAMPING
C      ..................................................
      DATA AG,S2,AM4,AM5,AK,P45/0.5,0.05,200.,800.,1.D C6,0.2/
     1,ALF,ALF3,ALF4,OMGAO,N1,N2/149.,57.,120.,9.,5,4/
      TIME=0.1DO
      S3=0.8DO
      NMR=0
      PI=4.DC*DATAN(1.DO)
      FCTR=PI/180.DO
      F=ALF*FCTR
      F3=ALF3*FCTR
      F4=ALF4*FCTR
      SF3=DSIN(F3)
      CF3=DCCS(F3)
      SF4=DSIN(F4)
      CF4=DCCS(F4)
      SF43=DSIN(F4-F3)
      CF43=DCOS(F4-F3)
      CF04=DSIN(F-F4)
      CF03=DCOS(F-F3)
   17 C=-SF43**2+S2*CF43*(-CF03+CF04/S3)
      AA=-AG*CF3**2+AG*S2/S3*(SF3*CF3*CF04)/SF43
      G1=AG*S2/S3*SF3*CF3/SF43
      G2=S2*CF43
      H2=AG*S2/S3*SF3*CF4/SF43
      BB=G2*CF3-G2/S3*CF4
      CC=G2*SF3-G2/S3*SF4
      D=P45*H2*CF3
      E=P45*H2*SF3
      P=C+P45*AA
      Q=G2*CF3-(G2/S3+P45*G1)*CF4
      R=G2*SF3-(G2/S3+P45*G1)*SF4
      AO=C/P
      A1=(BB-AO*Q)/C
      B1=(CC-AO*R)/C
      A2=0.5DO*((Q**2-R**2)/P**2-(BB*Q-CC*R)/(C*P))
      B2=Q*R/P**2-(BB*R+CC*Q)/(2.DO*C*P)
      A3=D/P
      B3=E/P
      AN1=(A1/4.DO+A3)**2+(B1/4.DO+B3)**2
      AN2=1.DO/2.DO*DSQRT(AN1)
      ALOW=1.DO/(4.DO*AC)-AN2
      HIGH=1.DO/(4.DO*AO)+AN2
      WRITE(6,100)S3,ALOW,HIGH,AN2,AO
  100 FORMAT(5D15.6)
      S3=S3+0.01DO
      IF(S3.LE.1.2DO)GO TO 17
      STOP
      END
```

A P P E N D I X 4

```
£CO MCE1:F4
      IMPLICIT REAL*8(A-H,O-Z)
C
C     THIS PROG. INVISTIGATES STABILITY IN PRESENCE OF DAMPING
C
      DIMENSION F(5)
      COMMON /FIRST/ AO,A1,B1,A2,B2,A3,B3,A4,B4,GAK,GAC
      COMMON /SECOND/ IA,NU
      EXTERNAL VDET
C       DATA OF MECHANISM
      DATA S2,S3,AM4,AM5,AK,P45/0.05,1.,200.,800.,1.D 06,0.2/
     1,ALF,ALF3,ALF4,OMGAO,N1,N2/149.,57.,120.,15.2,5,4/
C       INITIALISATION OF PARAMETERS AND INITIAL CALCULATIONS
      N=2
      IA=9
      NU=9
      ERR=1.D-12
      READ(5,100)AG,VISC
  100 FORMAT(2D9.2)
      WRITE(6,300)AG,VISC
  300 FORMAT(7X,2HAG,14X,4HVISC,/2D16.3)
      NMR=0
      PI=4.DO*DATAN(1.DO)
      FCTR=PI/180.DO
      FA=ALF*FCTR
      F3=ALF3*FCTR
      F4=ALF4*FCTR
      SF3=DSIN(F3)
      CF3=DCOS(F3)
      SF4=DSIN(F4)
      CF4=DCOS(F4)
      SF43=DSIN(F4-F3)
      CF43=DCOS(F4-F3)
      CF04=DCOS(FA-F4)
      CF03=DCOS(FA-F3)
C       LOOP OPTIONAL FOR VARYING INETIAS,MASSES,OR LENGTHS
   17 C=-SF43**2+S2*CF43*(-CF03+CF04/S3)
      AA=-AG*CF3**2+AG*S2/S3*(SF3*CF3*CF04)/SF43
      G1=AG*S2/S3*SF3*CF3/SF43
      G2=S2*CF43
      H2=AG*S2/S3*SF3*CF4/SF43
      BB=G2*CF3-G2/S3*CF4
      CC=G2*SF3-G2/S3*SF4
      AD=P45*H2*CF3
      E=P45*H2*SF3
      P=C+P45*AA
      Q=G2*CF3-(G2/S3+P45*G1)*CF4
      R=G2*SF3-(G2/S3+P45*G1)*SF4
      AO=C/P
      A1=(BB-AO*Q)/C
      B1=(CC-AO*R)/C
      A2=0.5DO*((C**2-R**2)/P**2-(BB*Q-CC*R)/(C*P))
      B2=Q*R/P**2-(BB*R+CC*Q)/(2.DO*C*P)
      A3=AD/P
      B3=E/P
      A4=0.5DO*(E*R-AD*Q)/P**2
      B4=-0.5DO*(AD*R+E*Q)/P**2
      U=P45*AG*S2*CF3**2
      V=P45*AG*S2*SF3*CF3
```

```
      GAK=AK/(AM4+AM5)
      GAC=VISC/(AM4+AM5)
      ABO=(0.25D0+0.125D0*(A1**2+B1**2))*A0**2
      CALL SIMPLX(VDET,F,N,ERR)
      STOP
      END
      FUNCTION VDET(V,JJ)
      IMPLICIT REAL*8(E-H,O-Z)
      IMPLICIT COMPLEX*16(A-D)
      COMMON /FIRST/ FA0,FA1,FB1,FA2,FB2,FA3,FB3,FA4,FB4,GAK,GAC
      COMMON /SECOND/ IA,NU
      COMMON /THIRD/ NOK
      DIMENSION A(9,9),AW(9,9),V(1)
      P1=DABS(V(JJ+1))
      V(JJ+1)=P1
      P2=V(JJ+2)
      AP2=DCMPLX(0.D0,P2)
      FLC=GAC*DSQRT(P1/GAK)
      FW1=P1*FA1+FA3
      FW2=P1*FB1+FB3
      FW3=P1*FA2+FA4
      FW4=P1*FB2+FB4
      FZ1=FLC*FA1
      FZ2=FLC*FB1
      FZ3=FLC*FA2
      FZ4=FLC*FB2
      FK0=2.D0*P1*FA0
      FC0=2.D0*FLC*FAC
C       INITIALISATION OF MATRIX EQUATION'S COEFFECIENTS
      DO 2 I=1,NU
      DO 2 J=1,NU
    2 A(I,J)=(0.D0,0.D0)
      FNF1=-2.D0*(P2**2+0.25D0)+FK0
      FNF2=FNF1-1.5D0
      FNF3=FNF1-4.D0
      FNF4=FNF1-7.5D0
      FL1=FW1-0.5D0*FZ2
      FL2=FW2+0.5D0*FZ1
      FL3=FW1-1.5D0*FZ2
      FL4=FW3-1.5D0*FZ4
      FL5=FW2+1.5D0*FZ1
      FL6=FW4+1.5D0*FZ3
      FM1=FW3-FZ4
      FM2=FW4+FZ3
      FM3=FW1-2.D0*FZ2
      FM4=FW2+2.D0*FZ1
      FN1=FW1+0.5D0*FZ2
      FN2=FW3-0.5D0*FZ4
      FN3=FW2-0.5D0*FZ1
      FN4=FW4+0.5D0*FZ3
      FO1=FW1+FZ2
      FO2=FW2-FZ1
      A(1,1)=FK0
      A(1,4)=-FZ2+FW1+FZ1*AP2
      A(1,5)=FZ1+FW2+FZ2*AP2
      A(1,8)=-2.D0*FZ4+FW3+FZ3*AP2
      A(1,9)=2.D0*FZ3+FW4+FZ4*AP2
      A(2,2)=FNF1+FL1+(FC0+FZ1)*AP2
      A(2,3)=0.5D0*FC0+FZ1+FL2+(2.D0+FZ2)*AP2
      A(2,6)=FL3+FL4+(FZ1+FZ3)*AP2
```

```
      A(2,7)=FL5+FL6+(FZ2+FZ4)*AP2
      A(3,2)=-0.5D0*FC0+FL2+(-2.D0+FZ2)*AP2
      A(3,3)=FNF1-FL1+(FC0-FZ1)*AP2
      A(3,6)=FL5+FL6+(-FZ2+FZ4)*AP2
      A(3,7)=FL3-FL4+(FZ1-FZ3)*AP2
      A(4,1)=2.D0*FW1
      A(4,4)=FNF2+FM1+(FC0+FZ3)*AP2
      A(4,5)=FC0+FM2+(4.D0+FZ4)*AP2
      A(4,8)=FM3+FZ1*AP2
      A(4,9)=FM4+FZ2*AP2
      A(5,1)=2.D0*FW2
      A(5,4)=-FC0+FM2+(-4.D0+FZ4)*AP2
      A(5,5)=FNF2-FM1+(FC0-FZ3)*AP2
      A(5,8)=-FM4-FZ2*AP2
      A(5,9)=FM3+FZ1*AP2
      A(6,2)=FN1+FN2+(FZ1+FZ3)*AP2
      A(6,3)=-FN3+FN4+(-FZ2+FZ4)*AP2
      A(6,6)=FNF3+FC0*AP2
      A(6,7)=1.5D0*FC0+6.D0*AP2
      A(7,2)=FN3+FN4+(FZ3+FZ4)*AP2
      A(7,3)=FN1-FN2+(FZ1-FZ3)*AP2
      A(7,6)=-1.5D0*FC0-6.D0*AP2
      A(7,7)=FNF3+FC0*AP2
      A(8,1)=2.D0*FW3
      A(8,4)=F01+FZ1*AP2
      A(8,5)=-F02-FZ2*AP2
      A(8,8)=FNF4+FC0*AP2
      A(8,9)=2.D0*FC0+8.D0*AP2
      A(9,1)=2.D0*FW4
      A(9,4)=F02+FZ2*AP2
      A(9,5)=F01+FZ1*AP2
      A(9,8)=-2.D0*FC0-8.D0*AP2
      A(9,9)=FNF4+FC0*AP2
      CALL MA23CD(A,IA,NU,DET,IDET,AW)
      VDET=CDABS(DET)
C      WRITE(3,100)DET,VDET,P1,P2
100   FORMAT(5D20.10)
      IF(NOK.LT.1) GO TO 3
      WRITE(6,100)DET,VDET,P1,P2
3     CONTINUE
      RETURN
      END
      SUBROUTINE SIMPLX(FUNC,F,N,ERR)
      IMPLICIT REAL*8(A-H,O-Z)
C      ACTUAL   NO. OF PARAMETERS = N
C      DIMENSION OF 'V' IS V(N*(N+3))
C      DIMENSION OF 'F' IS F(N+3)
      DIMENSION V(10),F(1)
      COMMON /THIRD/ NOK
      EXTERNAL MA23CD
      DATA LP,LC,ITER,MAX,MIN/20,5,0,2*1/
      DO 31 I=1,10
31    V(I)=0.D0
      READ(5,199)(V(I),I=1,6)
199   FORMAT(6D9.2)
150   FORMAT(12X,2HP1,24X,2HP2,/2D26.14)
 101  FORMAT('INIT. FUNCTION VALUES',/12X,2HF1,24X,2HF2,24X,2HF3)
 107  FORMAT(3D26.14)
 102  FORMAT('SIMPLEX IS BEEING HALVED')
119   FORMAT(12X,2HP1,24X,2HP2,24X,4HFMAX)
```

APPENDIX 5

```
      DIMENSION F(20)
      COMMON /DEVICE/ IDEV1,IDEV3,IDEV5,IDEV6,IDEV8,IDEV9
      COMMON /ALL/ PI,FCTR,EPS2,EPS3,M,MA,N,LEXT,IPATH,ICP
      COMMON /DESACT/ XDES(72),YDES(72),XACT(72),YACT(72),D(72)
      COMMON /THIRD/ DESX(72),DESY(72),DELT(72)
      COMMON /BOUNDS/ PLOW(20),PHIGH(20)
      COMMON /OUT/ NOUT1,NOUT2
      COMMON /CONV/ FMIN,NITER,LP,LC,NGUESS
      COMMON /APEX/ V(500)
      COMMON /RANGE/ VLOW(20),VHIGH(20),RAND,DRAND
      COMMON /FLGS/ SLINK,NFLG1,LCNEG,LCPOS,NCL
      COMMON /MRKS/ SROT,NFLG3,NCR1,NCR2,NCR
      EXTERNAL ERROR
C
C
C     N=NUMBER OF CONTROLLING PARAMETERS
C     M = NUMBER OF DESIRED POINTS;MAXIMUM VALUE 72
C     MA = NUMBER OF ACTUAL POINTS;MAXIMUM VALUE  361
C          IN FUNC. GEN. MA=M ; IN PATH GEN. MA >> M
C     NITER = LIMIT ON NUMBER OF ITERATIONS
C     FMIN = CONVERGENCE IF VALUE OF ERROR FALLS BELOW FMIN
C     NREAD = 1 IF DESIRED OUTPUT TO BE READ OR = -1 IF NOT
C     EPS1 = SMALL CONVERGENCE PARAMETER
C     EPS2 = 0 OR POSITIVE VALUE ; 0 ADMITTS A CRANK-CRANK MECHANISM
C            THE LARGER EPS2 THE SMALLER THE SWING OF THE ROCKER
C     EPS3 = A SMALL CONSTANT ; PARAMETERS ARE SET EPS3 WITHIN
C            THE EXTERNAL CONSTRAINTS
C     NOUT1,NOUT2 = OUTPUT FLAGS
C     LEXT = 1 IF THERE ARE EXTERNAL CONSTRAINTS
C          = -1 IF THERE ARE NO EXTERNAL CONSTRAINTS
C     LP = WRITE VALUES OF CONTROLLING PARAMETERS AND VALUES
C          OF MAX. & AND MIN. ERRORS AT EVERY LP ITERATIONS
C     LC = CHECK ON CONVERGENCE EVERY LC ITERATIONS
C     NGUESS = -1 IF ALL INITIAL SETS OF GUESSES ARE SUPPLIED
C              +1 IF ONLY ONE SET IS SUPPLIED ; MUST BE GOOD
C     IPATH = 1 FOR FUNCTION GENERATION
C           =-1 FOR PATH GENERATION
C     ICP = PARAM. FOR ADJUSTING THE AREA ERROR CALCULATION
C           IT IS USED IN PATH GENERATION ONLY AND IT PLAYS AN
C           IMPORTANT PART IN THE INITIAL 50 ITERATIONS
C           IF MA IS >>>> M AND DESIRED POINTS ARE EQUALLY SPACED,
C           (NOT STRICTLY), ICP MAY GIVEN THE VALUE OF ZERO I.E IGNORED
C     IDEV1,2,3,5,6,8,9 = ARE OUTPUT DEVICES
C
      N=9
      M=19
      MA=72
      PI=4.*ATAN(1.)
      FCTR=180./PI
      NITER=2000
      FMIN=1.
      EPS1=1.E-02
      EPS2=0.
      EPS3=1.E-05
      NOUT1=-1
      NOUT2=1
```

```
      NREAD=+1
      LEXT=-1
      LP=50
      LC=1
      NGUESS=-1
      IPATH=-1
      ICP=2
      IDEV1=1
      IDEV2=2
      IDEV3=3
      IDEV4=4
      IDEV5=5
      IDEV6=6
      IDEV8=8
      IDEV9=9
C
C     DATA FOR FLGS AND MRKS LABELLED COMMONS
C     NFLG1,NFLG3 = -1 COMBINED WITH VALUES OF SLINK AND SROT
C     ALLOWES FOR CHOICE OF LINK-CLOSURE AND ROT. DIRN. OF CRANK
C     IF NO CHOICE IS DESIRED THEN LEAVE AS BELOW
C
      SLINK=1.
      SROT=1.
      NFLG1=1
      NFLG3=1
      LCNEG=0
      NCR1=0
      LCPOS=0
      NCR2=0
      NCL=200
      NCR=200
C
      WRITE(IDEV6,110)M,MA
      WRITE(IDEV6,111)
C
C     DESIRED OUTPUT
C
      IF(NREAD.LE.0)GO TO 1
      READ(IDEV1,101)(XDES(I),I=1,M)
      READ(IDEV1,101)(YDES(I),I=1,M)
      IF(IPATH.LT.0) GO TO 4
      READ(IDEV1,101)(DELT(I),I=1,M)
      GO TO 4
C
C     DESIRED X & Y COORDINATES
C
 1    CONTINUE
      XADD=50.
      YADD=350.
      XDES(1)=164.+XADD
      YDES(1)=8.+YADD
      XDES(2)=164.+XADD
      YDES(2)=0.+YADD
      XDES(3)=100.+XADD
      YDES(3)=0.+YADD
```

```
      XDES(4)=50.+XADD
      YDES(4)=0.+YADD
      XDES(5)=0.+XADD
      YDES(5)=0.+YADD
      XDES(6)=0.+XADD
      YDES(6)=30.+YADD
      XDES(7)=0.+XADD
      YDES(7)=61.+YADD
      XDES(8)=45.+XADD
      YDES(8)=61.+YADD
      XDES(9)=92.+XADD
      YDES(9)=61.+YADD
      XDES(10)=128.+XADD
      YDES(10)=34.5+YADD
C
C     PRESCRIBED TIME OR CRANK ANGLE FOR DESIRED OUTPUT
C
      IF(IPATH.LT.0)GO TO 4
      DELT(1)=57./FCTR
      DELT(2)=69./FCTR
      DELT(3)=183./FCTR
      DELT(4)=277./FCTR
      DELT(5)=22./FCTR
 4    CONTINUE
C
C     IN PATH GENERATION THE STARTING POINT IS COUNTED TWICE
C
      IF(IPATH.GE.0) GO TO 10
      XDES(M+1)=XDES(1)
      YDES(M+1)=YDES(1)
 10   CONTINUE
C
C     AUX. STORAGE OF DESIRED PATH
C
      MLAST=M+1
      DO 11 I=1,MLAST
      DESX(I)=XDES(I)
 11   DESY(I)=YDES(I)
C
      IF(NGUESS)7,8,8
C
C
C     GENERATE (N) SETS OF INITIAL VALUES
C
 8    WRITE(IDEV6,107)
      READ(IDEV4,116)(V(I),I=1,N)
      WRITE(IDEV6,108)
      READ(IDEV4,116)(VLOW(I),I=1,N)
      WRITE(IDEV6,109)
      READ(IDEV4,116)(VHIGH(I),I=1,N)
      WRITE(IDEV6,105)
      READ(IDEV4,106)RAND,DRAND
      WRITE(IDEV2,102)
      WRITE(IDEV2,103)
      WRITE(IDEV2,116)(VLOW(I),I=1,N)
```

```
      WRITE(IDEV2,104)
      WRITE(IDEV2,116)(VHIGH(I),I=1,N)
      GO TO 9
C
C     READ (N+1) SETS OF INITIAL GUESSES
C
 7    CONTINUE
      NSETS=N+1
      DO 6 I=1,NSETS
      NV1=(I-1)*N+1
      NV2=I*N
      READ(IDEV5,116)(V(J),J=NV1,NV2)
 6    CONTINUE
 9    N1=N*(N+1)
      N3=N+3
      NF=N3*N
      NI=N1+1
      DO 5 I=NI,NF
 5    V(I)=0.
C
C     EXTERNAL CONSTRAINTS LEXT=1 FOR YES , LEXT=-1 FOR NO
C
      IF(LEXT)3,2,2
 2    READ (IDEV1,100)(PLOW(I),I=1,N)
      READ (IDEV1,100)(PHIGH(I),I=1,N)
 3    CONTINUE
      WRITE(IDEV3,112)
C
C     OUTPUT FORMATS
C
 102  FORMAT(' OUTPUT OF AUTOMATICALLY GENERATED INIT. VALUES')
 103  FORMAT('      VLOW      ')
 104  FORMAT('      VHIGH     ')
 116  FORMAT(10F7.2)
 100  FORMAT(10E10.3)
 101  FORMAT(5E12.4)
 112  FORMAT(4X,2HL1,8X,2HL2,8X,2HL3,8X,2HL4,8X,2H R,8X
     1,2HX0,8X,2HY0,7X,4HALF1,6X,4HALF2,6X,4HTH20)
 105  FORMAT('* WHAT ARE "RAND & DRAND" ? IN 2F7.4 FORMAT *')
 106  FORMAT(2F7.4)
 107  FORMAT('INTIAL GUESS ? IN 10F7.2 FORMAT')
 108  FORMAT('MINIMUM RANGE OR VLOW ? IN 10F7.2 FORMAT')
 109  FORMAT('MAXIMUM RANGE OR VHIGH ? IN 10F7.2 FORMAT')
 110  FORMAT('DESIRED POINTS M    ACTUAL POINTS MA',/,7X,I3,16X,I3)
 111  FORMAT('MA=M IN FUNC. GEN.',/,'MA>>M IN PATH GEN.')
      CALL SIMPLX(ERROR,F,N,EPS1)
      STOP
      END
```

MEMORY REQUIREMENTS 000D38 BYTES

```
      FUNCTION ERROR(V,J)
C
C     CLINK = +1 & -1 REPRESENTING BOTH LOOP CLOSURE CONFIGURATIONS
C
      DIMENSION V(1),XA(361),YA(361),XER(361),YER(361),THETA(361)
      COMMON /DEVICE/ IDEV1,IDEV3,IDEV5,IDEV6,IDEV8,IDEV9
      COMMON /ALL/ PI,FCTR,EPS2,EPS3,M,MA,N,LEXT,IPATH,ICP
      COMMON /OUT/ NOUT1,NOUT2
      COMMON /THIRD/ DESX(72),DESY(72),DELT(72)
      COMMON /FLGS/ SLINK,NFLG1,LCNEG,LCPOS,NCL
  104 FORMAT(10E10.3)
  105 FORMAT(11H CRANK ANG.,5X,4HXDES,8X,4HXACT,8X,4HYDES,8X,4HYACT
     1,8X,3HXER,8X,3HYER)
  112  FORMAT(4X,2HL1,8X,2HL2,8X,2HL3,8X,2HL4,8X,2H R,8X
     1,2HXC,8X,2HYC,7X,4HALF1,6X,4HALF2,6X,4HTH20)
  200  FORMAT(7E12.4)
  204  FORMAT('TOTAL ERROR & LINKAGE FORM',/,2E12.4)
  201  FORMAT(2E12.4)
  202  FORMAT('  ACTUAL X    ACTUAL Y')
  203  FORMAT(' DESIRED X   DESIRED Y')
C
C     MAKE SURE THAT LINK SIZES ARE POSITIVE
C
      DO 21 I=1,4
  21  V(J+I)=ABS(V(J+I))
C
C     INITIAL CALCULATIONS
C
      CLINK=SLINK
   4  TIME=0.
      NVIOL=+1
      ERROR=0.
      NFLAG2=-1
      CL=COS((V(J+8)+V(J+9))/FCTR)
      SL=SIN((V(J+8)+V(J+9))/FCTR)
C
   6  CYCLE=0.
      DO 3 I=1,MA
C
C     KINEMATICS
C
      IF(IPATH)30,31,31
  31  T2=DELT(I)
      GO TO 32
  30  T2=CYCLE
  32  CONTINUE
      ST2=SIN(T2)
      CT2=COS(T2)
      C1=V(J+3)**2-V(J+4)**2-V(J+2)**2
      C2=2.*V(J+2)*V(J+4)
      C3=2.*V(J+4)*(V(J+1)-V(J+2)*CT2)
      C4=C2*ST2
      C5=C1+(2.*V(J+2)*CT2-V(J+1))*V(J+1)
      ARG1=(C3**2-C5**2)*C3**2+(C3*C4)**2
C
```

```
C       ARE CONSTRAINTS VIOLATED
C
        CALL CONSTR(ARG1,V,J,NVIOL)
C
C       LOOP CONSTRAINTS HAVE BEEN VIOLATED
C
        IF(NVIOL)22,23,23
 22     GO TO 4
 23     CONTINUE
C
C       CONTINUE WITH THE KINEMATICS
C
        ST4=(-C4*C5+CLINK*SQRT(ARG1))/(C3**2+C4**2)
        CT4=(C5+C4*ST4)/C3
        ST3=(V(J+4)*ST4-V(J+2)*ST2)/V(J+3)
        CT3=(V(J+1)+V(J+4)*CT4-V(J+2)*CT2)/V(J+3)
C
C       ACTUAL MOTION
C
        XA(I)=V(J+6)+V(J+2)*COS(T2+V(J+8)/FCTR)+V(J+5)*(CL*CT3-SL*ST3)
        YA(I)=V(J+7)+V(J+2)*SIN(T2+V(J+8)/FCTR)+V(J+5)*(SL*CT3+CL*ST3)
C
        IF(IPATH)33,34,34
C
C       EVALUATION OF OBJECTIVE FUNCTION.I.E ERROR CRITERION
C
 34     XER(I)=(XA(I)-DESX(I))**2
        YER(I)=(YA(I)-DESY(I))**2
        ERROR=ERROR+XER(I)+YER(I)
        GO TO 3
C
 33     CYCLE=CYCLE+2.*PI/MA
 3      CONTINUE
C
C       IF PATH GENERATION CALL PATH SUBRCUTINE
C
        IF(IPATH.GE.0) GO TO 35
        CALL PATH(SUM,XA,YA)
        ERROR=SUM
C
C       SORT OUT LINKAGE CLOSURE CONFIGURATION
C
 35     IF(NFLAG2.GT.0) GO TO 13
        IF(NFLG1.LT.0) GO TO 41
        IF(CLINK)7,8,8
 8      CLINK=-1.
        TERR=ERROR
        ERROR=0.
        GO TO 6
 7      IF(TERR-ERROR)9,11,11
 9      ERROR=TERR
        CLINK=1.
        LCPOS=LCPOS+1
        GO TO 40
 11     LCNEG=LCNEG+1
```

```
 40   CONTINUE
      IF(LCPOS.GE.NCL)SLINK=1.
      IF(LCNEG.GE.NCL)SLINK=-1.
      IF((LCPOS.GE.NCL).OR.(LCNEG.GE.NCL))NFLG1=-1
 41   CONTINUE
C
C     OUTPUT
C
      IF(NOUT2)17,18,18
 18   KP=J+1
      KPAR=KP+N-1
      WRITE(IDEV3,104)(V(I),I=KP,KPAR)
 17   CONTINUE
C
C     THIS IS THE OPTIMISED OUTPUT
C     OPTIMISATION SUCCESS  *****
C
      IF(NOUT1)12,12,5
C
C     ORGANISE FINAL CALL AND OUTPUT RESULTS
C
  5   NFLAG2=1.
      ERROR=0.
      GO TO 6
 13   CONTINUE
C
      IF(IPATH)36,37,37
C
C     PATH GENERATION OUTPUT
C
 36   WRITE(IDEV6,112)
      WRITE(IDEV6,104)(V(I),I=1,N)
      WRITE(IDEV6,202)
      DO 38 I=1,MA
      WRITE(IDEV6,201)XA(I),YA(I)
 38   CONTINUE
      WRITE(IDEV6,203)
      DO 39 I=1,M
      WRITE(IDEV6,201)DESX(I),DESY(I)
 39   CONTINUE
      GO TO 60
C
 37   CONTINUE
C
C     FUNCTION GENERATION OUTPUT
C
      WRITE(IDEV6,112)
      WRITE(IDEV6,104)(V(I),I=1,N)
      WRITE(IDEV6,105)
      DO 16 I=1,M
      THETA(I)=DELT(I)*FCTR
      WRITE(IDEV6,200)THETA(I),DESX(I),XA(I),DESY(I),YA(I)
     1,XER(I),YER(I)
16    CONTINUE
60    CONTINUE
```

```
      WRITE(IDEV6,204)ERROR,CLINK
   12 CONTINUE
      RETURN
      END
```

MEMORY REQUIREMENTS 002890 BYTES

```
      SUBROUTINE SIMPLX(FUNC,F,N,EPS1)
C     ACTUAL   NO. OF PARAMETERS = N
C     DIMENSION OF 'V' IS V(N*(N+3))
C     DIMENSION OF 'F' IS F(N+3)
C     DIMENSION OF 'VC' IS VC(N)
      EXTERNAL FUNC
      COMMON /DEVICE/ IDEV1,IDEV3,IDEV5,IDEV6,IDEV8,IDEV9
      COMMON /CONV/ FMIN,NITER,LP,LC,NGUESS
      COMMON /OUT/ NOUT1,NOUT2
      COMMON /CENTRE/ VC(20)
      COMMON /APEX/ V(500)
      DIMENSION F(1)
      DATA ITER,MAX,MM,MIN/0,3*1/
  101 FORMAT('INITIAL FUNCTION VALUES,F1,..F(N+1) ARE:')
  107 FORMAT(1X,5E15.5)
  102 FORMAT('SIMPLEX IS BEEING HALVED')
  103 FORMAT(' THIS THE END OF SUBROUTINE "START"')
  119 FORMAT('PARAMS. FOR F(MAX)')
  120 FORMAT('PARAMS. FOR F(MIN)')
  104 FORMAT('MAX. ERROR VALUE IN CURRENT SIMPLEX',/,E15.6)
  105 FORMAT('MIN. ERROR VALUE IN CURRENT SIMPLEX',/,E15.6)
  117 FORMAT('CONVERGENCE***SUCCESS****',/)
  112 FORMAT('ITERATIONS =',I10)
  121 FORMAT('FINAL VALUES OF LINKAGE PARAMETERS')
  115 FORMAT(1X,5E15.6)
  122 FORMAT('MINIMUM ERROR',/E15.6)
C
C     CALCULATE STARTING VERTICES AND FUNCTION VALUES
C
      N1 = N + 1
      N3 = N + 3
      NN = N*N1
C
      IF(NGUESS)42,43,43
C
C     GENERATE INITIAL VALUES
C
 43   CONTINUE
      CALL START(FUNC,F,V,N)
      WRITE(IDEV4,103)
      GO TO 44
C
C     INITIAL SETS ARE GIVEN
C
 42   CONTINUE
      DO 45 I=1,N
      VC(I)=0.
      DO 46 L=1,N1
46    VC(I)=VC(I)+0.5*V(I+(L-1)*N)
45    CONTINUE
      DO 2 I=1,N1
2     F(I) = FUNC(V,(I-1)*N)
44    CONTINUE
      WRITE(IDEV3,101)
      WRITE(IDEV3,107)(F(I),I=1,N1)
```

```
C
C       CALCULATE HIGHEST(MAX),NEXT HIGHEST(MM),&LOWEST(MIN) FUNCTION
C
        NOUT2=-1
        DO 4 I=1,N1
        IF(F(I).GT.F(MAX))MAX=I
        IF(F(I).LT.F(MIN))MIN=I
    4   CONTINUE
        MM=MIN
        DO 5 I=1,N1
        IF(I.EQ.MAX) GO TO 5
        IF(F(I).GT.F(MM))MM=I
    5   CONTINUE
C
C       BEGIN NEW ITERATION
C
    3 CONTINUE
C       SELECT NEW VERTEX V*=V(N1+1) & EVALUATE F*=F(N1+1)
C
        DO 9 I=1,N
        V(I+NN) = -(1.+N/2.)*V(I+(MAX-1)*N)
        DO 8 J=1,N1
    8   V(I+NN) = V(I+NN) + V(I+(J-1)*N)
        V(I+NN) = V(I+NN)*2./N
    9 VC(I)=V(I+(MAX-1)*N)
        F(N1+1) = FUNC(V,NN)
C
C       CHECK IF F* .LT. F(MIN)
C
        IF(F(N1+1).GE.F(MIN)) GO TO 149
C
C       DIRECTION IS ADVANTAGEOUS SO TRY DOUBLE MOVE TO V**=2V*-V(MAX)
C
        DO 10 I=1,N
        V(I+N+NN) = 2.*V(I+NN) - V(I+(MAX-1)*N)
   10 VC(I)=V(I+NN)
        F(N1+2) = FUNC(V,N+NN)
C
C       CHECK IF DOUBLE MOVE IS IMPROVEMENT ON ORIGINAL MOVE
C
        IF(F(N1+2)-F(N1+1)) 11,12,12
   11   NEW = N1+2
        GO TO 13
   12   NEW = N1+1
C
C       RESET V(MAX) TO NEW VALUES
C
   13   CONTINUE
        DO 14 I=1,N
   14   V(I+(MAX-1)*N) = V(I+(NEW-1)*N)
        F(MAX) = F(NEW)
        GO TO 24
C
C       ORIGINAL MOVE NO GOOD. CHECK IF REFLECTED POINT
C       WILL HAVE THE LARGEST FUNCTION VALUE
```

```
C
 149  IF(F(N1+1) - F(MM)) 15,15,16
 15   NEW = N1+1
      GO TO 13
C
C     REFLECTED POINT WILL HAVE LARGEST FUNCTION VALUE
C     PREPARE FOR THE REDUCTION OF SIMPLEX ETC.
C
 16   DO 18 I=1,N
C
C     SET V** TEMPORARILY TO V=(V* + VMAX)/2
C
      V(I+N+NN) = (V(I+NN) + V(I+(MAX-1)*N))/2.
C
C     SET VMAX TO V* IF NECESSARY AND FINALISE CALC. FOR V** & F**
C
      IF(F(N1+1)-F(MAX)) 17,17,18
 17   V(I+(MAX-1)*N) = V(I+NN)
 18   V(I+N+NN) = (V(I+N+NN) + V(I+(MAX-1)*N))/2.
      F(N1+2) = FUNC(V,N+NN)
      IF(F(N1+1).LE.F(MAX)) F(MAX)=F(N1+1)
C
C     IF V** STILL HAS GREATEST FUNCTION VALUE, HALVE SIMPLEX ABOUT V(MIN)
C
      IF(F(N1+2)-F(MAX)) 19,19,20
 19   NEW = N1+2
      GO TO 13
C
C     HALVE SIZE OF SIMPLEX
C
   20 CONTINUE
C     WRITE(IDEV3,102)
      DO 23 I=1,N1
      IF(I-MIN) 21,23,21
 21   DO 22 J=1,N
      VC(J)=V(J+(I-1)*N)
 22   V(J+(I-1)*N) = (V(J+(I-1)*N) + V(J+(MIN-1)*N))/2.
      F(I) = FUNC(V,(I-1)*N)
 23   CONTINUE
C
   24 DO 6 I=1,N1
      IF(F(I).GT.F(MAX))MAX=I
      IF(F(I).LT.F(MIN))MIN=I
 6    CONTINUE
      MM=MIN
      DO 7 I=1,N1
      IF(I.EQ.MAX) GO TO 7
      IF(F(I).GT.F(MM))MM=I
 7    CONTINUE
C
C     TEST FOR CONVERGENCE
C
      ITER=ITER+1
      IF(ITER.GE.NITER) GO TO 41
C
```

```
C       WRITE PROGRESS OF OPTIMISATION EVERY LP ITERATIONS
C
        IF(ITER/LP-(ITER-1)/LP.EQ.0) GO TO 40
        WRITE(IDEV3,112)ITER
        I=(MAX-1)*N+1
        J=MAX*N
        WRITE(IDEV3,119)
        WRITE(IDEV3,115)(V(K),K=I,J)
        WRITE(IDEV3,104)F(MAX)
        I=(MIN-1)*N+1
        J=MIN*N
        WRITE(IDEV3,120)
        WRITE(IDEV3,115)(V(K),K=I,J)
        WRITE(IDEV3,105)F(MIN)
C
C       CHECK CONVERGENCE EVERY LC ITERATIONS
C
 40     IF(ITER/LC-(ITER-1)/LC.EQ.0) GO TO 3
        IF(F(MIN).LE.FMIN) GO TO 41
C
C       CONVERGENCE IF ABS.(FMAX-FMIN) LESS THAN ABS.(EPS1 * FMIN)
C
C       IF(F(MAX)-F(MIN).GT.ABS(EPS1*F(MIN)))GO TO 3
C
C       CONVERGENCE IF ABS.(VMAX-VMIN) LESS THAN ABS.(EPS1 * VMIN)
C
        DO 99 I=1,N
        IF(ABS(V(I+(MAX-1)*N)-V(I+(MIN-1)*N)).GT.ABS(EPS1*V(I+(MIN-1)*N))
       1)GO TO 3
 99     CONTINUE
    41 CONTINUE
C
C       FILL F WITH PARAMETER VALUES AND F(MIN)
C
 26     WRITE(IDEV6,117)
        WRITE(IDEV6,112)ITER
        DO 27 I=1,N
    27  V(I) = V(I+(MIN-1)*N)
        WRITE(IDEV6,121)
        WRITE(IDEV6,115)(V(I),I=1,N)
        WRITE(IDEV6,122)F(MIN)
        NOUT1=1
        F(N1)=FUNC(V,0)
        RETURN
        END
```

MORY REQUIREMENTS 001272 BYTES

```
      SUBROUTINE CONSTR(ARG1,V,J,NVIOL)
      DIMENSION V(1)
      COMMON /DEVICE/ IDEV1,IDEV3,IDEV5,IDEV6,IDEV8,IDEV9
      COMMON /CENTRE/ VC(20)
      COMMON /BOUNDS/ PLOW(20),PHIGH(20)
      COMMON /ALL/ PI,FCTR,EPS2,EPS3,M,MA,N,LEXT,IPATH,ICP
  110 FORMAT('VIOLATION OF CONSTRAINTS ARG1 = ',E15.5)
      IF(ARG1.GE.0.)GO TO 50
C     WRITE(3,110)ARG1
C
C     CHECK LOOP CONSTRAINTS,IF VIOLATED MOVE BACK QUARTER THE
C     DISTANCE BETWEEN CURRENT APEX AND MAX. ERR. APEX
C     THE MOVE IS TOWARDS THE CENTROID OF THE SIMPLEX
C
      DO 2 L=1,N
    2 V(L+J)=0.25*(3.*V(L+J)+VC(L))
      NVIOL=-1
   50 CONTINUE
C
C     EXTERNAL CONSTRAINTS;  EITHER PLACE THEM
C     EPS3 WITHIN THE GIVEN BOUNDS OR MOVE BACK 1/4. THE
C     DISTANCE TOWARDS THE CENTROID OF THE SIMPLEX
C
      IF(LEXT)18,17,17
   17 DO 19 I=1,N
      IF(V(I).GE.PLOW(I).AND.V(I).LE.PHIGH(I)) GO TO 19
      IF(ABS(V(I)-PLOW(I)).LE.ABS(V(I)-PHIGH(I))) GO TO 20
      V(I)=PHIGH(I)-EPS3
      GO TO 19
   20 V(I)=PLOW(I)+EPS3
   19 CONTINUE
   18 CONTINUE
      RETURN
      END
```

EMORY REQUIREMENTS 00033E BYTES

```
      SUBROUTINE START(FUNC,F,V,N)
      DIMENSION V(1),F(1)
      COMMON /CENTRE/ VC(20)
      COMMON /DEVICE/ IDEV1,IDEV3,IDEV5,IDEV6,IDEV8,IDEV9
      COMMON /RANGE/ VLOW(20),VHIGH(20),RAND,DRAND
  105 FORMAT('  RAND        DRAND',/,1X,2E10.3)
  101 FORMAT(10E10.4)
      WRITE(IDEV2,105)(V(I),I=1,N)
      NP=N
      ONE=1.
C
C     EVALUATE ERROR FUNCTION FOR THE SUPPLIED GUESS
C
      F(1)=FUNC(V,0)
C
      DO 4 J=1,N
      IF(J.GE.2)ONE=0.5
      DO 1 I=1,N
C
C     FIND THE THE V VECTOR OF INITIAL VALUES
C
      IF(RAND.GT.1.6)RAND=0.
      V(NP+I)=VLOW(I)+(VHIGH(I)-VLOW(I))*(SIN(RAND))**2
      RAND=RAND+DRAND
    1 CONTINUE
      JV=NP+1
      JVP=JV+N-1
      WRITE(IDEV2,101)(V(KV),KV=JV,JVP)
C
C     FIND THE CENTROID OF THE EXISTING SET OF VALUES
C
      DO 3 K=1,N
      VC(K)=0.
      DO 2 L=1,J
      VC(K)=VC(K)+ONE*V(K+(L-1)*N)
    2 CONTINUE
    3 CONTINUE
C
C     EVALUAT ERROR
C
      F(J+1)=FUNC(V,J*N)
      NP=NP+N
    4 CONTINUE
      RETURN
      END
```

EMORY REQUIREMENTS 00044E BYTES

```
      SUBROUTINE PATH(SUM,XA,YA)
      DIMENSION XA(361),YA(361),TXA(361),TYA(361),DA(361)
      COMMON /ALL/ PI,FCTR,EPS2,EPS3,M,MA,N,LEXT,IPATH,ICP
      COMMON /DESACT/ XDES(72),YDES(72),XACT(72),YACT(72),D(72)
      COMMON /MRKS/ SROT,NFLG3,NCR1,NCR2,NCR
C
C     FIND STARTING POINT FOR CALCULATION OF THE AREA ERROR
C
      SUM=0.
      ROT=SROT
      NRN=1
      DO 1 I=1,MA
      TXA(I)=XA(I)
    1 TYA(I)=YA(I)
      D(1)=SQRT((XDES(1)-XA(1))**2+(YDES(1)-YA(1))**2)
      DA(1)=D(1)
      MK1=1
      DO 2 I=2,MA
      DA(I)=SQRT((XDES(1)-XA(I))**2+(YDES(1)-YA(I))**2)
      IF(DA(I).LT.DA(MK1))MK1=I
    2 CONTINUE
C
C     INDEX ACTUAL OUTPUT ACCORDING TO POSITION OF STARTING POINT
C     ALSO MAKE WINDOW SEARCH IN THE NEIGHBOURHOOD OTHE DESIRED POINT
C
      MR2=MK1-1
      MR1=MA-MR2
      DO 4 I=1,MR1
      XA(I)=TXA(MK1+I-1)
    4 YA(I)=TYA(MK1+I-1)
      IF(MR2.EQ.0) GO TO 10
      DO 9 J=1,MR2
      MR1=MR1+1
      XA(MR1)=TXA(J)
    9 YA(MR1)=TYA(J)
   10 CONTINUE
   27 CONTINUE
      IF(ROT)19,19,20
   20 IF(NFLG3.LT.0) GO TO 21
      ROT=-1.
      GO TO 21
   19 DO 17 I=1,MA
      TXA(I)=XA(MA-I+1)
   17 TYA(I)=YA(MA-I+1)
      DO 18 I=1,MA
      XA(I)=TXA(I)
      YA(I)=TYA(I)
   18 CONTINUE
   21 XACT(1)=XA(1)
      YACT(1)=YA(1)
      XACT(M+1)=XA(1)
      YACT(M+1)=YA(1)
      MK=3
      MKP=2
      DO 5 I=2,M
```

```
      D(I)=SQRT((XDES(I)-XA(MKP))**2+(YDES(I)-YA(MKP))**2)
      MK1=MKP
      NCNT=0
      DA(MK1)=D(I)
      DO 7 J=MK,MA
      DA(J)=SQRT((XDES(I)-XA(J))**2+(YDES(I)-YA(J))**2)
      IF(DA(J).LT.DA(MK1))MK1=J
      NCNT=NCNT+1
      IF((MA-J)-(M-I))12,12,30
 30   IF(NCNT.GE.ICP*MA/M)GO TO 11
 7    CONTINUE
      GO TO 11
 12   IF((MA-MK1)-(M-I))16,16,11
 11   MK=MK1+2
      XACT(I)=XA(MK1)
      YACT(I)=YA(MK1)
      IF(MK-MA)29,29,15
 15   MKP=MA
      MK=MA
      GO TO 5
 29   MKP=MK-1
 5    CONTINUE
 16   DO 32 K=I,M
      XACT(K)=XA(MK1)
      YACT(K)=YA(MK1)
 32   MK1=MK1+1
C
C      WE HAVE NOW EQUAL NUMBER OF DESIRED AND ACTUAL POINTS
C     ALSO THEY ARE CHOSEN SO AS TO MAKE CALCULATION OF AREA ACCURATE
C
C      AREA ERROR BETWEEN DESIRED AND ACTUAL FUNCTIONS
C
      DO 8 K=1,M
      AREA=0.5*(ABS((XDES(K)*YACT(K)-YDES(K)*XACT(K))
     1+(XACT(K)*YACT(K+1)-YACT(K)*XACT(K+1))
     2+(XACT(K+1)*YDES(K)-YACT(K+1)*XDES(K)))
     3+ABS((XDES(K)*YDES(K+1)-YDES(K)*XDES(K+1))
     4+(XDES(K+1)*YACT(K+1)-YDES(K+1)*XACT(K+1))
     5+(XACT(K+1)*YDES(K)-YACT(K+1)*XDES(K))))
 8    SUM=SUM+AREA
      IF(NFLG3.LT.0) GO TO 22
      IF(NRN)23,23,24
 24   NRN=-1
      SUM1=SUM
      SUM=0.
      GO TO 27
 23   IF(SUM1-SUM)25,26,26
 25   SUM=SUM1
      NCR1=NCR1+1
      GO TO 28
 26   NCR2=NCR2+1
 28   IF(NCR1.GE.NCR)SROT=1.
      IF(NCR2.GE.NCR)SROT=-1.
      IF((NCR1.GE.NCR).OR.(NCR2.GE.NCR))NFLG3=-1
 22   CONTINUE
```

```
        RETURN
        END

MORY REQUIREMENTS 001B50 BYTES
RMINATED
```